

Uncovering the Mechanism of Action of a Novel Therapeutic Compound for the Treatment of Parkinson's Disease



Rachel Mary Hughes

Thesis submitted for the degree of Doctor of Philosophy (PhD)

June 2022

Sheffield Institute for Translational Neuroscience

The University of Sheffield

Acknowledgments

Firstly, I would like to thank my supervisor and mentor Professor Heather Mortiboys. Her dedication and passion for furthering the scientific field is forever inspiring. Without her knowledge, support and guidance I would not be where I am today. Also, for her belief and confidence in me when I lacked it the most. To my secondary supervisor Professor Oliver Bandmann, thank you for your ever enthusiastic input, it was truly motivating. I extend my thanks to the team at NZP UK Ltd, particularly Dr Alex Weymouth-Wilson, without who this work would not have been possible. Also, to Dr Gemma Packer for making NZP meetings all the more entertaining. I would also like to thank Dr Ryan West for his patience and for sharing his wealth of *Drosophila* knowledge with me.

These acknowledgments would not be complete without mentioning the generous donors who provided us with valuable skin biopsies, enabling us to generate the model used throughout this thesis. Thank you also to the DiMeN team and the MRC for funding this research.

I would like to thank all past and present members of the Mortiboys lab group, specifically the weekend neurone feeding team; Aurelie, Ruby, Tom(20), Fernanda, Lizzie, Naomi, Pauline, James and Toby. Also, Chris Hastings for the work on the initial drug screen. A special mention has to go to Katy Barnes for not only being my first (forced) friend but also becoming my lab-wife, sounding post and general go-to woman for all things science and life.

I will be forever grateful to the people I've met while working in SITraN but particularly to Martyna Matuszyk, Bridget Ashford and Sarah Roscoe. Your constant support hasn't gone unnoticed and it has been a privilege to get to know you and call you my friends.

Furthermore, to both my childhood friends Rachel Hussey and Gemma Roe, as well as my university friends, particularly Ruth Perkins. I would not have remained quite as sane through all these years of education if it was not for you.

To Paddy, thank you for sticking by me and supporting me through both my masters and PhD. You make life that little bit brighter and your infectious optimism and sense of humour carried me through lockdowns and stress. Not forcing me to talk about science 24/7 has kept my passion alive, yet your willingness to try and learn about some of the things I do has been inspiring. A special mention has to go to Poppy for being the best 4-legged friend a girl could wish for, a hurricane at times, but the perfect reason to take a break and appreciate the world around me.

My biggest thanks of all has to go to my two biggest cheerleaders, Mum and Dad. Without the constant barrage of love, support and encouragement, I would not be where I am today. For nurturing my determination as a child, to always telling me that I can do whatever I set my mind to and for forever supporting me physically, emotionally, and at times financially, I will be forever indebted. Thank you will never seem enough.

Finally, I would like to dedicate this thesis to my grandparents who are no longer with us, Margaret, Geoff, Beatrice and Jack.

Abstract

This section has been redacted by the author for commercial reasons.

Contents

Acknowledgments	i
Abstract	iii
Contents	iv
List of Figures	x
List of Tables	xiv
List of Abbreviations	xv
1 Introduction	1
1.1 Parkinson's disease	1
1.1.1 Parkinson's Disease Pathology	1
1.1.2 Causes of Parkinson's Disease	2
1.1.3 Current Treatments	4
1.2 Mitochondria.....	7
1.2.1 Cellular ATP Generation.....	8
1.2.2 Mitochondrial Dynamics.....	8
1.2.3 Reactive Oxygen Species.....	9
1.2.4 Other Mitochondrial Functions.....	9
1.3 Mitochondria and Their Role in Parkinson's Disease	10
1.3.1 Familial Parkinson's Disease.....	10
1.3.2 Sporadic Parkinson's Disease	12
1.4 Non-Mitochondrial Drivers of Parkinson's Disease	14
1.4.1 Lysosomal Dysfunction.....	14
1.4.2 Inflammation	14
1.4.3 Protein Aggregation.....	15
1.5 Bile Acids	15
1.5.1 Historical Uses.....	16
1.5.2 Bile Acids and Neurodegenerative Disease.....	16

1.5.3	Bile Acids as Treatments for Neurodegenerative Diseases.....	18
1.5.4	Possible Mechanism of Action of UDCA.....	19
1.5.5	Possible Mechanism of Action of TUDCA.....	20
1.6	Project Background.....	22
1.7	Aims and Objectives	27
1.8	Project Hypothesis	27
2	Materials and Methods.....	28
2.1	Ethics	28
2.2	Participant Characteristics	28
2.3	Cell Culture	28
2.3.1	Cell Culture of Fibroblasts.....	28
2.3.2	Generation of Induced Neuronal Progenitor Cells.....	29
2.3.3	Cell Culture of iNPCs	29
2.3.4	Cell Culture of iNPC Derived Dopaminergic Neurones	29
2.4	Drug Treatment.....	30
2.5	siRNA Treatment.....	31
2.5.1	Optimisation.....	31
2.5.2	RNA Extraction	32
2.5.3	Complementary DNA (cDNA) Synthesis.....	32
2.6	qPCR	33
2.6.1	Analysis	34
2.7	ATP Assays.....	35
2.7.1	Analysis	35
2.8	Immunocytochemistry	36
2.9	Western Blotting.....	38
2.9.1	Protein Quantification	38
2.9.2	Gel Electrophoresis	39

2.10	Mitophagy Assays.....	44
2.10.1	Live Basal Mitophagy Assay.....	44
2.10.2	Induced Mitophagy	44
2.11	Mitochondrial Membrane Potential and Mitochondrial Reactive Oxygen Species (MitoROS).....	46
2.11.1	siRNA Treatment.....	46
2.11.2	MMP/MitoROS Live Assay	46
2.11.3	Analysis.....	46
2.12	Confirming Knockdown Efficacy	47
2.12.1	Cell Lysis.....	47
2.12.2	Reverse Transcription	47
2.12.3	Real Time qPCR	47
2.12.4	Analysis.....	48
2.13	Cardiolipin.....	49
2.13.1	Analysis.....	49
2.14	Opera Phenix Harmony 4.9 Image Analysis	51
2.15	Drosophila Work	56
2.15.1	Virgin Selection	56
2.15.2	Crosses	57
2.15.3	Larval Locomotor Assay.....	57
2.15.4	Survival Assays.....	59
2.16	Statistics	61
3	Characterising the Neuronal Model.....	62
3.1	Background.....	62
3.2	Aims and Objectives	67
3.3	Results	68
3.3.1	Functional Characterisation.....	68

3.3.2	iNPC-Derived Dopaminergic Neurone Characterisation	80
3.4	Discussion.....	116
4	Parkinson’s Disease Relevant Mechanisms	123
4.1	Background.....	123
4.1.1	Alpha Synuclein.....	123
4.1.2	Alpha Synuclein and its Interaction with the Mitochondria	126
4.1.3	Mitophagy	127
4.2	Aims and Objectives	129
4.3	Results	130
4.3.1	Alpha Synuclein Expression	130
4.3.2	Total and Phosphorylated Alpha Synuclein Expression	132
4.3.3	ATP5a and Alpha Synuclein Filament Expression.....	144
4.3.4	Alpha Synuclein Results Overview	161
4.3.5	Basal Mitophagy	162
4.3.6	Induced Mitophagy	173
4.3.7	Mitophagy Results Overview	181
4.4	Discussion.....	182
4.4.1	Alpha Synuclein.....	182
4.4.2	Mitophagy	190
5	Target Characterisation.....	194
5.1	Background.....	Error! Bookmark not defined.
5.2	Aims and Objectives	Error! Bookmark not defined.
5.3	Results	Error! Bookmark not defined.
5.3.1	Concentration in Induced Dopaminergic Neurones	Error! Bookmark not defined.

5.3.2	Expression of Target A in iNPCs and Induced Dopaminergic Neurones	Error!
	or! Bookmark not defined.	
5.3.3	Measuring MMP in Dopaminergic Neurones with Expression of targets Knocked Down	Error! Bookmark not defined.
5.3.4	Verifying the Mitochondria Phenotype	Error! Bookmark not defined.
5.3.5	Mitochondrial Phenotype Results Overview	Error! Bookmark not defined.
5.3.6	Assessing the Knockdown Effect of Targets.....	Error! Bookmark not defined.
5.3.7	Assessing the Knockdown Efficiency of Targets Following MMP Investigations	Error! Bookmark not defined.
5.4	Discussion.....	Error! Bookmark not defined.
5.4.1	xxx	Error! Bookmark not defined.
5.4.2	Target Expression	Error! Bookmark not defined.
5.4.3	MMP and MitoROS Assay	Error! Bookmark not defined.
5.4.4	Knockdown	Error! Bookmark not defined.
6	In Vivo Drosophila Model	253
6.1	Background	253
6.1.1	Drosophila as a Model Organism	253
6.1.2	Drosophila to Model Parkinson's Disease	255
6.1.3	Drosophila Used in This Study	256
6.2	Aims and Objectives	258
6.3	Results	259
6.3.1	Phenotype Identification	259
6.3.2	Phenotype Rescue	Error! Bookmark not defined.
6.3.3	Survival Assay	Error! Bookmark not defined.
6.4	Discussion.....	269

7	General Discussion	276
7.1	Results Overview	276
7.2	Drug Screening	276
7.3	Modelling Parkinson's Disease	281
7.3.1	Cell Model.....	281
7.3.2	Animal Model.....	282
7.4	Alpha Synuclein	282
7.5	Future Work	282
7.6	Conclusion	288
8	Appendix	289
8.1	Alpha Synuclein Expression in Control 2 and sPD2.....	289
8.2	Expression	290
8.3	Knockout Drosophila.....	291
9	References.....	293

List of Figures

Figure 1.1 Chemical structures of compounds	22
Figure 1.2 Complex I activity of MPTP treated isolated left striatum homogenate treated with Jed135.....	25
Figure 2.1 Image region and cytoplasm segmentation	52
Figure 2.2 Representative images of mitochondrial segmentation.....	53
Figure 2.3 Neuronal marker positive image regions based on intensity	54
Figure 2.4 Representative images portraying areas where two stains co-localise	55
Figure 2.5 Schematic depicting set up of Drosophila cross and larvae selection	58
Figure 2.6 Schematic of the Drosophila mating scheme for survival assays.....	60
Figure 3.1 Phenotypes observed in iPSC derived dopaminergic neurones of varying PD genotypes	65
Figure 3.2 ATP production and metabolic status of sPD1 and control 1 iNPCs.	69
Figure 3.3 ATP production and metabolic status of sPD2 and control 2 iNPCs	71
Figure 3.4 ATP production and metabolic status of the SNCA mutant and control 3 iNPCs	73
Figure 3.5 Basal mitochondrial phenotyping, control 1 and sPD1.....	76
Figure 3.6 Basal mitochondrial phenotyping, control 2 and sPD2.....	79
Figure 3.7 Tuj and TH expression in sPD1 and Control 1 end stage dopaminergic neurones.	81
Figure 3.8 Effect of Jed135 or UDCA treatment on Tuj and TH in end stage dopaminergic neurones, control 1 and sPD1.....	Error! Bookmark not defined.
Figure 3.9 Tuj and TH expression in the iNPCs and Neurones as shown via Western Blotting, Control 1 and sPD1.....	Error! Bookmark not defined.
Figure 3.10 MAP2 and DAT expression in control 1 and sPD1 end stage dopaminergic neurones.....	87
Figure 3.11 MAP2 and DAT expression in control 1 and sPD1 when treated with Jed135 or UDCA	Error! Bookmark not defined.
Figure 3.12 PSD95 and Synaptophysin expression in control 1 and sPD1 end stage dopaminergic neurones.....	91
Figure 3.13 Effect of Jed135 or UDCA treatment on PSD95 and synaptophysin expression.	Error! Bookmark not defined.
Figure 3.14 Co-localisation of PSD95 and synaptophysin in control 1 and sPD1 dopaminergic neurones.....	Error! Bookmark not defined.
Figure 3.15 Tuj and TH expression in sPD2 and control 2 end stage dopaminergic neurones.	97

Figure 3.16 Effect of Jed135 or UDCA treatment on Tuj and TH in end stage dopaminergic neurones, control 2 and sPD2.....	Error! Bookmark not defined.
Figure 3.17 Tuj and TH expression in the iNPCs and neurones as shown via Western Blotting, Control 2 and sPD2	Error! Bookmark not defined.
Figure 3.18 MAP2 and DAT expression in control 2 and sPD2 end stage dopaminergic neurones.....	103
Figure 3.19 MAP2 and DAT expression in control 2 and sPD2 when treated with Jed135 or UDCA.	Error! Bookmark not defined.
Figure 3.20 Tuj and TH expression in SNCA mutant and Control 3 end stage dopaminergic neurones.....	107
Figure 3.21 Effect of Jed135 or UDCA treatment on Tuj and TH in end stage dopaminergic neurones, control 3 and the alpha synuclein mutant	Error! Bookmark not defined.
Figure 3.22 Tuj and TH expression in untreated and Jed135 treated neurones as shown via Western Blotting, Control 3 and SNCA mutant.....	Error! Bookmark not defined.
Figure 3.23 MAP2 and DAT expression in control 3 and alpha synuclein mutant end stage dopaminergic neurones.....	113
Figure 3.24 MAP2 and DAT expression in control 3 and the alpha synuclein mutant when treated with Jed135 or UDCA.....	Error! Bookmark not defined.
Figure 4.1 Illustrating the Parkin/PINK1 dependent mitophagy pathway	128
Figure 4.2 Alpha synuclein expression in sPD1/control1 and SNCA mutant/control 3 ...	Error! Bookmark not defined.
Figure 4.3 Total and serine129 phosphorylated alpha synuclein expression in control 1 and sPD1	Error! Bookmark not defined.
Figure 4.4 Assessing the size of alpha synuclein puncta in control 1 and sPD1	Error! Bookmark not defined.
Figure 4.5 Total and serine129 phosphorylated alpha synuclein expression in control 2 and sPD2.....	Error! Bookmark not defined.
Figure 4.6 Assessing the size of alpha synuclein puncta in control 2 and sPD2.	Error! Bookmark not defined.
Figure 4.7 ATP5a and alpha synuclein filament expression, control 1 and sPD1.	Error! Bookmark not defined.
Figure 4.8 Colocalisation of ATP5a and alpha synuclein filament stains, control 1 and sPD1.	Error! Bookmark not defined.
Figure 4.9 ATP5a and alpha synuclein filament expression, control 2 and sPD2	152
Figure 4.10 Colocalisation of ATP5a and alpha synuclein filament stains, control 2 and sPD2	Error! Bookmark not defined.

Figure 4.11 ATP5a and alpha synuclein filament expression, control 3 and alpha synuclein mutant..... **Error! Bookmark not defined.**

Figure 4.12 Colocalisation of ATP5a and alpha synuclein filament stains, control 3 and alpha synuclein mutant. **Error! Bookmark not defined.**

Figure 4.13 Mitochondrial and Lysosomal Number per Cell, Control 1 and sPD1..... **Error! Bookmark not defined.**

Figure 4.14 Mitochondrial and Lysosomal Number per Cell, Control 2 and sPD2..... **Error! Bookmark not defined.**

Figure 4.15 Mitophagy levels and network fragmentation of control 1 and sPD1..... **Error! Bookmark not defined.**

Figure 4.16 Mitophagy levels and network fragmentation of control 2 and sPD2..... **Error! Bookmark not defined.**

Figure 4.17 Mitochondrial and lysosomal counts, control 1 and sPD1...**Error! Bookmark not defined.**

Figure 4.18 Mitochondrial and lysosomal counts, control 2 and sPD2...**Error! Bookmark not defined.**

Figure 4.19 Percentage mitophagy and mitochondrial fragmentation, control 1 and sPD1 **Error! Bookmark not defined.**

Figure 4.20 Percentage of induced mitophagy and mitochondrial fragmentation, control 2 and sPD2..... **Error! Bookmark not defined.**

Figure 5.1 xxx concentration per mg of protein..... **Error! Bookmark not defined.**

Figure 5.2 Concentration of xxx across three PD patient and three control dopaminergic neurone lines **Error! Bookmark not defined.**

Figure 5.3 Target A expression across patient and control iNPC and induced dopaminergic neurones..... **Error! Bookmark not defined.**

Figure 5.4 Knock down effect of four different Target A clones in induced dopaminergic neurones..... **Error! Bookmark not defined.**

Figure 5.5 Knock down effect of four different Target B clones in induced dopaminergic neurones..... **Error! Bookmark not defined.**

Figure 5.6 Basal phenotype of controls vs patients All data generated without any form of knockdown treatment **Error! Bookmark not defined.**

Figure 5.7 Number of MitoROS spots per cell and percentage of mitochondria positive for MitoROS. **Error! Bookmark not defined.**

Figure 5.8 Effects of Target A single knockdown, control 1 and sPD1...**Error! Bookmark not defined.**

Figure 5.9 Effects of Target A single knockdown, control 2 and sPD2...**Error! Bookmark not defined.**

Figure 5.10 Effects of Target B single knockdown, control 1 and sPD1.**Error! Bookmark not defined.**

Figure 5.11 Effects of Target B single knockdown, control 2 and sPD2.**Error! Bookmark not defined.**

Figure 5.12 Effects of Target A and B double knockdown, control 1 and sPD1 **Error! Bookmark not defined.**

Figure 5.13 Effects of Target A and B double knockdown, control 2 and sPD2 **Error! Bookmark not defined.**

Figure 5.14 Knockdown efficiency of Target A and B following completion of mitochondrial membrane potential and mitochondrial reactive oxygen species investigations..... **Error! Bookmark not defined.**

Figure 6.1 Identifying the phenotype previously observed in Parkin mutant Drosophila larvae. 260

Figure 6.2 Initial locomotor assays with larvae treated with 60µM Jed135 and 600µM UDCA. **Error! Bookmark not defined.**

Figure 6.3 The effect of different doses of Jed135 and UDCA on larval locomotor speed **Error! Bookmark not defined.**

Figure 6.4 Total number of eclosed F1 progeny Drosophila ... **Error! Bookmark not defined.**

Figure 6.5 Investigating whether Jed135 harbours a toxic effect on the survival of adult Drosophila..... **Error! Bookmark not defined.**

Appendix Figure 8.1 Alpha synuclein expression for sPD2 and control 2 289

Appendix Figure 8.2 xxx expression in control 2 and sPD2 290

Appendix Figure 8.3 Phenotyping a novel mutant Drosophila larvae strain and assessing the effect of Jed135 and UDCA treatment..... 292

List of Tables

Table 1.1 Outlining the effect of Jed135 on MMP and cellular ATP in sPD fibroblasts.....	23
Table 1.2 Effect of UDCA and Jed135 on induced dopaminergic neurones over a variety of parameters.....	24
Table 2.1 Details of Fibroblast Lines Used for Reprogramming into iNPCs	28
Table 2.2 Primer Sequences of the siRNA Clones Taken Forward	31
Table 2.3 Reagents for Genomic DNA Elimination.....	32
Table 2.4 Reagents for Reverse Transcription Master Mix.....	33
Table 2.5 Reagents for SYBR Green Reaction Master Mix	33
Table 2.6 Forward and Reverse Primer Sequences Used.....	34
Table 2.7 List of Primary Antibodies Used for Immunocytochemistry	37
Table 2.8 Sample Buffer Reagents	38
Table 2.9 Reagents for 12% Resolving Gel.....	40
Table 2.10 Reagents for 10% Stacking Gel.....	40
Table 2.11 Reagents for SDS-PAGE Running Buffer.....	40
Table 2.12 Reagents for 5x Transfer Buffer	41
Table 2.13 Reagents for TBST.....	41
Table 2.14 Primary and Secondary Antibodies Used for Western Blotting	43
Table 2.15 Reagents for qPCR Master Mix per Well	48
Table 2.16 Recipe for Drosophila stock food.....	56
Table 4.1 Summary Table of Alpha Synuclein Results.....	161
Table 4.2 Summary Table of Mitophagy Results	181
Table 5.1 Summary Table of Mitochondrial Phenotype Results	Error! Bookmark not defined.

List of Abbreviations

2DG	2-DeoxyGlucose
AD	Alzheimer's Disease
ADP	Adenosine Monophosphate
AKAP1	A-Kinase Anchoring Protein 1
ALCAT	Lysocardiolipin Acyltransferase
ALS	Amyotrophic Lateral Sclerosis
ANOVA	Analysis of Variance
ATP	Adenosine Triphosphate
ATX-LPA	Autotaxin-Lysophosphatidic
BBB	Blood Brain Barrier
BDNF	Brain Derived Neurotrophic Factor
BSA	Bovine Serum Albumin
CA	Cholic Acid
CDCA	Chenodeoxycholic Acid
CDP-DAG	Cytidine Diphosphate Diacylglycerol
CL	Cardiolipin
CS	Canton S
DAPT	N-[N-(3,5-difluorophenacetyl)-l-alanyl]-S-phenylglycine t-butyl ester
DAT	Dopamine Transporter
DBS	Deep Brain Stimulation
DCA	Deoxycholic Acid
d-cAMP	d-cyclic Adenosine Monophosphate
DMSO	Dimethyl Sulfoxide

Dnm2	Dynamin 2
Drp1	Dynamin Related Protein 1
DSP	Dithiobis[succinimidylpropionate]
EB	Embryoid Body
EBV	Ebola Virus
ETC	Electron Transport Chain
FADH ₂	Flavin Adenine Dinucleotide
FBS	Foetal Bovine Serum
FGF8	Fibroblast Growth Factor 8
GBA	Glucocerebrosidase
GCA	Glycocholic acid
GDNF	Glial Derived Neurotrophic Factor
GFP	Green Fluorescent Protein
GWAS	Genome Wide Association Study
HPLC	High Performance Liquid Chromatography
Hsp90	Heat Shock Protein 90
HSV	Herpes Simplex Virus
ICC	Immunocytochemistry
IMM	Inner Mitochondrial Membrane
iNPC	Induced Neuronal Progenitor Cell
iPSC	Induced Pluripotent Stem Cell
JNK	c-Jun N-terminal kinase
LC3	Light Chain 3
LCA	Lithocholic Acid
LRRK2	Leucine-rich Repeating Kinase
MAP2	Microtubule Associated Protein 2

MCI	Mild Cognitive Impairment
MEM	Minimum Essential Medium
Mfn1	Mitofusin 1
Mfn2	Mitofusin 2
Mid49	Mitochondrial Dynamics Protein 49
Mid51	Mitochondrial Dynamics Protein 51
MMP	Mitochondrial Membrane Potential
MND	Motor Neurone Disease
MPP+	1-methyl-4-phenylpyridinium
MPPP	1-methyl-4-phenyl-4-propionpiperidine
MPTP	1-methyl-4-phenyl-1,2,3,6-tetrahydropyridine
NADH	Nicotinamide Adenine Dinucleotide
OMM	Outer Mitochondrial Membrane
Opa1	Optic Atrophy 1
OR	Oregon R
OXPHOS	Oxidative Phosphorylation
PA	Phosphatidic Acid
PARIS	Parkin Interaction Substrate
PC	Phosphatidylcholine
PD	Parkinson's Disease
PE	Phosphatidylethanolamine
PFA	Paraformaldehyde
PG	Phosphatidylglycerol
PGC1 α	Peroxisome Proliferator-Activated Receptor Gamma Coactivator 1-alpha
PI	Phosphatidylinositol

PINK1	Phosphatase and Tensin Homologue Induced Kinase 1
PS	Phosphatidylserine
PSD95	Post-Synaptic Density Protein 95
PTEN	Phosphatase and Tensin Homologue
PVDF	Poly-Vinylidene Difluoride Membrane
RBD	REM Behaviour Disorder
REM	Rapid Eye Movement
ROS	Reactive Oxygen Species
SAG	Smoothened Agonist
SNpc	Substantia Nigra Pars Compacta
SOD1	Superoxidase Dismutase 1
TBST	Tris Buffered Saline with Tween20
TCA	Taurocholic Acid
TGF β	Transforming Growth Factor Beta
TH	Tyrosine Hydroxylase
TM6B	Third Multiple 6B
TMRM	Tetramethylrhodamine Methyl Ester Perchlorate
TOM20	Translocase of Outer Membrane 20
TOM40	Translocase of Outer Membrane 40
TUDCA	Tauroursodeoxycholic Acid
UDCA	Ursodeoxycholic Acid
UPDRS	Unified Parkinson's Disease Rating Scale
US FDA	United States Food and Drug Administration
VDAC1	Voltage-dependent Anion-selective Channel 1
VPS35	Vacuolar Protein Sorting-associated Protein 35

1 Introduction

Disease modifying therapies for the treatment of neurodegenerative diseases are fast becoming the greatest challenge in biomedical research. Although pathologically and phenotypically different, Parkinson's disease (PD), Alzheimer's disease (AD) and motor neurone disease (MND) share a common feature: the loss of structure and function in discrete areas of the brain, with minimal effective therapies available to delay disease progression (Przedborski et al., 2003).

1.1 *Parkinson's disease*

Initially described as the 'shaking palsy' by James Parkinson in 1817, PD is now the second most common neurodegenerative disease and most common neurodegenerative movement disorder. It is thought to affect approximately 7 million people worldwide, a figure which is expected to double by 2040 (Jankovic and Tan, 2020), highlighting the importance of drug discovery, particularly to generate disease modifying therapies.

In order to satisfy a diagnosis of PD, a patient must exhibit the core motor symptoms of resting tremor, bradykinesia and rigidity, all of which are often asymmetric, as well as a degree of postural instability. Furthermore, these symptoms should be somewhat improved following dopaminergic treatment in order for a PD diagnosis to be given. In many cases, the severity of the main motor symptoms can differ, allowing motor subtypes to be formed, for example tremor-dominant (Balestrino and Schapira, 2020). Phenotypically, PD is an extremely heterogeneous disease and patients experience a myriad of other motor and non-motor symptoms. Additional motor symptoms include gait disturbances, freezing and alterations in blinking and eye movements (Balestrino and Schapira, 2020). The main disease heterogeneity in PD lies within the broad range of non-motor symptoms patients can experience. It has been reported that although often under-reported by patients and under-investigated by clinicians, the non-motor symptoms are usually the most debilitating to patients and have the largest effect on quality of life. There are a plethora of non-motor symptoms experienced in PD including, but not limited to, psychiatric symptoms such as depression, anxiety and hallucinations, gastrointestinal symptoms such as constipation and sleep disturbances (Balestrino and Schapira, 2020).

1.1.1 *Parkinson's Disease Pathology*

PD is characterised by a progressive loss of dopaminergic neurones in the substantia nigra pars compacta (SNpc), part of the nigrostriatal pathway, as well as the presence of cytoplasmic protein inclusions known as Lewy bodies (Simon et al., 2020). The main proteinaceous component of Lewy bodies is alpha synuclein, encoded by the *SNCA* gene,

and will be discussed in greater detail during chapter 4. By the time patients present to clinic with symptoms, approximately 40-60%, or more, of their dopaminergic neurones have already degenerated (Váradi, 2020). However, it is universally accepted that early degeneration begins 10-15 years prior to symptom onset, a stage widely referred to as the prodromal phase of PD (Balestrino and Schapira, 2020). This is further supported by the proposed spread of alpha synuclein which suggests early involvement of both the enteric nervous system and the olfactory bulb, with the SNpc only becoming affected during the third stage (Braak et al., 2003a, Hawkes et al., 2007). Furthermore, the presence of non-motor symptoms hyposmia (loss of smell), constipation and sleep disturbances known as rapid eye movement (REM) behaviour disorder (RBD) in otherwise healthy individuals displays an increased risk for the development of PD in later life (Mahlknecht et al., 2015). The long latency period that exists between initial pathology development and symptom onset presents a unique opportunity for early therapeutic intervention in order to preserve remaining dopaminergic neurones, as well as understanding disease processes and development (Balestrino and Schapira, 2020). However, the caveat remains in identifying this population as, excluding RBD, the prodromal symptoms are both subtle and lack specificity (Mahlknecht et al., 2015), highlighting the importance of identifying robust biomarkers to uncover PD.

1.1.2 Causes of Parkinson's Disease

In the majority of cases, the aetiology of PD is unknown and likely linked to a variety of lifestyle and environmental factors. However, approximately 5-10% of PD cases are linked to known genetic mutations, with 20 monogenic mutations and over 100 risk loci having been identified (Balestrino and Schapira, 2020, Jankovic and Tan, 2020). Different genetic causes present in slightly different ways, with differences in age of onset, motor sub-type and pathological burden. The first genetic mutations linked to PD were described in 1997 in the *SNCA* gene and so far, at least 14 pathogenic or likely pathogenic point mutations have been uncovered well as gene multiplications, frequently causing early onset PD (Siddiqui et al., 2016, Guo et al., 2021). Both gene duplications and triplications have been reported, with triplication mutations resulting in earlier onset than duplications (Simon et al., 2020), indicating a role for endogenous protein levels in PD.

A second genetic cause of PD, and the most common autosomal recessive mutation, is in the gene encoding *Parkin*. Parkin is an E3 ubiquitin ligase that is heavily involved in mitophagy, the removal of damaged and dysfunctional mitochondrial from a cell (Jankovic and Tan, 2020) but is also involved in mitochondrial dynamics, the repair of mildly damaged mitochondria via the formation of mitochondrial derived vesicles and it may also have a role

in promoting cell survival, although this is yet to be fully elucidated (Seirafi et al., 2015). Patients with *Parkin* mutations typically present with a more symmetrical phenotype and although they initially respond well to dopamine treatment, they exhibit dopamine-induced dyskinesias earlier than typically expected (Jankovic and Tan, 2020). Interestingly, upon post-mortem examination, cases of *Parkin* PD rarely show Lewy body pathology (Jankovic and Tan, 2020).

The most common cause of autosomal dominant PD is via mutation in the leucine-rich repeat kinase 2 (*LRRK2*) gene, however they frequently possess incomplete penetrance (Jankovic and Tan, 2020) and are sub-typed into manifesting and non-manifesting groups. Although still a rare cause of PD, *LRRK2* mutations are more commonly found in the Ashkenazi Jewish population, as well as in some regions of North Africa, with fewer cases described in Caucasians (Simon et al., 2020). There have been a number of *LRRK2* mutations described that result in PD via alterations within the kinase domain, likely via a toxic gain of function, therefore treatment with *LRRK2* kinase inhibitors may be of benefit to this PD population (Jeong and Lee, 2020). Pathologically, *LRRK2* PD patients may or may not exhibit Lewy bodies, while clinically, they often present with atypical Parkinsonian features such as orthostatic hypotension, dementia and hallucinations (Jankovic and Tan, 2020).

Other PD causing mutations exist in the genes that encode phosphatase and tensin homologue (*PTEN*) induced kinase 1 (*PINK1*), *DJ1* and *glucocerebrosidase* (*GBA*) which cause autosomal recessive (and autosomal dominant for *GBA*) disease (Simon et al., 2020). However, as mentioned, the majority of PD cases are idiopathic, having no known cause. That said, risk genes and environmental triggers have been described that can increase the risk of developing PD. By far the biggest risk factor for developing PD is age, however links have also been made to heavy metal exposure via an increase in oxidative stress in dopaminergic neurones (Emamzadeh and Surguchov, 2018). Similarly, exposure to pesticides and rural living have been associated with a higher risk of developing PD, as well as traumatic brain injury and the consumption of dairy products (Jankovic and Tan, 2020). On the contrary, smoking and caffeine intake through drinking coffee have been associated with lower risk of PD (Jankovic and Tan, 2020), however these should be balanced against the risk of developing other diseases as a result of their consumption. These potential risk and neuroprotective factors highlight the complexities in PD development and further illustrate why different disease modifying therapies may be needed.

1.1.3 Current Treatments

There are a number of treatments options available for PD, both pharmacological and non-pharmacological, however both options only offer symptomatic relief, not disease modifying. As mentioned, PD is caused by the loss of dopaminergic neurones, and thus less dopamine is available in the brain. Many of the available pharmacological interventions currently centre around increasing dopamine concentration in the synapse. Physiologically, dopamine is synthesised from phenylalanine via enzymatic reactions and the creation of the intermediates tyrosine and L-Dopa, with tyrosine hydroxylase being the rate limiting enzyme of the reaction (Daubner et al., 2011). The generation of further catecholamines norepinephrine and epinephrine are also possible via enzymatic reactions of dopamine (Daubner et al., 2011). Direct administration of dopamine is not possible due to its electrical charge, meaning it cannot cross the blood brain barrier (BBB), therefore the precursor, levodopa, is administered (LeWitt, 2015). However, levodopa presents a challenge of its own due to its uptake and bioavailability (Tambasco et al., 2018). Levodopa competes for uptake via facilitated sodium dependent L-neutral amino acid transport within the gut alongside neutral amino acids generated following the digestion of food (Tambasco et al., 2018). Following uptake, levodopa undergoes extensive first pass metabolism as well as degradation and clearance and consequently only approximately 1% of orally administered levodopa is available for uptake by the brain (Tambasco et al., 2018). In order to counteract a portion of levodopa degradation in the periphery, it is often administered in conjunction with carbidopa, a peripheral decarboxylase inhibitor, allowing for increased (up to 10%) bioavailability and consequently increased efficacy of levodopa (Tambasco et al., 2018). Levodopa is currently the most effective treatment for PD, however longer term use can result in the generation of new motor and non-motor symptoms, namely dopamine-induced dyskinesias which often negatively affect the patient's quality of life (Daubner et al., 2011). It is likely that long term, intermittent levodopa administration results in dyskinesias due to downstream effects that alter the serotonergic neurones of the striatal system (Thanvi et al., 2007, Emamzadeh and Surguchov, 2018).

In addition to levodopa, dopamine receptor agonists and monoamine oxidase inhibitors can also be used to treat PD. Dopamine receptor agonists are often used as the first line treatment for PD as they can delay motor complications and also delay the onset of dopamine induced dyskinesias, therefore of benefit to people with early onset PD (Borovac, 2016). There are two generations of dopamine receptors agonists, older, ergoline based, and newer, non-ergoline based. The older generation of dopamine receptor agonists are now rarely used due to their off target effects on other subsets of dopamine receptors, whereas the newer generation are specific to dopamine receptors D2 and D3 (Borovac,

2016). This is of critical importance as dopamine receptors D2 and D3 are involved in locomotor activities, whereas receptor D4 is linked to stimulant use and drug relapse while D1 also affects the renal system (Borovac, 2016). Dopamine receptor agonists primarily function by binding to dopamine receptors in the absence of endogenous dopamine, therefore mimicking its signalling and producing the desired effect. That said, they continue to have inherent disadvantages, in particular impulse-control disorder, peripheral oedema and excessive day time sleepiness (Borovac, 2016).

Monoamine oxidase B inhibitors function by halting the action of monoamine oxidase B, the enzyme responsible for the breakdown of dopamine in the brain, hence increasing the concentration of dopamine in the synaptic cleft, allowing dopamine signalling to ensue for longer (Dezsi and Vecsei, 2017).

The side effect profiles associated with these three groups of pharmacological therapies, as well as their symptomatic nature and typically limited efficacy, in particular in patients with advanced disease, highlight the need for alternative therapies that provide either a neuroprotective or neuro-restorative approach. Since its inception in 2000, approximately 2700 clinical trials have been undertaken in PD and their progress published on the 'clinicaltrials.gov' web registry (Prasad and Hung, 2021), with 3185 listed as of May 2022. In many instances, novel pharmacological therapies have looked promising during *in vitro* and *in vivo* studies, however once into clinical trials, they fail to meet their primary end points. Different phases of clinical trials exist to ensure their safety and tolerability in the first instance before conducting further in-depth studies to determine their efficacy, side effect profile and potency (Prasad and Hung, 2021). Only approximately 33% of compounds reach phase III clinical trials (Prasad and Hung, 2021) in which it can be determined whether a compound reaches its primary end point. Perhaps one of the most high-profile PD clinical trials of recent years was investigating the effect of a dopaminergic neurotrophic factor, glial cell line-derived neurotrophic factor (GDNF). This study was a large step into the unknown as they designed a novel drug administration technique. Four micro-catheters were inserted into the putamen with a transcutaneous delivery port mounted onto the skull allowing for intermittent delivery of GDNF or placebo throughout the trial (Whone et al., 2019). Interestingly, despite many participants experiencing a subjective improvement of their symptoms, the primary end point of this trial was not met, meaning that there was no statistically significant change in unified Parkinson's disease rating scale (UPDRS) score in the defined OFF state (Whone et al., 2019). GDNF clearly illustrated visual improvements in patient motor symptoms, however the drug delivery system required extensive neurosurgery

that is likely not suitable for all PD patients, therefore it may be of benefit to develop an oral or subcutaneous delivery system for GDNF.

As mentioned, Lewy bodies are found within the brain of the majority people with PD as a result of alpha synuclein aggregation. Alpha synuclein exists as different strains, with some strains believed to be more toxic than others. There are currently immunotherapies in clinical trials which aim to restrict the spread of pathogenic alpha synuclein by targeting it for degradation with antibodies (Stoker and Barker, 2020). However, the question remains regarding the effect of alpha synuclein spread in physiological disease. It is evidently important pathologically, but PD incorporates many other factors so it is likely immunotherapy would be needed in conjunction with other therapies. Moreover, the normal physiological function of alpha synuclein is, at present, poorly understood, therefore targeting it for degradation could create unexpected off target effects.

The drug discovery process from initial concept and target identification to licensing for clinical use often takes 12-15 years, if not longer, with a cost of over \$1 billion (Mohs and Greig, 2017). However, drug repurposing offers a cheaper, more efficient method to develop compounds. Briefly, drug repurposing investigates the potential for using compounds that are already licenced for one condition, in the treatment of another condition (Xue et al., 2018). The major benefit of drug repurposing is that the safety and tolerability profile of the drug, as well as the side effect profile, is already known and understood. One of the first examples of drug repurposing was acetylsalicylic acid, more commonly known as aspirin. Initially used as an analgesic, it can also be used at low doses as an anti-platelet aggregation therapy to prevent cardiac events (Jourdan et al., 2020).

Drug repurposing studies have also been conducted to discover new therapies for PD. Most notably, a repurposing study in 2013 uncovered the potential benefits of bile acids, namely ursodeoxycholic acid (UDCA), in restoring mitochondrial health in a number of different PD models (Mortiboys et al., 2013, Mortiboys et al., 2015). UDCA is currently used for the treatment of cholestatic liver diseases (Paumgartner and Beuers, 2002) however it has since entered human clinical trials to assess its effect in people with PD. The primary end points of this trial are primarily to determine safety and tolerability in PD patients but, as a secondary outcome, to investigate differences in UPDRS score, target engagement and imaging between baseline and end of trial. The trial was expected to end in July 2021; however, results are yet to be published (Payne et al., 2020).

Non-pharmacological therapies are also available for the treatment of PD, primarily in the form of deep brain stimulation (DBS). DBS requires the implantation of electrodes targeted

to specific brain regions (usually the subthalamic nuclei or globus pallidus internus) in order to deliver constant or intermittent electrical pulses and provides significant and persistent improvement in motor function for 5-10 years (Lozano et al., 2019). However, due to the multifaceted nature of PD and the underlying neurodegeneration that continues to occur, it is unable to provide respite from gait, speech or cognitive issues (Lozano et al., 2019). DBS is believed only to be beneficial to a small subset of patients, those in more advanced stages of disease who suffer with motor fluctuations and dopamine induced dyskinesias. Furthermore, the risk benefit ratio must be carefully considered due to the inherent possibility of brain infection (Emamzadeh and Surguchov, 2018).

The lack of long term, effective pharmacological and non-pharmacological treatments highlights the importance of continued research and drug development in the PD field. Unfortunately, it is common for novel compounds to show promise in cellular and animal models of PD, however struggle to translate to humans upon clinical trial. This is likely due to the struggles associated with identifying a suitable, measurable primary end point. Measuring dopaminergic cell survival is not possible as cells may survive, but without function. Therefore, therapies are often assessed on their ability to modify disease progression through changes in UPDRS score and measurable biomarkers from blood and cerebral spinal fluid (Rascol, 2009). Moreover, identifying the correct patient population to use to difficult. As mentioned, PD pathology is likely initiated 10-15 years prior to symptom onset. Therefore, treating once symptom burden has arisen may be too late and reliable biomarkers for early diagnosis need identifying to enable treatment within the preclinical or prodromal phases.

1.2 Mitochondria

Mitochondria are double membraned organelles that are pivotal for the survival of eukaryotes and are responsible for producing adenosine triphosphate (ATP), the energy required for cells to survive. Initially identified in the 1840s, mitochondria were first officially recognised by Altmann in 1890 who described them 'elementary organisms' that were able to live symbiotically with eukaryotic cells, aiding their function, an idea that was later revisited when scientists uncovered mitochondria's bacterial roots (Ernster and Schatz, 1981, Roger et al., 2017). In support of the endosymbiosis theory, mitochondria possess their own, circular, DNA, mtDNA, that encodes 37 genes, 13 of which are translated into proteins of the electron transport chain (ETC) (Gray, 2012, Nunnari and Suomalainen, 2012). The remaining genes encode ribosomal and transfer RNAs involved in mitochondrial protein translation (Gray, 2012).

1.2.1 Cellular ATP Generation

As mentioned, ATP is the cellular energy that is needed in order to cells to survive. There are two primary mechanisms by which ATP can be generated, namely glycolysis and oxidative phosphorylation (OXPHOS). Glycolysis is the conversion of glucose to either pyruvate or lactate, with conversion to the latter resulting in a more rapid generation of ATP, however the overall net gain of ATP is much lower than via OXPHOS (Bell et al., 2020b). If converted to pyruvate, it is able to enter the citric acid cycle following conversion to acetyl-CoA. The citric acid cycle is a series of 8 enzymatic reactions, which primarily occur in the mitochondrial matrix, and result in the generation of reducing agents nicotinamide adenine dinucleotide (NADH) and flavin adenine dinucleotide (FADH₂) (Haddad A, 2021). These substrates then enter the ETC by donating electrons to complex I (NADH: ubiquinone oxidoreductase) or complex II (succinate dehydrogenase) (Nolfi-Donagan et al., 2020). Electrons are then passed down the ETC via a series of redox reactions and are coupled to the pumping of hydrogen ions from the matrix to the intermembrane space at complexes I, III (co-enzyme q: cytochrome c reductase) and IV (cytochrome c oxidase). This generates a proton gradient across the membrane, which is finally utilised at complex V (ATP synthase). Complex V is a large multi-subunit complex, existing both extra membranous (F₀) and trans-membranous (F₁), in which protons are pumped down their concentration gradient from the intermembrane space back into the matrix via F₀. This is coupled to the rotation of the F₁ head, resulting in the addition of a phosphate group to adenosine diphosphate (ADP), generating ATP (Nolfi-Donagan et al., 2020). The process of ATP generation via OXPHOS is much more energy efficient, resulting in a net gain of approximately 32 ATP molecules compared to 4 generated via glycolysis (Bell et al., 2020b, Deshpande OA, 2021).

1.2.2 Mitochondrial Dynamics

Mitochondria were once believed to be static, isolated organelles, however thanks to improvements in live cell imaging over the last 30 years, this was proved to be incorrect. In contrast, mitochondria are now known to form a vast, dynamic cellular network owing to their ability to alter their morphology in response to the needs of the cell (Tilokani et al., 2018). Mitochondrial dynamics are governed by the balance between fission and fusion. Mitochondrial fission is the ability of one mitochondrion to split into two daughter organelles and is primarily regulated by mitochondrial protein dynamin related protein 1 (Drp1) and its receptor proteins mitochondrial fission factor and mitochondrial dynamics proteins 49 and 51 (Mid49 and Mid51). Briefly, Drp1, a cytosolic protein, is dynamically recruited to the mitochondrion where it forms a ring like structure at the scission site. This causes membrane constriction and the final step likely requires dynamin 2 (Dnm2) to catalyse the final scission (Tilokani et al., 2018). Conversely, mitochondrial fusion is the merging of two

mitochondria, forming one mitochondrion and is regulated by optic atrophy 1 (Opa1) and mitofusins 1 and 2 (Mfn1 and Mfn2). Fusion occurs in a 3-step process. Initially, two mitochondria are tethered via Mfn1 and Mfn2 at the outer mitochondrial membrane (OMM), docking surface area is increased and distance between the two mitochondria is reduced. A conformational change occurs via a GTP hydrolysis mechanism resulting in the fusion of the OMM. Finally, Opa1 interacts with cardiolipin (CL) on the opposing inner mitochondrial membrane (IMM), tethering them together and the resulting GTP hydrolysis completes the fusion process (Tilokani et al., 2018).

1.2.3 Reactive Oxygen Species

Reactive oxygen species (ROS) are derived from molecular oxygen and formed via its partial reduction to create species such as superoxide, hydrogen peroxide and hydroxyl radicals (Ray et al., 2012). ROS are widely accepted to play a physiological role in cell signalling, particularly via the NF- κ B pathway, whilst also being involved in immunity as anti-microbial effectors molecules (Dan Dunn et al., 2015). Mitochondria are the major source of cellular ROS generation, producing approximately 90% (Kausar et al., 2018), and occurring primarily via the production of superoxide at complex I of the ETC due to leakage of electrons (Dan Dunn et al., 2015, Murphy et al., 2016). There is a fine balance between physiological and pathological ROS that is governed by antioxidants, molecules able donate an electron, in order to stabilise free radicals and prevent oxidative stress (Lobo et al., 2010). It is thought that when this system becomes imbalanced, ROS and hence oxidative stress can have negative impacts upon the cell and contribute to many different diseases.

1.2.4 Other Mitochondrial Functions

As mentioned, the primary function of the mitochondria are to generate ATP, however the mitochondria are key players in other cellular processes including apoptosis. Furthermore, mitochondria are known to be involved in cholesterol metabolism. Briefly, although mitochondrial cholesterol levels are 40 times lower than the plasma membrane and 4.5 times lower than the endoplasmic reticulum, the importance of cholesterol at the mitochondrial membrane shouldn't be overlooked. In fact, it could be argued that the lower cholesterol levels mean the mitochondria are more susceptible to cholesterol dysregulation than the plasma membrane or endoplasmic reticulum (Martin et al., 2016). Cholesterol must be transported to the mitochondria from elsewhere in the cell, internalised through the outer and inner mitochondrial membranes and in instances where cholesterol import is altered, changes in the mitochondrial membrane properties and overall mitochondrial functions occur (Martin et al., 2016). Furthermore, the presence of cholesterol at the IMM is vital for steroid, oxysterols and hepatic bile acid synthesis (Elustondo et al., 2017). Increased mitochondrial

cholesterol has been linked to AD however evidence linking it to PD is currently inconclusive. However, increased mitochondrial cholesterol was found to cause oxidative stress and mitochondrial dysfunction in a 1-methyl-4-phenyl-1,2,3,6-tetrahydropyridine (MPTP) mouse model of PD, increasing the vulnerability of the mid-brain dopaminergic neurones (Paul et al., 2017).

Furthermore, the maintenance of a healthy mitochondrial population is pivotal and, in association with mitochondrial fission and fusion, mitochondria are able to undergo a process called mitophagy to maintain a healthy mitochondria pool. The process of mitophagy will be discussed at greater length during chapter 4. Mitochondria also have a role in calcium signalling (Murphy et al., 2016) and although an extremely important function within its own right, it is outside the scope of this thesis and therefore won't be discussed at length.

1.3 Mitochondria and Their Role in Parkinson's Disease

As we age, efficiency of the mitochondria is known to decrease, both in quality and activity, contributing to age-related decline in organ function (Sun et al., 2016). Moreover, there is an increased risk of mitochondrial mutations, particularly within the mtDNA, which in turn contributes to the process of ageing (Sun et al., 2016). It is now widely accepted that mitochondria are dysfunctional in many neurodegenerative diseases, including PD. The deficits that we observe in normal ageing appear to be exacerbated, with additional defects also present. Furthermore, many of the genetic causes of PD already mentioned are centred around the mitochondria, further highlighting their role in pathogenesis. The discovery of familial causes of PD has allowed us to investigate the role that the mitochondria play in disease pathogenesis, however these pathways may not be an accurate representation of sporadic disease.

1.3.1 Familial Parkinson's Disease

Understanding the impact of genetic mutations on disease progression has allowed researchers to identify roles that the mitochondria may play in PD pathogenesis. As mentioned, genetic mutations have been found in a number of genes that are now known to cause both autosomal dominant (*SNCA*, *LRRK2*, *vacuolar protein sorting-associated protein 35 (VPS35)*) and autosomal recessive (*Parkin*, *PINK1*, *ATP13A2*) PD. Many of the genes implicated in familial PD have direct effects on mitochondrial function (Park et al., 2018).

SNCA

Alpha synuclein overexpression in a mouse model of PD, synonymous with alpha synuclein gene multiplications, highlighted differences in mitochondrial ETC disruption depending upon brain region, with no differences in regional aggregation. For example, defects in complexes

I, II, IV and V were observed in the midbrain, whereas only defects in complexes IV and V were observed in the striatum (Subramaniam et al., 2014). This highlights the selective vulnerability of dopaminergic neurones within the SNpc to PD.

Alpha synuclein oligomers have also been associated with the production of a more fragmented mitochondrial network, contributing to the imbalances in mitochondrial dynamics and morphology that are observed in PD (Plotegher et al., 2014). Furthermore, pathogenic gene mutations in alpha synuclein have also showed similar pathogenic mechanisms through the creation of more fragmented mitochondrial network, as well as increased ROS production and ETC complex deficiencies (Khalaf et al., 2014, Park et al., 2018).

LRRK2

LRRK2 is a kinase that, under physiological conditions, interacts with mitochondrial fission and fusion proteins, particularly Drp1, resulting in regulation of mitochondrial dynamics (Wang et al., 2012). It is believed that mutations in *LRRK2* result in a toxic gain of function and consequently increased Drp1 activity, with a more fragmented mitochondrial population being formed (Ryan et al., 2015). The most common *LRRK2* mutation, G2019S, is able to enhance the alterations in mitochondrial morphology through increased interactions with Drp1, a phenomenon that can be rescued with Drp1 inhibitors (Ryan et al., 2015). Furthermore, the G2019S mutation is able to interact with fusion protein Opa1, reducing the amount of mature protein available, hence further altering the fission and fusion balance (Stafa et al., 2014). Mutations in VPS35 have also been linked to mitochondrial dynamic alterations via interactions with fission and fusion proteins (Park et al., 2018).

Parkin

Mutations in genes causing autosomal recessive PD have also been directly linked to mitochondrial function. There are over 120 known mutations within *Parkin* that cause PD and its protein function has been linked to regulating the overall health of the mitochondrial population, both through mitophagy and mitochondrial biogenesis. The mechanism by which mitophagy is disrupted depends upon the *Parkin* mutation present; some mutations decrease the recruitment of Parkin to the mitochondria, while others result in a loss of ligase activity (Lee et al., 2010). That said, the outcome in all cases remains constant, removal of damaged mitochondria is impaired, affecting the overall health of the mitochondrial population. As well as mitophagy defects, *Parkin* mutations have also been linked to defective mitochondrial biogenesis. Under physiological conditions, Parkin ubiquitinates parkin interaction substrate (PARIS), targeting it for degradation via the proteasome. Degradation of PARIS is pivotal for normal function as it is a repressor of peroxisome proliferator-activated receptor gamma coactivator 1-alpha (PGC1 α), a protein vital for

mitochondrial biogenesis (Castillo-Quan, 2011, Park et al., 2018). Therefore mutations in *Parkin* result in the accumulation of PARIS and consequently decreased mitochondrial biogenesis (Castillo-Quan, 2011).

PINK1

Physiologically, PINK1 works upstream of Parkin in the mitophagy pathway by means of accumulation at the OMM, recruiting Parkin and tagging the mitochondria for degradation. Therefore, mutations in *PINK1* also primarily affect the mitophagy pathway. However similarly to *Parkin*, mutations in *PINK1* have other effects on the mitochondria, namely perturbations in calcium buffering (Kostic et al., 2015) and deficiencies in ETC complex I and III activity, leading to decreased ATP (Amo et al., 2014). Furthermore, PINK1 acts as a pro-fission regulator by displacing protein kinase A from A-kinase anchoring protein 1 (AKAP1) and activating Parkin and Drp1 to drive mitochondrial fission, however this pathway is disrupted in the presence of *PINK1* mutations (Pryde et al., 2016).

1.3.2 Sporadic Parkinson's Disease

The majority of PD patients have no known underlying cause; however, we are able to understand some of the pathways affected due to our knowledge about dysregulated systems in familial cases of PD. It is also likely that environmental factors play a role in the development of sporadic PD (Park et al., 2018).

Complex I Deficiencies

Mitochondria were first implicated in sporadic PD pathogenesis during the 1980s when a group of seven people presented at a number of different hospitals, all possessing similar symptoms that didn't fit any clinical psychiatric or neurological diagnoses. They presented with Parkinsonian like features including rigidity and cog-wheeling (a jerky-like feeling when the limbs are rotated) (Langston, 2017). As well as the rapid onset of motor symptoms, the patients also experienced some non-motor symptoms in the form of deficits of higher cognitive function and levodopa responsiveness (Langston, 2017). The common denominator between the seven patients was their drug use, having all tried a new, synthetic heroin that they believed to be 1-methyl-4-phenyl-4-propionpiperidine (MPPP). However, upon testing a batch, it was discovered that the synthetic drug was almost exclusively pure MPTP. MPTP is able to cross the BBB where it is rapidly converted into 1-methyl-4-phenylpyridinium (MPP⁺), acting as a substrate at the dopamine transporter on dopaminergic neurones of the SNpc. However, the ventral dopaminergic neurones appeared to be relatively spared, likely due to differences in uptake affinity (Langston, 2017). MPP⁺ was found to exhibit its neurotoxic effects through inhibition of ETC complex I, resulting in decreased ATP production and an increase in ROS, hence oxidative stress, and

consequently neuronal cell death (Langston, 2017). This provided evidence for the role of complex I inhibition in PD, however the rapid onset of symptoms is not representative of sporadic PD. In 1990 Schapira et al studied the ETC in post-mortem tissue from patients with sporadic PD. They described a significant reduction in the activity of mitochondrial complex I compared to age and sex matched controls, yet they were unable to explain why (Schapira et al., 1990). Since then, decreased complex I activity has been repeatedly described in brain tissue from people with PD (Hattori et al., 1991, Janetzky et al., 1994, Mann et al., 1994), however total protein amount remains unchanged (Schägger, 1995). Therefore it is likely that the defects lie primarily within the enzymatic activity of complex I and not within complex assembly (Schägger, 1995). Further evidence for the role of complex I defects in PD have arisen in the form of alternative mitochondrial toxins such as rotenone and 6-hydroxydopamine (Glinka et al., 1997, Marella et al., 2009, Tanner et al., 2011) which have been proven to act via complex I dependent mechanisms and are now routinely used to induce Parkinsonian phenotypes in PD research.

Alternative Mechanisms of Mitochondrial Dysfunction

The production of ROS, which in turn contributes to overall oxidative stress, is locked in vicious cycle with alpha synuclein aggregation. As mentioned, and as will be discussed in greater depth during chapter 4, alpha synuclein aggregates are found pathologically in PD. These aggregates interact with the mitochondria, specifically at complex I, resulting in increased ROS production and oxidative stress (Park et al., 2018). Furthermore, alpha synuclein has been found to interact with OMM proteins translocase of outer membrane 20 and 40 (Tom20 and Tom40), as well as voltage-dependent anion-selective channel 1 (VDAC1), levels of which were found to be reduced in sporadic PD (Chu et al., 2014, Park et al., 2018). It is also possible that alpha synuclein is able to open the mitochondrial permeability transition pore, resulting in the loss of mitochondrial membrane potential (MMP) and a subsequent fragmentation of the network (Park et al., 2018).

Dysfunction within mitochondrial dynamics have also been implicated in sporadic PD, namely via the proteolysis of Opa1 and phosphorylation of Drp1 at serine 616, promoting mitochondrial fission and reducing mitochondrial fusion (Santos et al., 2015). Moreover, levels of PGC1 α have also been discovered to be decreased in sporadic PD and exacerbated by oligomeric alpha synuclein, resulting in decreased mitochondrial biogenesis (Eschbach et al., 2015).

Mitochondria evidently play a pivotal role in the development and pathogenesis of both sporadic and familial PD. It is likely that each patient with PD has deficits in several of the mechanisms discussed and therefore many potential drug targets exist. It is also possible

that the heterogeneity observed within PD is due to different pathways being affected, highlighting the possibility for patient stratification in order to effectively treat PD.

1.4 Non-Mitochondrial Drivers of Parkinson's Disease

1.4.1 Lysosomal Dysfunction

Although linked to mitochondrial dysfunction through mitophagy, lysosomal dysfunction can be a driver of PD in its own right. Lysosomes are small vesicles containing acid hydrolases that play a pivotal role in the degradation and recycling of intra- and extra-cellular macromolecules such as proteins, lipids and carbohydrates (Navarro-Romero et al., 2020). Lysosomal dysfunction occurs when the lysosome is unable to break down the macromolecules, resulting in their accumulation within the lysosome which can ultimately lead to cellular dysfunction.

Functional and effective clearance systems are pivotal in postmitotic cells such as neurones, however similarly to mitochondrial function, lysosomal function declines with age. Moreover, lysosomal dysfunction has been linked to PD. Mutations in *ATP13A2*, a gene that encodes an ATPase involved in lysosomal degradation, have been associated with a rare form of early-onset parkinsonism, while recent genome wide association studies (GWAS) have linked several lysosomal genes to increased risk of PD (Navarro-Romero et al., 2020).

Lysosomal storage disorders have also been associated with neurodegenerative diseases such as PD. Lysosomal storage disorders occur when a mutation, commonly a loss of function mutation, is present in the acidic hydrolases, causing a build-up of substrate inside the lysosome that is unable to be digested. This leads to lysosomal, and consequently cellular, dysfunction.

1.4.2 Inflammation

There is extensive evidence linking inflammation and the development of PD. Briefly, inflammation is an innate, highly regulated mechanism that is able to protect the body from damage and aid in tissue repair (Pajares et al., 2020). Inflammation can also occur following viral infection and links have been made between PD and influenza A, herpes simplex virus 1 (HSV) and Ebola virus (EBV), to name a few, with the viruses believed to reach the basal ganglia via the olfactory bulb and/or the enteric nervous system. Furthermore, some viruses, such as HSV and EBV, are able to mimic alpha synuclein, promoting aggregation and contributing to the endless cycle of alpha synuclein spreading and entering a vicious cycle of alpha synuclein aggregation and inflammation (Pajares et al., 2020). Tackling neuroinflammation represents a large therapeutic intervention option in PD, however it is yet

to be understood whether targeting neuroinflammation would result in symptomatic relief or neuroprotection.

1.4.3 Protein Aggregation

We know that protein aggregation itself is able to cause PD, as mutations in the gene encoding alpha synuclein, *SNCA*, were the first to be linked to PD and cause an early onset, rapidly progressing disease, with higher risk of developing an associated dementia (Gundersen, 2010, Klein and Westenberger, 2012). Mutations in *SNCA* are relatively rare and there is evidence to suggest that wild-type alpha synuclein is able to cause neurodegeneration. This has been further elucidated as *SNCA* multiplications are able to cause disease progression and alpha synuclein over expression in invertebrates and neuronal cell cultures is able to induce toxicity in endogenous dopamine (Gundersen, 2010). However, the question remains as to whether alpha synuclein toxicity alone is able to drive PD in sporadic cases or whether the toxicity of alpha synuclein is a result of another, as yet unidentified, cause. Furthermore, will therapeutically targeting alpha synuclein alter disease progression or is this futile and attention should be channelled into targeting other aspects and potential causes of PD?

1.5 Bile Acids

Bile acids form a group of amphiphilic molecules, containing both hydrophobic and hydrophilic areas, with a rigid ring-like structure and branched side chains (Šarenac and Mikov, 2018). They are produced by cholesterol catabolism in the liver (Chiang, 2013) and stored in the gall bladder until the ingestion of food (Schonewille et al., 2016) when they are released and act as a detergent to aid in the solubilisation and absorption of dietary lipids and fat soluble vitamins in the duodenum (Ackerman and Gerhard, 2016, Grant and DeMorrow, 2020). Upon reaching the ileum, bile acids are recycled, a process that is highly efficient, with approximately 95% of bile acids reabsorbed into the liver and the remaining 5% excreted via the stool (Ackerman and Gerhard, 2016). Bile acids also possess a secondary role, functioning as steroid hormones, binding to receptors such as sphingosine-1-phosphate receptor 2 (S1PR2), Takeda G-protein coupled bile acid receptor 5 (TGR5) and farnesoid X receptor (FXR) to aid in physiological metabolic processes (Grant and DeMorrow, 2020). Bile acids are produced in hepatocytes via the conversion of cholesterol in association with 17 enzymes. The enzymes are responsible for altering the steroid core of cholesterol and are able to produce the two primary bile acids found in humans, cholic acid (CA) and chenodeoxycholic acid (CDCA) (Chiang, 2013, Šarenac and Mikov, 2018). Bile acid synthesis can take place via 2 different pathways, classical or alternative with the former accounting for 90% of bile acid synthesis (Šarenac and Mikov, 2018, Grant and

DeMorrow, 2020). Conversion of cholesterol into the primary bile acids occurs via a specific family of cytochrome P450 enzymes (Grant and DeMorrow, 2020). Pathways are initiated by specific CYPs, with CYP7A1 initiating the classical pathways, resulting in the formation of CA and CDCA, and the alternative pathway being initiated by CYP27A1 (Chiang, 2013). CA and CDCA undergo dihydroxylation by gut bacteria to form secondary bile acids deoxycholic acid (DCA) and lithocholic acid (LCA), with the majority of LCA excreted (Monte et al., 2009, Chiang, 2013). A small amount, approximately 3%, of UDCA exists endogenously in humans and is the 7 β epimer of CDCA (Lazaridis et al., 2001). Before release from the liver, CA and CDCA undergo conjugation with either glycine or taurine (at a 3:1 ratio) allowing for increased water solubility and reduced cytotoxicity, aiding in bile acid ability to solubilise dietary fats (Chiang, 2013, Grant and DeMorrow, 2020). The conjugation of bile acids means that a vast range of bile acid derivatives are created, including, but not limited to, taurocholic acid (TCA), tauroursodeoxycholic acid (TUDCA) and glycocholic acid (GCA) (Nagana Gowda et al., 2009, Ackerman and Gerhard, 2016).

1.5.1 Historical Uses

Animal bile has been used for over 2500 years in Chinese medicine (Wang and Carey, 2014) for the treatment of colds, swelling and liver diseases, such as primary biliary cirrhosis (Li et al., 2016). In the 1950s, pharmaceutical company Tokyo Tanabe produced UDCA for use as a liver tonic (Hofmann and Hagey, 2014) and by the 1970s, it was discovered that UDCA was able to dissolve gallstones without causing hepatotoxicity, replacing CDCA as the primary treatment (Okumura et al., 1977, Hofmann and Hagey, 2014). UDCA has since become a popular treatment in the management of cholestatic liver disease (Kumar and Tandon, 2001), however, recently there is an emerging role developing for the use of bile acids, particularly UDCA, as potential treatments for neurodegenerative diseases.

1.5.2 Bile Acids and Neurodegenerative Disease

There is a growing body of evidence to suggest that UDCA and its taurine conjugate TUDCA may have beneficial effects for the treatment of neurodegenerative diseases, including PD. A major difficulty in uncovering therapies for neurodegenerative disease is assessing a compounds ability to cross the BBB. The BBB is a tightly regulated layer consisting of cerebral endothelial cells that have formed tight junctions with adjacent cells and their proteins, namely occludin and claudin-5 (Quinn et al., 2014). Only when these tight junctions are compromised via a specific pathway or occludin and claudin-5 phosphorylation, are molecules able to diffuse freely across (Quinn et al., 2014). It has been illustrated numerous times that bile acids are involved in the pathogenic breakdown of the BBB during liver disease (Livingstone et al., 1977, Quinn et al., 2014, McMillin et al., 2016) and similarly,

administration of bile salts to rats was also found to cause disruption to the BBB (Greenwood et al., 1991). Bile acids have been described in the brains of both human and rats (Mano et al., 2004, Zheng et al., 2016, Pan et al., 2017) and it is likely that unconjugated bile acids, such as CA and CDCA, are able to cross into the brain via passive diffusion through the BBB, whereas conjugated bile acids are larger and negatively charged, thus require the help of transporters such as the bile salt export pump to enter the brain (Kiryama and Nochi, 2019).

Concentrations of endogenous bile acids have been suggested as a biomarker for AD. A recent study using plasma from 30 healthy individuals, 20 patients with mild cognitive impairment (MCI) and 30 patients with AD revealed that LCA was significantly increased in AD compared to controls, with a number of glycine conjugated bile acids also increased in AD compared to those with MCI (Marksteiner et al., 2018). Pathogenically, the relevance of these findings are unknown, however like many other neurodegenerative diseases, AD lacks reliable biomarkers, therefore the presence of altered levels of bile acids may propose a novel biomarker (Grant and DeMorrow, 2020).

Relevant to PD is the early involvement of constipation, highlighting a role for gastrointestinal upset early in disease. Furthermore, aggregated alpha synuclein has been described in the gastrointestinal tract of PD patients, particularly within the appendix and interestingly, some epidemiological studies have identified a link to suggest that removal of the appendix confers a decreased risk to PD (Li et al., 2021). A recent study identified alterations in the gut microbiota of the appendix in PD patients along with increases in secondary bile acids LCA and DCA in the ileum and impaired bile acid reuptake via decreases in fatty acid binding protein 6 (FABP6). It has been suggested that these alterations could lead to peripheral inflammation as well as alpha synuclein aggregation (Li et al., 2021). Moreover, studies using human plasma have yielded similar results, identifying increases in the level of unconjugated bile acids (CA, DCA and LCA) in individuals with both sporadic and familial PD (Yakhine-Diop et al., 2020). With more robust research, it is possible that analysis of plasma, the gut microbiome and bile acid pool could be used as biomarkers for PD.

Furthermore, mouse models of PD have highlighted potential dysregulation in taurine and hypotaurine metabolism, bile acid synthesis, the citric acid cycle and glycine, serine and threonine metabolism following injection with human alpha synuclein fibrils (Graham et al., 2018b, Grant and DeMorrow, 2020). They postulated that the dysregulation, particularly with taurine metabolism and bile acid synthesis, may point to the brain increasing the production of secondary bile acids in response to alpha synuclein aggregation and neurotoxicity, corroborating the finding of increased secondary bile acids in the ileum referred to previously

(Graham et al., 2018b, Li et al., 2021). Furthermore, the same group were also able to distinguish between prodromal and control mice via the downregulation in UDCA and TUDCA concentrations in the prodromal mice, again highlighting a potential new biomarker that could translate to human PD (Graham et al., 2018a).

1.5.3 Bile Acids as Treatments for Neurodegenerative Diseases

Bile acid therapy represents a novel treatment approach for neurodegenerative diseases and research has already begun to elucidate whether there is a beneficial treatment effect. Daily injections with CDCA administered to an aluminium chloride rat model of AD illustrated a rescue effect in cognitive and spatial defects to near control levels, alongside decreased amyloid beta₄₂ production in the hippocampus (Bazzari et al., 2019). Furthermore, treatment of sporadic and familial AD patient fibroblasts with UDCA resulted in an increase in MMP as well as changes in mitochondrial morphology in the form of reduced mitochondrial number, likely through a Drp1 related mechanism (Bell et al., 2018). This highlights the potential therapeutic effect of bile acids in the treatment of AD.

Bile acid treatment has already been trialled in humans suffering with amyotrophic lateral sclerosis (ALS). A phase II clinical trial was undertaken in the form of a 54-week trial in which 34 ALS patients began taking TUDCA as an add-on therapy in association with riluzole. Results suggested that the therapy was well tolerated, with only mild gastrointestinal complaints reported, as well as potential neuroprotective effects detected via a 15% increase in the ALS functioning scale and slowed deterioration (Elia et al., 2016, Grant and DeMorrow, 2020). Following this, a phase III clinical trial is currently underway to assess the safety and efficacy of TUDCA add-on therapy in a larger cohort of 440 patients, with the study expected to complete in December 2022, clinical trial identifier: NCT03800524 (Sever et al., 2022). In June 2022, Health Canada approved ALBRIOZA for the treatment of ALS, the first drug approved for ALS treatment since 2018. Briefly, ALBRIOZA is a combination of sodium phenylbutyrate and TUDCA which have been found to reduce neuronal cell death through regulation of endoplasmic reticulum stress and mitochondrial dysfunction (Paganoni et al., 2021). The recent CENTAUR trial was a randomised double-blind, placebo controlled study that met its primary end point of slowing decline on the ALS functional rating scale, however although approved by the Canadian board, it is yet to be approved by the United States Food and Drug Administration (US FDA) or the UK and European Medicines Agency. Research with alternative bile acids has also been undertaken *in vitro*. For example, the effects of GUDCA treatment was investigated using motor neurone-like cells NSC-34, expressing either wild type or mutant superoxidase dismutase 1 (SOD1). GUDCA treatment was found to decrease caspase 9 levels, consequently decreasing apoptotic nuclei present

within the cells. There was also found to be a decrease in oxidative stress and neuroinflammatory markers, however no effect was noted on levels of ATP (Vaz et al., 2015, Grant and DeMorrow, 2020).

In PD research, an MPTP mouse model was treated with TUDCA prior to and following MPTP exposure and found that motor capabilities and the ability to initiate movements were improved in the MPTP+TUDCA group compared to the MPTP only group (Rosa et al., 2018). Previously in our group, a drug re-purposing study was undertaken that identified bile acids, particularly UDCA, as having mitochondrial rescue effects in a number of different PD models (Mortiboys et al., 2013, Mortiboys et al., 2015, Carling et al., 2020). The process of the drug screen will be discussed in chapter 3, however the paper published in 2015 detailed a similar reduction in ATP across both manifesting and non-manifesting *LRRK2* PD patient fibroblasts, but interestingly discovered that while *parkin* mutant cells possess mitochondrial complex I deficiencies, mimicking the effects seen after MPTP exposure (Schapira et al., 1990), a complex IV deficiency was observed in *LRRK2*^{G2019S} mutant patient fibroblasts (Mortiboys et al., 2015). Furthermore, a functional mitochondrial rescue effect was observed following UDCA treatment in both manifesting and non-manifesting *LRRK2* PD patient fibroblasts, as well as a rescue effect on visual function in *drosophila* harbouring the *LRRK2*^{G2019S} mutation (Mortiboys et al., 2015). This research provided the basis for the clinical trial discussed in section 1.1.3 that has now been completed (Payne et al., 2020).

1.5.4 Possible Mechanism of Action of UDCA

The full mechanism of action of UDCA for the treatment of PD has not yet been elucidated, however theories have been postulated.

Following the 2015 paper by Mortiboys et al that uncovered beneficial effects of UDCA on both *Parkin* and *LRRK2* mediated PD, it is clear that UDCA is functioning through either a complex I or complex IV mediated mechanism (Mortiboys et al., 2015).

In 2012, the human dopaminergic cell line SH-SY5Y was used to investigate the effect of pre-treatment with UDCA on cellular cytotoxicity, following treatment with potent neurotoxin sodium nitroprusside (Chun and Low, 2012). UDCA rescued cell viability with evidence suggesting it was acting by decreasing apoptosis rate through the increase of the Bcl2/Bax ratio. Briefly, the apoptotic cascade is a highly regulated form of programmed cell death controlled by pro- and anti- apoptotic proteins of the Bcl-2 family (Elmore, 2007). There are two pathways of apoptosis, extrinsic and intrinsic. The intrinsic pathway involves the mitochondria and can be activated by Bax which usually resides in the cytoplasm. However, upon apoptosis activation, Bax is able to translocate to the OMM where it forms oligomers,

causing a loss of MMP and culminating in the release of cytochrome C (Antonsson, 2001). At this point cellular recovery is impossible and the cell dies. Further investigations on UDCA and the apoptotic pathways were undertaken using specific inhibitors, however the data proved inconclusive (Chun and Low, 2012).

Further work using a rotenone rat model of PD discovered that rotenone treatment increased mRNA expression levels of pro-apoptotic factors Bax and caspase 9 and decreased anti-apoptotic protein Bcl-2. These effects were significantly reversed with UDCA treatment (Abdelkader et al., 2016).

The full mechanism of action is yet to be elucidated; however, research currently suggests that the apoptotic pathways may play a key role. However, it should be noted that the concentration of UDCA used in studies appears to differ. In the current study, as well as the study by Mortiboys et al, 2015, UDCA was added to cells at a concentration of 10nM (Mortiboys et al., 2015), whereas Chun and Low, 2012, using SH-SY5Y cells utilised UDCA at a concentration of 50µM to 200µM (Chun and Low, 2012). Furthermore, dosing of animal models with UDCA has also differed, with the study mentioned above dosing at 50mg/kg (Abdelkader et al., 2016) while a previous PhD linked to this project dosed mice with 12mg/kg, 30mg/kg and 50mg/kg. It is possible that UDCA does not exert its effect via one mechanism alone, rather via a number of mechanisms and also in a dose dependent manner.

1.5.5 Possible Mechanism of Action of TUDCA

TUDCA, the taurine conjugate of UDCA, has also shown potential benefit in the treatment of neurodegenerative diseases. It is currently approved by the US FDA for the treatment of cholestatic liver disease (Rosa et al., 2017). The effects of TUDCA in PD models have been investigated both *in vivo* and *in vitro* with the emphasis being on oxidative stress and cell death pathways.

A 2012 study illustrated that pre-treatment with TUDCA prior to MPTP infusion in mice resulted in a 30% decrease in TH positive cells, compared to a 65% decrease in controls. The authors suggested the protective effect was due to TUDCA negatively modulating the c-Jun N-terminal kinase (JNK) pathway, decreasing ROS (Castro-Caldas et al., 2012b). JNKs are a type of mitogen-activated protein (MAP) kinase that phosphorylate serine or threonine residues on their target proteins and have been previously implicated in apoptosis, cell differentiation and cell survival (Peng and Andersen, 2003). The JNK pathway is activated upon recognition of cellular stress (Kim and Choi, 2015) including oxidative stress, seen in PD. Once activated, the JNK pathway can phosphorylate c-Jun which has downstream

effects on pro- and anti-apoptotic genes. Similarly, the JNK pathway can affect the mitochondria and result in direct phosphorylation of the Bcl-2 family of proteins, potentially resulting in apoptosis (Castro-Caldas et al., 2012a).

More recently, the same research group investigated the effects of TUDCA in both SH-SY5Y cells and a mouse model of PD. They were able to characterise the ability of TUDCA to activate the nuclear factor erythroid 2 related factor 2 (Nrf2) pathway (Moreira et al., 2017). Nrf2 is usually repressed in the cytoplasm by kelch-like ECH-associated protein 1 (Keap1) however under conditions of oxidative stress, Keap1 dissociates from Nrf2, causing its translocation to the nucleus and binding to target antioxidant response elements. Antioxidant genes are consequently transcribed and translated, releasing antioxidants into the cell to tackle the increasing oxidative burden (Pistollato et al., 2017). Treatment with TUDCA prior to MPP+ exposure resulted in increased translocation of Nrf2 to the nucleus and consequently increased antioxidant production (Moreira et al., 2017).

Similarly to UDCA, it is likely that TUDCA may exert its effect via multiple mechanisms, many of which haven't yet been identified.

Alternative mechanisms of UDCA/TUDCA action have also been suggested. Firstly, the autotaxin-lysophosphatidic (ATX-LPA) pathway. Briefly, ATX is a glycoprotein that produces LPA, a bioactive lipid acting as a ligand at LPA receptors resulting in activation of several signalling pathways (Keune et al., 2016, Salgado-Polo et al., 2018). UDCA and TUDCA have been shown to bind to an allosteric binding pocket on ATX resulting in modulation of the ATX-LPA pathway (Keune et al., 2016), however the significance of this has not yet been investigated in PD.

Secondly, multiple studies have described TUDCA to function via the Akt pathway in a number of different models of neurodegeneration, namely traumatic brain injury (Sun et al., 2017a), acute haemorrhagic stroke (Rodrigues et al., 2003) and PD (Castro-Caldas et al., 2012b). Akt is an intermediary that is able to phosphorylate a number of substrates leading to downstream regulation of survival, proliferation, metabolism and growth (Manning and Toker, 2017). TUDCA is thought to activate the Akt pro-survival pathway via the regulation of its downstream effectors such as pro-apoptotic factor Bad (Castro-Caldas et al., 2012b). Bad is known to bind to anti-apoptotic factors Bcl-2 and Bcl-x_L causing their inactivation. However, TUDCA appears to phosphorylate Bad, disrupting its ability to bind the anti-apoptotic factors, hence promoting cellular survival (Rodrigues et al., 2003).

Finally, both UDCA and TUDCA have been linked with glucocorticoid receptor function. Briefly, glucocorticoids are steroid hormones secreted by the adrenal glands and their receptors are found in almost all tissues of the human body (Nicolaidis NC, 2020). Evidence

suggests that UDCA and TUDCA bind to glucocorticoid receptors at an alternative ligand binding domain (Sharma et al., 2011), causing dissociation from its cytosolic chaperone, heat shock protein 90 (Hsp90), allowing for translocation to the nucleus where it is able to modulate apoptotic processes (Solá et al., 2005, Solá et al., 2006).

1.6 Project Background

This section has been redacted by the author for commercial reasons.

This section has been redacted by the author for commercial reasons.

This section has been redacted by the author for commercial reasons.

This section has been redacted by the author for commercial reasons.

This section has been redacted by the author for commercial reasons.

1.7 Aims and Objectives

The aim of this project was to identify the mechanism of action of a novel therapeutic compound, Jed135, in patient derived induced dopaminergic neurones. Throughout the course of the project we compared Jed135 to UDCA, a compound with known mitochondrial rescue effects. In order to do this, we identified four main objectives which form the basis of the results chapters for this thesis.

1. To characterise the iNPC and induced dopaminergic model by investigating ATP levels, pan neuronal and dopaminergic markers and understand basal mitochondrial phenotypes
2. To investigate mechanisms relevant to PD in the form of alpha synuclein expression and mitophagy and to study the effects that Jed135 may have on this
3. To knockdown the putative targets of Jed135 and assess any changes in drug effect
4. To assess the effect of Jed135 on an *in vivo Drosophila* model of PD

1.8 Project Hypothesis

We hypothesise that novel small molecules, in this instance Jed135, can restore neuronal health in a cellular model of sporadic PD via multiple mitochondrial targeted mechanisms. Furthermore, we hypothesise that Jed135 will be able to rescue a reduced crawling speed of *Parkin* mutant *Drosophila* larvae.

2 Materials and Methods

2.1 Ethics

Ethics approval was gained from the National Health Service National Research Ethics Service (approval number 12/YH0367). The alpha synuclein mutant and control 3 lines were sourced from NINDS Cell Repository via MTA (<https://stemcells.nindsgenetics.org/>)

2.2 Participant Characteristics

Skin biopsies were collected from two sporadic PD patients (53.5 ± 3.5 years), one alpha synuclein triplication mutant (55 years) and three neurologically normal controls (56 ± 1.7 years) with full informed consent, **table 2.1**. Sporadic PD fibroblasts and their controls were set up at the University of Sheffield while the alpha synuclein mutant and its control were bought from the NINDS human cell and data repository.

Table 2.1 Details of Fibroblast Lines Used for Reprogramming into iNPCs

Sample	Type	Sex	Age at Biopsy (Years)
sPD1 (OB182)	Sporadic PD	F	51
sPD2 (OB209)	Sporadic PD	F	56
Alpha Synuclein Mutant (ND27760)	SNCA Triplication	F	55
Control 1 (OB248)	Control	M	55
Control 2 (OB247)	Control	M	58
Control 3 (ND29510)	Control	F	55

2.3 Cell Culture

2.3.1 Cell Culture of Fibroblasts

A 2mm skin biopsy was taken from the forearm of the donor and fibroblast monolayers were cultured in Eagles minimum essential fibroblast media (EMEM) (Lonza) supplemented with 10% foetal bovine serum (FBS) (Biosera), 50mg/ml uridine (Sigma), 1% sodium pyruvate (Sigma), 1% non-essential amino acids (Lonza) and 1% minimum essential medium (MEM) vitamins (Lonza). These were incubated at 37°C, supplemented with 5% CO₂. Cells were routinely tested for mycoplasma and treated with ciprofloxacin if necessary. This was carried out by Dr Philippa Carling prior to the start of this project.

2.3.2 Generation of Induced Neuronal Progenitor Cells

iNPCs were generated prior to the start of this project by Professor Heather Mortiboys in accordance with a previous published protocol (Meyer et al., 2014). Briefly, fibroblasts were transduced using the Oct3/4, Sox2, Klf4, Lin28 and Nanog viruses for 48 hours. Following this, cells were maintained in Dulbeccos modified eagle medium (DMEM)/nutrient mixture F12 glutamax with 1% N2 (Gibco), 1% B27 (Gibco), 20ng/ml epidermal growth factor (EGF) and 20ng/ml fibroblast growth factor 2 (FGF2) until the cell morphology changed.

2.3.3 Cell Culture of iNPCs

iNPCs were maintained in DMEM/F12 glutamax, supplemented with 1% N2, 1% B27, 1% penicillin/streptomycin (Lonza) and 40ng/ml basic fibroblast growth factor (FGF basic) (Peprotech). Cells were split twice per week until passage 20 by incubating with accutase (Sigma) to detach, before placing a small proportion into a fresh 10cm² dish, coated for 5-10 minutes with 1:200 fibronectin (Millipore) in PBS to aid with cell adherence. iNPCs were incubated at 37°C, supplemented with 5% CO₂.

For neurone differentiation, iNPCs were plated into a fibronectin coated 6 well plate at a density of 70,000-100,000 cells per well and differentiation started at approximately 80-90% confluency.

For ATP assays, iNPCs were plated at a density of 5000 cells per well into a fibronectin coated white, clear bottom 96 well plate (Greiner BioOne). ATP assays were carried out the day after plating.

2.3.4 Cell Culture of iNPC Derived Dopaminergic Neurones

iNPCs began the neurone differentiation protocol when they were 80-90% confluent. The standard differentiation protocol has been outlined in two previous papers (Carling et al., 2020, Schwartzenruber et al., 2020), however the protocol was slightly modified to optimise for each pair of lines used in this project.

Regardless of protocol stage, the base medium remained the same and cells were maintained in DMEM/F12 glutamax media supplemented with 1% N2, 2% B27 and 1% penicillin/streptomycin.

iNPCs were initially put into neuronal base media with 5µM N-[N-(3,5-difluorophenacetyl)-l-alanyl]-S-phenylglycine t-butyl ester (DAPT) for 48 hours to ensure a neuronal lineage. 2ml of DAPT media solution was added to each well and left for 48 hours.

During the second stage of the differentiation protocol, cells were incubated with neuronal base media with 16.5ng/ml fibroblast growth factor 8 (FGF8) (Peprotech) and 0.5µM

smoothened agonist (SAG) (Millipore). Media was refreshed every 24 hours from this point. This stage of the protocol lasted for 10 days, however sPD2 and control 2 were in this stage for 4 days due to cell death.

Following FGF8/SAG treatment, cells were re-plated into appropriate vessels. Cells were detached by incubating with accutase for 4-5 minutes before adding 500 μ l of PBS, placing cell suspension in a 15ml falcon tube and centrifuging for 4 minutes at 200rcf, brake speed 9.

For live assays and immunocytochemistry (ICC), cells were replated at a density of 10,000 cells per well (20,000 cells per well for sPD2), accounting for cell death, in black, clear bottom 96 well plates (Greiner BioOne). For Western blot and CL experiments, cells were replated at a density of 500,000 cells per well in a 6 well plate. For knockdown optimisation, cells were replated at a density of 250,000 cells per well in a 12 well plate. All plates were fibronectin coated.

For the following 15 days, or until cell morphology was altered causing a bundling of projections and cell bodies, cells were incubated with neuronal base media with 30ng/ml brain derived neurotrophic factor (BDNF) (Peprotech), 30ng/ml GDNF (Peprotech), 75ng/ml transforming growth factor beta (TGF β) (Peprotech), 2mM d-cyclic adenosine monophosphate (d-cAMP) (Sigma) and 1 μ g/ml ciprofloxacin (LKT Laboratories) to prevent contamination with mycoplasma.

2.4 Drug Treatment

Induced dopaminergic neurones were treated with the compounds of interest 24 hours prior to the end of differentiation. The concentrations chosen had previously been determined to show mitochondrial restorative properties in the same dopaminergic neurone lines (work completed by Camilla Boschian, Katy Barnes and Professor Heather Mortiboys).

Compounds were diluted in the media used in stage 3 of differentiation.

Neurones for live assays or fixing were treated under one of four conditions; untreated, vehicle treated using dimethyl sulfoxide (DMSO), 10nM Jed135 or 10nM UDCA.

Cells in 6 well plates for Western blots or CL experiments were treated under one of 2 conditions: untreated or 10nM Jed135.

2.5 siRNA Treatment

A subset of induced neurones were treated with siRNA oligonucleotides to knock down the putative targets. The optimisation process also included siRNA oligonucleotides against GAPDH and a scramble condition as controls. Once clone choices were verified, only a scramble condition was included in the live assays.

2.5.1 Optimisation

Initial optimisation used 4 different siRNA clones, along with control conditions of; media only, GAPDH housekeeping gene and scramble siRNA. 5x siRNA buffer (Dharmacon) was diluted 1:5 in RNase free water to create a 1x solution. Sequences for the siRNA clones chosen, along with GAPDH and non-targeting scramble, are in **table 2.2**. 50µl or 200µl of 1x siRNA buffer was added to 5nmol or 20nmol siRNA respectively to generate a 100uM stock, as per manufacturer's instructions. Solution was then subjected to gentle shaking for 90 minutes at room temperature, aliquoted and stored at -20°C until needed.

48 hours prior to the end of neuronal differentiation, siRNA stock solution was diluted to a working solution of 1µM in siRNA delivery media (Accell) and 300µl was added cells in 12 well plates. This was incubated for 24 hours at 37°C, supplemented with 5% CO₂ before being removed and replaced with normal dopaminergic neuronal media supplemented with BDNF, GDNF, TGFβ, d-cAMP and ciprofloxacin for a further 24 hours. Cells were then detached from the plate using accutase, centrifuged and pelleted as previously described in section 2.3.4. Supernatant was removed and pellets stored at -80°C until required.

Table 2.2 Primer Sequences of the siRNA Clones Taken Forward

siRNA	Sequence
GAPDH	GUGUGAACCAUGAGAAGUA
Non-targeting Scramble	UGGUUUACAUGUCGACUAA
Target A	Redacted
Target B	Redacted

2.5.2 RNA Extraction

In order to assess the knockdown effect of the target A and B siRNA oligonucleotides, firstly, RNA extraction was performed using the Qiagen RNeasy mini-kit. Protocol was performed as per manufacturer's instructions. Briefly, 350µl of RLT was added and samples vortexed for 30 seconds. 350µl of 70% ethanol was added, pellets re-suspended and solution transferred into an RNeasy spin column with 2ml collection tube and centrifuged at 8000g for 15 seconds. Flow through was discarded and 700µl of RW1 buffer added and solution centrifuged for 15 seconds at 8000g. Flow through was discarded and 500µl of RPE buffer added. Solution was centrifuged for 2 minutes at 8000g. 30µl of RNase free water was added and centrifuged for 1 minute at 8000g, this was repeated. The RNeasy spin column was discarded. RNA content was measured using the Nanodrop spectrophotometer (Thermo Scientific) and samples frozen at -80°C until required.

2.5.3 Complementary DNA (cDNA) Synthesis

Following RNA extraction, cDNA was synthesised using the QuantiTect Reverse Transcription Kit (Qiagen), following manufacturer's protocol. Genomic DNA elimination reaction was undertaken using 7x gDNA wipe out buffer and RNase free water provided, along with the template RNA extracted previously and incubated for 2 minutes at 42°C, **table 2.3**. The reverse transcription master mix was made, **table 2.4**, and incubated for 15 minutes at 42°C before being incubated for 3 minutes at 95°C to inactivate the reverse transcriptase. This was then used for the qPCR reaction.

Table 2.3 Reagents for Genomic DNA Elimination

Component	Volume/Concentration
gDNA Wipeout Buffer	2µl of 7x Buffer
Template RNA	Variable up to 1µg
RNase free water	Variable – make up to a final volume of 14µl

Table 2.4 Reagents for Reverse Transcription Master Mix

Component	Volume/Concentration
Quantiscript Reverse Transcriptase	1 μ l
Quantiscript RT Buffer	4 μ l of 5x buffer
RT Primer Mix	1 μ l
Genomic DNA Elimination Reaction	14 μ l

2.6 qPCR

For qPCR, the QuantiTect SYBR green PCR kit (Qiagen) was used and the manufacturer's protocol was followed. The reaction mix was prepared, **table 2.5**, and primers of interest added as appropriate, sequences and concentrations in **table 2.6**, including GAPDH as a house keeping protein. Where possible, samples were plated in duplicate or triplicate. qPCR was undertaken using a CFX Connect qPCR machine (BioRad) and the following cycle was programmed; PCR initial activation step, 15 minutes at 95°C, denaturation, 15 seconds at 94°C, annealing, 30 seconds at 55°C and extension, 30 seconds at 72°C. This cycle was repeated 45 times.

Table 2.5 Reagents for SYBR Green Reaction Master Mix

Component	Volume/Concentration	Final Concentration
QuantiTect SYBR Green PCR Master Mix	25 μ l of 2x solution	1x
Primer A	Variable	0.3 μ M or 1 μ M
Primer B	Variable	0.3 μ M or 1 μ M
Template DNA or cDNA	Variable	<500ng/reaction
RNase Free Water	Variable	

Table 2.6 Forward and Reverse Primer Sequences Used

This table has been redacted by the author for commercial reasons.

2.6.1 Analysis

Relative gene expression was calculated using the equation ' $2^{-\Delta\Delta CT}$ ' method, described previously in the literature (Winer et al., 1999, Livak and Schmittgen, 2001). Briefly, data was analysed with the use of Microsoft Excel and, where appropriate, an average CT value was determined for both the genes of interest and the GAPDH housekeeper. Delta CT was calculated by subtracting the CT value for the gene of interest from the GAPDH CT value. Delta delta CT was calculated by subtracting each delta CT value from the delta CT value of the media only control, resulting in this value becoming 0. The relative concentration was then generated using the following equation: ' 2^{-x} ' where x is the delta delta CT value. This caused the media only control value to become 1 and the other samples became relative to this.

2.7 ATP Assays

iNPCs were plated in clear bottom, white well 96 well plate at a density of 5000 cells per well and ATP assays were undertaken approximately 24 hours after plating. Cells were incubated under one of four conditions for 30 minutes; phenol red free MEM (Gibco) only, phenol red free MEM plus 1 μ M oligomycin (Sigma) (to inhibit OXPHOS), phenol red free MEM plus 50mM 2-deoxyglucose (2DG) (Sigma) (to inhibit glycolysis) or phenol red free MEM plus oligomycin and 2DG, 3 wells per condition.

Following inhibitor treatment, we used the ATPlite kit (Perkin Elmer) following supplier's protocol. Briefly, inhibitors were removed and wells washed with PBS. 100 μ l of PBS plus 50 μ l of lysis buffer were added to each well and shaken at 700rpm for 5 minutes at room temperature. 50 μ l of substrate solution was then added to each well and shaken for a further 5 minutes at 700rpm, room temperature. The plate was dark adapted for 10 minutes and the luminescence read on the PHERAstar plate reader (BMG Labtech).

A cell quantification analysis was carried out using the CyQuant Cell Proliferation Assay kit (Invitrogen). 2ml of CyQuant solution was made up by adding 400 μ l of Hanks balanced salt solution (HBSS), 1.6ml PBS and 2 μ l CyQuant and 50 μ l of this solution was added to each well. Plate was incubated for 1-3 hours at 37°C, supplemented with 5% CO₂, before measuring fluorescence on the PHERAstar plate reader (485nm excitation, 520nm emission).

Blank wells were included in the measurements by adding ATP reagents to wells that did not contain cells in order to generate a background reading.

2.7.1 Analysis

The average of the background reading was subtracted from the ATP and CyQuant values. Raw ATP data was normalised to the corresponding CyQuant values to control for cell number. The mean was then produced for each treatment condition and the graphs plotted using GraphPad Prism 8 (GraphPad software Inc.). To determine any ATP deficit, values for each repeat were normalised to their untreated control. The percentage by which each line was undergoing glycolysis or OXPHOS was determined by normalising the control values to the untreated controls and the patient values to the untreated patients for each repeat.

2.8 Immunocytochemistry

Following completion of the neurone differentiation protocol, cells in black 96 well plates were fixed by adding 4% paraformaldehyde (PFA) at a 1:1 ratio with neuronal media and incubated for 30 minutes at 37°C. PFA and neuronal media mix was removed and replaced with 4% PFA in PBS and incubated for a further 10-15 minutes at room temperature. PFA solution was removed, cells washed 3 times with PBS and stored in PBS until needed.

For ICC, cells were permeabilised using 0.1% TritonX in PBS-Tween20 (PBST) for 10 minutes and then put into blocking solution (5% horse serum in PBST) for at least 1 hour. Blocking solution was removed and replaced with blocking solution plus antibodies of interest, **table 2.7**, and incubated overnight at 4°C with gentle rocking. The following day, wells were washed 3 times, for at least 5 minutes, in PBST. They were then incubated in the dark with fluorescent secondary antibodies (AlexaFluor anti-rabbit 488 and 568, AlexaFluor anti-mouse 488 and 568 or AlexaFluor anti-chicken 488 (Invitrogen)) diluted 1:1000 in PBST, at room temperature for 1 hour.

Wells were washed 3 times in PBST and incubated for 2 minutes, at room temperature, with 20µM bisBenzimide (Hoechst) in PBST before a further 3 PBST washes. They were stored in PBS until imaging.

Dopaminergic neurones that had undergone ICC were imaged on the Opera Phenix High Content Screening System (Perkin Elmer) using the 40x water objective with at least 6 Z stacks per field of view and 17 fields of view per well. Fluorescent secondary antibodies were imaged using the following channels: AlexaFluor 488 (488nm excitation, 500-550nm emission), AlexaFluor 568 (561nm excitation, 570-630nm emission) and Hoechst using the DAPI channel (405nm excitation, 435-480nm emission).

Table 2.7 List of Primary Antibodies Used for Immunocytochemistry

Primary Antibody	Species	Dilution	Source	Catalogue Number
Beta III Tubulin (Tuj1)	Chicken	1:1000	Sigma Aldrich	AB9354
Tyrosine Hydroxylase (TH)	Rabbit	1:1000	Abcam	ab112
Microtubule Associated Protein 2 (MAP2)	Rabbit	1:1000	Abcam	ab32454
Dopamine Transporter (DAT)	Mouse	1:1000	Invitrogen	ma5-24796
PSD95	Rabbit	3µg/ml	Abcam	ab18258
Synaptophysin	Mouse	1:1000	Abcam	ab8049
Total Alpha Synuclein	Rabbit	1:1000	Sigma Aldrich	ab5038
Phosphorylated (Serine 129) Alpha Synuclein	Rabbit	1:250	Abcam	ab51253
ATP5a	Mouse	1:1000	Abcam	ab14748
Alpha Synuclein Filament	Rabbit	1:1000	Abcam	ab209538
Mitochondrial Import Receptor Subunit (TOM20)	Mouse	1:1000	BD Transduction Laboratories	612278
Microtubule associated proteins 1A/1B light chain 3B (LC3)	Rabbit	1:1000	MBL International	PM036

2.9 Western Blotting

Neurones grown in 6 well plates were harvested for pellets using accutase and centrifuged for 4 minutes at 200rcf, brake speed 9.

Following splitting of iNPCs, remaining cells were also pelleted for Western blotting. In both cases, supernatant was removed and pellets frozen at -80°C until required.

2.9.1 Protein Quantification

Each cell pellet was lysed in 50µl of radioimmunoprecipitation assay (RIPA) buffer (Sigma), 5µl of 10x protease inhibitor cocktail (Sigma) and 5µl phosphatase inhibitor cocktail (Sigma) and incubated on ice for 30 minutes. Samples were then centrifuged for 10 minutes at 16,000g and supernatant transferred into a 1.5ml Eppendorf. A Bradford assay was undertaken to determine the protein concentration of the samples. 5µl of dH₂O and bovine serum albumin (BSA) standards (100, 125, 250, 500, 750, 1000, 1200 µg/ml) were plated in triplicate into a clear 96 well plate. Samples were diluted 1:4 in distilled water and 2µl was added in triplicate to the 96 well plate. 250µl of Coomassie blue was added to each well and absorbance was then read at 595nm on the PHERAstar plate reader.

Using GraphPad Prism, a standard curve was created and unknown values interpolated. Using an excel template, the volume needed for 20µg of protein was calculated. Samples were boiled at 95°C for 5 minutes following the addition of 10µl of 4X sample buffer, **table 2.8**. After cooling, samples were aliquoted into 20µg aliquots and stored at -80°C until needed.

Table 2.8 Sample Buffer Reagents

Reagent	Amount	Source
Tris HCl	0.62g	Melford
Glycerol	8ml	Sigma
Sodium Dodecyl Sulphate (SDS)	1.8g	Fisher Chemical
Bromophenol Blue	0.008g	Sigma
Dithiothretiol (DTT)	0.8g	Sigma
2-mercaptoethanol	10ml	Gibco

2.9.2 *Gel Electrophoresis*

All Western blotting equipment was supplied by BioRad.

Gel Preparation

Prior to the Covid19 pandemic, gels were hand poured following the method outlined below. However, due to building restrictions and subsequent time pressures, during the period that followed the lockdowns, 12% pre-cast gels (BioRad) were used.

In order to prepare the gels, glass plates were first cleaned and assembled into the gel casting apparatus. A 12% resolving gel was made using the reagents in **table 2.9** and poured between the glass plates. A layer of isopropanol was added to prevent bubble formation and the gel was left to polymerise for 20-30 minutes. The isopropanol layer was then poured off. A 10% stacking gel was made using the reagents in **table 2.10** and poured between the glass plates, on top of the resolving gel. A 1cm comb was placed into the stacking gel before it set to create 10 wells. The stacking gel was left to polymerise for 20-30 minutes.

While the gels were setting, samples and the BioRad Precision Plus Dual Colour Standards Ladder were thawed on ice.

Once set, gels were removed from the casting apparatus, combs removed and placed into the mini-PROTEAN tetra vertical electrophoresis cell tank. 20µg of protein was loaded for each sample, along with 5µl of the standards ladder and the tank was filled to the appropriate level with SDS-PAGE running buffer, **table 2.11**. The tank as connected to the PowerPac basic power supply and run at a constant voltage of 50V for 30 minutes followed by 120V for 60-90 minutes.

Transfer

A wet transfer method was used to transfer the proteins from the gel onto poly-vinylidene difluoride membrane (PVDF). Briefly, PVDF membrane was pre-soaked in methanol while 1x transfer buffer was prepared (200ml 5x transfer buffer, **table 2.12**, 100ml methanol (Merck), 700ml dH₂O). The gel holder assembly was removed from the running buffer which was then discarded. Transfer cassette, foam pads and filter paper were pre-soaked in transfer buffer, with the black side of the cassette at the bottom with a foam pad and piece of filter paper resting on top. Glass plates were carefully taken apart to expose the gel, stacking gel removed and resolving gel placed onto the prepared transfer cassette. PVDF membrane was placed on top, followed by filter paper and foam pad, ensuring all air bubbles were rolled out. The cassette was closed and placed into the mini trans-blot central core and back into

the cell tank. Transfer buffer and ice pack were added and the transfer was run at a constant 250mAmps for 60 minutes.

Table 2.9 Reagents for 12% Resolving Gel

Reagent	Amount	Source
30% Acrylamide	4ml	National Diagnostics
1.5M Tris HCl pH 8.8	2.5ml	Melford
Nanopure Water	3.3ml	
10% Sodium Dodecyl Sulphate (SDS)	100µl	Fisher Chemical
Tetramethylethylenediamine (TEMED)	4µl	Melford
10% Ammonium Persulphate (APS)	100µl	Sigma

Table 2.10 Reagents for 10% Stacking Gel

Reagent	Amount	Source
30% Acrylamide	500µl	National Diagnostics
1.5M Tris HCl pH 6.8	380µl	Melford
Nanopure Water	2.1ml	
TEMED	5µl	Melford
10% APS	20µl	Sigma

Table 2.11 Reagents for SDS-PAGE Running Buffer

Reagent	Amount	Source
Tris Base	30g	Melford
Glycine	144g	Sigma
SDS	10g	Fisher Scientific
Nanopure dH ₂ O	Make up to 10 litres	

Table 2.12 Reagents for 5x Transfer Buffer

Reagent	Amount	Source
Tris Base	150g	Melford
Glycine	720g	Sigma
Nanopure dH ₂ O	Make up to 10 litres	

Fixing and Blocking

Membranes were removed from the transfer cassette and in most cases, incubated with blocking buffer straight away. However, when blotting for total alpha synuclein, membranes were fixed in 4% PFA for 30 minutes prior to blocking. Alpha synuclein is a small and extremely labile protein that does not transfer well onto membranes. It was found that a fixation step, prior to blocking, increases the detection of endogenous alpha synuclein (Lee and Kamitani, 2011).

In all instances, membranes were blocked in 5% non-fat dry milk dissolved in Tris-buffered saline with tween20 (TBST), **table 2.13** for at least 60 minutes at room temperature.

Table 2.13 Reagents for TBST

Reagent	Amount	Source
Tris Base	30g	Melford
Sodium Chloride	80g	Fisher Scientific
Potassium Chloride	2g	Fisher Scientific
Nanopure dH ₂ O	Made up to 10 litres	
Tween20	5ml	Sigma Aldrich

Antibodies

Membranes were incubated over night at 4°C with antibodies against proteins of interest diluted in TBST, **table 2.14**.

The following day, membranes were washed for 3 x10 minutes in TBST before being incubated with the appropriate horseradish peroxidase (HRP) conjugated secondary

antibody, **table 2.14**, diluted in TBST for one hour at room temperature. Membranes were then washed again for 3 x10 minutes.

Before imaging, membranes were incubated in 2ml of chemiluminescence solution (EZ-ECL HRP Kit, Biological Industries) and then imaged on the G-Box (Syngene) using intelli-chemi mode to include the protein ladder to ensure the protein of interest was present at the correct molecular weight. Images then taken on classic sub-saturating mode to allow for quantification.

Following imaging, membranes were incubated with a primary antibody against a housekeeping protein at 4°C overnight. The process of washing, secondary antibody incubation and imaging was then repeated as previously explained.

Table 2.14 Primary and Secondary Antibodies Used for Western Blotting

Antibody	Species	Dilution	Incubation	Source	Catalogue Number
Tuj1	Chicken	1:1000	4°C Overnight	Millipore	AB9354
TH	Rabbit	1:200	4°C Overnight	Abcam	ab137869
Target A	Rabbit	1:2000	4°C Overnight	Redacted	Redacted
Total Alpha Synuclein	Rabbit	1:10000	4°C Overnight	Abcam	ab138501
GAPDH	Mouse	1:2000	4°C Overnight	Proteintech	60004-1
Anti-Chicken HRP Secondary	Goat	1:3000	Room Temperature, 1 Hour	Invitrogen	A16054
Anti-Rabbit HRP Secondary	Goat	1:5000	Room Temperature, 1 Hour	Dako	P0448
Anti-Mouse HRP Secondary	Goat	1:10000	Room Temperature, 1 Hour	Abcam	Ab97040

Densitometry

Densitometry was undertaken using the GeneTools software (version 4.3.9, Syngene). Rolling background correction was used for each sample lane when analysing. Raw values were exported to excel and the protein of interest was normalised to the GAPDH loading control for the corresponding lane. Values were then normalised against the control, untreated iNPC.

2.10 Mitophagy Assays

Two different mitophagy assays were performed to assess either basal mitophagy or induced mitophagy. Basal mitophagy was assessed via a live assay whereas induced mitophagy was assessed via ICC.

2.10.1 Live Basal Mitophagy Assay

Live mitophagy assays were completed as described previously (Schwartzentruber et al., 2020). Briefly, dyes were prepared by diluting 80nM tetramethylrhodamine methyl ester perchlorate (TMRM) (Invitrogen), 1 μ M lysotracker green (Invitrogen) and 2 μ M Hoechst (Sigma) in phenol free MEM. Cell culture medium was removed from the well and 100 μ l of dye solution added and plates incubated for 60 minutes at 37°C supplemented with 5% CO₂.

Following incubation, dyes were removed and replaced with 100 μ l phenol free MEM. Images were optimised on the Opera Phenix before capture, with intensity levels adjusted and corrected. Images were captured over a time course to include 12 time points using the 40x water objective with 4 z stacks and at least 10 fields of view. Opera Phenix settings allowed a temperature of 37°C to be set with 5% CO₂. TMRM was imaged on the Cy3 channel (561nm excitation, 570-630nm emission), lysotracker using AlexaFluor488 (488nm excitation, 500-550nm emission) and Hoechst using the DAPI channel (405nm excitation, 435-480nm emission).

Analysis

Analysis was completed using the Harmony 4.9 software (Perkin Elmer). A protocol was produced to segment nuclei, cytoplasm, image region, mitochondrial spots and lysosomal spots and investigated mitochondrial morphology and intensities of mitochondrial and lysosomal markers. In order to identify mitophagy events, a 100% colocalisation of the mitochondrial and lysosomal signal was identified; details of this and optimisation of the assay are detailed in a later chapter.

Parameters were graphed from at least 3 separate rounds of differentiation per line using GraphPad Prism 8.

2.10.2 Induced Mitophagy

Due to difficulties imaging so many wells per plate, induced mitophagy was quantified using a fixed assay instead.

On the final day of neuronal differentiation, cells were treated with 4 μ M antimycin A (Sigma) and 10 μ M oligomycin (Sigma) diluted in phenol red free MEM and incubated at 37°C supplemented with 5% CO₂ for 30 minutes. Cells were then fixed in 4% PFA as outlined

previously and stored until needed. ICC was also carried out as previously described using antibodies against LC3 to label autophagosomes and TOM20 to label mitochondria.

Plates were imaged on the Opera Phenix using the 40x water objective with at least 6 Z stacks and 17 fields of view per well.

Analysis

Data was analysed using Harmony version 4.9. The protocol investigated the same parameters as the basal mitophagy, and parameters were graphed and analysed in GraphPad Prism 8.

2.11 Mitochondrial Membrane Potential and Mitochondrial Reactive Oxygen Species (MitoROS)

MMP/MitoROS experiments were undertaken on dopaminergic neurones differentiated in black 96 well plates. NpFR2 probe was supplied by our collaborator Elizabeth New at the University of Sydney (Yeow et al., 2014, Kaur et al., 2015).

2.11.1 siRNA Treatment

48 hours prior to the end of neuronal differentiation, cells were treated with siRNA oligonucleotides targeted against either target A or target B singularly, target A and target B together, a scramble condition or a media only control. siRNA treatment lasted for 24 hours before media was removed and replaced with stage 3 neuronal differentiation media plus drug treatment (no treatment, vehicle, 10nM Jed135 or 10nM UDCA) for a further 24 hours.

2.11.2 MMP/MitoROS Live Assay

Media was removed and replaced with phenol free MEM with the addition of 100nM TMRM, 20µM NpFR2 (MitoROS) probe and 40µM Hoechst. This was incubated for 30 minutes at 37°C supplemented with 5% CO₂. Dye mix was then removed and replaced with phenol free MEM and imaged on the Opera Phenix using the 40x water objective. At least 20 fields of view were imaged per well with 6 Z stacks per field. TMRM was imaged using the Cy3 channel (561nm excitation, 570-630nm emission), NpFR2 using the FITC channel (488nm excitation, 500-550nm emission) and Hoechst using the DAPI channel (405nm excitation, 435-480nm emission). Temperature settings on the Opera Phenix were set to 37°C with 5% CO₂.

2.11.3 Analysis

Data was analysed using Harmony version 4.9. The protocol was set up to determine nuclei number, region of the image that contained cells, mitochondrial morphology and co-localisation of TMRM and MitoROS signal. This produced a spreadsheet and selected parameters were graphed using GraphPad Prism 8.

2.12 Confirming Knockdown Efficacy

In order to confirm the knockdown efficacy was as expected following optimisation, we used the Cells to CT (Invitrogen) kit enabling us to perform cell lysis in the 96 well plates. Primers against target A, target B and GAPDH were used as previously described.

2.12.1 Cell Lysis

Following the MMP/MitoROS assay, plate was removed from the Opera Phenix and 50µl of cold PBS added to each well to wash. Lysis solution was made using 50µl of lysis buffer and 0.5µl DNase per well, PBS removed, and lysis solution added. Wells aspirated 3-5 times, avoiding the creation of bubbles and left to incubate for 5 minutes at room temperature. 5µl of stop solution per well was then added directly to cell lysate to halt the lysis reaction, wells aspirated 5 times, avoiding the creation of bubbles, and left to incubate at room temperature for 2 minutes. Plates could be frozen at -80°C at this point, until needed.

2.12.2 Reverse Transcription

Reverse transcription master mix was made using 25µl of 2x SYBR RT buffer and 2.5µl of RT enzyme mix per well as supplied. This was distributed into a nuclease free multi-well plate. 27.5µl of cell lysate was added to each well with master mix, sealed and incubated on the thermal cycle at 42°C for 60 minutes followed by 5 minutes at 95°C to denature the enzyme.

2.12.3 Real Time qPCR

qPCR reaction master mix was made up according to **table 2.15**. 35µl of master mix was plated into a nuclease free multi-well plate and 15µl of cDNA added as appropriate, resulting in a final volume per well of 50µl. Plates were sealed and qPCR programme run as follows: 95°C for 15 minutes for 1 cycle only, followed by 94°C for 15 seconds, 60°C for 30 seconds and 72°C for 30 seconds. This was repeated for 44 cycles before being cooled to 65°C for 40 seconds.

Table 2.15 Reagents for qPCR Master Mix per Well

Reagent	Amount	Concentration
PowerSYBR Green PCR Master Mix	25µl	
Forward Primer	Variable	1µM
Reverse Primer	Variable	1µM
cDNA	15µl	
RNase Free Water	Variable	
Final Volume	50µl	

2.12.4 Analysis

Analysis was performed as described previously in section 2.6.1.

2.13 Cardiolipin

CL content was investigated using untreated and Jed135 treated dopaminergic neurone pellets that had been differentiated in 6 well tissue culture plates, detached and pelleted as previously described and stored at -80°C until needed.

The CL assay kit, purchased from BioVision, is able to specifically measure the amount of CL in a sample, not reacting with other phospholipids. It contains a proprietary fluorescent probe that, when in the presence of CL, fluoresces. It is directly linked to the amount of CL within a sample, the higher fluorescence output, the more CL present.

Assay was completed as per manufacturer's instructions. Briefly, kit components were thawed and reconstituted as per instructions. Cell pellets were resuspended in 1ml of CL assay buffer, transferred into Eppendorfs and rapidly freeze-thawed 3 times in liquid nitrogen. Samples were then centrifuged at 4°C for 10 minutes at 10,000g and supernatant transferred into a fresh Eppendorf. Protein concentration of each sample was determined using a Bradford assay as previously described in section 2.9.1, however in this instance, samples were not diluted, meaning 2µl of sample was directly plated in triplicate.

Absorbance was then read at 595nm on the PHERAstar plate reader. Initially, to optimise the assay, different volumes (5µl, 10µl and 20µl) of sample were plated for the CL assay. However, it was then decided that going forward, only 20µl of each sample would be plated.

For each sample, 20µl was plated in duplicate, one well for the experimental condition and one well for background control. 30µl of CL assay buffer was added to experimental condition wells and 80µl to the background control wells.

5mM CL standard was diluted 1:20 in CL assay buffer and known standards were plated (0, 0.5, 1.0, 1.5, 2.0, 2.5 and 3.0nM) and the volume of each well brought up to 50µl using CL assay buffer.

CL reaction mix was made up using 48µl of CL assay buffer and 2µl of CL probe per well and this was added to every well except the background control wells.

Plate was incubated at room temperature for 5-10 minutes before the fluorescence was read on the FLUOStar Omega plate reader (BMG Labtech), 340nm excitation, 480nm emission.

2.13.1 Analysis

Analysis was conducted as per manufacturers guidelines. Values from the 0 CL standard was subtracted from all readings, unless the sample background control was higher, in which case this value was subtracted from its corresponding experimental sample condition.

CL standard curve was generated, and unknowns interpolated. Concentration of CL in each sample was calculated using the following formula:

$$C = (B/V)*D \text{ nmol/ml}$$

where C = concentration of CL, B = amount of CL in the sample from standard curve (nmol), V = volume of sample added to the well (ml) and D = dilution factor.

Protein concentration per well was calculated from the Bradford assay results by creating a standard curve of the averages from the BSA standards and interpolating the averages from the unknown samples. Volume of sample needed to obtain 1mg of protein was calculated.

We were then able to calculate the CL content per mg of protein by dividing the value generated from the CL concentration per sample by the volume containing 1mg of protein. These values were then normalised to the untreated control neurone from each assay.

2.14 Opera Phenix Harmony 4.9 Image Analysis

All data collected via Opera Phenix imaging was analysed using the Harmony 4.9 software.

In all instances, Z stacks were combined to produce a maximum intensity projection and basic flat field correction was applied. Protocols were generated on an assay-by-assay basis depending upon what was being investigated however it was standard procedure to segment the nuclei. Due to limitations with the analysis software, portions of the cell that exist at a distance from the nuclei were difficult to segment, therefore both cytoplasm region and full image region were identified. In most cases, image region provided a better selection of the cells area than the cytoplasm building block, **figure 2.1**.

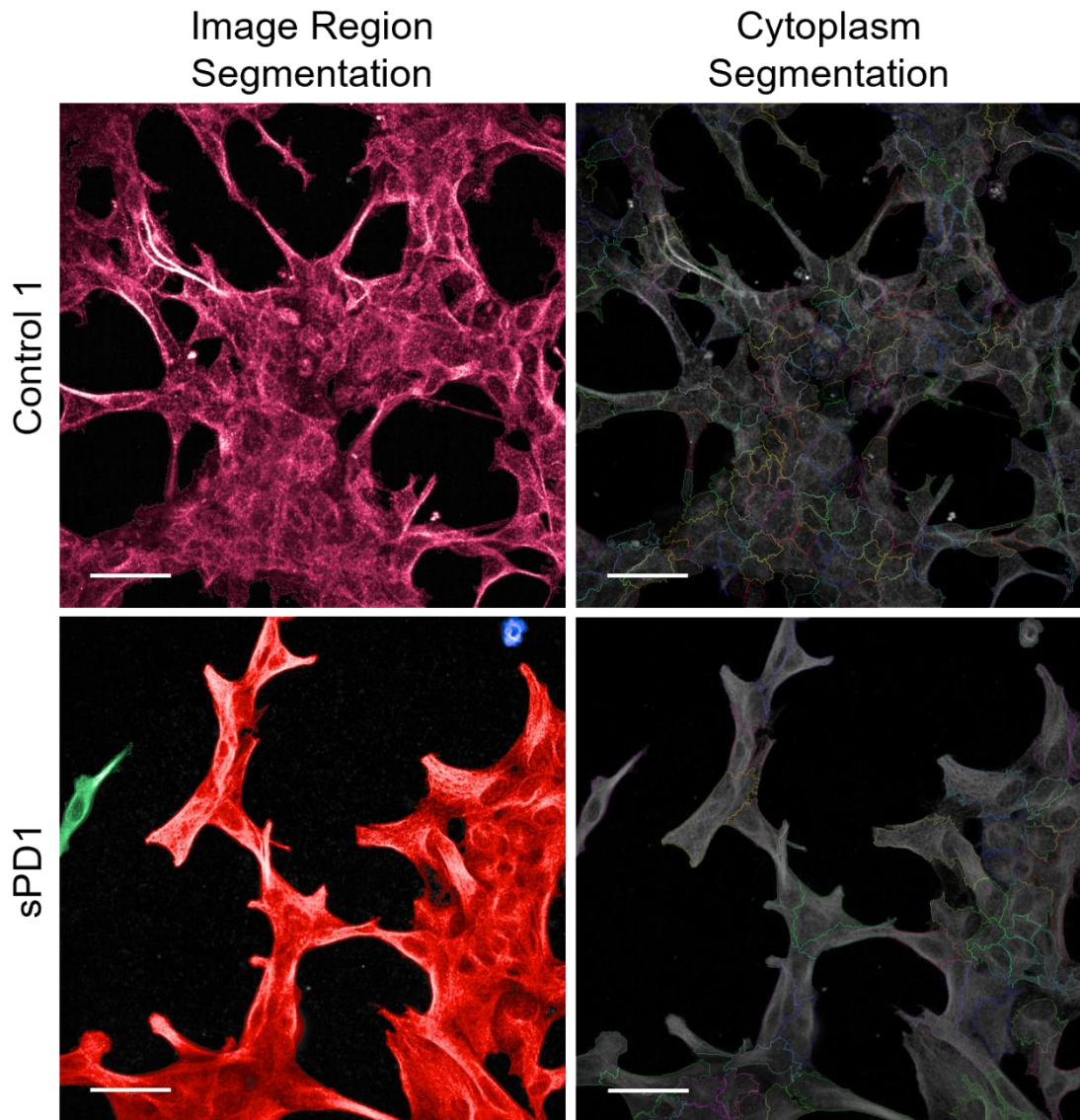


Figure 2.1 Image region and cytoplasm segmentation

Example images portraying image region segmentation (left) and cytoplasm segmentation (right), highlighting the differences between the two parameters, including how variable they can be between cell lines. Image region segmentation was able to highlight the whole area of the image covered by cells whereas the cytoplasm segmentation was unable to reliably outline the cell area consistently. Representative images taken from Tuj and TH immunocytochemistry; however the same phenomenon was true for all images captured on Opera Phenix, scale bar represents 50 μ M.

In cases where mitochondria were being investigated, texture settings using the SER edge or ridge features, **figure 2.2B**, followed by 'find spots', **figure 2.2C**, were applied in order to segment individual mitochondrion. Population was then further refined by using area and/or intensity settings to remove false positives and ensure a representative population were being selected, **figure 2.2D**.

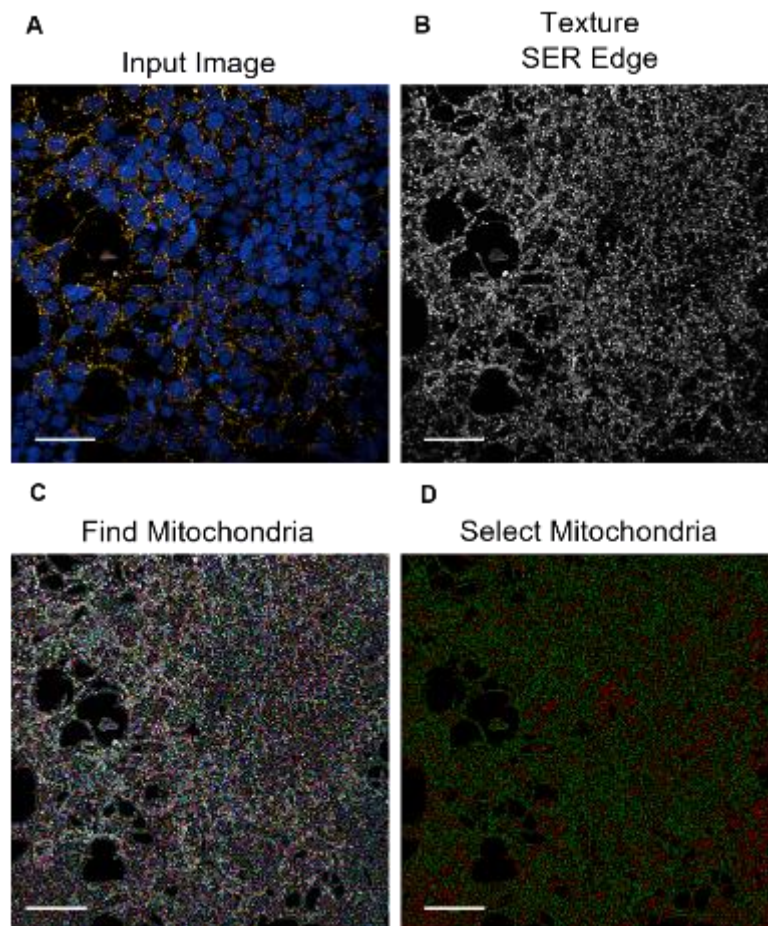


Figure 2.2 Representative images of mitochondrial segmentation

Representative images taken from control 1 ATP5a and alpha synuclein filament immunocytochemistry. The above images are only depicting the ATP5a stain. This method was employed for any assay that involved finding and segmenting mitochondria (A) input image (B) texture SER edge feature applied (C) finding mitochondria 'spots' (D) selecting the spots based on their area. Scale bar represents 50 μ M

When investigating neuronal markers, image regions of neuronal marker positive cell populations were identified by intensity. Maximum background intensity from a secondary only control was identified and those cell populations with intensity higher than the secondary only control maximum intensity were deemed neuronal marker positive, **figure 2.3**.

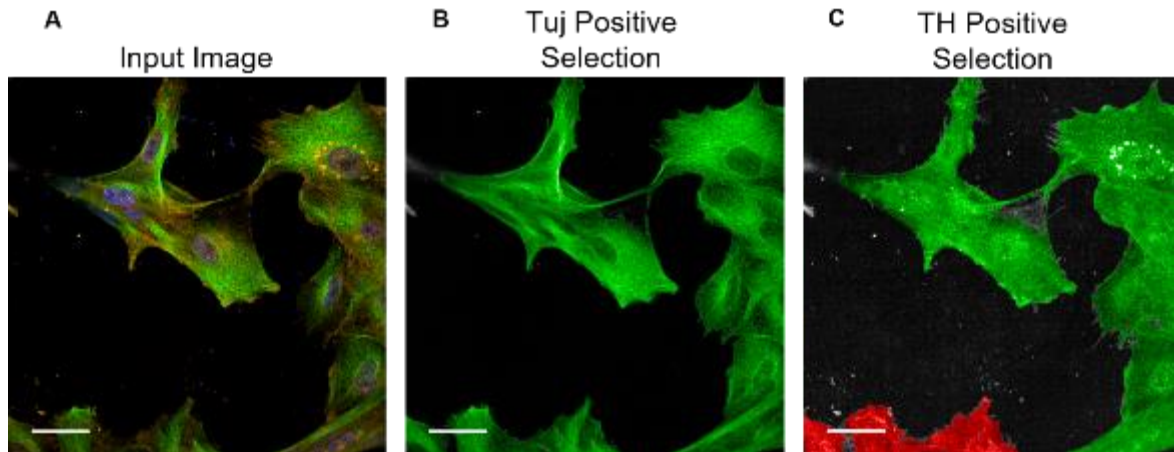


Figure 2.3 Neuronal marker positive image regions based on intensity

Representative images from sPD1 Tuj and TH immunocytochemistry. This method was employed for any immunocytochemistry in which the proportion of marker positive staining was assessed (A) Input image, Tuj (green), TH (red), nuclei (blue) (B) Tuj positive image regions depicted in green (C) TH positive image regions depicted in green, TH negative image regions depicted in red. Scale bar represents 50 μ M

In any instances where we were interested in the co-localisation of two stains, we added a 'find spots' parameter to each channel to first identify positive staining, usually puncta. In the example below, we illustrate total alpha synuclein spots, **figure 2.4B** and phosphorylated alpha synuclein spots, **figure 2.4C**. We were then able to assess co-localisation by identifying where the two stains directly overlap, **figure 2.4D**.

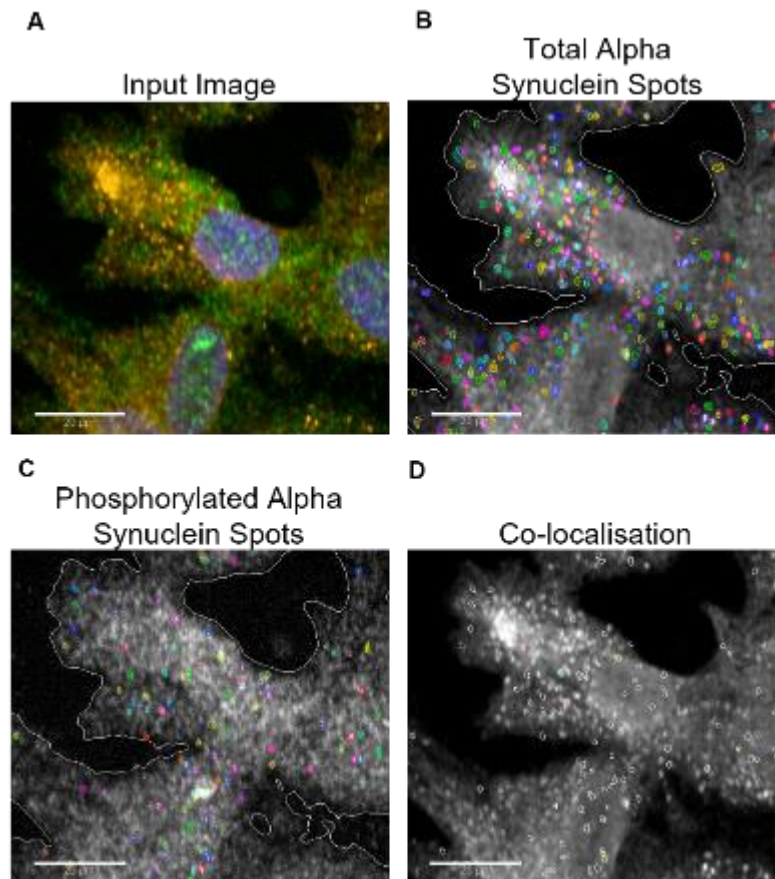


Figure 2.4 Representative images portraying areas where two stains co-localise

Representative images from control 2 total and serine 129 phosphorylated alpha synuclein immunocytochemistry. This method was employed for any work in which we were interested in the co-localisation of two stains (A) Input image, total alpha synuclein (red), serine 129 phosphorylated alpha synuclein (green), nuclei (blue) (B) Total alpha synuclein spots (C) Serine 129 phosphorylated alpha synuclein spots (D) Co-localisation of the two stains. Scale bar represents 20µM

In all instances, following optimisation of the assay specific protocol, analyses were run, generating an excel spreadsheet and parameters of interest were graphed via GraphPad Prism 8.

2.15 *Drosophila* Work

Drosophila containing two different *Parkin* mutations were used, *Park*^{Z472} and *Park*²⁵. These were obtained from Dr Chris Elliott (The University of York). In each case, the *Parkin* mutation was present on the third chromosome and was balanced to the balancer chromosome Third Multiple 6B (TM6B).

Alongside this, two wildtype strains were utilised, Canton S (CS) and Oregon R (OR).

Stocks were maintained on a yeast-cornmeal media, **table 2.16**, at 18°C, with a 12 hour light:dark cycle.

Table 2.16 Recipe for *Drosophila* stock food

Ingredient	Amount	Manufacturer	Supplier
Cold tap water	1 litre		
Medium cornmeal	80g	Triple Lion	Lembas/Easton Enterprises
Dried Yeast	18g	Kerry Ingredients	BTP Drewitt
Soya Flour	10g	Lembas Wholefoods	Lembas
Malt Extract	80g	Rayner's Essentials	Lembas
Molasses	40g	Rayner's Essentials	Lembas
Agar	8g		BTP Drewitt
10% Nipagin in Absolute Ethanol	25ml	Clariant UK Ltd	Chemolink Specialties Ltd
Propionic Acid	4ml	Fisher	Fisher

2.15.1 *Virgin Selection*

Female virgins were collected from all stains as often as possible. This varied due to the Covid19 building restrictions, however it was usually every 2-4 hours. Virgins were selected either by the presence of wings that were not yet expanded, indicating eclosion occurred within the previous 30 minutes or the presence of meconium, a small dark spot within the abdomen, indicating eclosion within the previous 2 hours. In order to do this, flies were emptied onto a gas pad with a small amount of CO₂ present to temporarily anaesthetise them. Assessment was done using a standard light microscope (Zeiss) and flies were categorised into males, females or female virgins. Female virgins were kept at room temperature, separate to the stocks.

Stocks were regularly maintained by providing fresh yeast-cornmeal media as necessary and stored at 25°C, with a 12 hour light:dark cycle.

2.15.2 Crosses

Crosses were set up once 12-15 virgin females had been collected. Female virgins possessing the *Park*^{Z472} mutations were crossed with males harbouring the *Park*²⁵ mutation and vice versa. Similarly, CS virgin females were crossed with OR males and vice versa. Crosses were initially set up on yeast-cornmeal media to ensure it was going to take before being flipped onto food containing either vehicle (ethanol), Jed135 or UDCA (both at concentrations of 60µM, 300µM or 600µM) 2-3 days later. In order to incorporate the drug, food was made manually using a solution of 5% yeast and 10% sucrose which was autoclaved to denature the yeast. 3ml of solution, with added drug treatment, was used per vial before adding an equal quantity of NutriFly instant formulation fly food flakes (Genesee Scientific), **figure 2.5**.

Flies were allowed to lay eggs on this food and once larvae were observed, adult flies were removed to allow the growth of the larvae.

2.15.3 Larval Locomotor Assay

Larval locomotor assays were undertaken as previously described (West et al., 2018, West et al., 2020). Briefly, larvae in the wandering phase of the third instar developmental stage were selected and placed onto a 10cm² petri dish containing 2% agar and left to acclimatise, **figure 2.5**. Up to five larvae at a time were videoed from above for 60 seconds using a digital webcam and recorded at a frame rate of 30 frames per second using the Virtual Dub software (Avery Lee). Locomotor assays were performed once per day, at the same time, with a room temperature of approximately 21°C.

Only larvae that were still within the wandering phase were used, those that had already begun to pupate were discarded. Any larvae from the wildtype cross were available for use, however only the *Parkin transheterozygous* (*Park*^{Z472}/*Park*²⁵) mutant larvae were utilised. These were selected by the absence of the TM6B larval marker, tubby. We identified larvae that had a standard appearance as opposed to those that were shorter and with a more rounded appearance.

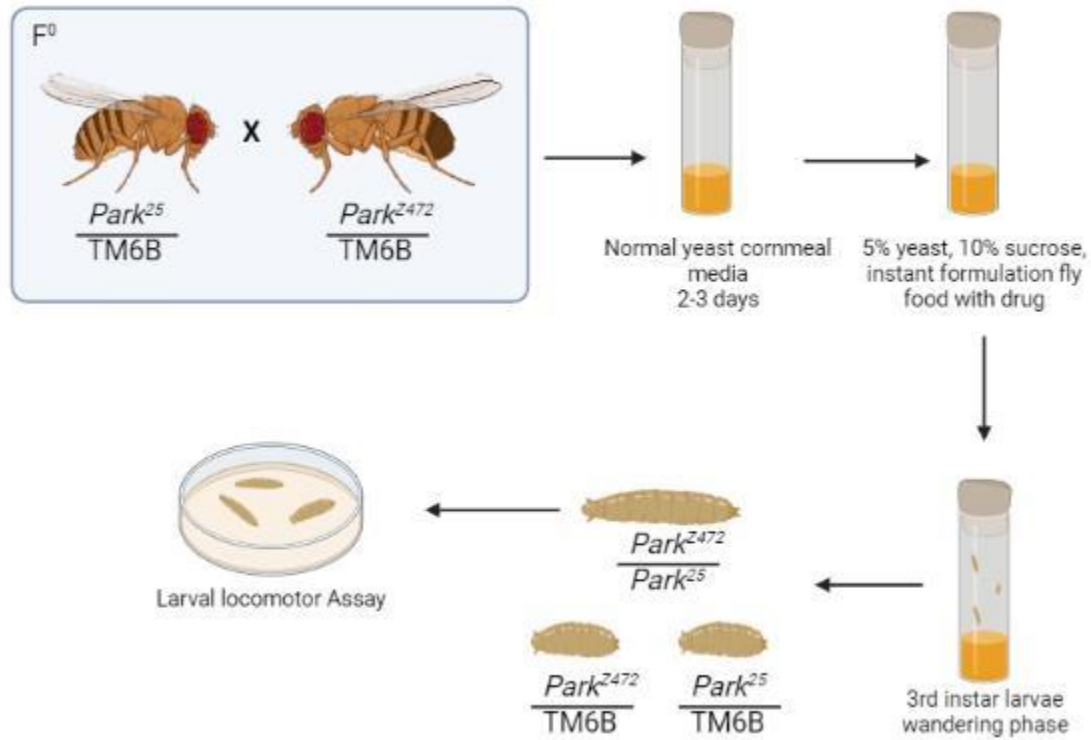


Figure 2.5 Schematic depicting set up of *Drosophila* cross and larvae selection

Two different *Parkin* mutant strains of *Drosophila* are crossed. Initially set up on normal yeast cornmeal media, after 2-3 days they are flipped onto food containing either vehicle, Jed135 or UDCA, made up using a solution of 5% yeast and 10% sucrose, with added NutriFly instant formulation food. Eggs are laid and develop into larvae, which are left until the 3rd instar wandering phase, at which point *Parkin* transheterozygous larvae are selected for larval locomotor assay. Schematic created using biorender.com

Analysis

Raw video files were analysed using ImageJ. As previously described (West et al., 2018, West et al., 2020), images were batch thresholded and a custom macro applied allowing the larval coordinates to be generated and an excel spreadsheet produced. Spreadsheets were then manually checked to ensure larval tracking was correct. This data was able to determine the mean speed of the larvae.

2.15.4 Survival Assays

In order to determine whether Jed135 had a toxic effect on the flies, survival assays were undertaken. Female virgins harbouring the *Park*²⁵ mutation were crossed with males possessing the *Park*^{Z472} mutation, as well as CS virgin females crossed with OR males. As before, crosses were set up on yeast-cornmeal media and given a period of 2-3 days to ensure they would take. Food was made up as previously described using either vehicle or 60µM Jed135. Flies were flipped onto this food, allowed to lay until larvae were observed and then removed. Larvae were left to pupate, and progeny counted for a period of 7 days post first eclosion.

All wildtype progeny were counted, however as previous, we were interested in *Parkin* transheterozygous (*Park*^{Z472}/*Park*²⁵) mutant progeny. The TM6B balancer chromosome carries the adult marker humeral, which is characterised phenotypically by the presence of extra macrochaetes (large bristles) on their humeral callus (shoulder area). Therefore, flies were anaesthetised as previously described and categorised and counted based on the presence or absence of the humeral marker. Results from this assay were based on 3 separate crosses.

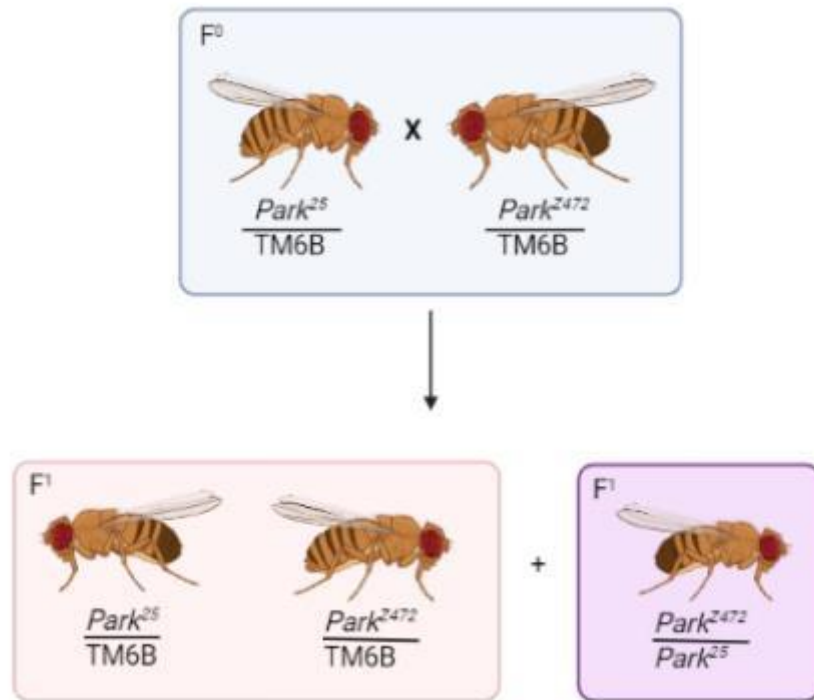


Figure 2.6 Schematic of the *Drosophila* mating scheme for survival assays

Female $Park^{25}$ *Drosophila* crossed with male $Park^{2472}$ *Drosophila*. Eggs are laid on food containing either vehicle or Jed135 and larvae allowed to develop and pupate until F^1 progeny begin to eclose. Adult F^1 *Drosophila* are counted for 7 days post first eclosion, identifying the adult TM6B humeral marker. Schematic made using biorender.com

2.16 Statistics

All statistical analyses were undertaken using GraphPad Prism version 8 or 9.0.2. When appropriate, statistical significance was defined as * $p < 0.05$, ** $p < 0.005$, *** $p < 0.0005$ and **** $p < 0.0001$.

When comparing 2 groups, normality was tested using Shapiro Wilks test for normality. Following confirmation of normally distributed data, an unpaired t-test with Welch's correction was completed. If data was not normally distributed, a Mann Whitney U test was undertaken.

When comparing multiple groups, normality was tested using the Shapiro Wilks test for normality. If data was normally distributed, a one-way analysis of variance (ANOVA) with Sidak's or Tukey's multiple comparisons test were undertaken. If data was not normally distributed, a Kruskal-Wallis one-way ANOVA with Dunn's multiple comparisons test was completed.

When two independent variables were present, for example genotype and drug treatment, normality was assumed and a two-way ANOVA with Sidak's multiple comparisons test was undertaken.

3 Characterising the Neuronal Model

3.1 Background

In this project, we chose to model PD in a two-dimensional system using iNPCs reprogrammed from fibroblasts. The iNPCs then underwent a version of the neuronal differentiation protocol described previously (Schwartzentruber et al., 2020).

In 2007, Takahashi and Yamanaka detailed the conversion of adult human dermal fibroblasts into induced pluripotent stem cells (iPSCs) using a combination of four factors; Oct3/4, Sox2, Klf4 and c-Myc, commonly referred to as Yamanaka factors (Takahashi et al., 2007). iPSCs harness the ability to differentiate into any cell type of the three primary germ layers, ectoderm, mesoderm and endoderm (Medvedev et al., 2010). Of particular interest for the neuroscience field is that iPSCs are able to be pushed down an ectodermal lineage and are able to form neuronal precursor cells with the ability to become neurones, astrocytes or oligodendrocytes. Interestingly, in order to generate microglia, iPSCs are required to enter a mesodermal lineage (Ginhoux and Prinz, 2015). This protocol revolutionised research, particularly in the neuroscience field as we are unable to use live primary human cells and as such, iPSCs have provided a method to study disease mechanisms *in vitro* that weren't available before (Wu et al., 2019). However, modelling of neurodegenerative diseases using iPSCs comes with its inherent disadvantages. The generation of fibroblasts into iPSCs is relatively inefficient, with only 0.02% efficiency 30 days after transduction (Takahashi et al., 2007, Malik and Rao, 2013, Meyer et al., 2014). Also, iPSCs grow in colonies and as such, each colony may differ slightly, increasing the variability (Gatto et al., 2021). iPSCs require full characterisation prior to further differentiation which includes investigating known pluripotency markers via ICC, gene expression profiling and ensuring that the iPSCs can differentiate into all three germ layers (McKinney, 2017).

However, the major pitfall when modelling neurodegenerative diseases using iPSCs is that the Yamanaka factors used to induce pluripotency are highly expressed in embryonic stem cells (Liu et al., 2008). Minimal differences in gene expression were found between human iPSCs and human embryonic stem cells (Patterson et al., 2012). In addition, there is also evidence to suggest that iPSCs from older donors possess increased telomere length (Agarwal et al., 2010, Miller et al., 2013), loss of senescent markers (Agarwal et al., 2010, Lapasset et al., 2011) and improved mitochondrial health (Suhr et al., 2010, Miller et al., 2013), indicative of an embryonic-like state and a loss of cellular ageing (Gatto et al., 2021).

Age is the biggest risk factor in the development of neurodegenerative diseases and as such, is extremely important for disease modelling *in vitro*. In 2014, Meyer et al described

the direct conversion of adult fibroblasts into tripotent iNPCs, donated by people with ALS (Meyer et al., 2014). The tripotent status of these progenitor cells allows the differentiation of neurones, astrocytes or oligodendrocytes (Meyer et al., 2014). iNPC derived astrocytes differentiated from young and old donors have been found to retain the ageing phenotype of the donors (Gatto et al., 2021). During ageing, there is an accumulation of ROS. A 2021 paper investigated differences in ROS between young and old donor induced astrocytes from iNPCs, illustrating significantly higher ROS in astrocytes from old donors compared to young donors. When subjected to stress conditions, the induced astrocytes from older donors required longer to return to baseline ROS levels than the cells from young donors (Gatto et al., 2021). This provides evidence to support the retention of age-related changes from donors and hence supports the notion that iNPCs are a more disease relevant model to study neurodegenerative diseases than iPSCs.

The iNPCs utilised for this thesis were reprogrammed from human adult fibroblasts prior to starting this project and were fully characterised previously using neuronal progenitor markers Pax6 and Nestin (data not shown). Previous studies using the same methodology also demonstrated Pax6 and Nestin expression (Meyer et al., 2014, Ferraiuolo et al., 2016, Schwartzenruber et al., 2020).

iPSCs and iNPCs both provide an intermediary for the generation of neurones from fibroblasts, however the methodology of producing dopaminergic neurones differs slightly. Differentiation of iPSCs into induced dopaminergic neurones is a time-consuming and multistep process involving 3 key steps, neuralisation, specification and maturation (Wang et al., 2020). However, iPSCs require the generation of a further intermediary. This intermediate cell type can vary from embryoid bodies (EBs) to neural rosettes to neural progenitor cells, with these believed to mimic *in utero* neurogenesis (Tran et al., 2020). There are a number of different protocols for the generation of induced dopaminergic neurones from iPSCs which are beyond the scope of this thesis, however the following description is true for induced dopaminergic neurones generated from iPSCs via a neural progenitor lineage. Firstly, inhibition and activation of key signalling pathways results in the iPSCs undertaking an ectodermal lineage, and this remains similar between the protocols. This is done by inhibiting two pathways, dual-mothers against decapentaplegic homologue (SMAD), preventing the mesodermal and endodermal lineages (Wang et al., 2020). Early and prolonged exposure to the sonic hedgehog protein and the Wnt signalling pathways increase the expression of FOXA2, a protein with roles in development, particularly in the generation of dopaminergic neurones during development (Kittappa et al., 2007, Wang et al., 2020). The activation of FGF8 was also found to be required for the differentiation of

dopaminergic neurones from iPSCs. The inhibition or activation of the above pathways paves the way for the generation of neural stem cells, expressing pan neuronal markers and takes approximately 30 days. A cocktail of dopaminergic factors including BDNF, GDNF, cAMP, TGF β , ascorbic acid and DAPT, are then added for 20 or more days to produce the desired dopaminergic neurones (Xu et al., 2017, Wang et al., 2020). The exact combination of factors appears to differ between groups; however they are similar to the ones used in our iNPC differentiation protocol. A 2020 meta-analysis discovered that since 2011, 385 different iPSC lines have been used in studies investigating PD (215 patients and 170 controls). However, of these 215 PD patient lines, less than 20% were from sporadic cases of PD despite the fact that sporadic PD accounts for approximately 90% of cases (Tran et al., 2020). The most common genetic mutations modelled were from cases of *LRRK2-G2019S*, *Parkin*, *PINK1* and alpha synuclein mutant individuals, and although in reality these only represent a small proportion of PD cases, the data generated from them still provides valuable insight into PD (Tran et al., 2020). Further data from the meta-analysis assessed the most common phenotypes described from the 385 iPSC lines, used across 67 different studies. They noted impairments in cellular waste recycling, mitochondria, neuronal morphology, oxidative stress, neuronal survival and development and neuroinflammation. The heat map in **figure 3.1** is taken from figure 4 of the meta-analysis and eloquently highlights the phenotypes that were observed in iPSC derived induced dopaminergic neurones of different PD genotypes (Tran et al., 2020). Interestingly, none of the papers assessed in this meta-analysis highlighted any mitochondrial and metabolic deficiencies in the sporadic dopaminergic neurones. The sporadic dopaminergic neurones appeared to display alterations primarily in neuronal morphology and function but also, to a lesser extent, neuroinflammation and neuronal survival (Tran et al., 2020).

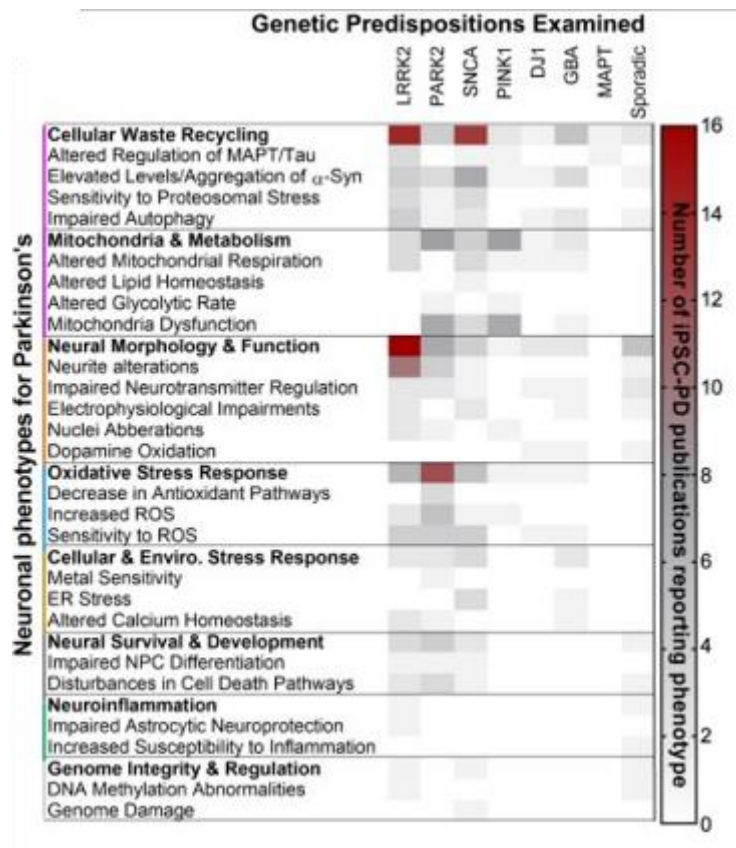


Figure 3.1 Phenotypes observed in iPSC derived dopaminergic neurones of varying PD genotypes

Heat map highlighting specific dysfunctions observed in iPSC derived dopaminergic neurones. Taken from meta-analysis conducted by (Tran et al., 2020) in which common phenotypes were assessed from 385 iPSC-derived dopaminergic neurones generated from PD patients. Impairments were noted in a number of different categories including cellular waste and recycling and mitochondria and metabolism. However, the majority of these impairments were uncovered in iPSC-derived dopaminergic neurones generated from genetic forms of PD. No impairments in mitochondria and metabolism were described in induced dopaminergic neurones generated from sporadic PD. Figure used under the creative commons attribution license (CC-BY)

An alternative method of generating induced dopaminergic neurones is via a direct reprogramming method. Direct reprogramming does not require the formation of a pluripotent intermediate, using exogenous genes to alter lineage-specific genes of somatic cells such as fibroblasts (Han et al., 2021). Using transcription factors *Mash1*, *Nurr1* and *Lmx1a*, Caiazzo et al were able to illustrate that both mouse embryonic fibroblasts and human fibroblasts could be directly reprogrammed into dopaminergic neurones and were able to release dopamine as well as exhibit organised electrical activity, in a process taking approximately 20 days (Caiazzo et al., 2011). The benefit of a direct reprogramming method

over the iPSC pluripotency intermediate is due to the difference in tumour potential. Some studies are investigating the utility of implanting a patient's own iPSC derived dopaminergic neurones directly into their brain in order to replenish the lost dopaminergic neurones (Schweitzer et al., 2020). However, this carries a risk of tumour growth due to the proliferative nature of the iPSCs (Caiazzo et al., 2011).

Conversely, standard differentiation of the dopaminergic neurones from iNPCs takes 27 days (Schwartzentruber et al., 2020), with alterations to the protocol made on a line by line basis. Furthermore, once generated, the iNPCs are continually proliferative, enabling us to freeze and build up large repositories of stocks following each passage. The benefit of this compared to both iPSCs and directly reprogrammed dopaminergic neurones is that each individual differentiation is ultimately from the same fibroblast reprogramming cycle, hence removing any heterogeneity.

In this chapter we show characterisation of the metabolic status of 2 sporadic PD patients, 1 alpha synuclein mutant (triplication) and 3 control iNPC lines. We also present data detailing the basal mitochondrial phenotypes of these lines and finish by extensively characterising the iNPC-derived dopaminergic neurones of the same cohort.

3.2 Aims and Objectives

The aim of this chapter was to characterise the neuronal progenitor cells, and dopaminergic neurones generated from them, in two sporadic PD and one alpha synuclein mutant line plus age and sex matched controls. This was achieved by:

- Measuring the metabolic status of the iNPCs via ATP assay
- Understanding any differences in mitochondrial phenotypes including number of mitochondria per cell, percentage mitophagy and MMP
- Investigating the expression of pan neuronal and dopaminergic specific markers in the iNPC-derived dopaminergic neurones via ICC and Western blotting
- Assessing the effect of Jed135 or UDCA treatment on the pan neuronal and dopaminergic markers

3.3 Results

3.3.1 Functional Characterisation

Metabolic Status of iNPCs

The overall ATP content of the iNPCs was investigated, along with assessing the metabolic status. This was done by measuring ATP levels under one of four conditions; untreated, oligomycin treatment to inhibit OXPHOS via complex V, 2DG treatment to inhibit glycolysis via hexokinase or both inhibitors together.

Sporadic PD1 and Control 1

Previous data from our group found no significant differences in ATP production between sPD1 and control 1 in the fibroblasts (data not shown and generated by previous lab members, patient included in (Carling et al., 2020)).

The sPD1 iNPCs display an ATP deficiency (mean \pm SD) of 54% (\pm 9.2) compared to control 1, as seen in **figure 3.2A**. This was significant ($p < 0.0001$) following two-way ANOVA with Sidak's multiple comparisons test. When OXPHOS was inhibited, via the use of oligomycin, we also discovered a significant ($p < 0.0001$) ATP deficit of 57.9% (\pm 4.7) in the sPD1. The data presented here suggests the iNPCs are heavily reliant on glycolysis as their main source of respiration. When OXPHOS is inhibited, there is a decrease in ATP production of 22% in control 1 and 28% in sPD1 iNPCs, meaning that glycolysis is accounting for 78% and 72% of ATP production respectively, **figure 3.2B**. Whereas when glycolysis is inhibited, the decrease in ATP production is 76% and 74% respectively, illustrating that OXPHOS accounts for 24% and 26% of ATP production in the iNPCs.

No significant differences were observed between control 1 and sPD1 when glycolysis was inhibited, or when both OXPHOS and glycolysis were inhibited.

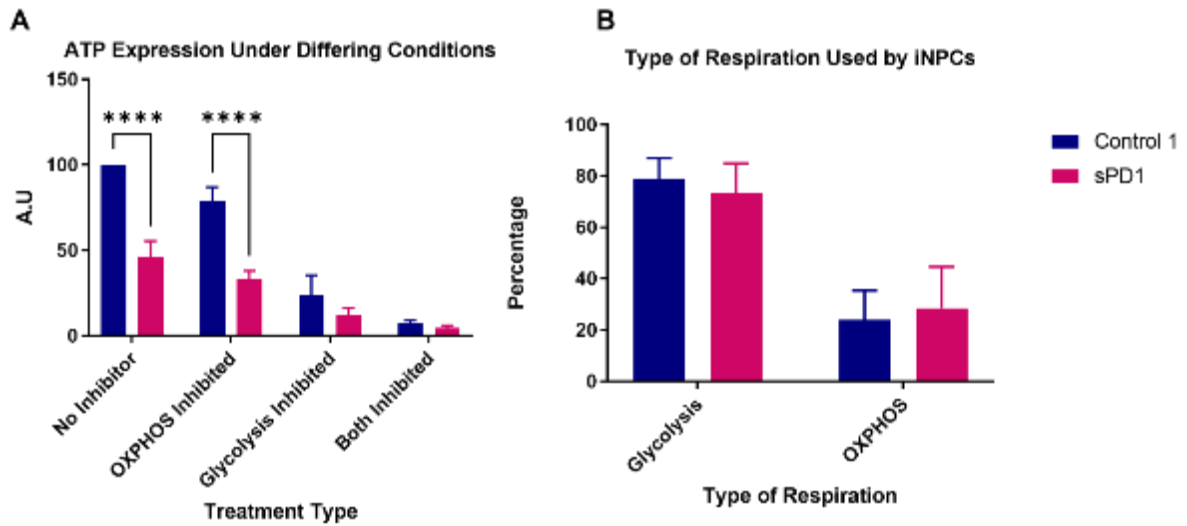


Figure 3.2 ATP production and metabolic status of sPD1 and control 1 iNPCs

Results are expressed as mean \pm standard deviation, $n=3$ (A) ATP production under four different treatment conditions; untreated, oligomycin treated (inhibiting complex V of the electron transport chain and hence giving information on ATP generated by glycolysis), 2-deoxyglucose treated (inhibiting hexokinase, giving information on ATP generated by OXPPOS) and both inhibitors. sPD1 displays a 54% ATP deficiency compared to control 1. ATP/Cyquant normalised to untreated control per repeat (B) Percentage of ATP produced via glycolysis and oxidative phosphorylation. Glycolysis accounts for 78% of ATP production in control 1 and 72% in sPD2 while OXPPOS accounts for 24% and 26% of ATP production respectively. Data was normally distributed following Shapiro Wilks tests for normality and a two-way ANOVA with Sidak's multiple comparisons tests completed, **** $p < 0.0001$.

Sporadic PD Patient 2 and Non-PD Control 2

Previous data collected by past members of the group showed sPD2 to have a 31% deficit in ATP production when compared to control 2 in the fibroblasts (data not shown, patient line included in (Carling et al., 2020)).

However, sPD2 iNPCs did not show an ATP deficit under basal conditions compared to control 2, with a difference of only 1.6% between control 2 and sPD2, **figure 3.3A**. Similarly, the data here also suggest the iNPCs are heavily reliant upon glycolysis. When OXPHOS is inhibited, there is a decrease in ATP production of 12% in control 2 and 32% in sPD2 meaning the cells rely on glycolysis for 88% and 68% of the ATP production respectively. Whereas, when glycolysis is inhibited, the decrease in ATP production is 71% in control 2 and 78% in sPD2 meaning that OXPHOS accounts for 29% and 22% of ATP production respectively, **figure 3.3B**.

When comparing the four treatment types individually, no condition showed any significant differences between control 2 and sPD2, however it should be noted that in some cases, sPD2 showed a high degree of variability.

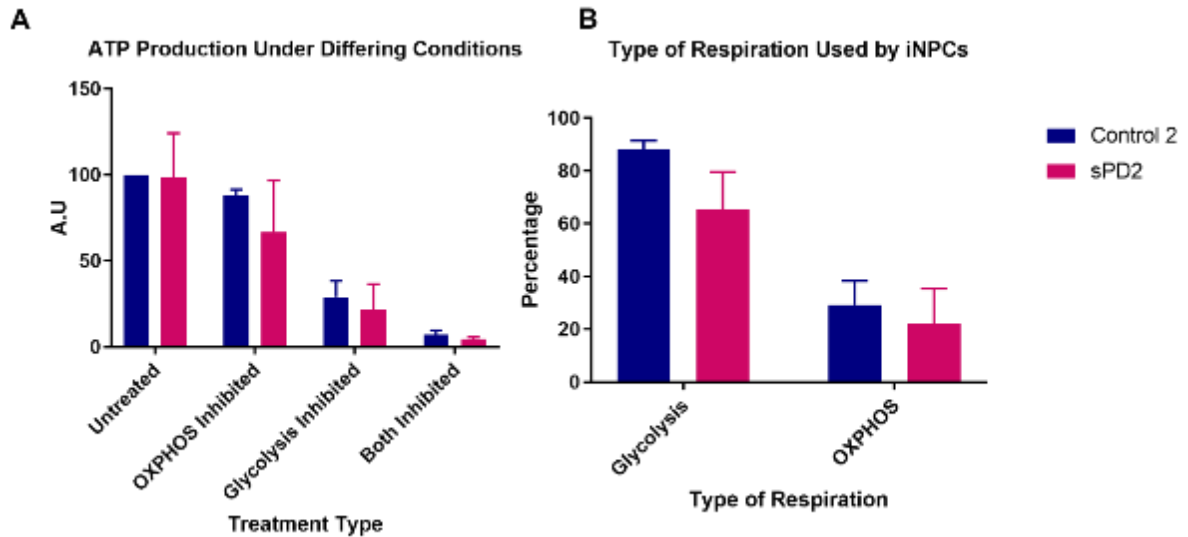


Figure 3.3 ATP production and metabolic status of sPD2 and control 2 iNPCs

Results are expressed as mean \pm standard deviation, $n=4$ (A) ATP production under four different treatment conditions; untreated, oligomycin treated, 2DG treated and treatment with both inhibitors. No difference in ATP production between control 2 and sPD2 was observed. ATP/Cyquant normalised to untreated control per repeat (B) Percentage of ATP produced via glycolysis and oxidative phosphorylation. In control 2, glycolysis accounted for 88% of ATP production and OXPHOS 29%. Conversely in sPD2, glycolysis accounts for 68% of ATP production while OXPHOS accounts for 22%. Normality confirmed by Shapiro Wilks test for normality and two-way ANOVA with Sidak's multiple comparisons test undertaken.

SNCA mutant and Control 3

Previous data collected by another member of the lab group illustrated no difference in ATP levels between the alpha synuclein mutant line and control 3 in the fibroblasts. This result was expected due to inherently low levels of alpha synuclein expressed in fibroblasts.

We also observed no differences in ATP production between control 3 and the alpha synuclein mutant iNPCs under basal conditions, with the alpha synuclein mutant exhibiting only 3.5% less ATP production than control 3, **figure 3.4A**. In agreement with the data from the sporadic PD lines, the iNPCs main source of ATP production was via glycolysis. When OXPHOS is inhibited, there is a decrease in ATP production of 17% in control 3 and 24% in the alpha synuclein mutant meaning that glycolysis accounts for 83% and 76% of ATP production respectively. Whereas, when glycolysis is inhibited, ATP production decreases by 55% in control 3 and 75% in the alpha synuclein mutant meaning that OXPHOS accounts for 45% and 25% of ATP production respectively, **figure 3.4B**.

No significant differences were observed between control 3 and the alpha synuclein mutant line following treatment with any of the inhibitors.

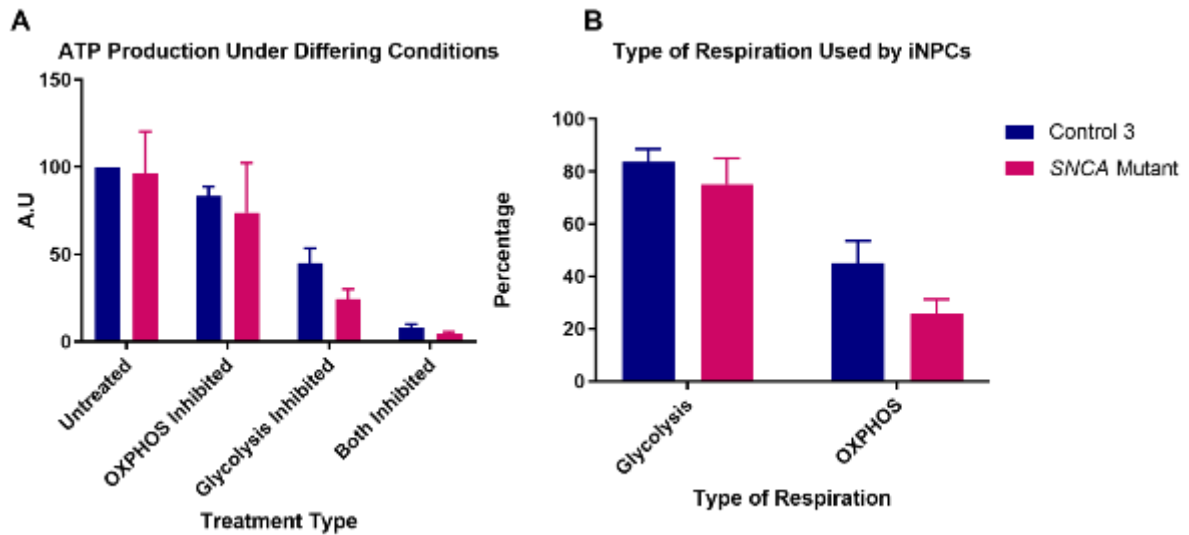


Figure 3.4 ATP production and metabolic status of the SNCA mutant and control 3 iNPCs

Results are expressed as mean \pm standard deviation, $n=3$ (A) ATP production under four different treatment conditions; untreated, oligomycin treated, 2DG treated and treatment with both inhibitors. We do not observe any ATP deficit in the alpha synuclein mutant compared to control 3. ATP/Cyquant normalised to untreated control per repeat (B) Percentage of ATP produced via glycolysis and oxidative phosphorylation. Glycolysis accounts for 83% and 76% of ATP production in control 3 and the alpha synuclein mutant respectively while OXPHOS accounts for 45% and 25% of ATP production. Normality confirmed via Shapiro Wilks test for normality and two-way ANOVA with Sidak's multiple comparisons test confirmed no differences.

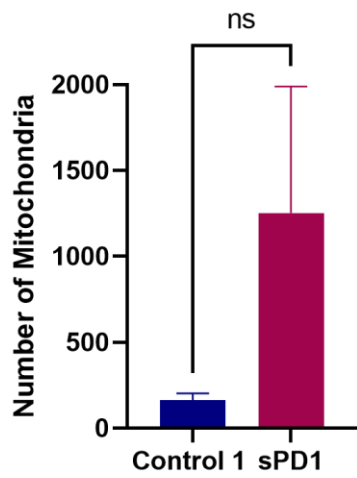
Basal Mitochondrial Phenotypes of iNPC Derived Dopaminergic Neurones

We sought to characterise any basal mitochondrial phenotypes present within the dopaminergic neurones by considering mitochondrial and lysosomal number per cell, percentage of mitochondria undergoing mitophagy, mitochondrial fragmentation score and MMP. This information enabled us to understand any mitochondrial abnormalities present before we assessed the effect of Jed135 or UDCA. Data presented here are from untreated conditions and any drug effects will be considered and discussed in chapter 4.

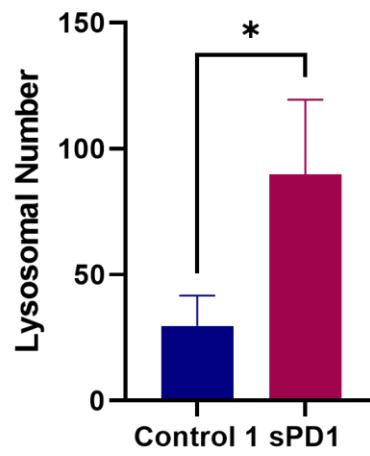
Control 1 and sPD1

There are clear differences between control 1 and sPD1 over a number of different mitochondrial parameters, however likely due to variability they aren't always significant. sPD1 appeared to average 1252 (± 736) mitochondria per cell whilst on average, control 1 exhibited 162 (± 40) mitochondria per cell. This illustrates an increase of 673% between control 1 and sPD1, however, this difference was not found to be significant following an unpaired t-test, likely due to the variability observed in the patient line, **figure 3.5A**. We also illustrated a significantly ($p < 0.02$) increased number of lysosomes per cell in sPD1 compared to control 1, **figure 3.5B**. Control 1 possessed an average of 30 (± 11.9) lysosomes per cell, while sPD1 had approximately 200% more, averaging 90 (± 29.6) lysosomes per cell. A mitophagy event was defined as the co-localisation of the mitochondrial and lysosomal stain and this data is presented as a percentage of the total mitochondrial population. Although not significant, there is a trend towards reduced levels of mitophagy occurring in sPD1 compared to control 1, with averages of 1.8% (± 0.5) and 3.9% (± 1.6) respectively, **figure 3.5C**. Mitochondria produce a vast network that is highly interconnected and the mitochondrial fragmentation score reported provides information on this. The lower the mitochondrial fragmentation score, the more fragmented the network. Therefore the data presented illustrates that, although not significant, sPD1 has a more fragmented network when compared to control 1 and this may account for the increased number of mitochondria per cell, **figure 3.5D**. On average, the mitochondrial fragmentation score for control 1 was 85.5 (± 39.5) while for sPD1 it was 14.4 (± 5.7), a decrease of 81.1%. Finally, we observed no difference in MMP between control 1 and sPD1, with a decrease in MMP of only 23.5%. However, sPD1 exhibits some variability and therefore there may be a trend to suggest that sPD1 has a lower membrane potential, **figure 3.5E**.

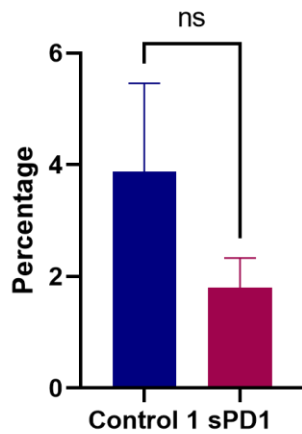
A
Number of Mitochondria
per Cell



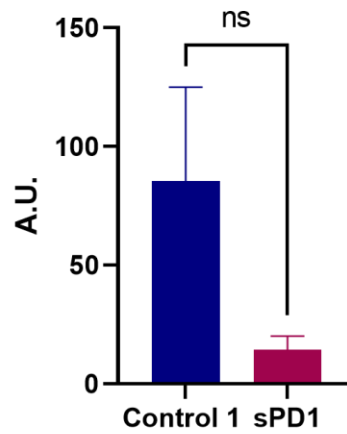
B
Number of Lysosomes
per Cell



C
Percentage of Mitochondria
Undergoing Mitophagy



D
Mitochondrial
Fragmentation



E
Mitochondrial Membrane
Potential

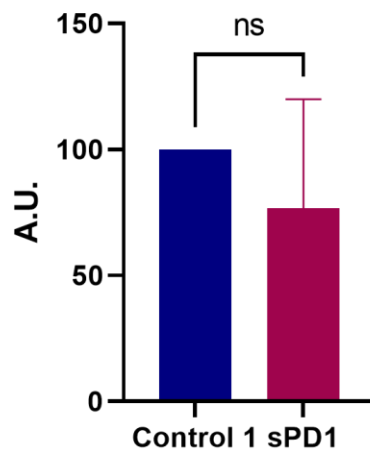


Figure 3.5 Basal mitochondrial phenotyping, control 1 and sPD1

Results are expressed as mean \pm standard deviation, n= at least 3 (A) Mitochondrial number per cell. sPD1 exhibited a 673% increase in mitochondrial number per cell compared to control 1, however this did not reach significance, likely due to the amount of variability observed (B) Lysosomal number per cell. sPD1 had significantly more lysosomes per cell than control 1, with an increase of roughly 200% (C) Percentage mitophagy calculated as the number of mitochondria undergoing mitophagy as a percentage of the full mitochondrial population. sPD1 exhibited a decrease in the percentage of mitochondria undergoing mitophagy compared to control 1, however this did not reach significance. 3.9% of mitochondria were undergoing mitophagy in control 1, whereas in sPD1 this was only 1.8% (D) Mitochondrial fragmentation score. A lower score is indicative of a more fragmented mitochondrial network. Although non-significant, sPD1 displayed a decreased mitochondrial fragmentation score of 81.1%, suggesting that the mitochondrial network in sPD1 was more fragmented and less interconnected (E) Mitochondrial membrane potential normalised to control 1. We observed a small, 23.5%, decrease in MMP in sPD1 compared to control 1, a difference that was not significant. For (A) to (E) all data was normally distributed following Shapiro-Wilks test and unpaired t-tests with Welch's correction were performed. * $p < 0.05$.

Control 2 and sPD2

We considered the same parameters as above for control 2 and sPD2, observing different mitochondrial phenotypes. No significant differences were uncovered in mitochondrial number per cell, although sPD2 did exhibit a trend to having an increased number, **figure 3.6A**. More specifically, control 2 displayed on average 565.5 (± 30.6) mitochondria per cell whereas sPD2 had, on average, 687.7 (± 107.2) mitochondria per cell, exhibiting an increase of 21.6%. Similarly, there were also no differences in number of lysosomes per cell with control 2 having 184.4 (± 16.2) lysosomes per cell, while sPD2 had 187.6 (± 25.1) lysosomes per cell, a difference of only 1.8%, **figure 3.6B**. However, sPD2 appeared to have a significantly ($p < 0.027$) reduced percentage mitophagy compared to control 2, at 4.8% (± 0.4) and 6.03% (± 0.5) respectively, meaning that sPD2 exhibited a decrease in mitophagy of 20.2%, **figure 3.6C**. sPD2 also had a significantly ($p < 0.0005$) more fragmented mitochondrial network than control 2, with average fragmentations scores of 37.2 (± 2.9) and 107.8 (± 6.1) respectively, illustrating a difference of 65.5%, **figure 3.6D**. Mitochondrial health in the form of MMP also appeared to be significantly ($p < 0.0001$) reduced in sPD2, **figure 3.6E**, exhibiting 79.1% lower MMP than control 2.

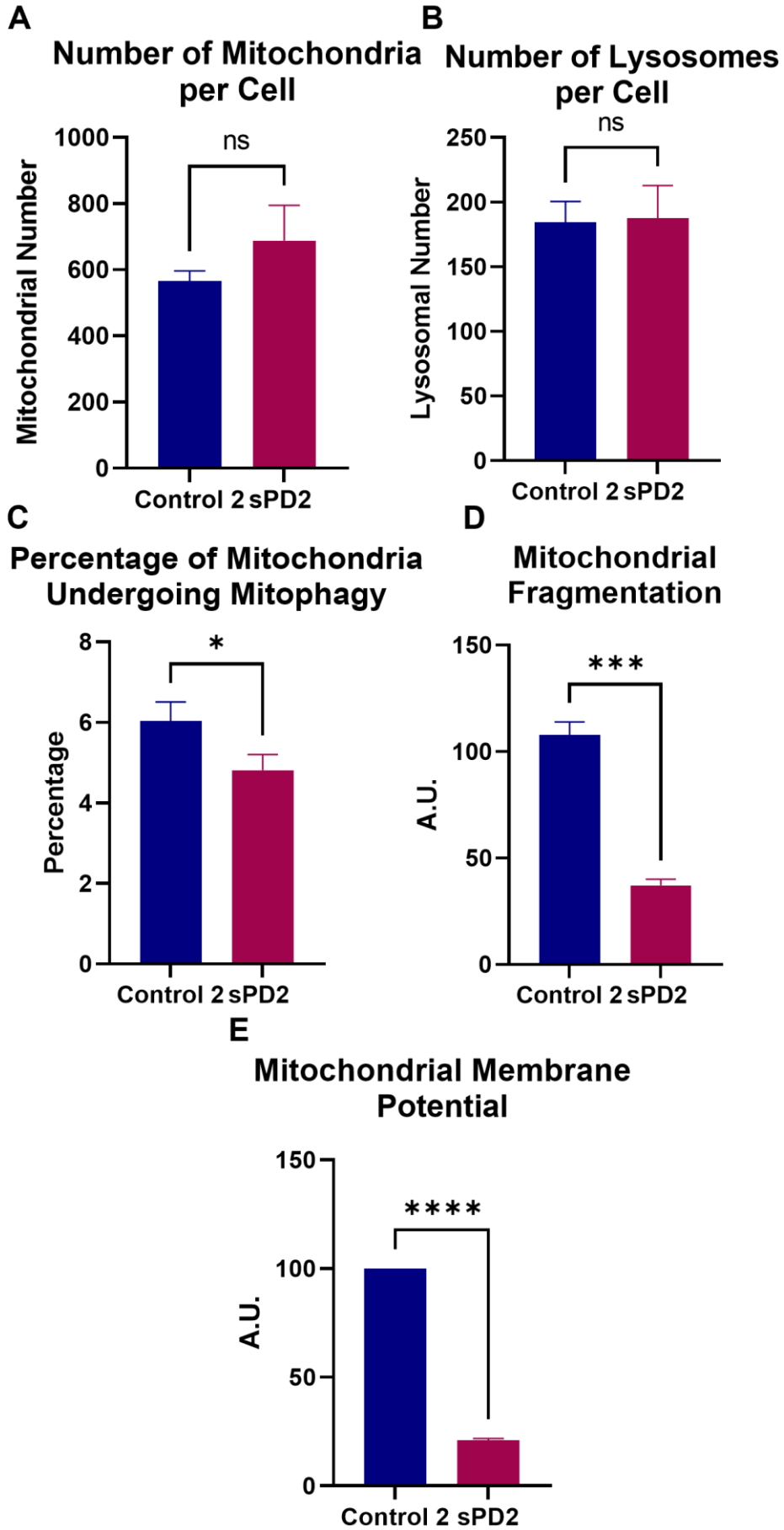


Figure 3.6 Basal mitochondrial phenotyping, control 2 and sPD2

Results are expressed as mean \pm standard deviation, n=3 (A) Mitochondrial number per cell. We observed a small, 21.6%, increase in mitochondrial number per cell in sPD2 compared to control 2 however this did not reach significance (B) Lysosomal number per cell. No differences were observed between control 2 and sPD2 (C) Percentage mitophagy calculated as the number of mitochondria undergoing mitophagy as a percentage of the full mitochondrial population. sPD2 had significantly fewer mitochondria undergoing mitophagy than control 2. We observed a difference of 1.23% between patient and control (D) Mitochondrial fragmentation score. A lower fragmentation score is indicative of a more fragmented, less interconnected mitochondrial network. sPD2 exhibited a significantly lower mitochondrial fragmentation score, with a 65.5% decrease, suggesting that the mitochondrial network in sPD2 is more fragmented (E) Mitochondrial membrane potential normalised to control 2. MMP in sPD2 was 79.1% lower than control 2, a difference that was found to be significant. For (A) to (E) all data was normally distributed following Shapiro-Wilks test and unpaired t-tests with Welch's corrections were performed. * $p < 0.05$, *** $p < 0.0005$, **** $p < 0.0001$.

3.3.2 *iNPC-Derived Dopaminergic Neurone Characterisation*

For the purpose of this chapter, each pair of cell lines will be considered in isolation as the length of the differentiation protocol was slightly altered due to changes in morphology with the clustering of cell bodies and formation of large projection tracts which led to detachment of the cells from the cell culture plates, therefore a direct comparison isn't possible.

Sporadic PD 1 and Control 1

Control 1 and sPD1 were cultured as per the standard protocol outlined in the methods for the first two stages of differentiation. Once into the third stage of differentiation, the morphology of sPD1 was quick to change and as such, the protocol was terminated approximately 7 days after third stage initiation.

In order to characterise the neurones generated, ICC and Western blotting were undertaken to investigate a range of pan neuronal and dopaminergic specific markers.

Firstly, we studied the percentage of cells expressing Tuj, a neurone specific cytoskeletal marker, and TH, the rate limiting enzyme in the formation of dopamine and therefore a dopaminergic specific marker. Tuj expression was observed as an overall cytosolic stain whereas TH positive staining was identified as small, high intensity puncta. Our ICC shows both control 1 and sPD1 to express high levels of Tuj, 92% (± 10.05) and 96.5% (± 2.99) respectively, **figure 3.7B**. TH expression was more variable between the two cell lines, with control 1 containing 56% (± 18.9) of cells positive for TH and sPD1 83% (± 18.2), **figure 3.7C**. The Shapiro-Wilk test for normality found the data for both Tuj and TH expression to be normally distributed and the resulting unpaired t-test with Welch's correction exhibited no significant difference in either marker expression between the two cell lines.

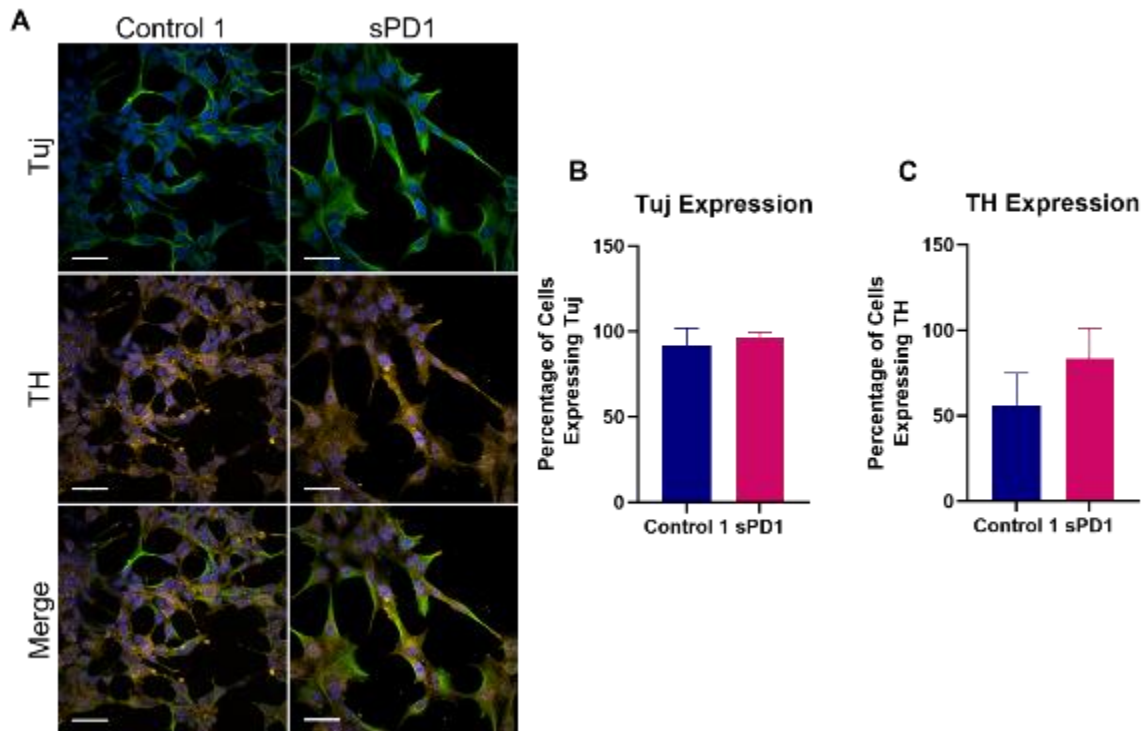


Figure 3.7 Tuj and TH expression in sPD1 and Control 1 end stage dopaminergic neurones

Results are expressed as mean \pm standard deviation, $n=3$. (A) Representative images using Tuj (green) as a pan neuronal marker and TH (orange) as a dopaminergic specific marker with Hoechst (blue) to label nuclei. Scale bar = $50\mu\text{m}$. At least 17 fields of view were imaged per well (B) Percentage of cells expressing Tuj. We found no significant difference between patient and control, with them exhibiting 96.5% and 92% Tuj expression respectively (C) Percentage of cells expressing TH. Control 1 had 56% of cells positive for TH, while sPD1 had 83% of cells positive for TH. The difference between patient and control was 27% however this was not significant. Quantification for (B) and (C) was done on three separate rounds of differentiation; Shapiro-Wilk test for normality showed the data to be normally distributed. No differences in Tuj or TH expression were found following unpaired t -test with Welch's correction.

This section has been redacted by the author for commercial reasons.

This section has been redacted by the author for commercial reasons.

This section has been redacted by the author for commercial reasons.

This section has been redacted by the author for commercial reasons.

Neurons were further characterised via ICC using antibodies targeted to pan-neuronal marker MAP2, a neuronal microtubule associated protein, and DAT, the dopamine transporter. MAP2 is a member of the microtubule associated protein family that bind and stabilise microtubules, with MAP2 primarily being associated with neurons (Soltani et al., 2005). There are 3 isoforms of MAP2, a, b and c, with MAP2c representing a more juvenile form of the protein and is therefore only expressed in immature neurons (Soltani et al., 2005). MAP2 is primarily expressed within the dendrites, therefore we expect to observe expression within the projections of the cells (Rehbach et al., 2019), however the antibody we utilised is unable to differentiate between the MAP2 isoforms and therefore in some instances less MAP2 expression may be synonymous with more mature neurons as we have less of the juvenile MAP2c. Similarly, DAT is usually localised to the cytoplasmic surfaces of plasma membranes as well as the smooth endoplasmic reticulum of the dendrites (Nirenberg et al., 1996). Therefore, in our model, we expect to observe DAT as small, high intensity puncta, primarily within the projections.

We observed that control 1 had a neuronal population that had 76.3% (± 18.9) of cells positive for MAP2 while SPD1 had 67.3% (± 25.1), **figure 3.10B**. Meanwhile, DAT expression was much lower with 31.6% (± 1.0) and 32.6% (± 5.8) of positive cells respectively, **figure 3.10C**. Data was found to be normally distributed and unpaired t-test with Welch's correction showed no difference in MAP2 or DAT expression between control 1 and SPD1.

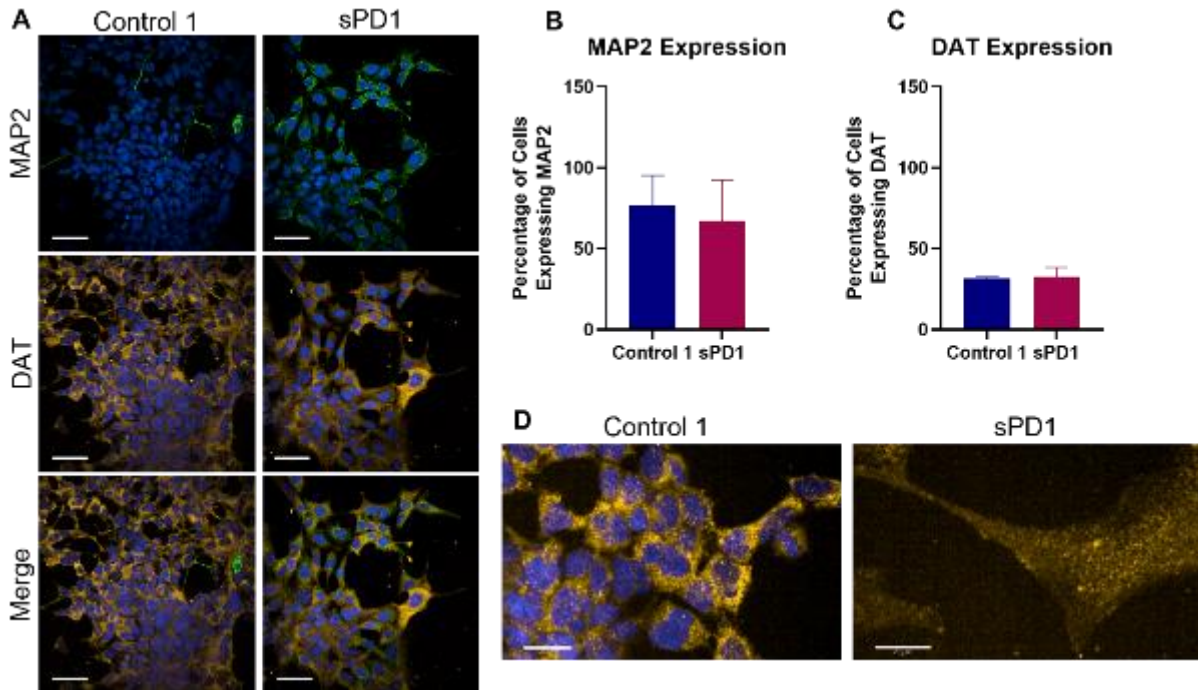


Figure 3.8 MAP2 and DAT expression in control 1 and sPD1 end stage dopaminergic neurones
 Results are expressed as mean \pm standard deviation, $n=3$. (A) Representative images using MAP2 (green) as a pan neuronal marker and DAT (orange) as a dopaminergic specific marker with Hoechst (blue) to label nuclei. Scale bar = 50 μ m. 17 fields of view imaged per well (B) Percentage of cells expressing MAP2. Control 1 had a slightly higher percentage of cells expressing MAP2, 76.3%, compared to sPD1, 67.3%, however this difference was not significant (C) Percentage of cells expressing DAT. This was similar between the two cell lines, 31.6% and 32.6% in control 1 and sPD1 respectively. Quantification for (B) and (C) was done on three separate rounds of differentiation; Shapiro-Wilk test for normality showed the data to be normally distributed. No differences in MAP2 or DAT expression were found following unpaired *t*-test. (D) DAT high intensity puncta, characterised and discovered primarily within the projection of cells.

This section has been redacted by the author for commercial reasons.

This section has been redacted by the author for commercial reasons.

We sought to further characterise this pair of induced dopaminergic neurones by studying the expression of presynaptic protein synaptophysin and post-synaptic density protein 95 (PSD95). Evidence suggests that synaptophysin is expressed earlier in development and levels are liable to decrease with age (Fletcher et al., 1994, Petralia et al., 2014). Therefore, if we were to assess synaptophysin expression throughout the differentiation protocol, we would expect to observe inverse proportionality, with higher expression at the start of the protocol, which decreased over time. On the contrary, PSD95 expression has been found to increase as neurones mature. During neuronal development, PSD95 is regulated post-transcriptionally by polypyrimidine tract binding proteins 1 and 2 (PTBP1 and PTBP2). During embryonic development, the expression of PTBP1 and PTBP2 decreases, allowing the expression of PSD95 to increase with neuronal maturation (Zheng et al., 2012). As our reprogramming protocol doesn't take the cells to an embryonic-like phase, we would potentially not expect to see many changes in PSD95 expression over the course of the differentiation protocol. Furthermore, as neuronal development occurs, it is likely that the distribution of both PSD95 and synaptophysin changes, moving from the cell body to the axons (Chai et al., 2016).

The ICC presented below is the result of preliminary investigations and as such, characterisation was only carried out with control 1 and sPD1 due to time constraints and limited laboratory access due to Covid19 restrictions. However, optimisation wasn't completed fully for sPD1 therefore even though data has been included below, it should be interpreted with caution as further optimisation would have been beneficial.

PSD95 expression was similar between control 1 and sPD1 at 52.6% (± 13.8) and 51.5% (± 32.9) respectively, **figure 3.12B**, meaning there was no difference between the two lines. Synaptophysin expression differed between the lines a small amount with control 1 exhibiting 62.4% (± 16.6) synaptophysin positive cells and sPD1 only 53.6% (± 24.5), **figure 3.12C**. However, this difference was found to be insignificant.

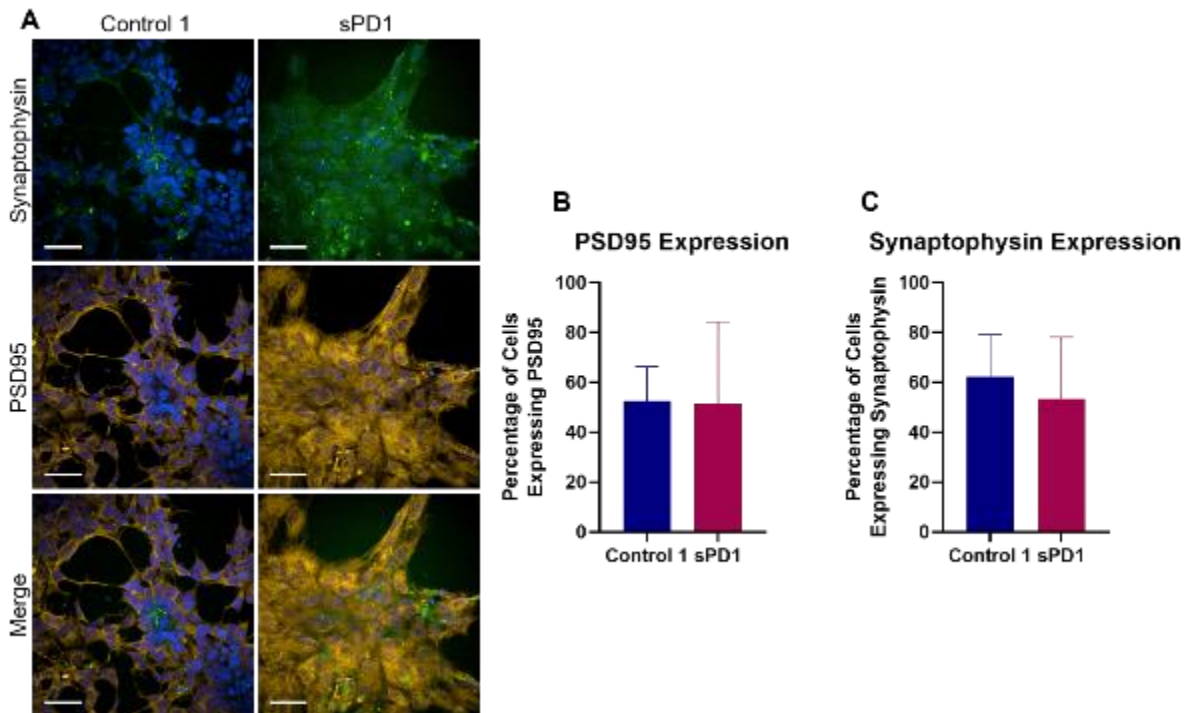


Figure 3.9 PSD95 and Synaptophysin expression in control 1 and sPD1 end stage dopaminergic neurones

Results are expressed as mean \pm standard deviation, $n=3$. (A) Representative images using synaptophysin (green) as a presynaptic marker and PSD95 (orange) as a postsynaptic marker with Hoechst (blue) to label nuclei. Scale bar = $50\mu\text{m}$. 17 fields of view imaged per well (B) Percentage of cells expressing PSD95. Similar percentages of PSD95 positive cells were observed between control 1 and sPD1, however sPD1 was much more variable. We found 52.6% and 51.5% of cells were positive for PSD95 in control 1 and sPD1 respectively. Data normally distributed and unpaired t -test revealed no difference in PSD95 expression (C) Percentage of cells expressing synaptophysin. Control 1 had slightly higher expression than sPD1, 62.5% to 53.6% respectively. Data not normally distributed and t -test followed by Mann Whitney U post-hoc test revealed no difference in synaptophysin expression. Quantification for (B) and (C) was done on three different rounds of differentiation.

This section has been redacted by the author for commercial reasons.

This section has been redacted by the author for commercial reasons.

This section has been redacted by the author for commercial reasons.

This section has been redacted by the author for commercial reasons.

Sporadic PD 2 and Control 2

The neurone differentiation protocol for control 2 and sPD2 differed from the standard protocol in the second stage of differentiation. This is because cell number dramatically decreased over the 10-day FGF/SAG stage, therefore the middle stage of differentiation was reduced to 4 days, followed by the 15-day third stage of differentiation.

Tuj and TH expression was again investigated using ICC and Western blotting. Beginning with ICC, we outlined control 2 to have 87.7% (± 11.3) Tuj positive cells while sPD2 had 75.6% (± 26.0), **figure 3.15B**. Similarly to sPD1, sPD2 had higher TH expression than control 2, 71.1% (± 33.5) and 39.0% (± 15.3) respectively, **figure 3.15C**. Data for both Tuj and TH were normally distributed following Shapiro-Wilk test and the resulting unpaired t-test with Welch's correction highlighted no differences in either Tuj or TH expression between control 2 and sPD2.

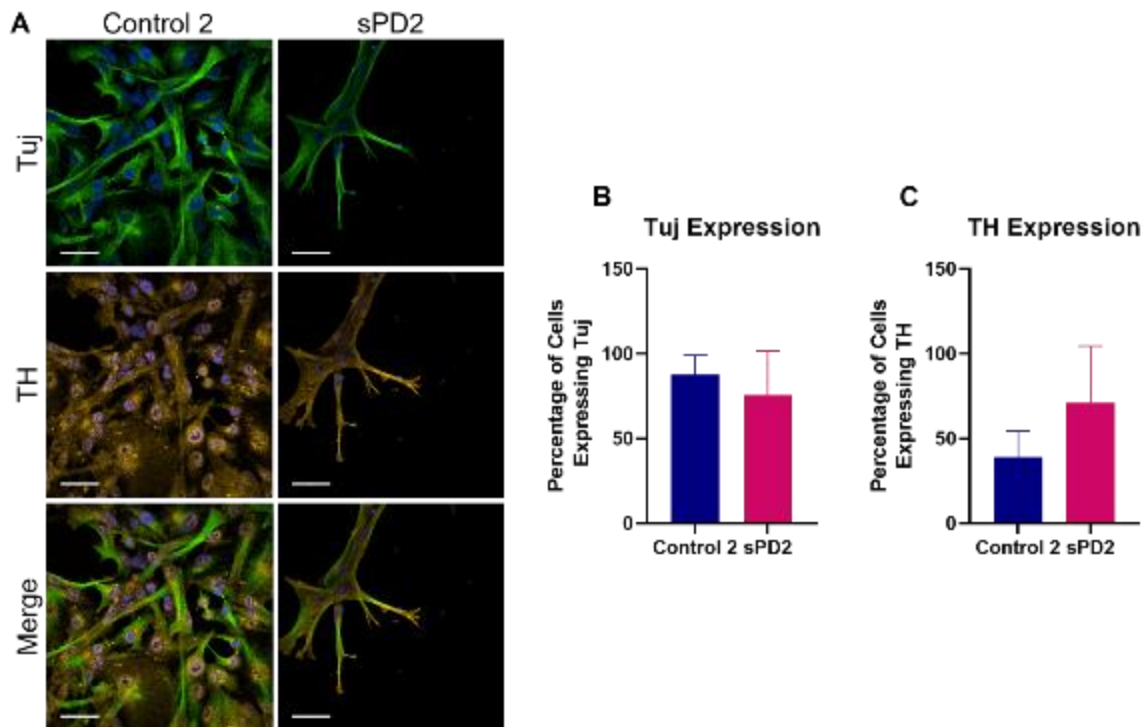


Figure 3.10 Tuj and TH expression in sPD2 and control 2 end stage dopaminergic neurones

Results are expressed as mean \pm standard deviation, $n=3$. (A) Representative images using Tuj (green) as a pan neuronal marker and TH (orange) as a dopaminergic specific marker with Hoechst (blue) to label nuclei. Scale bar = 50 μ m. 17 fields of view imaged per well (B) Percentage of cells expressing Tuj. We found control 2 to contain 87.7% of cells positive for Tuj while sPD2 had 75.6% of Tuj positive cells (C) Percentage of cells expressing TH. TH expression was higher in sPD2 than control 2, 71.1% to 39% respectively. Quantification for (B) and (C) was done on three separate rounds of differentiation; Shapiro-Wilk test for normality followed by unpaired t-test with Welch's correction detailed no significant differences in Tuj or TH expression between control 2 and sPD2.

This section has been redacted by the author for commercial reasons.

This section has been redacted by the author for commercial reasons.

This section has been redacted by the author for commercial reasons.

This section has been redacted by the author for commercial reasons.

Further characterisation of control 2 and sPD2 was also undertaken by investigating MAP2 and DAT expression. ICC revealed 67.1% (± 19.1) of control 2 cells were MAP2 positive while 53.9% (± 28.7) were positive in sPD2, **figure 3.18B**. No difference was observed in MAP2 expression between control 2 and sPD2 following unpaired t-test with Welch's correction. DAT expression was significantly ($p < 0.03$) different between the two cell lines with control 2 exhibiting 15.9% (± 2.2) DAT positive cells while sPD2 had 57.1% (± 13.1), **figure 3.18C**.

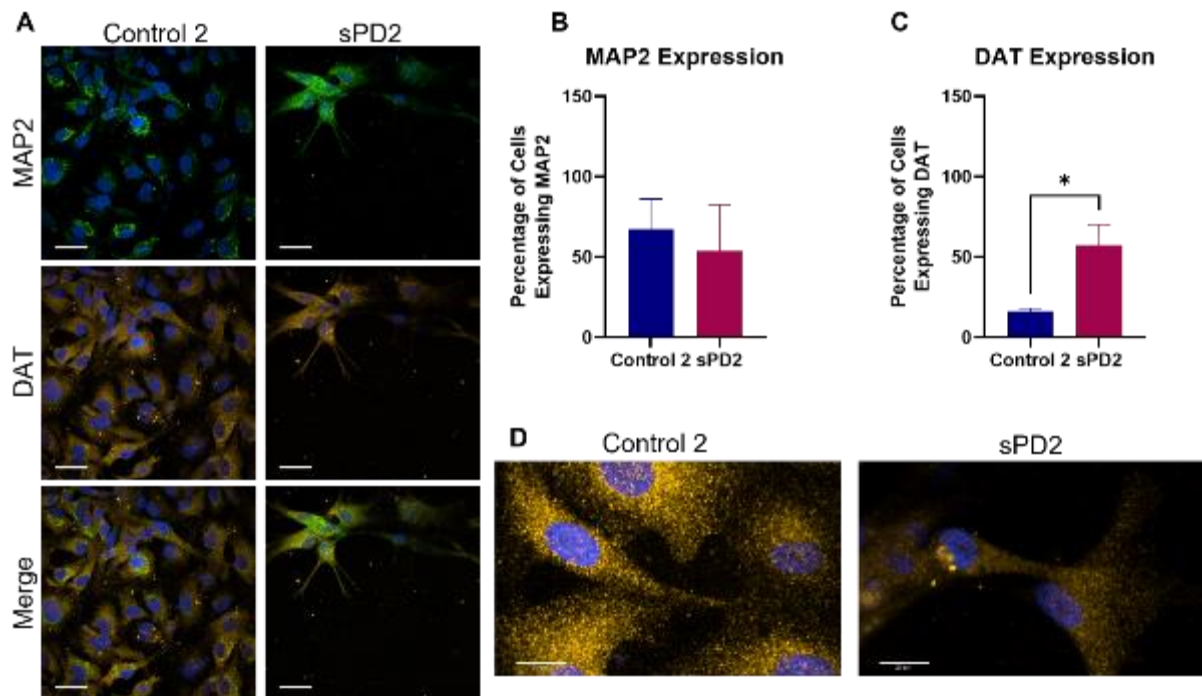


Figure 3.11 MAP2 and DAT expression in control 2 and sPD2 end stage dopaminergic neurones

Results are expressed as mean \pm standard deviation, $n=3$. (A) Representative images using MAP2 (green) as a pan neuronal marker and DAT (orange) as a dopaminergic specific marker with Hoechst (blue) to label nuclei. Scale bar = 50 μ m. 17 fields of view were imaged per well (B) Percentage of cells expressing MAP2. In control 2 this was 67.1% while in sPD2 it was 53.9% (C) Percentage of cells expressing DAT. DAT expression was higher in sPD2 compared to control 2, 57.1% to 15.9% respectively. Quantification for (B) and (C) was done on three separate rounds of differentiation; Shapiro-Wilk test for normality showed the data to be normally distributed. Unpaired t -test with Welch's correction detailed no significant differences in MAP2 expression. A significant difference in DAT expression was observed, $*p<0.05$ (D) DAT high intensity puncta, characterised and discovered primarily within the projection of cells.

This section has been redacted by the author for commercial reasons.

This section has been redacted by the author for commercial reasons.

Alpha Synuclein Mutant and Control 3

The neurone differentiation protocol for the alpha synuclein mutant and control 3 differs from the standard differentiation protocol outlined in the Schwartzenruber (2020) paper. The first two stages of differentiation are the same however due to quickly changing morphology, detachment from the cell culture plates and exhibiting typical neuronal features of clustered cell bodies and elongated projections, the final stage of differentiation is 7-9 days after initiation of stage 3. This is similar to control 1 and sPD1.

ICC revealed 95.6% (± 1.2) of control 3 cells were positive for Tuj, while 84.7% (± 10.9) of the alpha synuclein mutant cells were Tuj positive. Data were normally distributed and quantification via unpaired t-test with Welch's correction highlighted no significance difference in Tuj expression between the pair, **figure 3.20B**.

TH expression was more variable within each line, however 82.4% (± 26.4) and 77.0% (± 37.4) of cells were TH positive in control 3 and the alpha synuclein mutant respectively. Shapiro-Wilks normality tests showed that the data was not normally distributed therefore a Mann Whitney U test was carried out, showing no significant difference in TH expression between control 3 and the alpha synuclein mutant, **figure 3.20C**.

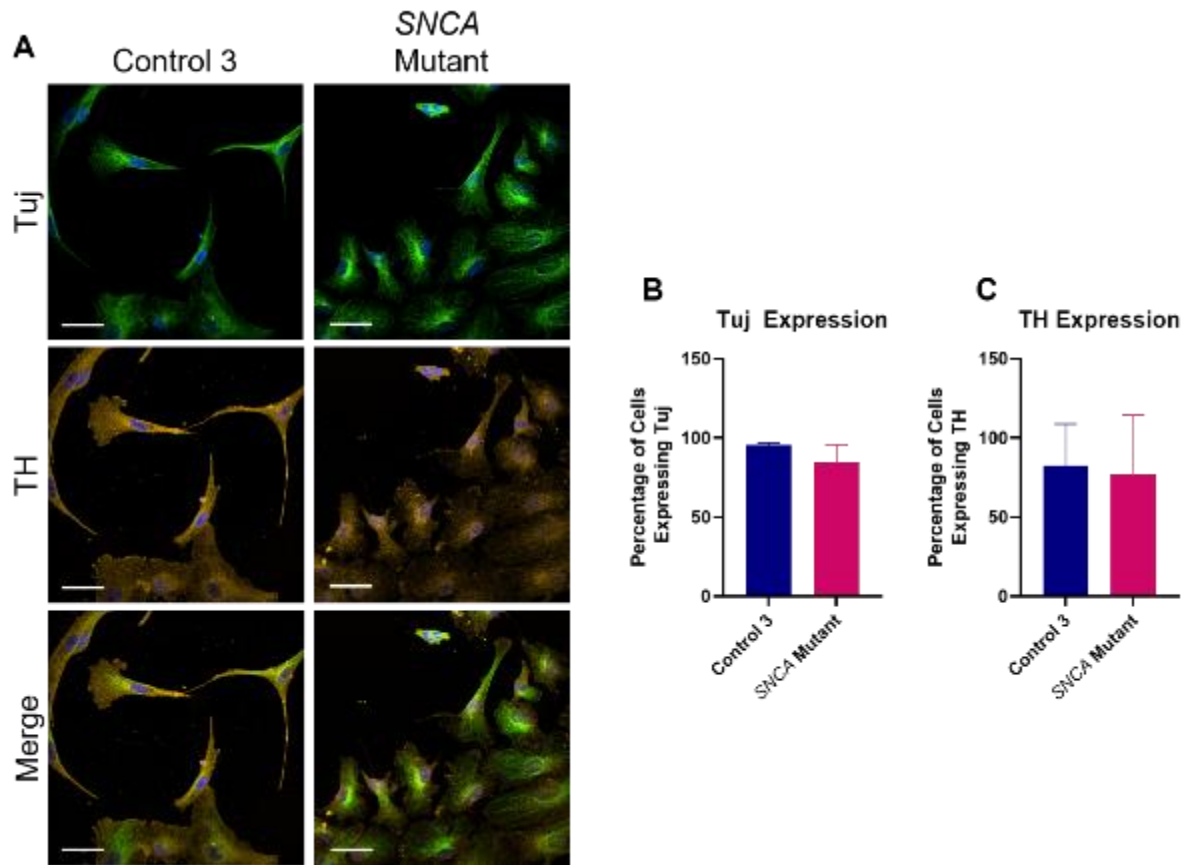


Figure 3.12 TuJ and TH expression in SNCA mutant and Control 3 end stage dopaminergic neurones

Results are expressed as mean \pm standard deviation, $n=3$. (A) Representative images using TuJ (green) as a pan neuronal marker and TH (orange) as a dopaminergic specific marker with Hoechst (blue) to label nuclei. Scale bar = $50\mu\text{m}$. 17 fields of view imaged per well (B) Percentage of cells expressing TuJ. This was found to be 95.6% in control 3 and 84.7% in the alpha synuclein mutant line. Unpaired *t*-test showed no significant difference (C) Percentage of cells expressing TH. This was similar between the two cell lines, 82.4% in control 3 and 77% in the alpha synuclein mutant. *t*-test with Mann Whitney *U* post hoc correction showed no differences in TH expression. Quantification for (B) and (C) was done on three separate rounds of differentiation.

This section has been redacted by the author for commercial reasons.

This section has been redacted by the author for commercial reasons.

This section has been redacted by the author for commercial reasons.

This section has been redacted by the author for commercial reasons.

Further characterisation with MAP2 and DAT discovered that control 3 and the alpha synuclein mutant line exhibited 46.8% (± 16.6) and 46.2% (± 7.0) MAP2 positive cells respectively, **figure 3.23B**.

However, DAT expression was discovered to differ between the two cell lines with control 3 possessing 61.9% (± 3.6) DAT positive while the alpha synuclein mutant line had 43.5% (± 7.4) of cells positive for DAT. This difference was significant ($p < 0.03$) when quantified via unpaired t-test with Welch's correction, **figure 3.23B**.

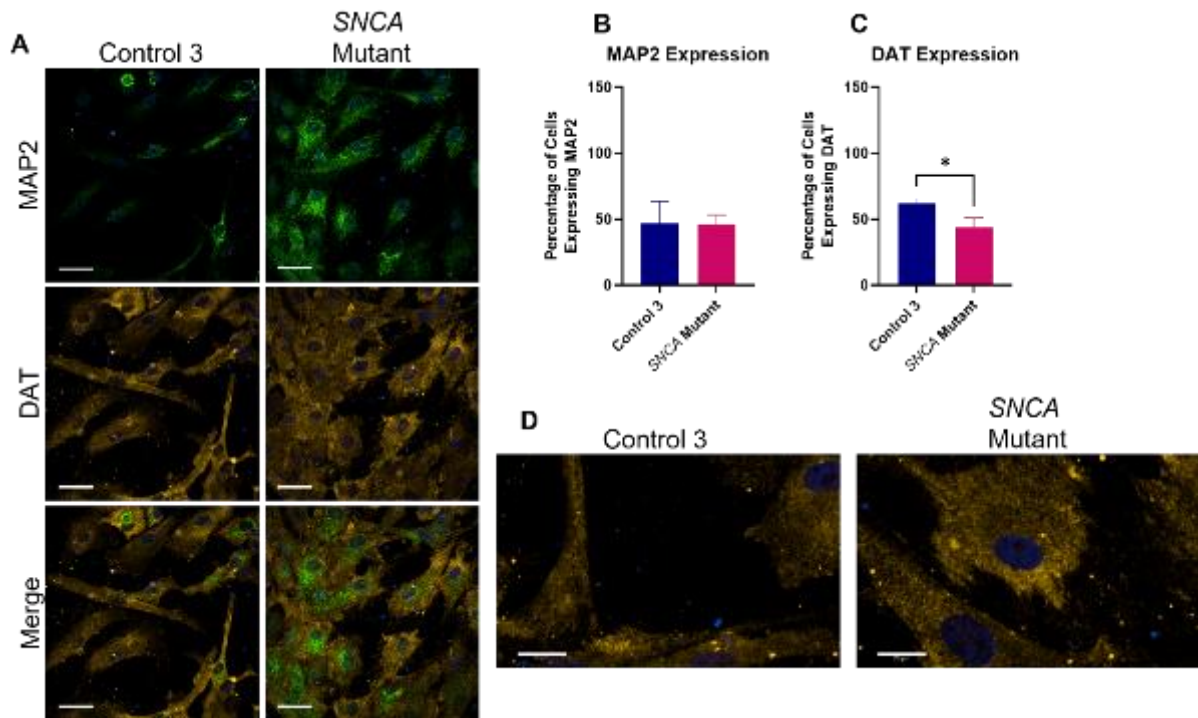


Figure 3.13 MAP2 and DAT expression in control 3 and alpha synuclein mutant end stage dopaminergic neurones

Results are expressed as mean \pm standard deviation, $n=3$. (A) Representative images using MAP2 (green) as a pan neuronal marker and DAT (orange) as a dopaminergic specific marker with Hoechst (blue) to label nuclei. Scale bar = 50 μ m. 17 fields of view were imaged per well (B) Percentage of cells expressing MAP2. This was similar between control 3 and the alpha synuclein mutant line, 46.8% and 46.2% respectively (C) Percentage of cells expressing DAT. DAT expression was higher in control 3, at 61.9% compared to 43.5% in the alpha synuclein mutant line. Quantification for (B) and (C) was done on three separate rounds of differentiation; Shapiro-Wilk test for normality showed the data to be normally distributed. Unpaired t-test with Welch's correction detailed no differences in MAP2 expression but a small, significant, decrease in DAT expression in the alpha synuclein mutant $*p<0.05$ (D) DAT high intensity puncta, characterised and discovered primarily within the projection of cells.

This section has been redacted by the author for commercial reasons.

This section has been redacted by the author for commercial reasons.

3.4 Discussion

Data within this chapter focussed upon characterising the dopaminergic neuronal model used, from the iNPCs to the end stage dopaminergic neurones.

However, the initial drug screen that led to this project utilised fibroblasts to identify Jed135 as the lead compound. Fibroblasts are an extremely valuable tool for studying neurodegenerative diseases. Readily available and relatively low cost, fibroblasts are robust cells that are easy to culture and maintain, providing an excellent model for large primary drug screens. They possess environmental and epigenetic alterations that a person has acquired throughout their life, an important factor for neurodegenerative diseases in which prevalence increases with age (Auburger et al., 2012). However, there are also inherent disadvantages for the use of fibroblasts in neuroscience research. First and foremost, fibroblasts are not the cell type affected in neurodegeneration, in this instance PD, therefore there is a limit to their utility, particularly in drug screening. Early passages (pre passage 3) of fibroblasts are mixed with keratinocytes and infection with skin microorganism *mycoplasma* is possible, potentially causing artificial phenotypes, highlighting the need for regular testing (Auburger et al., 2012). On the contrary, many cells can become post-mitotic at higher passages, hence reducing the proliferation rate (Kálmán et al., 2016). There are major differences in gene expression profiles between fibroblasts and neurones which are important factors to consider when studying neurodegenerative diseases. For example, alpha synuclein is readily expressed in neurones and the protein aggregates within the brain. However, alpha synuclein expression in fibroblasts is minimal (Auburger et al., 2012, Kálmán et al., 2016). Fibroblasts are also much more resilient than neurones and don't form synapses meaning they don't rely on a synergistic relationship, unlike neurones and glial cells (Kálmán et al., 2016).

It is important to consider the role that fibroblasts play in neurodegenerative research, particularly in relation to primary drug screens, before discussing the neuronal model used in this study. Previous drug screens have utilised the beneficial properties of fibroblasts to screen large drug libraries for their mitochondrial rescue effects. In 2013, Mortiboys et al screened a library of 2000 compounds, investigating their effect on MMP, as well as understanding any associated toxicity. This was a 3 stage drug discovery study with more in-depth investigations being performed at each stage. Of the original 2000 compounds, 35 compounds passed through to stage 2 where cellular ATP levels were investigated, leaving a possible 15 compounds to reach stage 3. However following a literature search, only 2 compounds were subjected to more in-depth assessments in understanding the effect of the compounds on the mitochondrial respiratory complexes (Mortiboys et al., 2013). This study

is prime example for the utility of fibroblasts in large scale drug screens and the primary screen associated with the current project was completed in fibroblasts. However, as mentioned, fibroblasts don't possess all the qualities we would expect of neurones and hence the ability to reprogramme fibroblasts into iPSCs or iNPCs and further into induced neurones is invaluable.

As highlighted in the introduction, iPSC derived neurones have provided a method to study disease mechanisms *in vitro* that wasn't available before, allowing us to study brain disease mechanisms in a physiologically relevant model (Wu et al., 2019). iPSCs can be reprogrammed from a variety of somatic cells other than fibroblasts, including blood, urine and dental tissue and there are far fewer ethical implications in generating pluripotent cells via this method compared to collecting human embryonic stem cells (Chang et al., 2019). The similarities of iPSCs to embryonic stem cells are not beneficial when studying neurodegenerative diseases and hence the discovery of iNPCs, a tripotent stem cell able to retain the ageing phenotype of the donor, are a more relevant disease model (Meyer et al., 2014, Gatto et al., 2021) and utilised in this study.

Initially, we sought to functionally characterise the model being used. Fibroblasts have a relatively low metabolic requirement compared to neurones and as such rely on glycolysis as their main source of ATP (Kim et al., 2018). Although less efficient, producing a net gain of 2 ATP molecules per cycle, glycolysis generates ATP more readily than OXPHOS (Bonora et al., 2012, Bell et al., 2020b). In contrast, although the brain represents only 2% of total body mass, it is responsible for 20% of the body's energy demand, highlighting how metabolically active neurones are (Heger et al., 2021). As such, an oxidative switch has been described; ATP generation in neurones is primarily via OXPHOS (Kim et al., 2018, Schwartzentruber et al., 2020), producing approximately 32-34 ATP molecules per cycle in order to keep up with the energy requirements of the neurone (Bonora et al., 2012). Previously, we had not identified the metabolic status of the sporadic and alpha synuclein mutant iNPCs lines that were used in this study; hence, we were interested in investigating whether they were glycolytic or relied upon OXPHOS. In agreement with Schwartzentruber et al (2020), our iNPCs were glycolysis dependent and although ATP was not investigated throughout the differentiation protocol, we can be confident that the oxidative switch would occur and the resulting end stage dopaminergic neurones would be reliant upon OXPHOS (Schwartzentruber et al., 2020).

The dopaminergic neurone differentiation protocol utilised in this study was described previously (Schwartzentruber et al., 2020). Although the protocol length varied, the same neuronal factors were used throughout, albeit at different concentrations due to batch

variations in stocks from our supplier, and it is important to understand their relevance. The first stage of the protocol used DAPT, a gamma secretase inhibitor blocking the Notch signalling pathway (Qi et al., 2017). Notch signalling inhibits the differentiation of neurones and promotes gliogenesis, highlighting the importance of its inhibition (Koch et al., 2013).

The second stage of differentiation utilised FGF8 and SAG. FGF8 has been found to promote the maturation of the iNPCs into dopaminergic neurones (Lim et al., 2015) and improve survival (Stathakos et al., 2021), while SAG activates the sonic hedgehog signalling pathway, promoting neurogenesis and the survival of neuronal cells *in vitro* (Bragina et al., 2010).

In the third stage of the differentiation protocol, cells were incubated with a cocktail of 5 different factors that all played a pivotal role in the final differentiation. BDNF has been described as being able to enhance both neuronal growth and the activity of synapses in hippocampal cells in culture (Bartrup et al., 1997), while also activating NTRK2 receptors to enhance survival of neurones (Stathakos et al., 2021). GDNF is a member of the TGF β superfamily and used to support the differentiation of dopaminergic neurones in culture (Roussa and Krieglstein, 2004). Previous studies have highlighted TGF β as being able to increase TH expression in cultures as it is able to promote a dopaminergic lineage (Roussa et al., 2009), while d-cAMP also aids in the upregulation of TH synthesis (Stathakos et al., 2021). Although not directly linked to neuronal or dopaminergic differentiation, ciprofloxacin is an important addition to the culture medium as it is an antibiotic, part of the fluoroquinolone family, and able to prevent *mycoplasma* infection (Schmitt et al., 1988). This was particularly important as our cells were in culture plates for a long length of time. There is conflicting evidence in the literature surrounding the addition of ciprofloxacin to cell culture models and the impact this may have on the cells. Some studies suggest that ciprofloxacin can diminish cell growth rate (Romorini et al., 2013), as well as causing the upregulation of apoptotic and inflammation related genes (Salimiaghdam et al., 2020), while others have noted no side effects. More specifically, those who didn't find ciprofloxacin to have any effect on their cell culture model reported that concentrations up to 5 μ g/ml had no inhibitory effect, however concentrations of 25-50 μ g/ml were able to inhibit colony formation in healthy and leukemic bone marrow cells (Somekh et al., 1989). However, the above mentioned studies are all carried out in different cell models systems, which are seemingly all different to the model system used in this study, therefore we cannot draw any solid conclusions. In relation to this study, at the stage in which ciprofloxacin is added to our cultures, the induced dopaminergic neurones are no longer proliferative, therefore ciprofloxacin will not influence growth rate. However, we should be aware of the potential to increase apoptotic and

inflammatory related genes. This was not something that we investigated in this study and as such we are unable to comment on the impact it would have but considering the role that the mitochondria play in apoptosis, we should be aware when interpreting our data. On the contrary, it should be noted that we only used ciprofloxacin at a concentration of 1 µg/ml, a concentration that was deemed to have no effect on cells in a previous paper (Somekh et al., 1989).

We sought to identify any basal mitochondrial phenotypes in the differentiated neurones. Neurones are post-mitotic meaning they no longer divide, therefore rely upon the dynamics of the mitochondrial network to ensure the equal distribution of metabolites as well as meeting the energy demand of different parts of the cell (Heger et al., 2021). Mitochondrial dynamics incorporates fission and fusion and was mentioned previously in section 1.2.2. The balance between fission and fusion is responsible for mitochondrial size and length and also isolating dysfunctional mitochondria, enabling them to be degraded via mitophagy. Our characterisation was able to identify distinct mitochondrial phenotypes within the pairs of sporadic lines. sPD1 showed a significant increase in number of mitochondria per cell whilst also possessing a more fragmented mitochondrial network which may account for this increase. Whereas there was no difference in mitochondrial number in sPD2, yet it still had a more fragmented network. In contrast to sPD1, sPD2 had a deficit in percentage of mitochondria undergoing mitophagy as well as harbouring more depolarised mitochondria. The observation here of differing mitochondrial phenotypes is not uncommon. Several studies have highlighted differences in total number of mitochondria as well as fragmentation state, with different genetic factors potentially having an impact. A paper in 2012 described abnormal morphology and turnover of mitochondria in iPSC-derived neurones from *Parkin* patients but not in the fibroblasts or iPSCs of the same lines. They also observed a decrease in cytoplasmic volume density of mitochondria compared to controls (Imaizumi et al., 2012), synonymous with a reduced number of mitochondria. On the contrary, iPSC-derived neuroepithelial cells (NESCs) with the *LRRK2-G2019S* mutation have significantly more mitochondria per cell than their isogenic controls which were also found to be more fragmented via the Feret ratio (Walter et al., 2019). In contrast, mitochondria from *Parkin* knockout cells have been described to possess a more elongated phenotype (Bogetofte et al., 2019). This evidence suggests that opposing phenotypes are possible within the PD population and although cells from sporadic patients are being used here, it is possible that different genetic influences are at play that are unidentified. There is evidence to suggest that stratification of patients may be beneficial in future treatments for PD. Carling et al (2020) were recently able to identify sub-groups within a cohort of iNPC-derived dopaminergic neurones from sporadic patients, stratifying into groups based on

mitochondrial or lysosomal dysfunction (Carling et al., 2020). Therefore, it is possible that the two sporadic patient lines used here could be further sub-grouped.

The overarching aim of this project wasn't to fully characterise the functionality of the model used; therefore, we didn't investigate this any further. However, it is important to consider how we could have investigated the functionality of the *in vitro* model used if needed. Neurones rely upon electrical impulses within the brain and reliable *in vitro* models would also possess this characteristic. An alternative method to measure cellular membrane potential in a stem cell derived neuronal population is via patch-clamp. The patch-clamp method is able to measure single-channel currents or whole cells and relies on a small glass pipette filled with solution being inserted into a membrane (Petersen, 2017), allowing the current flowing across the membrane to be measured. However, a second alternative method to measure neuronal membrane potential has been described. FluoVolt is a voltage sensitive, fast responding dye that responds to membrane potential changes in sub-milliseconds, releasing a high emission signal (Pakhomov et al., 2017). It is a relatively new, commercially available probe, with few studies having been published at present, however it has been proven to be accurate and reliable at measuring membrane potential (Bedut et al., 2016, Pakhomov et al., 2017).

We also completed a comprehensive characterisation of our dopaminergic neurones by investigating their expression of pan neuronal and dopaminergic markers. Although the protocol was altered for each of the cell lines, the expression of the neuronal and dopaminergic markers were still present, albeit in varying amounts. Pan neuronal markers Tuj and MAP2 were convincingly apparent in all lines and the distribution pattern we observed was as expected. Previous work from our group has demonstrated that dopaminergic neurones differentiated from other iNPCs express a range of pan neuronal and dopaminergic makers which increase throughout the differentiation protocol. Most notably, at the end stage of differentiation, they observed 94.5% of Tuj positive cells and 87.9% of MAP2 positive cells (Schwartzentruber et al., 2020). Conversely to iNPCs, a recent meta-analysis was able to illustrate the vast heterogeneity in Tuj expression following differentiation of dopaminergic neurones from iPSCs, regardless of whether the same differentiation protocol was used. They reported an average Tuj expression of 64% of the total cellular population across the 67 studies analysed (Tran et al., 2020). A third neuronal specific stain that could have been utilised in this project is neuronal nuclear protein (NeuN). NeuN is commonly investigated following stem cell differentiation as it is a marker of mature neurones (Gusel'nikova and Korzhevskiy, 2015). Discovered in 1992, it is found exclusively in nervous tissues with no evidence of its existence in glial cells (Gusel'nikova and

Korzhevskiy, 2015). Furthermore, our group have previously identified 76.5% of induced dopaminergic neurones, generated from iNPCs, to be positive for NeuN (Schwartzentruber et al., 2020).

Expression of dopaminergic markers TH and DAT varied throughout the lines; however we observed a distribution pattern that we would expect. We illustrated high intensity puncta of both TH and DAT with varying localisations, TH within the cell body and DAT primarily within the processes. Although not significant, it appears that in most cases, the patient lines possessed increased TH and DAT expression levels compared to the controls. Although not ideal, this is potentially because the differentiation protocols were altered and shortened due to the patient lines being unpredictable. As such, differentiation of the controls lines could have been extended to increase dopaminergic marker expression however this would have meant differing differentiation times between control and patient lines and therefore was not used. Previous work from our group using different lines was able to identify 89.9% of cells positive for TH using the same protocol (Schwartzentruber et al., 2020), providing further evidence that the lower TH expression observed in this thesis is likely due to the shortened protocol. The aforementioned meta-analysis investigating iPSC derived dopaminergic neurones discovered that throughout the 67 studies analysed, dopaminergic neurones, assessed via TH expression, made up 27% of the total cellular population. However, this figure varied greatly between papers, likely due to assays and analyses being completed at different time points of the maturation process (Tran et al., 2020). Furthermore, differences in arbitrary intensity levels may differ between studies, as well as considering single cell populations vs multicellular populations, with some groups reporting the presence of astrocytes and other neuronal subtypes within their populations, thus adding to the discordance between papers (Tran et al., 2020).

We also observed DAT expression to be lower than TH. The previous paper from our group also found this to be true, indicating that 82.4% of cells were positive for DAT. However, it should be noted that it was more challenging to segment the DAT puncta on the analysis software.

An alternative method of investigating dopamine content is via neurosensor521. Neurosensor521 was developed to selectively recognise catecholamines present within neurosecretory vesicles in both live and fixed cells (Hettie et al., 2013). This stain would have allowed us to measure the dopamine content throughout differentiation and assess how the dopamine content increases throughout the protocol. However, as alluded to previously, neurosensor521 is not dopamine specific, it is able to recognise other

catecholamines, for example noradrenaline (Hettie et al., 2013) and therefore the results should be interpreted with caution.

Other neuronal markers are available to assess the success of the differentiation protocol. In this project we utilised synaptophysin, an abundant molecule found on synaptic vesicles in nervous tissue (Glantz et al., 2007, Kokotos et al., 2019) and PSD95, a post-synaptic protein.

Overall, this chapter has provided a comprehensive characterisation of the iNPC and dopaminergic neuronal model used. It has highlighted the advantages of an iNPC derived neuronal model compared to an iPSC derived neuronal model and has considered the basal mitochondrial deficits of the samples used. It should be taken into consideration however that the data presented in this chapter is from two sporadic cases of PD and one alpha synuclein triplication and the results may not be indicative of an entire PD cohort.

4 Parkinson's Disease Relevant Mechanisms

4.1 Background

Our understanding regarding the complexities of PD has increased over the years however there are still a multitude of unanswered questions. As mentioned previously, there are some known causes of PD such as genetic mutations and exposure to pesticides, herbicides and mitochondrial toxins such as MPTP and rotenone that cause Parkinsonian-like features or increase the risk of developing PD (Balestrino and Schapira, 2020). However, these only account for a small proportion of PD cases meaning the majority have no known cause. That said, the same pathophysiology is observed between sporadic and familial; a loss of dopaminergic neurones in the SNpc of the brain, resulting in the characteristic triad of main motor symptoms.

4.1.1 Alpha Synuclein

The key underlying factor in PD pathology is the aggregation of alpha synuclein, a small, 14kDa, protein encoded by the *SNCA* gene (Emamzadeh, 2016), found at position 21 of the long arm of chromosome 4 (Manzanza et al., 2021). Alpha synuclein is primarily expressed in the central nervous system (Jakes et al., 1994) however it is also ubiquitously expressed throughout the body, with reports identifying it in the heart, muscle, blood and kidney to name a few (Burré et al., 2018). Cellularly, alpha synuclein exists in the cytosol in a natively disordered, unfolded state, accounting for approximately 1% of the total cytosolic protein (Fauvet et al., 2012, Manzanza et al., 2021). Localisation of alpha synuclein has been debated within the literature. Initially characterised in the Pacific electric ray (*Torpedo Californica*) in 1988 by Maroteaux et al, they described alpha synuclein at both the presynaptic terminal and the nucleus (Maroteaux et al., 1988), giving it the name synuclein, however very few subsequent studies have corroborated the nuclear localisation (Goers et al., 2003, Yu et al., 2007).

Alpha synuclein has been linked to a number of different functions within the cell, however the physiological relevance of these remains undetermined (Burré et al., 2018). There is no over-riding consensus regarding the physiological function of alpha synuclein (Villar-Piqué et al., 2016) thus understanding its pathological role in disease is difficult. That said, it has been suggested to be involved in the following processes: suppression of apoptosis by reducing expression of protein kinase C (Jin et al., 2011), regulation of glucose levels via interaction with insulin secretory vesicles (Geng et al., 2011), chaperone activity through interaction with synaptobrevin 2, regulating the assembly and disassembly of the SNARE complex (Burré et al., 2010), antioxidation via the interaction of monomers with membrane

phospholipids (Zhu et al., 2006) and regulation of dopamine biosynthesis through interaction with its precursor tyrosine hydroxylase (Yu et al., 2004). Furthermore, alpha synuclein's presynaptic localisation and role in the SNARE complex assembly also suggests that it is involved in neurotransmitter release and synaptic plasticity, although loss of alpha synuclein has no effect on neurotransmitter release, therefore its function here may be transient (Burré et al., 2018).

Alpha synuclein is composed of three domains, a lipid-binding N-terminus (residues 1-60), the non-amyloid beta component (NAC region, residues 61-95) and the acidic carboxyl tail (residues 96-140) (Cho et al., 2009, Lashuel et al., 2013, Emamzadeh, 2016). The N-terminal domain has the ability to interact with phospholipids in cell and organelle membranes in an alpha helical confirmation (Emamzadeh, 2016, Manzanza et al., 2021) and is comprised of four eleven-dimer repeats (Manzanza et al., 2021). Evidence suggests that alpha synuclein has a preference towards binding lipids possessing a negatively charged head group due to its plethora of lysine residues in the N-terminal domain (Emamzadeh, 2016). It has also been suggested that alpha synuclein bears preference to certain phospholipids over others, namely phosphatidic acid (PA), phosphatidylethanolamine (PE) and phosphatidylinositol (PI) (Emamzadeh, 2016). The NAC region is inherently hydrophobic (Manzanza et al., 2021) and able to alter the confirmation of alpha synuclein, allowing it to form beta-sheet structures which aid in its propensity to aggregate (Emamzadeh, 2016). Interestingly, many genetic mutations known to contribute to synucleinopathies are also located within the NAC region (Manzanza et al., 2021). Finally, the C-terminal domain contributes to the overall solubility of alpha synuclein. It possesses a net negative charge which provides flexibility and supports its unstructured confirmation (Emamzadeh, 2016, Manzanza et al., 2021). In addition, the C-terminal domain appears to be the site many post-translational modifications (Manzanza et al., 2021). Post-translational modifications are alterations to the protein which are able to alter its secondary structure as well as impact cellular localisation, binding affinity and degradation to name a few (Manzanza et al., 2021). Alpha synuclein is subjected to a large number of different post translational modifications including, but not limited to, phosphorylation, nitration, acetylation and glycosylation. However, by far the most studied is phosphorylation, particularly of serine 129 (Manzanza et al., 2021). Multiple kinases have been described to phosphorylate serine 129 including casein kinase II which promotes fibrilisation (Fujiwara et al., 2002) and G-protein coupled receptor kinase 2 which enhances the rate of alpha synuclein oligomerisation in *Drosophila* (Feany and Bender, 2000). Previous work described healthy individuals to possess only 4% of alpha synuclein phosphorylated at serine 129, compared to over 90% in people with PD, highlighting the probable pathogenic role of this modification (Kahle et al., 2000, Fujiwara et

al., 2002, Manzanza et al., 2021). Similarly, Anderson et al discovered that alpha synuclein present within Lewy bodies was also preferentially phosphorylated at serine 129 (Anderson et al., 2006). However, it has been postulated that phosphorylation of serine 129 isn't a prerequisite for Lewy body formation, it likely occurs once the Lewy body has been formed (Paleologou et al., 2010). Serine 129 phosphorylation is believed to increase neurotoxicity in PD by increasing the formation of alpha synuclein oligomers. In its natively disordered state, alpha synuclein exists as monomers with each monomer possessing a life span depending upon its intramolecular interactions (Alam et al., 2019). These monomers have the propensity to aggregate when the balance between production and clearance is altered, resulting in the formation of different sized oligomers, ranging from several to hundreds of monomers (Du et al., 2020). The heterogeneity that is present within the oligomeric alpha synuclein pool, coupled with the fact that the oligomers are soluble and unstable, means little is known about their structure and they represent a great challenge in the understanding of PD mechanisms (Du et al., 2020).

Oligomers are believed to represent alpha synuclein in its most toxic state, causing cytotoxicity via a plethora of mechanisms including mitochondrial dysfunction, neuroinflammation and apoptosis (Du et al., 2020). Larger aggregates of alpha synuclein exist in the form of fibrils; stable structures which exhibit less neurotoxicity than their oligomeric counterparts (Lashuel et al., 2013). Fibrils form the basis of Lewy bodies and it is believed they are created in a bid to sequester the toxic oligomers and act as a neuroprotective mechanism (Bengoa-Vergniory et al., 2017).

PD pathology is widely acknowledged to begin many years before symptom onset. This includes the spreading capabilities of alpha synuclein. There have been several mechanisms hypothesised for alpha synuclein spread throughout the brain, however, a single unified consensus has not been agreed (Jan et al., 2021). Perhaps the most widely accepted method of alpha synuclein spread was first described by Braak et al in 2003. Briefly, they began by hypothesising that alpha synuclein aggregation is initiated in peripheral regions such as the olfactory bulb, potentially due to the presence of a pathogen or toxin (Jan et al., 2021). They proposed a staging system (1-6) of alpha synuclein spread in which stages 1 and 2 detect alpha synuclein aggregation in the olfactory bulb with spread along the vagus nerve to the medulla oblongata, with caudal rostral spread to the pontine tegmentum (Braak et al., 2003b). Further spread into the midbrain, particularly the SNpc, and basal forebrain are indicative of stages 3 and 4 (Braak et al., 2003b). Finally, stage 5 and 6 includes pathology being observed in the neocortex, particularly in high order sensory areas (Braak et al., 2003b). The involvement of the midbrain at stage 3 suggests that pathological alpha

synuclein deposition can occur without a disease phenotype being present, suggesting that PD can be categorised into phases; stage 1 and 2 representing pre-symptomatic, stage 3 and 4 early symptomatic and stages 5 and 6 late symptomatic (Jan et al., 2021). More recently, it has been postulated that the enteric nervous system of the gut may also be involved in the initiation of alpha synuclein aggregation which may explain early non-motor symptoms of PD such as constipation (Krogh et al., 2008, Jan et al., 2021). Several animal studies have corroborated this hypothesis following gut inoculation with alpha synuclein pre-formed fibrils resulting in alpha synuclein aggregates being discovered in the dorsal motor nucleus, via the vagus nerve (Holmqvist et al., 2014, Uemura et al., 2018, Kim et al., 2019). However, spreading past the dorsal motor nucleus has not consistently been identified (Jan et al., 2021).

4.1.2 Alpha Synuclein and its Interaction with the Mitochondria

Alpha synuclein interacts with lipid membranes via its N-terminal domain and its interaction with the mitochondria has been reported in many experimental models, as reviewed by (Pozo Devoto and Falzone, 2017). Interestingly, much of the literature is conflicting regarding how alpha synuclein interacts with the mitochondria and in particular the physiological role it plays. Some report that alpha synuclein does not contain a mitochondrial targeting sequence and instead interacts with mitochondrial associated membranes (Guardia-Laguarta et al., 2014) whereas others suggest a 32 amino acid sequence present within the N-terminal domain that contains a cryptic mitochondrial targeting sequence (Devi et al., 2008). Reports also differ regarding the mitochondrial location of alpha synuclein, with some describing an OMM location (Cole et al., 2008, Pozo Devoto and Falzone, 2017), others an inner membrane location (Devi et al., 2008, Pozo Devoto and Falzone, 2017) and a further subset providing evidence that alpha synuclein exists in the mitochondrial matrix (Zhang et al., 2008, Pozo Devoto and Falzone, 2017). The mitochondrial location of alpha synuclein is likely linked to its function, with a role in mitophagy and mitochondrial bioenergetics having been proposed (Risiglione et al., 2021). It has also been reported that physiologically, alpha synuclein may play a role in mitochondrial respiration via the OXPHOS pathway. A 2005 study using *SNCA* null mice described not only a 23% reduction in CL content but also a decrease of 15% in linked complex I/III activity (Ellis et al., 2005). Similarly, alpha synuclein has also been associated with complex V, ATP synthase. It has been described that physiologically, monomeric alpha synuclein has a role in the maintenance of ATP synthase, regulating its activity (Ludtmann et al., 2016). However, under pathological conditions, the aggregation of alpha synuclein increases the formation of beta sheets that are able to interact with ATP synthase, as well as complex I, causing oxidative stress (Ludtmann et al., 2018) and a decrease in overall ATP concentrations within

the cell. It is likely that alpha synuclein's interaction with the mitochondria is tightly regulated and a threshold level may be present in order to maintain synergy (Vicario et al., 2018).

4.1.3 Mitophagy

The role of mitochondrial dysfunction has already been discussed in the introduction, however in this chapter, we are specifically investigating mitophagy. Mitophagy is the selective removal of old, damaged or dysfunctional mitochondria from a cell to ensure there is a constant pool of healthy mitochondria, therefore acting as a quality control mechanism (Corti, 2019). There are a number of different mitophagy pathways, however the most well characterised is the Parkin/PINK1 pathway. Briefly, PINK1 is targeted to the mitochondria via its mitochondrial targeting sequence (Geisler et al., 2010) and upon translocation, is imported into the mitochondria. Under normal physiological conditions, the PINK1 mitochondrial targeting sequence is degraded while presenilin-associated rhomboid-like protease (PARL) cleaves the transmembrane domain of PINK1 (Truban et al., 2017). These cleavage points result in a generalised break down of PINK1 and thus no accumulation of PINK1 at the OMM (Wei et al., 2015). However, under mitochondrial stress or depolarisation of the mitochondrial membrane, PINK1 is stabilised at the OMM by autophosphorylation at 3 residues, serine 228, threonine 257 and serine 402 (Truban et al., 2017) allowing recruitment of the E3 ubiquitin ligase, parkin through phosphorylation at serine 65 (Narendra et al., 2010, Truban et al., 2017). Parkin is able to ubiquitinate several proteins at the OMM, including mitofusin, mitochondrial fission protein and VDAC1, **figure 4.1**. The ubiquitination of OMM proteins allows for the recruitment of autophagy receptors such as P62 and optineurin, which are able to interact with light chain 3-II (LC3-II) on the surface of an extending phagophore membrane which, once fully encapsulated, forms the autophagosome. The autophagosome is then able to fuse with a lysosome for proteolytic degradation (Glick et al., 2010, Durcan and Fon, 2015).

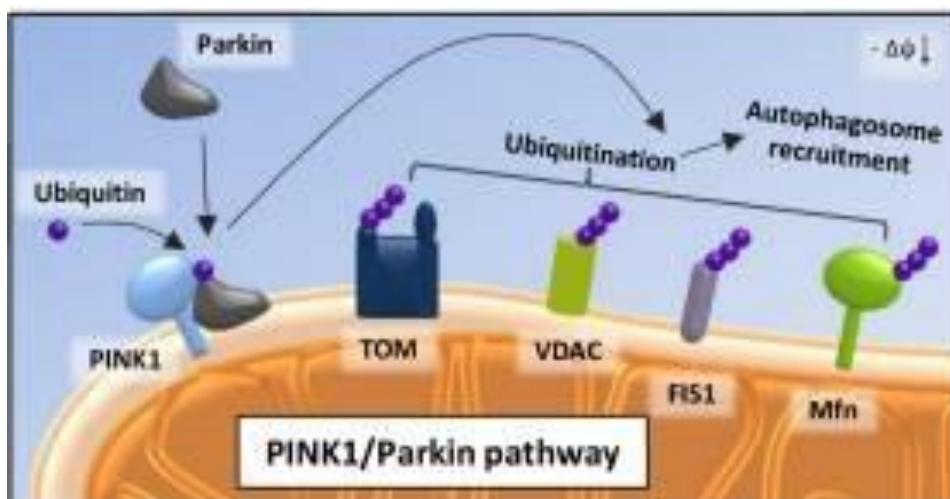


Figure 4.1 Illustrating the Parkin/PINK1 dependent mitophagy pathway

PINK1 accumulates at the outer mitochondrial membrane under mitochondrial stress. This recruits parkin to the mitochondria, resulting in the ubiquitination of several outer mitochondrial membrane proteins. Ubiquitination causes the recruitment of the LC3 positive autophagosome and thus the mitochondria is removed from the cell. Adapted from figure 1 (von Stockum et al., 2018). Used under the creative commons attribution license (CC-BY)

This pathway can become dysfunctional in PD. PINK1 is known to work directly upstream of parkin, and therefore functional PINK1 is vital for this pathway to proceed (Geisler et al., 2010). There are known genetic mutations in the genes that encode PINK1 and parkin. Mutations in these genes cause autosomal recessive disease, with symptom presentation below 40 years of age, however the phenotypes tend to be less aggressive, with slower progression and good response to medication (Truban et al., 2017). Drug targets within this pathway have since been identified, attempting to rectify the dysfunction observed. These include small molecules to target PINK1 via an increase in autophosphorylation, binding at allosteric sites (Miller and Muqit, 2019). *In vivo* studies are still in their infancy regarding these small molecules, however there is hope that they may yield efficacious results. Similarly, small molecules to activate parkin are also in development, however there is no *in vivo* data currently available (Miller and Muqit, 2019).

Mitochondrial dysfunction and alpha synuclein aggregates are both well characterised in PD in their own right, however it is reasonable to assume that dysregulation of both the mitochondria and alpha synuclein have the propensity to exacerbate further dysfunction on each other.

4.2 Aims and Objectives

The aim of this chapter was to investigate the alpha synuclein phenotype of the sporadic and alpha synuclein mutant patient and control cell lines and to discover whether Jed135 or UDCA could alter this phenotype. We also sought to characterise any differences in mitophagy and assess the effect of Jed135 and UDCA on basal and induced mitophagy. We achieved this by:

- Investigating total alpha synuclein expression via Western blotting
- Investigating total and phosphorylated alpha synuclein via ICC
- Assessing the interaction between ATP synthase and filamentous alpha synuclein via ICC
- Measuring mitophagy under both basal and induced conditions and assessing any drug effect

4.3 Results

4.3.1 Alpha Synuclein Expression

Total alpha synuclein expression was assessed via Western blotting. As mentioned in the materials and methods, alpha synuclein can be notoriously difficult to detect via Western blotting due to its small size and the fact it is extremely labile, washing off the membrane when a standard protocol is followed (Lee and Kamitani, 2011). Therefore, following transfer, we fixed the membrane in 4% PFA prior to blocking.

We were able to detect total alpha synuclein expression in both iNPCs and induced dopaminergic neurones in most lines, however we observed considerable variability.

Firstly, results generated from control 1 and sPD1 displayed a high level of variability. Both control 1 and sPD1 showed expression of alpha synuclein in iNPCs and induced dopaminergic neurones, however the difference between the 2 cell types and also between control and patient was too variable to be able to draw conclusions. There appears to be lower expression of alpha synuclein in the sPD1 induced dopaminergic neurones compared to the iNPCs which is counter to our expectations, **figure 4.2A**.

This section has been redacted by the author for commercial reasons.

This section has been redacted by the author for commercial reasons.

4.3.2 Total and Phosphorylated Alpha Synuclein Expression

This section has been redacted by the author for commercial reasons.

This section has been redacted by the author for commercial reasons.

This section has been redacted by the author for commercial reasons.

This section has been redacted by the author for commercial reasons.

This section has been redacted by the author for commercial reasons.

This section has been redacted by the author for commercial reasons.

This section has been redacted by the author for commercial reasons.

This section has been redacted by the author for commercial reasons.

This section has been redacted by the author for commercial reasons.

This section has been redacted by the author for commercial reasons.

This section has been redacted by the author for commercial reasons.

This section has been redacted by the author for commercial reasons.

4.3.3 ATP5a and Alpha Synuclein Filament Expression

Previous research has suggested a pathogenic role for oligomeric alpha synuclein at the mitochondria, specifically in association with ATP synthase (Ludtmann et al., 2018).

Therefore, we were interested in investigating this within our induced dopaminergic cell model and completed it by ICC. We used antibodies targeted against ATP5a, a subunit of ATP synthase, and a conformation specific alpha synuclein filament.

This section has been redacted by the author for commercial reasons.

This section has been redacted by the author for commercial reasons.

This section has been redacted by the author for commercial reasons.

This section has been redacted by the author for commercial reasons.

We were also interested in the amount of co-localisation of the two stains. We investigated this on the Harmony software by assessing where the signal from the two stains overlapped, **figure 4.8A**, and expressed this as a percentage of the total mitochondrial population.

This section has been redacted by the author for commercial reasons.

This section has been redacted by the author for commercial reasons.

This section has been redacted by the author for commercial reasons.

This section has been redacted by the author for commercial reasons.

This section has been redacted by the author for commercial reasons.

This section has been redacted by the author for commercial reasons.

This section has been redacted by the author for commercial reasons.

Control 3 and Alpha Synuclein Mutant

We were also able to assess ATP5a and alpha synuclein filament in control 3 and the alpha synuclein mutant line. However, it should be noted that the data presented below is from 1 technical repeat, therefore results should be interpreted with caution as more repeats are necessary for validation.

This section has been redacted by the author for commercial reasons.

This section has been redacted by the author for commercial reasons.

This section has been redacted by the author for commercial reasons.

This section has been redacted by the author for commercial reasons.

This section has been redacted by the author for commercial reasons.

This section has been redacted by the author for commercial reasons.

4.3.4 Alpha Synuclein Results Overview

In order to easily visualise the alpha synuclein results presented above, **table 4.1** has been generated.

Table 4.1 Summary Table of Alpha Synuclein Results

Green upwards arrows represent an increase compared to its paired line, red downwards arrow represents a decrease compared to its paired line and an orange = represents no difference between paired control and patient lines

	Control 1	Control 2	Control 3	sPD1	sPD2	SNCA Mutant
Total Alpha Synuclein Expression (Western Blot)	↑		↓	↓		↑
Total Alpha Synuclein Expression (ICC)	=	↑		=	↓	
Phosphorylated Alpha Synuclein Expression	↑	↓		↓	↑	
Colocalisation of Total and Phosphorylated Alpha Synuclein	=	↓		=	↑	
Mitochondrial Number (ICC)	↓	=	=	↑	=	=
Alpha Synuclein Filament Expression	↓	↓	↑	↑	↑	↓
Colocalisation of Alpha Synuclein and Mitochondria	↓	↑	↓	↑	↓	↑

4.3.5 Basal Mitophagy

Following from the data presented in chapter 3, neuronal characterisation, we performed live basal mitophagy assays to assess the number of mitochondria and lysosomes present per cell, as well as investigating the percentage of mitochondria undergoing mitophagy and measuring the fragmentation of the mitochondria. This information was gathered to present us with an understanding of any physiological differences in the aforementioned parameters between the control and patient induced dopaminergic neurones. The data presented in chapter 3 was gathered from the untreated condition of time point 3, whereas in this chapter, we were interested in investigating whether Jed135 or UDCA could affect these parameters.

This was a live, time lapse assay, however we observed minimal differences between the time points. In order to illustrate the lack of differences, we are presenting data from two time points, one close to the start, 3, and one towards the end of the assay, 11.

This section has been redacted by the author for commercial reasons.

This section has been redacted by the author for commercial reasons.

This section has been redacted by the author for commercial reasons.

This section has been redacted by the author for commercial reasons.

This section has been redacted by the author for commercial reasons.

This section has been redacted by the author for commercial reasons.

Percentage Mitophagy and Mitochondrial Fragmentation

Mitophagy was assessed by selecting the points at which the mitochondrial TMRM stain fully co-localised with the autolysosome LysoTracker stain. Mitophagy was then calculated as a percentage of the total mitochondrial population undergoing mitophagy.

This section has been redacted by the author for commercial reasons.

This section has been redacted by the author for commercial reasons.

This section has been redacted by the author for commercial reasons.

This section has been redacted by the author for commercial reasons.

This section has been redacted by the author for commercial reasons.

4.3.6 Induced Mitophagy

We also sought to induce mitophagy by the use of mitochondrial toxins. Briefly, prior to fixation, we incubated the cells with 4 μ M antimycin A to inhibit complex III of the ETC and 10 μ M oligomycin to inhibit ATP synthase. By doing this, we caused mitochondrial dysfunction through alterations in the ETC, thus causing mitochondrial depolarisation, fragmentation and hence mitophagy.

This section has been redacted by the author for commercial reasons.

This section has been redacted by the author for commercial reasons.

This section has been redacted by the author for commercial reasons.

This section has been redacted by the author for commercial reasons.

This section has been redacted by the author for commercial reasons.

This section has been redacted by the author for commercial reasons.

This section has been redacted by the author for commercial reasons.

This section has been redacted by the author for commercial reasons.

4.3.7 Mitophagy Results Overview

Table 4.2 was created to visually represent the mitophagy data presented above.

Table 4.2 Summary Table of Mitophagy Results

Green upwards arrows represent an increase compared to its paired line, red downwards arrow represents a decrease compared to its paired line and an orange = represents no difference between paired control and patient lines.

	Control 1	Control 2	sPD1	sPD2
Mitochondrial Number (Basal)	↓	=	↑	=
Lysosomal Number (Basal)	↓	=	↑	=
Percentage Mitophagy (Basal)	↑	=	↓	=
Mitochondrial Fragmentation (Basal)	↓	↓	↑	↑
Mitochondrial Number (Induced)	↑	↑	↓	↓
Lysosomal Number (Induced)	↓	↑	↑	↓
Percentage Mitophagy (Induced)	↓	=	↑	=
Mitochondrial Fragmentation (Induced)	↑	↓	↓	↑

4.4 Discussion

4.4.1 Alpha Synuclein

We began this chapter by investigating alpha synuclein expression in our induced dopaminergic neurone model. We were only able to do this successfully in two out of the three pairs of lines. Interestingly, although variable, we observed increased expression of alpha synuclein in the iNPCs of sPD1 compared to the induced dopaminergic neurones of sPD1, a finding we weren't necessarily expecting. Also, we decided not to continue with optimisation of control 2 and sPD2 as we repeatedly observed a strong band at the sPD2 iNPC, with no other bands visible. The iNPCs are continually cultured in growth medium supplemented with 0.001% FGF basic which is then removed once the cells begin the neurone differentiation protocol. There is evidence to suggest that FGF basic may have a role in alpha synuclein expression. More specifically it was discovered that when rat PC-12 cells were treated with neuronal growth factors including FGF basic, levels of alpha synuclein increased via the MAP/ERK and PI3K pathways (Stefanis et al., 2001, Lee Clough and Stefanis, 2007). Furthermore, in their model, they postulated that this was specific to the catecholaminergic family of neurones, comprising of dopaminergic and noradrenergic neurones (Lee Clough and Stefanis, 2007). This may explain the increase in alpha synuclein expression that we observe in both sPD1 and sPD2 iNPCs and also why alpha synuclein expression appears to decrease when sPD1 iNPCs are differentiated into dopaminergic neurones.

Alpha synuclein is notoriously difficult to identify via Western blotting, however, we were able to detect expression by adapting the protocol to include a fixation step in 4% PFA, prior to blocking (Lee and Kamitani, 2011). Protein transfer to membranes such as PVDF and nitrocellulose likely occur via non-covalent hydrophobic interactions and thus it is probable that alpha synuclein routinely washes off the membranes due to its size and hydrophilic nature (Newman et al., 2013). Newman et al, 2013, sought to utilise crosslinkers such as dithiobis[succinimidylpropionate] (DSP) to investigate whether endogenous alpha synuclein was more readily detected in neuroblastoma cells following treatment with 2mM DSP. Crosslinkers, such as DSP, are able to permeabilise cell membranes and stabilise proteins through the formation of amide bonds (Wang et al., 2019). More specifically, DSP contains an amine-reactive N-hydroxysuccinimide ester at each end which is able to interact with lysine residues, of which alpha synuclein has an abundance, in order to generate the stabilising amide bonds (Wang et al., 2019). Endogenous alpha synuclein expression was indeed increased following treatment with DSP (Newman et al., 2013) and this was later corroborated by Preterre et al, 2015, using a rat enteric nervous system model as well as

tissue homogenates from human small intestine (Preterre et al., 2015). They compared both fixation in PFA as well as 2.5mM DSP treatment and were able to illustrate increased detection of endogenous alpha synuclein following DSP treatment regardless of what antibody was used, whereas PFA only improved detection for 2 out of the 7 antibodies they trialled. (Preterre et al., 2015). It is possible that PFA and DSP crosslinker treatment improve the binding of alpha synuclein to PVDF or nitrocellulose membranes by masking the positive charge of lysine residues present within alpha synuclein resulting in increased hydrophobicity (Newman et al., 2013). Furthermore, they add a large hydrophobic moiety to alpha synuclein which enables increased membrane binding and thus greater detection capabilities (Newman et al., 2013). In future work, it may be beneficial to optimise the use of DSP in our induced dopaminergic neurone samples in order to blot for total alpha synuclein more successfully.

We also investigated total alpha synuclein via ICC and our results illustrated no difference between control 1 and sPD1, whereas control 2 appeared to have more total alpha synuclein than sPD2. These findings were interesting as initially, it would be assumed that the patient lines would display higher total alpha synuclein expression than controls. Alpha synuclein is a protein predominantly expressed in the brain but can also be expressed in other organs such as the heart, skeletal muscle and pancreas (Siddiqui et al., 2016). It is expressed in very small amounts in the skin, however endogenously, this expression is extremely low compared to the brain. Furthermore, it's expression in the skin has only been reliably linked to those that possess Lewy Bodies (Ikemura et al., 2008). We are unable to confirm the presence or absence of Lewy Bodies within our cell model, therefore it is possible that the total alpha synuclein expression we are observing is indicative of alpha synuclein that is 'free', or rather not sequestered within Lewy Bodies. Furthermore, conflicting results have been published surrounding alpha synuclein expression in iPSC-derived dopaminergic neurones harbouring *Parkin* mutations, with some failing to illustrate differences between patients and controls (Jiang et al., 2012) while others have identified alpha synuclein accumulation (Shaltouki et al., 2015, Chung et al., 2016). Moreover, further studies also reported no differences in alpha synuclein expression between iPSC-derived control, alpha synuclein mutant (triplication and A53T mutation) (Little et al., 2018) and idiopathic (Sánchez-Danés et al., 2012) dopaminergic neurones. However, in this study, we utilised an alpha synuclein triplication patient line and were able to robustly illustrate large increases in alpha synuclein expression, as would be expected. Our alpha synuclein mutant acted as a positive control and the variability we observed was primarily within the sporadic PD lines.

It is possible that limitations exist with the antibodies used within this research. At times, when imaging, the exposure settings on the Opera Phenix would have to be increased in order to get a good signal. Furthermore, it is possible that although we were able to identify alpha synuclein puncta, the antibodies used may not have been completely specific for alpha synuclein and hence we were picking up higher background levels than we would usually expect. This could potentially explain why our control induced dopaminergic neurones had a higher alpha synuclein expression than our patients. Moreover, it is possible that because our induced neurones were reprogrammed from fibroblasts, and alpha synuclein expression is inherently lower in fibroblasts, we do not observe alpha synuclein levels that are a true representation of endogenous brain levels. Therefore, we must be cautious in over-analysing the data we have presented and treat it as a guide.

As alluded to in the background to this chapter, alpha synuclein undergoes a number of post-translational modifications, with the phosphorylation of serine 129 believed to represent a more neurotoxic form of the protein. We were able to present data collected via ICC using an antibody targeted against alpha synuclein phosphorylated at serine 129. We also attempted to optimise this antibody for Western blotting, however after repeated attempts and optimisation it was unsuccessful and due to Covid19 restrictions and limited lab time, it was decided that we wouldn't continue with this. We made two alterations to the Western blotting protocol in order to try and investigate phosphorylated alpha synuclein expression. Firstly, during sample preparation, we included a phosphatase inhibitor cocktail as well as protease inhibitor cocktail. Briefly, cell pellets are lysed in order to access intracellular proteins through membrane disruption however a number of proteinases, kinases and phosphatases are released (Bass et al., 2017). Western blots that were undertaken for neuronal characterisation only included protease inhibitor cocktail in the cell lysis buffer as we were only interested in expression of total protein. However, during optimisation to detect phosphorylated alpha synuclein, we added phosphatase inhibitor cocktail to the cell lysis buffer in order to maintain the phosphorylation status of the proteins, in this case alpha synuclein. Secondly, we altered the blocking solution used. Ordinarily we used a 5% non-fat milk solution as this was cheap and readily available. However, milk contains its own phosphoprotein, casein, which was likely to cross-react (Bass et al., 2017) with our phosphorylated alpha synuclein antibody. Therefore, we blocked our membranes in a 5% BSA solution in TBST. Despite these alterations, alongside differing concentration of antibody, we were unable to successfully blot for alpha synuclein phosphorylated at serine 129. As well as the inherent difficulties of blotting not only for alpha synuclein but also for phosphorylated proteins in general, it is possible that this failed to work as much of the serine 129 phosphorylated alpha synuclein exists sequestered within Lewy Bodies and our

cellular model likely does not include Lewy Bodies. Therefore, in order to investigate this, the use of human post-mortem tissue may be of more benefit, however we would then be unable to consider the effect that Jed135 may have on this.

A wealth of work has investigated the pathological relevance of alpha synuclein phosphorylated at serine 129, describing it as a neurotoxic phosphorylation event contributing to the pathogenesis of PD. As such, surrounding residues have also been investigated and it has been discovered that alpha synuclein can also be phosphorylated at tyrosine 125, 133 and 136 (Fayyad et al., 2020). The pathological relevance of these residues is yet to be determined, however phosphorylation of tyrosine 125 has been investigated in brain tissue and the results present within the current literature have been conflicting. For example, a case study described both serine 129 and tyrosine 125 phosphorylation within Lewy Bodies from a PD patient with the G51D alpha synuclein mutation (Kiely et al., 2013) whereas others failed to detect tyrosine 125 phosphorylation in human brain tissue from people with PD (Chen et al., 2009). Interestingly, levels of tyrosine 125 phosphorylation decrease with age (Hejjaoui et al., 2012) while the risk of developing PD increases. Thus, it can be postulated that tyrosine 125 conveys a neuroprotective effect which, as we age, is lost, resulting in an imbalance between tyrosine 125 and the neurotoxic serine 129 phosphorylation. A study published in 2020 specifically investigating dual phosphorylation of serine 129 and tyrosine 125 in a cell model system, rodent model and human post-mortem tissue reported tyrosine 125 phosphorylation to not be present within alpha synuclein inclusions (Fayyad et al., 2020). With most papers in this field not reporting tyrosine 125 phosphorylation present within Lewy Bodies, it has been suggested that the case study by Kiely et al, 2013, included cross-reactivity in which tau was being detected using the tyrosine 125 antibody, although it is also possible that the G51D mutation represents a unique type of PD pathology (Fayyad et al., 2020).

We also initially set out to investigate different species of alpha synuclein. As mentioned, alpha synuclein exists as a number of different species, monomers, oligomers, and fibrils. We wanted to observe whether Jed135 was able to alter aggregated alpha synuclein. The Western blots carried out during this project were primarily done under reducing conditions meaning that the sample buffer contained reducing agents dithiothreitol (DTT) and beta-mercaptoethanol as well as samples being boiled at 95°C. This process resulted in the breakdown of di-sulphide bonds between cysteine residues (Bass et al., 2017). Furthermore, SDS was also present within the sample buffer, resolving gel and running buffer to coat hydrophobic protein regions with a negative charge, proportional to their molecular mass (Nowakowski et al., 2014, Bass et al., 2017). These factors ultimately caused the proteins to

lose their quaternary, tertiary and secondary structure, thus denaturing the protein to its primary amino acid sequence. We sought to investigate aggregated alpha synuclein, therefore the tertiary protein structure needed to remain intact. As such, we omitted DTT, beta-mercaptoethanol and SDS from the sample buffer, didn't boil the samples following addition of sample buffer and also did not add SDS to the resolving gel or running buffer. Regardless of this, we were unable to clearly detect alpha synuclein aggregates present within our samples and, due to time constraints, we did not continue to optimise this. The protocol that we attempted to optimise matches that of Roberts et al, 2015. They also omitted SDS from all steps of their sample preparation and gel electrophoresis however they were able to detect both alpha synuclein oligomers and fibrils of different sizes (Roberts et al., 2015). Given more time, we may have been able to investigate alpha synuclein oligomers within our dopaminergic cell model via an alternative method. Lassen et al, 2018, developed and described an enzyme-linked immunosorbent assay (ELISA) which utilised an oligomer conformation specific antibody. The method they described was based on a sandwich ELISA, in which the ELISA plate was initially coated with a capture antibody to bind the antigen of interest. A primary antibody was then added to recognise and bind to the antigen. Following this, an enzyme-labelled secondary antibody targeted to the primary antibody was added (Aydin, 2015). The ELISA developed by Lassen et al required the incubation of a 96 well plate with the MJF-14-6-4-2 antibody overnight, before washing and adding ELISA blocking buffer. The sample of interest was then added and incubated before the addition of another anti-alpha synuclein antibody. Following this, the plate was incubated with an HRP antibody to detect the primary antibody, and a visualisation agent, 3,3',5,5'-tetramethylbenzidine added (Lassen et al., 2018). The capture antibody used in this ELISA was specific to an epitope on filamentous and oligomeric alpha synuclein and it has been demonstrated that upon denaturation, the epitope is lost, confirming its specificity to oligomeric and filamentous alpha synuclein, as well as this assay being dependent upon protein confirmation (Lassen et al., 2018). Future work could optimise this ELISA protocol for use with our dopaminergic neurone cell model in order to investigate the effect of Jed135 on alpha synuclein oligomers and fibrils.

We utilised the same confirmation specific antibody as Lassen et al, 2018, for our ICC investigations. However, following work from Ludtmann et al, 2018, we were interested to assess oligomeric alpha synuclein in association with ATP synthase in our cell model system (Ludtmann et al., 2018). Interestingly, our results suggested that both control 1 and control 2 appeared to have more aggregated alpha synuclein in association with ATP synthase than their patient counterparts. These results are at odds with the aforementioned research from 2018. However, it should be noted that we used different methodology which may therefore

account for the variation. Initially, they were able to observe some areas of co-localisation of filamentous alpha synuclein and ATP synthase in wild type rat co-cultures exposed to oligomers, however conventional confocal microscopy possesses a diffraction limit (Ludtmann et al., 2018). Briefly, diffraction limits of light exist when a light is shone through a small hole, or aperture, as is true for microscopy, hence limiting the spread of the light wave (Huang et al., 2010). Although standard light microscopy has been an invaluable tool in research, enabling us to further our biological understanding by imaging cellular organelles and bacteria, its limited resolution began to become a hindrance. As such, a number of researchers have been able to shatter the diffraction barrier, developing several different methods of super-resolution microscopy, improving resolution by several orders of magnitude and further developing the scientific field (Huang et al., 2010). In order to overcome the diffraction limit of confocal microscopy, (Ludtmann et al., 2018) utilised a method called DNA points accumulation for imaging in nanoscale topography (DNA-PAINT) in order to better visualise oligomeric alpha synuclein and ATP synthase co-localisation. DNA-PAINT is a form of super resolution microscopy consisting of a docking strand and an imaging strand (Schnitzbauer et al., 2017). The docking strand is targeted to, and remains fixed to, the biological target, while the imager strand consists of a short, DNA oligonucleotide, usually 8-10 oligonucleotides in length and is complementary to the docking strand. Furthermore, the imager strand contains a fluorophore and is able to freely diffuse, allowing for transient binding to the docking strand (Schnitzbauer et al., 2017). It is during this binding that photon detection occurs, generating a stochastic, or random, series of blinking signals (Filius et al., 2020). Using this technique, Ludtmann et al, 2018, were able to measure more than 500,000 co-localisations of oligomeric alpha synuclein and ATP synthase (Ludtmann et al., 2018). The stark difference in methodology, along with the light diffraction barrier, is a likely reason for the differences observed between our results and those of the aforementioned paper. Therefore, future work on our part could consider using a super resolution imaging technique to assess whether we observe any differences in oligomeric alpha synuclein expression in association with ATP synthase. Moreover, Ludtmann et al, 2018, sought the further validate their super resolution microscopy by performing a proximity ligation assay (PLA), allowing them to again observe an interaction between oligomeric alpha synuclein and ATP synthase (Ludtmann et al., 2018). PLAs determine protein-protein interactions also by utilising DNA. Briefly, samples are incubated with primary antibodies of choice before secondary PLA probes, plus and minus, containing a unique DNA strand is applied. Proteins in close interaction are able to hybridise the DNA to produce circular DNA which is then amplified and detected as small puncta upon imaging

(Alam, 2018). With more time, we could also have utilised this method to determine oligomeric alpha synuclein and ATP synthase interactions.

Although we observed control 1 and control 2 to have more co-localisation, we were able to illustrate the alpha synuclein mutant to have more co-localisation than control 3, as expected. It should be noted however, that the work carried out by Ludtmann et al, 2018, was undertaken in wildtype rat co-cultures, treated with exogenous monomeric and oligomeric alpha synuclein, therefore potentially accounting for more differences with our results.

The addition of exogenous alpha synuclein to cell cultures represents an additional method to study alpha synuclein pathogenicity. This is particularly useful for studying alpha synuclein cell to cell propagation. A 2022 study hypothesised that levels of endogenous alpha synuclein expression influences the susceptibility of succumbing to the accumulation of pathological alpha synuclein (Vasili et al., 2022). They were particularly interested in assessing selective vulnerability of specific brain regions to alpha synuclein pathology. Using stable HEK293 cells with varying expression levels of alpha synuclein, they applied exogenous alpha synuclein preformed fibrils and assessed the uptake and pathological conversion of endogenous alpha synuclein into pathogenic aggregated species. They were able to illustrate that areas of the brain with naturally higher alpha synuclein expression likely contribute to the spread of toxic alpha synuclein species, including accumulation and spread of serine 129 phosphorylated alpha synuclein (Vasili et al., 2022). In the context of our study and in determining a mechanism of action of Jed135, exogenously expressing alpha synuclein may not be appropriate, however in order to fully understand the impact of Jed135 on alpha synuclein expression and spread, it may be beneficial in the future.

Alpha synuclein represents an attractive drug target for the treatment of PD, however alpha synuclein aggregation is not necessary for the development of PD neurodegeneration (Vijjaratnam et al., 2021b), as observed by some individuals with *Parkin* mutations not possessing Lewy bodies (Johansen et al., 2018). Several alpha synuclein targeted therapies are currently being developed or are in clinical trials, including antibodies targeted towards alpha synuclein in order to increase immune-mediated clearance (Vijjaratnam et al., 2021b). Numerous other alpha synuclein targeted therapies are in development, aiming to target mechanisms related to gene regulation and autophagy, however it could be postulated that specifically targeting alpha synuclein is futile due to the fact it may be too late in the disease course and only show symptomatic relief. This again highlights the need to uncover more robust biomarkers so that treatment can begin early to preserve the dopaminergic neurone pool from degradation.

Further to the evidence illustrating that alpha synuclein is able to interact with ATP synthase under both physiological and pathological conditions, the protein also interacts with other aspects of mitochondrial biology. The association of alpha synuclein with the mitochondria was first determined via Western blotting of mitochondrial and cytosolic fractions from a wildtype rat brain (Li et al., 2007) and later confirmed in human tissue due to pathological accumulations observed in areas such as the SNpc in PD patients (Devi et al., 2008, Bernal-Conde et al., 2020). Alpha synuclein interaction has been detailed at both the outer and inner mitochondrial membranes (Bernal-Conde et al., 2020) and it is the N terminal domain of alpha synuclein that is responsible for the translocation into the mitochondria. Under physiological conditions, alpha synuclein likely aids in the regulation of mitochondrial fusion, ensuring the normal function of the ETC and regulating the permeability of voltage dependent anion channels (Bernal-Conde et al., 2020). Pathological alpha synuclein can cause mitochondrial dysfunction in numerous ways. Firstly, small oligomers, as well as serine 129 phosphorylated alpha synuclein, are able to block protein import into the mitochondria by inhibiting the interaction between TOM20-TOM22 (Di Maio et al., 2016, Martínez et al., 2018, Bernal-Conde et al., 2020). Alpha synuclein has also been linked to complex I activity, both physiologically and pathologically. Firstly, evidence suggests that alpha synuclein plays a physiological role at complex I, as when knocked down, expression of complex I and III linked NADH cytochrome C reductase is reduced (Ellis et al., 2005, Bernal-Conde et al., 2020). Pathologically, alpha synuclein contributes to mitochondrial dysfunction, also through association with complex I. It causes the generation of ROS which, in turn, result in the generation of more pathological alpha synuclein species, creating a cycle in which these two processes continually exacerbate each other (Bernal-Conde et al., 2020). Our study only began to touch the surface of understanding what effect Jed135 could have on alpha synuclein, only considering overall expression levels and co-localisation with ATP synthase. However, with more time we could assess the activity of the mitochondrial complexes when induced dopaminergic neurones are treated with Jed135. Furthermore, we could investigate the TOM complexes in greater depth in order to characterise any phenotype in our model and assess whether this was altered with Jed135 treatment.

For the purposes of this thesis, we have focussed on the effects of alpha synuclein at the mitochondria, however there is a wealth of evidence detailing its effects at other organelles such as the endoplasmic reticulum and Golgi apparatus which has been reviewed elsewhere (Bernal-Conde et al., 2020).

4.4.2 Mitophagy

We moved on to assessing mitophagy under both basal and induced conditions, allowing us to understand what the cells are capable of physiologically and when placed under stress. Under basal conditions, we observed sPD1 to have increased mitochondrial and lysosomal number per cell along with more fragmented mitochondria and decreased mitophagy. On the contrary, data suggested no overall difference in most of these parameters between sPD2 and control 2, with mitochondrial fragmentation being the exception. Therefore, we illustrate our sporadic PD lines to have a more fragmented mitochondrial population, potentially pointing to problems with mitochondrial bioenergetics and/or mitochondrial clearance. Defective mitophagy has been implicated in both familial and sporadic PD (Hsieh et al., 2016, Clark et al., 2021) and our data suggests that Jed135 does not function in a mitophagy-mediated manner.

We displayed control 1 to have a more fragmented mitochondrial network than sPD1 under induced conditions, however it also showed slightly reduced mitophagy. Also, in both instances under induced conditions, the control lines appeared to have more mitochondria than the patients. In our experimental model, we incubated our cells with the inhibitors for 30 minutes and then fixed with 4% PFA. It is likely that the increase in mitochondria and fragmentation is indicative of initiation of the mitophagy pathway, however there were still many mitochondria yet to be removed. It would be interesting to have completed this assay as a live, time lapse assay, similar to the basal state, so that we would be able to observe mitophagic flux. We would have expected to observe an initial increase in mitochondrial number and fragmentation, followed by increased mitophagy, both of which would then be expected to decrease towards the end of the assay. Autophagic, or mitophagic, flux encapsulates the entire degradation process, whereas merely measuring the formation of autophagosomes or conversion rate of LC3-I to LC3-II is not sufficient to determine autophagy/mitophagy (Villanueva-Paz et al., 2020).

We assessed the effect of inducing mitophagy through ICC, labelling the OMM protein TOM20 to visualise the mitochondria and labelling LC3 to visualise autophagosomes. LC3 is a family of 3 proteins, LC3 A, B and C, with LC3A and LC3B possessing high sequence identity and being differentially expressed throughout a variety of human tissue, whereas LC3C is minimally expressed (Koukourakis et al., 2015). Studies relating to mitophagy, as well as autophagy, have primarily focused on LC3B, however a 2015 study detailed how many LC3 antibodies failed to distinguish between LC3A and LC3B isoforms meaning they aren't specific enough to detect purely LC3B (Koukourakis et al., 2015). It has been suggested that LC3A and LC3C have similar functions to LC3B, as well as also being

involved in signal transduction (Baeken et al., 2020). As mentioned, it is primarily LC3B that is believed to be involved in autophagy and mitophagy pathways and is present in two different states within the cell, LC3-I and LC3-II. Briefly, LC3-I represents LC3 in its non-lipidated state and is found diffusely within the cytoplasm. However, LC3-I is able to become conjugated to PE, hence forming the lipidated version LC3-II (Baeken et al., 2020). It is LC3-II that is recruited to autophagosomes and appears as high intensity puncta that we quantify during our investigations.

There are alternative methods to investigating mitophagy that we could have utilised to validate our results, namely mito-Keima or mito-QC. Keima is a fluorescent protein sourced from coral that is easily transfected into cells via plasmid or viral transfection (Sun et al., 2017b), with mito-Keima containing a specific COX8A mitochondrial targeting sequence (Clark et al., 2021). The emission wavelength of Keima is pH-independent, with a peak at 620nm, however it has a bimodal excitation spectrum that is pH-dependent (Sun et al., 2017b, Clark et al., 2021). In alkaline environments, such as the mitochondria (pH 8.0), mito-Keima excites at a shorter wavelength of 440nm, resulting in a green fluorescence, however in acidic conditions such as a lysosomal environment (pH 4.5), the excitation shifts to a longer wavelength, 568nm, causing fluorescence to gradually change to red. Calculation of the 568nm:440nm ratio generates a mitophagy index (Sun et al., 2017b, Clark et al., 2021) which can then be compared between cells lines and under different treatments/conditions. Some researchers suggest the mito-Keima probe to be resistant to proteolytic degradation meaning that mitophagic flux is easily measured (Sun et al., 2017b), however others state that the lysosomal fate of mito-Keima following mitochondrial degradation is poorly defined (Clark et al., 2021). However, one confirmed disadvantage of mito-Keima is that it can only be performed on live cells as the fixation process destroys the lysosomal pH gradient (Sun et al., 2017b, Clark et al., 2021).

Mito-QC takes advantage of the lysosomal quenching of green fluorescent protein (GFP) and was initially developed as a transgenic mouse model; however the construct has now been developed for use in cells (McWilliams et al., 2016, Rosignol et al., 2020). The mito-QC construct consists of an OMM protein targeting sequence, specifically targeted to mitochondrial fission 1 protein (Fis1), linked to a GFP-mCherry protein (Clark et al., 2021). Under physiological conditions, mito-QC is able to fluoresce both green and red, however upon delivery to the lysosomes, the GFP signal is quenched, hence only displaying the red signal and highlighting a mitophagic event (Rosignol et al., 2020, Clark et al., 2021). However, recently, a study questioned the reliability of mito-QC and its OMM localisation. As mentioned, the Fis1 tag localises mito-QC to the OMM and it has been suggested that

because it is cytosolic-facing, it may undergo proteasomal degradation. Indeed, their investigations appear to show this is true, therefore a Fis1 tag may not be the most appropriate mitochondrial targeting sequence and hence mito-QC data should be interpreted with caution as it may not be appropriate for studying mitophagy (Katayama et al., 2020). Our data does not suggest that any further mitophagy investigations are necessary, however it is good practice to consider alternative methodology that could have been undertaken.

As mentioned in the introduction to this chapter, the most well characterised mitophagy pathway is the PINK1/Parkin mediated pathway. However, PINK1 and Parkin have both been shown to affect other cellular processes such as the turnover of ETC complexes (Vincow et al., 2013) and the generation of mitochondrial derived vesicles triggered by ROS, in a mechanism distinct from canonical mitophagy, targeting them to endolysosomes in a syntaxin-17 dependent manner (McLelland et al., 2014, McLelland et al., 2016, Singh and Ganley, 2021). Similarly, alternative mitophagy pathways exist that can occur independently from, or branch into aspects of, the PINK1/Parkin pathway, generating two main alterations, ubiquitination by other ubiquitin ligases or alternative ways to target mitochondria to lysosomes (von Stockum et al., 2018). Evidence has suggested that other ubiquitin ligases such as seven in absentia homolog (SIAH)-1 (Szargel et al., 2016), glycoprotein 78 (GP78) (Fu et al., 2013) and mitochondrial E3 ubiquitin protein ligase 1 (MUL1) (Li et al., 2015, Georgakopoulos et al., 2017) are able to ubiquitinate OMM proteins in a similar fashion to Parkin, tagging the mitochondria for degradation. Furthermore, others have uncovered alternative mitophagy receptors, present on the OMM. Receptors such as Bcl-2 interacting protein 3 (Bnip3) and FUN domain containing 1 (FUNDC1) possess an LC3 interacting region allowing them to bind to LC3 on phagophores (Gottlieb et al., 2021). More specifically, both Bnip3 and FUNDC1 regulate mitophagy following a hypoxic challenge and interaction with LC3-B is dependent upon the phosphorylation status of the proteins, serine 17 and 24 for Bnip3 and serine 17 for FUNDC1 (Gottlieb et al., 2021). Another OMM receptor, FK506 binding protein 8 (FKBP8), has also been identified as an alternative mitophagy initiator, with its strong ability to bind to LC3-A to induce mitophagy (Bhujabal et al., 2017). The mitophagy assays completed in this study were unable to determine the pathway by which mitophagy was occurring, however we would be able to investigate the expression levels of different mitophagy receptors via qPCR or Western blotting in order to characterise the cause of mitophagy deficits, particularly in sPD1. However, in the context of this study and understanding the mechanism of Jed135, our results are fairly conclusive in determining that the mechanism of Jed135 is mitophagy independent and therefore we wouldn't expect to observe any difference in protein expression when treated with Jed135.

This chapter has characterised differences that exist between controls and patients in multiple aspects of alpha synuclein pathology as well as mitophagy under both basal and induced conditions. Our results conclusively reveal that there is minimal, if any, effect of Jed135 on these two mechanisms. That said, there are many more aspects of alpha synuclein pathology and mitochondrial dysfunction that could be investigated in the future.

5 Target Characterisation

This section has been redacted by the author for commercial reasons.

This section has been redacted by the author for commercial reasons.

This section has been redacted by the author for commercial reasons.

This section has been redacted by the author for commercial reasons.

This section has been redacted by the author for commercial reasons.

This section has been redacted by the author for commercial reasons.

This section has been redacted by the author for commercial reasons.

This section has been redacted by the author for commercial reasons.

This section has been redacted by the author for commercial reasons.

This section has been redacted by the author for commercial reasons.

This section has been redacted by the author for commercial reasons.

This section has been redacted by the author for commercial reasons.

This section has been redacted by the author for commercial reasons.

This section has been redacted by the author for commercial reasons.

This section has been redacted by the author for commercial reasons.

This section has been redacted by the author for commercial reasons.

This section has been redacted by the author for commercial reasons.

This section has been redacted by the author for commercial reasons.

This section has been redacted by the author for commercial reasons.

This section has been redacted by the author for commercial reasons.

This section has been redacted by the author for commercial reasons.

This section has been redacted by the author for commercial reasons.

This section has been redacted by the author for commercial reasons.

This section has been redacted by the author for commercial reasons.

This section has been redacted by the author for commercial reasons.

This section has been redacted by the author for commercial reasons.

This section has been redacted by the author for commercial reasons.

This section has been redacted by the author for commercial reasons.

This section has been redacted by the author for commercial reasons.

This section has been redacted by the author for commercial reasons.

This section has been redacted by the author for commercial reasons.

This section has been redacted by the author for commercial reasons.

This section has been redacted by the author for commercial reasons.

This section has been redacted by the author for commercial reasons.

This section has been redacted by the author for commercial reasons.

This section has been redacted by the author for commercial reasons.

This section has been redacted by the author for commercial reasons.

This section has been redacted by the author for commercial reasons.

This section has been redacted by the author for commercial reasons.

This section has been redacted by the author for commercial reasons.

This section has been redacted by the author for commercial reasons.

This section has been redacted by the author for commercial reasons.

This section has been redacted by the author for commercial reasons.

This section has been redacted by the author for commercial reasons.

This section has been redacted by the author for commercial reasons.

This section has been redacted by the author for commercial reasons.

This section has been redacted by the author for commercial reasons.

This section has been redacted by the author for commercial reasons.

This section has been redacted by the author for commercial reasons.

This section has been redacted by the author for commercial reasons.

This section has been redacted by the author for commercial reasons.

This section has been redacted by the author for commercial reasons.

This section has been redacted by the author for commercial reasons.

This section has been redacted by the author for commercial reasons.

This section has been redacted by the author for commercial reasons.

This section has been redacted by the author for commercial reasons.

This section has been redacted by the author for commercial reasons.

This section has been redacted by the author for commercial reasons.

This section has been redacted by the author for commercial reasons.

6 In Vivo *Drosophila* Model

6.1 Background

6.1.1 *Drosophila* as a Model Organism

Drosophila melanogaster, or more commonly, the fruit fly and hereby referred to as *Drosophila*, are one of the most commonly used model organisms in biomedical research (Tolwinski, 2017). William Castle's group at Harvard University are believed to have been the first group to use *Drosophila* as a model, utilising them to study experimental evolution (Jennings, 2011, Carlson, 2013). However, it wasn't until work was completed in 1933 by Thomas Hunt Morgan that people understood the full capabilities of *Drosophila* in order to study Mendelian inheritance patterns, winning him the 1933 Nobel Prize for 'discoveries concerning the role played by the chromosome in heredity' (Jennings, 2011). More specifically, he was able to illustrate that the *white* gene resided on the X chromosome and hence proved the chromosomal theory of inheritance (Tolwinski, 2017). Since then, Thomas Hunt Morgan has been seen as the 'father' of *Drosophila* and the use of *Drosophila* in biomedical research has increased due to its short life cycle, rapid generation time, low costs and genetic manipulability, not to mention they aren't covered by the modern day Home Office License in the UK (Tolwinski, 2017). Since 1933, *Drosophila* work has won the Nobel Prize on at least five more occasions, including by Hermann Muller in 1946 for his work on understanding how X-rays can cause mutations and again in 1995 by Edward B Lewis, Christiane Nüsslein-Volhard and Eric F Wieschaus for their work on embryonic development (Muller, 1928, Nüsslein-Volhard and Wieschaus, 1980, Tolwinski, 2017).

Drosophila were the first complex organism to have their genome fully sequenced, published in 2000, 11 months before the publication of the human genome (Adams et al., 2000, Jennings, 2011). They possess approximately 14,000 genes, spread over four pairs of chromosomes, although the bulk of the genetic information is present over three of the pairs (Pandey and Nichols, 2011). Briefly, the four pairs comprise of the sex chromosomes (XX or XY), also denoted as chromosome 1, 2 pairs of larger chromosomes (chromosomes 2 and 3) and a small dot chromosome (chromosome 4) (Kaufman, 2017). *Drosophila* possess a significantly smaller genome than most mammals, however crucially, with less gene redundancy (Nagoshi, 2018). Their genome has, on average, 60% homology with humans, however this can vary from 40% in some areas of the genome, up to 90% in functionally conserved regions. Approximately 75% of human disease causing genes have been found to have sequence homology in *Drosophila*, making them an attractive model organism to study human disease (Pandey and Nichols, 2011).

Another attractive quality for the use of *Drosophila* is their short life cycle and rapid generation time, meaning it is relatively simple to generate large numbers of animals for studies (Fernández-Moreno et al., 2007). The *Drosophila* life cycle can be easily manipulated with temperature, with most studies, including this one, opting to maintain experimental conditions at 25°C and stock vials at 18°C in order to slow the lifecycle (Fernández-Moreno et al., 2007). *Drosophila* are known to be holometabolous, meaning a complete metamorphic change occurs from infant to adulthood, in this case from larvae to adult fly, and its life cycle can be split in four stages; embryo, larvae, pupae and adult (Fernández-Moreno et al., 2007). The following life cycle timeline is correct if kept at 25°C. Upon eggs being laid, the embryo stage lasts for 24 hours before turning into larvae. The larval stage is further split in 3 phases, 1st, 2nd and 3rd instar. First instar larvae begin to feed on the surface of the food source and upon initiation of the second instar phase, begin to burrow into the food source. Once the third instar larval phase is reached, larvae are fully grown and begin to wander up the side of the vial in search of a pupation location. Pupation is the process in which complete metamorphosis occurs, larval tissues are broken down and adult physiology develops, after which, the adults eclose and the life cycle begins again (Fernández-Moreno et al., 2007). This whole process takes approximately 9-10 days from egg fertilisation; however, this is doubled when stored at a lower temperature (Fernández-Moreno et al., 2007).

Although *Drosophila* do not possess a complete repertoire of human disease-causing genes, as mentioned, there is 75% homology. Regardless of this, genetic manipulation techniques exist that enable researchers to model the disease of interest. CRISPR-Cas9 is able to insert point mutations, specific proteins are able to be overexpressed or knocked down using binary expression systems such as the Gal4- upstream activating sequence (UAS) system and genetic alleles can be created that mimic the disease-causing genes of interest (Vos and Klein, 2021). The use of toxins and their known targets mean that novel mutant *Drosophila* strains are able to be produced (Vos and Klein, 2021). Furthermore, an extensive number of mutant lines have been generated via mutagenesis using ionising radiation such as X-rays (Eeken et al., 1989) and ethyl methanesulfonate (Yang et al., 2001). Mutant lines can also be created via P-element mobilisation. Briefly, P elements were first identified in the 1970s and it has since been discovered that the progeny generated from wild type male strains and laboratory made female strains can possess aberrant genetic traits known as hybrid dysgenesis (Ghanim et al., 2020). These include high rates of mutation as well as sterility and chromosome rearrangements (Ghanim et al., 2020).

6.1.2 *Drosophila* to Model Parkinson's Disease

A wealth of different animal models of PD exist, ranging from zebra fish (Najib et al., 2020) to rodent models (Campos et al., 2013) to non-human primates (Blesa et al., 2018), all possessing their own unique advantages and challenges. *Drosophila* provide an additional method in which to model PD, also harbouring their own range of advantages and disadvantages, to be discussed. *Drosophila* present a relatively simple model of PD, however crucially, they possess approximately 200 dopaminergic neurones, organised into distinct clusters within their central nervous system, that are liable to degeneration, a feature that isn't always recapitulated in rodent models (West et al., 2015, Vos and Klein, 2021). Similarly to vertebrates, dopamine modulates movement and learning in *Drosophila*, as well as sleep via the regulation of circadian rhythms (West et al., 2015, Juárez Olguín et al., 2016), therefore we are able to understand the effect of PD specific mechanisms on dopaminergic neurones. As mentioned, motor symptoms are a pivotal aspect for a PD diagnosis in humans and, as such, *Drosophila* are able to replicate a number of motor phenotypes including reduced locomotion and altered flying, walking and climbing capabilities. Notably, climbing phenotypes are evident following the startle-induced negative geotaxis assay, climbing upwards in response to a startle stimulus such as being banged to the bottom of a tube (Nagoshi, 2018). *Drosophila* models of PD have repeatedly illustrated abnormalities in climbing ability, specifically harbouring a slowed climbing recovery compared to wild types (Sang et al., 2007, Tran et al., 2018, Pütz et al., 2021). Furthermore, *Drosophila* are also able to mirror a number of non-motor symptoms associated with PD such as sleep disturbances and problems with circadian rhythm, visual deficits, as well as changes in learning and memory (Nagoshi, 2018). The inherent disadvantages of *Drosophila* include the lack of endogenous *SNCA* meaning that endogenous Lewy bodies are not present, as well as lacking an adaptive immune system (Nagoshi, 2018).

Following the discovery of PD associated genes, endogenous mutants as well as transgenic models of PD are available. Moreover, as well as PD causing genes, GWAS have identified over 70 genes in which mutations confer increased risk for the development of sporadic PD (Nagoshi, 2018). The *Drosophila* genome is able to be easily manipulated, whether via the overexpression of exogenous genes, or knockdown, mutation or overexpression of endogenous genes and presents a unique, yet powerful genetic toolbox (West et al., 2015, Vos and Klein, 2021). Of particular importance is the Gal4-UAS system, developed as a binary expression system in *Drosophila* by Andrea Brand and Norbert Perrimon in the Department of Genetics at Harvard Medical School (Brand and Perrimon, 1993). Briefly, this system harnesses the Gal4 transcription factor present in yeast along with the UAS construct upstream of a reporter gene of interest (Homem and Davies, 2018) and was first

described in 1988 by Fischer et al (Fischer et al., 1988). The Gal4 and UAS constructs are usually present within separate *Drosophila* strains which, when crossed, result in the F1 progeny expressing the gene of interest due to the entire Gal4-UAS construct being present (Homem and Davies, 2018). Crucially for PD, mutant or wild type alpha synuclein is able to be expressed in *Drosophila* via the GAL4-UAS expression system, enabling the formation of Lewy bodies in the brain and the development of locomotor deficits and retinal degeneration (Bulus et al., 2020, Vos and Klein, 2021). Furthermore, other genetic causes of PD can be modelled in *Drosophila* via mutations in homologous genes of *Parkin*, *PINK1* and *LRRK2* as well as overexpression of Tau and *LRRK2*. PD-like phenotypes are also induced in *Drosophila* via the use of toxins, primarily rotenone or paraquat, both of which have been linked with increased risk of PD development following environmental exposure. Chronic exposure of *Drosophila* to rotenone, specifically when they were fed with less than 750µM rotenone over a 7-day period, resulted in reduced locomotor activity in the startle-induced negative geotaxis assay and was partially rescued by levodopa treatment. It was also found that rotenone was able to cause the loss of certain subtypes of dopaminergic neurones, however this was not rescued with levodopa treatment and was therefore deemed representative of human PD (Coulom and Birman, 2004, Nagoshi, 2018).

Paraquat is also able to induce PD-like motor phenotypes in *Drosophila*, with exposure to 20mM able to induce dopaminergic neurone loss after 6 hours, with locomotor defects visible within 12 hours and a high rate of lethality within days (Nagoshi, 2018). Although both rotenone and paraquat seemingly appear to cause motor phenotypes indicative of PD, they don't replicate the progressive nature that is observed in humans with PD, highlighting the probable multifactorial nature of sporadic PD (Nagoshi, 2018).

6.1.3 *Drosophila* Used in This Study

Motor phenotypes of PD are not only linked to adult *Drosophila* but are also evident in larvae. This study utilised *Drosophila* harbouring mutations of *Parkin* at position 25 and 472. More specifically, the *Park*²⁵ mutant was created by the mobilisation and excision of a P-element (EP(3)LA1) identified in the *Parkin* gene creating a loss of function allele (Greene Jessica et al., 2003) while the *Park*^{Z472} mutant was the result an A46T point mutation. When crossed, we were able to generate a double *Parkin* mutant, transheterozygous, strain. The transheterozygote larvae were then used to perform locomotor assays. Single *Parkin* mutations were balanced with the third chromosome balancer TM6B, not only to provide a phenotypic marker to allow for larval selection, but also to maintain the mutant stock by suppressing homologous recombination (Sun et al., 2012). In larvae, heterozygous *Parkin* mutants, or heterozygotes, balanced with TM6B were phenotypically smaller and tubby due

to the tubby marker carried on TM6B, whereas the transheterozygote *Parkin* mutants possessed regular morphology.

The *Parkin Drosophila* model used has been previously characterised elsewhere (Vincent et al., 2012). Briefly, they described a 38% reduction in crawling speed, as well as shorter crawling tracks in the *Parkin* transheterozygote larvae compared to that of the wild types. Furthermore, a rescue in velocity was observed following the global expression of wild type *Parkin* in the homozygote background via the Gal4-UAS system (Vincent et al., 2012). This characterisation provided us with an opportunity to observe whether Jed135 or UDCA was able to rescue locomotor velocity in this model. Larvae were treated with three different concentrations of Jed135 or UDCA; 60µM, 300µM and 600µM, however initial investigations began using Jed135 at a concentration of 60µM and UDCA at 600µM. Drug concentration was based on previous work which outlined that 600µM UDCA was able to partially rescue crawling velocity in a charged multivesicular body protein 2B (CHMP2B) model of frontotemporal dementia (FTD) (West et al., 2020).

6.2 Aims and Objectives

The aim of this chapter was to observe whether impaired locomotor velocity could be restored following the ingestion of Jed135 or UDCA in transheterozygote *Parkin* mutant *Drosophila* larvae. Furthermore, we sought to determine whether Jed135 had a toxic effect on survival to adulthood. This was achieved by:

- Performing larval locomotor assays following treatment with 60µM, 300µM and 600µM of Jed135 or UDCA and assessing the speed in which the larvae moved
- Performing survival assays following treatment with 60µM Jed135

6.3 Results

6.3.1 Phenotype Identification

Initially, we sought to identify whether we observed the same, or similar, phenotype described by Vincent et al in their 2012 paper. In each instance, larvae had been treated under vehicle conditions, meaning a small amount of ethanol was present within their food source. We observed wild type larvae to possess a mean locomotor speed of 0.67mm/sec while the locomotor speed of *Parkin* mutant larvae was significantly slower at 0.39mm/sec, **figure 6.1**. Therefore, our *Parkin* mutant larvae were crawling approximately 42.4% slower than the wild types, which corroborates what has been observed previously (Vincent et al., 2012).

Phenotype Identification

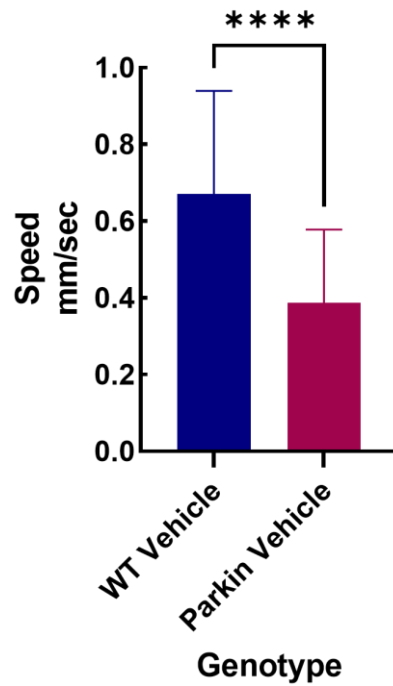


Figure 6.1 Identifying the phenotype previously observed in Parkin mutant *Drosophila* larvae
Parkin mutant larvae have a significantly slower locomotor speed than their wild type (WT) counterparts. A difference in locomotor speed of 42.4% was observed between the WT and *Parkin* mutant larvae. Data was found to not be normally distributed via Shapiro Wilks test for normality therefore a *t*-test with Mann Whitney correction was undertaken. **** $p < 0.0001$, $n =$ at least 61 biological replicates from at least 4 crosses (technical repeats), bars depict mean \pm SD.

This section has been redacted by the author for commercial reasons.

This section has been redacted by the author for commercial reasons.

This section has been redacted by the author for commercial reasons.

This section has been redacted by the author for commercial reasons.

This section has been redacted by the author for commercial reasons.

This section has been redacted by the author for commercial reasons.

This section has been redacted by the author for commercial reasons.

This section has been redacted by the author for commercial reasons.

6.4 Discussion

For this project, we chose to study the effects of Jed135 and UDCA in a *Drosophila* model of PD, however, initially, we had planned to use two different mouse models, an MPTP induced and a genetic, *LRRK2* PD model. This plan had to be altered due to the Covid19 pandemic, meaning we were unable to visit the labs of collaborators in the United States, but the *Drosophila* model available at the University of Sheffield provided a solid alternative. As mentioned in the introduction to this chapter, *Drosophila* offer a low cost model with a short life cycle, ideal for large scale drug screens, and are easily manipulated genetically (Chia et al., 2020). Furthermore, their nervous system is well characterised and they possess a dopamine synthesis pathway similar to humans. Toxin-induced *Drosophila* models also exhibit motor phenotypes similar to that in humans, as well as dopaminergic neurone degeneration and oxidative stress (Chia et al., 2020). However *Drosophila* are not an ideal organism to study all aspects of PD, owing to their lack of an homologous alpha synuclein gene.

A plethora of other animal models of PD exist, each with their own inherent advantages and disadvantages which must be considered before undertaking research.

Other, non-mammalian, animal models include *Caenorhabditis (C.) elegans* and *zebrafish*. Advantages of these are similar to that of *Drosophila*, with low maintenance costs, short life cycle and ability to manipulate their genomes making them attractive organisms to use. Both organisms also have well defined nervous systems, with *C.elegans* possessing 302 neurones, of which 8 are dopaminergic. However, these are difficult to target and make it more difficult to understand the effects of dopaminergic neurone degeneration, as well as understanding the effect of a novel therapeutic (Chia et al., 2020). Similarly to *Drosophila*, *C.elegans* also lack a homologue to the human *SNCA* gene, meaning that in order to study alpha synuclein, it has to be exogenously expressed.

Drosophila, *C.elegans* and *zebrafish* represent relatively simple organisms and, as such, many researchers opt to use rodents as a more complex organism in order to study PD. Similarly, both toxin and genetically induced rodent models of PD exist. Rodent models are well characterised and correlations with human disease have been identified. For example, degeneration of the nigrostriatal dopaminergic pathway in rodents directly correlates with motor deficits as assessed by the open field, rotarod and pole tests to study locomotion, strength and bradykinesia respectively (Chia et al., 2020). Rodents have also been found to exhibit non-motor symptoms associated with PD such as depression and weight loss, both of which can be monitored via behavioural assessments (Chia et al., 2020). Furthermore,

rodents offer a more expensive model organism that also possesses a longer life cycle and are more heavily regulated than non-mammalian models.

Perhaps the model organism that attracts the most ethical debates, is the use of non-human primates (NHP). Only approximately 10% of PD research using animals is conducted on NHP due to the extensive regulations, ethics and expenses that are associated with it (Chia et al., 2020). However, they represent the model closest to human disease with the presence of levodopa-induced dyskinesias, similar sleeping patterns to humans and comparable neuroimaging studies. Also, although currently unstandardised, motor phenotypes in NHP are able to be assessed via a UPDRS-like rating scale (Chia et al., 2020).

PD has only been found to develop naturally in humans (Potashkin et al., 2010), posing a major limitation to any animal model. The use of neurotoxins to induce a PD-like phenotype is therefore unavoidable in many situations. Acute treatment with MPTP, or other neurotoxins such as rotenone or paraquat, result in the rapid generation of a PD-like phenotype in animals, not indicative of human disease. Moreover, MPTP, which is frequently utilised to induce a PD-like phenotype in animals, has been described as having a different metabolism pathway in rodents compared to humans (Potashkin et al., 2010). However, a study in 2001 described that administration of MPTP alongside probenecid resulted in a chronic loss of striatal dopamine over a 6-month period, with a progressive decline in motor performance (Petroske et al., 2001). The probenecid adjuvant was used to prevent the rapid degradation and clearance of MPTP from the brain and kidneys (Petroske et al., 2001), resulting in a slowed and more progressive onset of symptoms. However, the major drawback of toxin induced animal models centres around the fact that they frequently don't develop Lewy bodies or Lewy body-like inclusions.

The discovery of genetic causes of PD resulted in the generation of genetically induced PD animal models. Alpha synuclein and *LRRK2* are frequently overexpressed in animal models while genes such as *Parkin*, *PINK1* and *DJ1* are knocked down or out (Chia et al., 2020). Genetic models of PD were initially extremely important in understanding disease pathogenesis, however similarly to the toxin-induced models, they were unable to recapitulate full human disease (Dawson et al., 2010). This is likely due to the inherent heterogeneity within human PD and the notion that an animal should replicate both motor and non-motor aspects of PD in a progressive fashion, as well as exhibiting the pathological burden of alpha synuclein inclusions.

Choosing a representative animal model for a study is an extremely difficult task, not only choosing the correct animal to model PD, but also deciding on the correct method by which to induce PD. All models and PD induction techniques have their own unique set of advantages and disadvantages to consider. Decades worth of biomedical research has been undertaken using animals to explore novel therapeutics, however in the context of neurodegenerative diseases, many of these therapeutics have failed once they reach human preclinical and clinical trials. For example, it has been estimated that approximately 99% of drug compounds developed to tackle AD have failed (Pistollato et al., 2020) and it's likely that this figure is similar for PD. Therefore it begs the question whether animal models need to be improved or whether, as a community, we need to work on developing new approach methodologies, such as organoids, in order to evaluate the safety, tolerability and efficacy of novel drug compounds (Pistollato et al., 2020). During this PhD project, a smaller patient and public involvement (PPI) project was undertaken in association with Parkinson's UK. We were interested in understanding what people with Parkinson's thought about animal models for PD research, specifically for drug development and two sessions, run by myself and Chris Hastings, were completed. The overall consensus from the sessions was that they believed animal models were, in part, responsible for the failure of drug development programmes and that they saw more value in modelling PD in cells from patients, followed by safety and tolerability studies in animals. They suggested that the inherent differences between animal models and humans, along with the fact that PD usually has to be induced in animal models, means that efficacy studies are generally not accurate and therefore providing novel compounds are safe, they should be taken straight into pre-clinical and clinical trials in humans. These PPI sessions were part of a larger study into developing a framework for researchers to follow in order to involve patients and the public in basic science research.

This project utilised the larvae of transheterozygous *Parkin* mutant *Drosophila*, however motor phenotypes have also been described in adult *Drosophila*. As mentioned in chapter 4, Parkin is an E3 ligase that plays a pivotal role in ubiquitinating OMM proteins, initiating the mitophagic response (Jin and Youle, 2012). Unsurprisingly therefore, mutations and deficiencies within the *Parkin* gene result in motor phenotypes in *Drosophila*. Specifically, they suffer mitochondrial deficits causing aberrations in muscle structure resulting in locomotor deficits and flying capabilities (Greene et al., 2003, Pesah et al., 2004, Saini et al., 2011). Furthermore, both male and female *Drosophila* lacking *Parkin* are unable to reproduce and have a significantly reduced lifespan (Pesah et al., 2004, Saini et al., 2011). *Parkin* null *Drosophila* also exhibit non-motor symptoms such as alterations in circadian rhythm, learning and memory (Julienne et al., 2017). It is frequently detailed that the non-

motor symptoms of PD are arguably more debilitating than the motor symptoms, therefore highlighting the usefulness of *Drosophila* to study non-motor symptoms.

It would have been interesting to have had the opportunity to define any motor or non-motor phenotypes within our transheterozygous *Parkin* mutant adult *Drosophila* and observe what rescue effects, if any, Jed135 would have on these phenotypes.

The set-up of our experimental protocol meant that we were unsure of the quantity of food, and hence drug, each larvae ate, possibly accounting for some of the variation. Other studies within the field have utilised dye-based feeding assays, involving the use of coloured food dyes for labelling. Following larval incubation for a desired amount of time, larvae can be washed and amount of food ingested quantified via spectrophotometer (Rodrigues et al., 2015, Almeida de Carvalho and Mirth, 2017, Keita et al., 2017). Furthermore, similar dye-based assays can also be used to quantify the amount of food present within the digestive tract of adult *Drosophila* using spectrophotometric or fluorescence readers (Wong et al., 2009, Shell et al., 2018, Eickelberg et al., 2022). This highlights a relatively simple method in which we could have quantified larval drug intake in this experiment. However several limitations to this methodology exist, primarily surrounding the incubation time given to the animals. Once excrement begins, the linearity between food consumption and dye accumulation ends, meaning this method is only beneficial to assess short term (30 minute) food intake (Eickelberg et al., 2022). Furthermore, in order for analysis to take place, *Drosophila* must be sacrificed (Eickelberg et al., 2022), which, in the context of this study, would mean we would be unable to assess the impact of Jed135 or UDCA on the characterised motor phenotypes.

Alternative food-intake assays are available, specifically to monitor the amount in which adult *Drosophila* ingest. One such assay is the Capillary FEeder (CAFE) assay in which a capillary containing liquid food is placed through the lid of the vial housing the *Drosophila*. Food intake is measured via the decrease in capillary volume (Diegelmann et al., 2017, Eickelberg et al., 2022). This method does not require the sacrifice of the *Drosophila* and therefore could provide a good alternative to measure food, and drug, consumption in our study if we were to continue to assess the Jed135 or UDCA effect in adult *Drosophila*. However, consideration should be given to the feasibility of *Drosophila* with a motor impairment to feed from a vertical food source placed at the top of the vial.

A further method by which we could analyse how much Jed135 or UDCA each larvae ingested would be via high performance liquid chromatography (HPLC). Briefly, the mobile phase (a sample dissolved in solvent) is passed through a column bearing a stationary

phase (immobilised chromatographic packing material). The inherent properties of the sample determine how long it takes for metabolites to pass through the column, those with the strongest interaction taking the longest amount of time to elute and vice versa, resulting in separation of the sample (Petrova and Sauer, 2017). HPLC is an improved version of standard column chromatography in which samples are passed through the column at a higher pressure, allowing for a faster separation time and higher resolution results (Makos et al., 2009). Previous studies have been able to separate dopamine, L-Dopa and methyldopa in the brains and retinas of *Drosophila* (Ramadan et al., 1993, Makos et al., 2009). Using a similar method, we would be able to investigate the exact quantity of Jed135 or UDCA that each larvae had ingested, allowing us to identify and exclude any larvae that had ingested below a threshold level of drug, thereby reducing variability and potentially observing more of a drug effect.

This section has been redacted by the author for commercial reasons.

One major consideration in the use of *Drosophila* for neurodegenerative research, particularly in drug discovery, is the formation and composition of the BBB. In neurodegenerative research it is vital to understand whether a novel therapeutic is permeating the BBB in order to reach its desired target. The composition of the BBB is extremely different between vertebrates and invertebrates, and hence between humans and *Drosophila*. Briefly, the insect BBB is primarily comprised of glial cells whereas in vertebrates, it is formed from the brain vascular epithelium (Hindle and Bainton, 2014). The function of the BBB is to protect the nervous system and its environment from the potentially damaging and often fluctuating components of the blood. Therefore, one of the major differences between the vertebrate and invertebrate BBB system is due, in part, to the fact that invertebrates such as insects do not possess the same blood capillary system as vertebrates and hence the BBB must completely surround the nervous system (Hindle and Bainton, 2014). Conversely however, the invertebrate BBB is a compound structure, analogous to the vertebrate neurovascular unit, meaning that they represent a structural multicellular unit that is able to function in unison (Hindle and Bainton, 2014, Bell et al., 2020a). Considering the ability of a novel compound to cross the human BBB is pivotal and often a hindrance in neuropharmacology. Generally, cells in culture are unable to replicate the full extent of the BBB and therefore *in vivo* assessments are necessary to decipher whether a novel compound will reach its brain destination.

Similarly, it is likely that rodents and humans display differences in the make-up of the BBB. In both human and rodent PD, the BBB has been described as 'leaky', meaning that immune mediators from the blood are likely able to cross over into the central nervous system (Carvey et al., 2009, Potashkin et al., 2010). However, crucially, rodents possess different enzymes to humans, therefore it can be postulated that the nutrients required by the brain, along with the toxins being removed from the brain, are different between the species (Carvey et al., 2009, Potashkin et al., 2010) and may account for some of the failures observed in human clinical trials following animal studies (Pound, 2020). Rodents are often deemed too expensive for this type of study and also have a longer life cycle, whereas *Drosophila* offer a lower cost alternative and changes in fluorescence intensity of the eye are able to determine the penetration of compound through the BBB (DeSalvo et al., 2011, Hindle and Bainton, 2014).

This section has been redacted by the author for commercial reasons.

7 General Discussion

PD is a progressive neurodegenerative disease of which there is currently no cure. Current available therapeutic interventions are solely focussed on alleviating symptomatic burden, with no effect on disease progression. The work presented in this thesis is a continuation of a PhD project undertaken in our group by Chris Hastings, also in collaboration with NZP UK Ltd. Following an initial drug screen of 144 compounds followed by a more in-depth screen of the top performing compounds, Jed135 was highlighted as the lead compound and the overarching aim of this project was to identify its mechanism of action. We identified four objectives which included (I) Characterising the cell model used (II) Understanding PD related mechanisms (III) Assessing the putative targets and (IV) Understanding the actions of Jed135 in an *in vivo* model.

7.1 Results Overview

This section has been redacted by the author for commercial reasons.

This section has been redacted by the author for commercial reasons.

This section has been redacted by the author for commercial reasons.

7.2 Drug Screening

This project was based upon a phenotypic drug screen, meaning that compounds were screened against known and quantitatively measured cellular deficits in order to determine their effectiveness at altering these phenotypes. On the contrary, different drug screening methodologies can be carried out, namely reverse pharmacology, more commonly referred to as a target-based approach. For this, a gene or protein target is identified and compounds are screened primarily for their interaction with this target (Lage et al., 2018). The benefit of a phenotypic approach over a target-based approach is that phenotypic studies are able to screen vast quantities of compounds at once in a high throughput fashion, especially given the fact that assays have since been miniaturised into 384- or 1536- well plates (Lage et al., 2018). For many years, target-based drug discovery was the main approach taken, however more recently, due to the lack of suitable targets identified, researchers have begun to adopt a phenotypic based approach which has led to recent advances in treatments for cystic fibrosis, spinal muscular atrophy and hepatitis C (Berg, 2021). The risks, however, with a phenotypic based approach is that because a target is yet to be identified, there is a higher probability of off target effects and toxicity occurring (Berg, 2021). The pipeline of a phenotypic drug screen involves screening a desired drug library in a phenotypic assay, such as an MMP assay for PD, with results highlighting any compounds that exhibit a rescue effect (full or partial) on the phenotype of interest. Any hits from this initial screen are then interrogated for undesirable effects, at which point lead optimisation can begin, with more in-depth phenotypic assays performed and an understanding of the mechanism formulated. This process may also include screening any leads in more disease relevant models such a cell-type specific, for example dopaminergic neurones for PD, or animal models. Preclinical studies can then be undertaken to assess both safety, tolerability and efficacy in animals, before being taken forward into human clinical trials (Berg, 2021). This process can take

anywhere up to 15 years at a cost of approximately £1 billion or more (Mohs and Greig, 2017).

As of June 2022, according to clinicaltrials.gov, there were 3206 clinical trials relating to PD listed on their website, of which 170 were based in the United Kingdom. This study, along with other work in our group, is centring around therapeutically targeting the mitochondria, however this represents just one potential target for the treatment of PD. Others are assessing the feasibility of immunotherapies, gene therapies and targeting alpha synuclein through decreasing expression or reducing aggregation, to name a few (Ntetsika et al., 2021). It is beyond the scope of this thesis to provide a comprehensive review of different PD targeted therapies; however we will consider one drug that has garnered interest in recent years. Exenatide, the synthetic version of exendin-4 found in the saliva of the Gila monster, is a glucagon-like peptide 1 (GLP1) receptor agonist which has been used in the treatment of type 2 diabetes mellitus (T2DM) since 2005 (Aviles-Olmos et al., 2013). Early *in vitro* work uncovered potential neurotrophic and neuroprotective effects of exendin-4, through the induction of neurite outgrowth, neuronal differentiation and the rescue of neuronal degeneration (Perry et al., 2002a, Perry et al., 2002b, Vijjaratnam et al., 2021a). Due to the fact exenatide was already approved for use in humans in the treatment of T2DM, a single-blinded randomised control trial was undertaken to assess the tolerability of exenatide in PD patients, in a rapid and cost-efficient manner (Aviles-Olmos et al., 2013). This study was able to provide evidence that exenatide was well tolerated in people with PD, as well as providing modest improvements in UPDRS score for those on drug vs those on placebo, providing supporting evidence to continue with larger scale trials (Aviles-Olmos et al., 2013). Following this, a double-blinded, placebo controlled, randomised trial was undertaken to assess the effect of once weekly exenatide injections on UPDRS score following 48 weeks of treatment. They observed an improvement of 1 point in the exenatide group and a worsening of 2.1 points in the control group, concluding that exenatide provided beneficial effects on PD although they were unable to prove whether this was due to extended symptomatic relief or an alteration in disease pathophysiology (Athauda et al., 2017). A further study has since begun with the aim of replicating or refuting the 2017 study, using a larger cohort of PD patients, assessed over a longer time period, 96 weeks. As before, the primary end point of this study will be the assessment and comparisons of UPDRS score in the practically define OFF state, as well as secondary outcomes to assess other motor, non-motor and cognitive scores. This trial is currently in process and results are expected in 2024 (Vijjaratnam et al., 2021a). Exenatide provides another perfect example of a drug repurposing study, a drug initially licensed for the treatment of T2DM that may provide beneficial effects in the treatment of PD, in a similar fashion to UDCA. However, it

further highlights the time scale of the drug development timeline, which remains evident in repurposing studies.

A further complication that often arises not only in PD but for neurodegenerative diseases as a whole, is the inability to identify the correct population of patients for clinical trials. It is likely that the number of neurones that have degenerated by the point of symptom presentation represents a stage in the disease process in which it is too late to begin a neuroprotective therapy. Although neuroprotective drugs may still be of benefit to protect the remaining neurones, they may be more beneficial earlier in the disease course. It can therefore be postulated that many potential therapies have failed in clinical trials as they are being tested on the wrong patient population. This again highlights the need to identify more robust disease biomarkers in order to recruit pre-clinical patients on neuroprotective drug clinical trials and follow their progress longitudinally.

As mentioned previously in this thesis, PD is an extremely heterogeneous disease, with different patients experiencing a wealth of different symptoms. Therefore, it is reasonable to assume that different patients are likely to have different underlying causes of their PD and consequently respond differently to prescribed medications. The aim of personalised medicine is to target a patient's treatment specifically to their clinical characteristics as well as genotype and biomarkers (Mishima et al., 2021). However, as mentioned, reliable, robust biomarkers are yet to be identified for PD and as such, diagnosis remains to be based on clinical characteristics. That said, there has been some evidence to suggest that patients can be grouped on clinical characteristics, with a 2017 paper performing a cluster analysis on 421 patients based on a number of factors including motor and non-motor symptoms and neuropsychological testing. They were able to determine 3 subgroups of patients; (I) mild motor predominant, patients with the mildest UPDRS scores as well as minimal sleep, olfactory and autonomic dysfunction (II) Intermediate, those whose symptoms lay between I and III (III) diffuse malignant, patients who had the most severe motor and non-motor symptoms (Fereshtehnejad et al., 2017). The ability to group clinical characteristics is beneficial, however this was unable to take into account the molecular driving factor behind their PD and therefore a paper briefly discussed earlier in this thesis, involving our group has furthered our molecular understanding of PD sub-grouping by identifying those with a mitochondrial or lysosomal driven phenotype. We described patients with mitochondrial driven PD to have a reduction in complex I and IV protein expression while those with lysosomal driven PD appeared to have activation in lysosomal pathways (Carling et al., 2020). Being able to mechanistically stratify patients through deep tissue phenotyping is a great step forward for precision medicine, however this work was undertaken on fibroblasts

following skin biopsy which presents challenges in itself. It involves an invasive procedure that isn't necessarily feasible within a clinical setting and consequently the lab work that would ensue following a skin biopsy may mean it is not a cost-effective method of stratification. It provides evidence to suggest that patients are able to be stratified into disease-relevant groups, however the techniques needed to make this a reality need refining.

7.3 Modelling Parkinson's Disease

Consideration should also be given to the models used within this project; the iNPC derived dopaminergic neurone and the *Parkin* mutant *Drosophila*. Unfortunately, as is true for the majority of neurodegenerative diseases, there is no perfect way to model human PD either by cell culture or with the use of animal models.

7.3.1 Cell Model

The induced dopaminergic neurones offer a cell-type specific method to model PD, however they are not fully representative of the human brain. In this instance we utilised a single cell type, whereas in reality, the brain consists not only of neurones, but also of astrocytes, microglia and oligodendrocytes, all of which likely interact with and influence the overall fate of the dopaminergic neurones. Therefore, in the future, utilising a co-culture model may be of benefit to understand the effects of novel drug compounds not only on the cell type affected, but also on the supporting cells of the brain. Furthermore, in relation to drug screening, the drug toxicity profile may not accurately represent the tissue-specific or whole-body response, often leading to unexpected toxicity reactions *in vivo* (Maitra and Ciesla, 2019). Investigation of Jed135 in a co-culture model may aid in reducing unexpected toxicity as it is more representative of the brain environment.

This study only investigated a limited number of patient lines, therefore although we observed both concordant and discordant results between the cell lines, data must be interpreted with caution. It would be pertinent to both increase the number of patient lines assessed, as well as broaden the genetic range from which we assess. For example increasing patient numbers for both sporadic and alpha synuclein triplications as well as investigating other alpha synuclein multiplications or mutations and utilising patients with *Parkin*, *LRRK2* or *PINK1* mutations before drawing any finite conclusions.

Modelling sporadic PD in cell culture is difficult. The use of iNPC derived dopaminergic neurones allows us to maintain any epigenetic alterations that an individual has accumulated over their life span, alterations that may have led to the development of disease. This is a large advantage over iPSC derived neurones that return to an embryonic-like state prior to

differentiation. Therefore, our iNPC derived dopaminergic neurones are one of the best ways to model an otherwise complex sporadic disease.

7.3.2 Animal Model

Similarly, all animal models possess advantages and disadvantages for modelling PD, with no one model incorporating all aspects of human disease. Perhaps one of the more difficult aspects of human PD to model is the alpha synuclein pathology that is observed. Mice are known to endogenously express alpha synuclein, hence this can be manipulated in a number of ways. Firstly, it is able to be knocked out, allowing researchers to investigate its physiological role within a biological system (Fernagut and Chesselet, 2004). Alpha synuclein knock out mice have been described as having reduced dopamine content in the striatum (Abeliovich et al., 2000) as well as impairments in spatial and working memory (Kokhan et al., 2012). Alternatively, transgenic mice can overexpress human wild type or mutated alpha synuclein in order to model PD (Chesselet, 2008), with the gene mutations administered under different promoters, generating different models. Another method of modelling alpha synuclein expression in animals is via the introduction of alpha synuclein preformed fibrils. This method requires the generation of preformed fibrils from monomeric recombinant alpha synuclein, although not all monomeric alpha synuclein has the potential to aggregate, highlighting the importance in choosing the correct starting material (Polinski et al., 2018). Preformed fibrils can be introduced into different models, both *in vivo* and *in vitro*. In cultured neurones pathology is generated relatively quickly, however, after direct injection into the brain of an animal, it can take up to 6 months for neurodegenerative changes to occur, potentially making it more representative of human disease (Thakur et al., 2017). Drug development projects such as this often use at least one, if not more, animal models to investigate safety and tolerability of a novel drug compound, as well as efficacy. It is likely that many drugs are discounted for use in human disease due to lack of positive results on efficacy in animals. However it is entirely possible that due to inherent differences in the genetic make-up of humans and animals, along with the discussed caveats in modelling of human diseases, drug compounds are being overlooked which may be of benefit in human disease.

7.4 Alpha Synuclein

This section has been redacted by the author for commercial reasons.

This section has been redacted by the author for commercial reasons.

7.5 Future Work

This section has been redacted by the author for commercial reasons.

This section has been redacted by the author for commercial reasons.

This section has been redacted by the author for commercial reasons.

This section has been redacted by the author for commercial reasons.

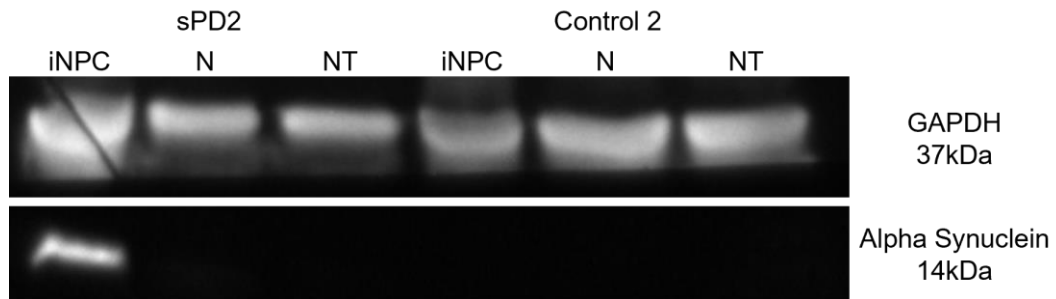
This section has been redacted by the author for commercial reasons.

7.6 Conclusion

This section has been redacted by the author for commercial reasons.

8 Appendix

8.1 Alpha Synuclein Expression in Control 2 and sPD2



Appendix Figure 8.1 Alpha synuclein expression for sPD2 and control 2

Representative Western blot for sPD2 and control 2 showing only one strong band at the sPD2 iNPC. This was the case for all repeats attempted (n=6), therefore the decision was made not to continue with this

8.2 Expression

This section has been redacted by the author for commercial reasons.

8.3 Knockout *Drosophila*

This section has been redacted by the author for commercial reasons.

This section has been redacted by the author for commercial reasons.

9 References

- ABDELKADER, N. F., SAFAR, M. M. & SALEM, H. A. 2016. Ursodeoxycholic Acid Ameliorates Apoptotic Cascade in the Rotenone Model of Parkinson's Disease: Modulation of Mitochondrial Perturbations. *Mol Neurobiol*, 53, 810-817.
- ABELIOVICH, A., SCHMITZ, Y., FARIÑAS, I., CHOI-LUNDBERG, D., HO, W. H., CASTILLO, P. E., SHINSKY, N., VERDUGO, J. M., ARMANINI, M., RYAN, A., HYNES, M., PHILLIPS, H., SULZER, D. & ROSENTHAL, A. 2000. Mice lacking alpha-synuclein display functional deficits in the nigrostriatal dopamine system. *Neuron*, 25, 239-52.
- ACKERMAN, H. D. & GERHARD, G. S. 2016. Bile Acids in Neurodegenerative Disorders. *Frontiers in aging neuroscience*, 8, 263-263.
- ADAMS, M. D., CELNIKER, S. E., HOLT, R. A., EVANS, C. A., GOCAYNE, J. D., AMANATIDES, P. G., SCHERER, S. E., LI, P. W., HOSKINS, R. A., GALLE, R. F., GEORGE, R. A., LEWIS, S. E., RICHARDS, S., ASHBURNER, M., HENDERSON, S. N., SUTTON, G. G., WORTMAN, J. R., YANDELL, M. D., ZHANG, Q., CHEN, L. X., BRANDON, R. C., ROGERS, Y. H., BLAZEJ, R. G., CHAMPE, M., PFEIFFER, B. D., WAN, K. H., DOYLE, C., BAXTER, E. G., HELT, G., NELSON, C. R., GABOR, G. L., ABRIL, J. F., AGBAYANI, A., AN, H. J., ANDREWS-PFANNKOCH, C., BALDWIN, D., BALLEW, R. M., BASU, A., BAXENDALE, J., BAYRAKTAROGLU, L., BEASLEY, E. M., BEESON, K. Y., BENOS, P. V., BERMAN, B. P., BHANDARI, D., BOLSHAKOV, S., BORKOVA, D., BOTCHAN, M. R., BOUCK, J., BROKSTEIN, P., BROTTIER, P., BURTIS, K. C., BUSAM, D. A., BUTLER, H., CADIEU, E., CENTER, A., CHANDRA, I., CHERRY, J. M., CAWLEY, S., DAHLKE, C., DAVENPORT, L. B., DAVIES, P., DE PABLOS, B., DELCHER, A., DENG, Z., MAYS, A. D., DEW, I., DIETZ, S. M., DODSON, K., DOUP, L. E., DOWNES, M., DUGAN-ROCHA, S., DUNKOV, B. C., DUNN, P., DURBIN, K. J., EVANGELISTA, C. C., FERRAZ, C., FERRIERA, S., FLEISCHMANN, W., FOSLER, C., GABRIELIAN, A. E., GARG, N. S., GELBART, W. M., GLASSER, K., GLODEK, A., GONG, F., GORRELL, J. H., GU, Z., GUAN, P., HARRIS, M., HARRIS, N. L., HARVEY, D., HEIMAN, T. J., HERNANDEZ, J. R., HOUCK, J., HOSTIN, D., HOUSTON, K. A., HOWLAND, T. J., WEI, M. H., IBEGWAM, C., et al. 2000. The genome sequence of *Drosophila melanogaster*. *Science*, 287, 2185-95.
- AGARWAL, S., LOH, Y. H., MCLOUGHLIN, E. M., HUANG, J., PARK, I. H., MILLER, J. D., HUO, H., OKUKA, M., DOS REIS, R. M., LOEWER, S., NG, H. H., KEEFE, D. L., GOLDMAN, F. D., KLINGELHUTZ, A. J., LIU, L. & DALEY, G. Q. 2010. Telomere elongation in induced pluripotent stem cells from dyskeratosis congenita patients. *Nature*, 464, 292-6.
- ALAM, M. S. 2018. Proximity Ligation Assay (PLA). *Current protocols in immunology*, 123, e58-e58.
- ALAM, P., BOUSSET, L., MELKI, R. & OTZEN, D. E. 2019. α -synuclein oligomers and fibrils: a spectrum of species, a spectrum of toxicities. *Journal of Neurochemistry*, 150, 522-534.
- ALMEIDA DE CARVALHO, M. J. & MIRTH, C. K. 2017. Food intake and food choice are altered by the developmental transition at critical weight in *Drosophila melanogaster*. *Animal Behaviour*, 126, 195-208.
- AMO, T., SAIKI, S., SAWAYAMA, T., SATO, S. & HATTORI, N. 2014. Detailed analysis of mitochondrial respiratory chain defects caused by loss of PINK1. *Neurosci Lett*, 580, 37-40.
- ANDERSON, J. P., WALKER, D. E., GOLDSTEIN, J. M., DE LAAT, R., BANDUCCI, K., CACCAVELLO, R. J., BARBOUR, R., HUANG, J., KLING, K., LEE, M., DIEP, L., KEIM, P. S., SHEN, X., CHATAWAY, T., SCHLOSSMACHER, M. G., SEUBERT, P., SCHENK, D., SINHA, S., GAI, W. P. & CHILCOTE, T. J. 2006. Phosphorylation of Ser-129 is the dominant pathological modification of alpha-synuclein in familial and sporadic Lewy body disease. *J Biol Chem*, 281, 29739-52.
- ANTONSSON, B. 2001. Bax and other pro-apoptotic Bcl-2 family "killer-proteins" and their victim the mitochondrion. *Cell and Tissue Research*, 306, 347-361.
- ATHAUDA, D., MACLAGAN, K., SKENE, S. S., BAJWA-JOSEPH, M., LETCHFORD, D., CHOWDHURY, K., HIBBERT, S., BUDNIK, N., ZAMPEDRI, L., DICKSON, J., LI, Y., AVILES-OLMOS, I., WARNER, T. T., LIMOUSIN, P., LEES, A. J., GREIG, N. H., TEBBS, S. & FOLTYNIE, T. 2017. Exenatide once

- weekly versus placebo in Parkinson's disease: a randomised, double-blind, placebo-controlled trial. *Lancet (London, England)*, 390, 1664-1675.
- AUBURGER, G., KLINKENBERG, M., DROST, J., MARCUS, K., MORALES-GORDO, B., KUNZ, W. S., BRANDT, U., BROCCOLI, V., REICHMANN, H., GISPERT, S. & JENDRACH, M. 2012. Primary skin fibroblasts as a model of Parkinson's disease. *Molecular neurobiology*, 46, 20-27.
- AVILES-OLMOS, I., DICKSON, J., KEFALOPOULOU, Z., DJAMSHIDIAN, A., ELL, P., SODERLUND, T., WHITTON, P., WYSE, R., ISAACS, T., LEES, A., LIMOUSIN, P. & FOLTYNIE, T. 2013. Exenatide and the treatment of patients with Parkinson's disease. *The Journal of clinical investigation*, 123, 2730-2736.
- AYDIN, S. 2015. A short history, principles, and types of ELISA, and our laboratory experience with peptide/protein analyses using ELISA. *Peptides*, 72, 4-15.
- BAEKEN, M. W., WECKMANN, K., DIEFENTHÄLER, P., SCHULTE, J., YUSIFLI, K., MOOSMANN, B., BEHL, C. & HAJIEVA, P. 2020. Novel Insights into the Cellular Localization and Regulation of the Autophagosomal Proteins LC3A, LC3B and LC3C. *Cells*, 9, 2315.
- BALESTRINO, R. & SCHAPIRA, A. H. V. 2020. Parkinson disease. *European Journal of Neurology*, 27, 27-42.
- BARTRUP, J. T., MOORMAN, J. M. & NEWBERRY, N. R. 1997. BDNF enhances neuronal growth and synaptic activity in hippocampal cell cultures. *Neuroreport*, 8, 3791-4.
- BASS, J. J., WILKINSON, D. J., RANKIN, D., PHILLIPS, B. E., SZEWCZYK, N. J., SMITH, K. & ATHERTON, P. J. 2017. An overview of technical considerations for Western blotting applications to physiological research. *Scandinavian journal of medicine & science in sports*, 27, 4-25.
- BAYIR, H., KAPRALOV, A. A., JIANG, J., HUANG, Z., TYURINA, Y. Y., TYURIN, V. A., ZHAO, Q., BELIKOVA, N. A., VLASOVA, II, MAEDA, A., ZHU, J., NA, H. M., MASTROBERARDINO, P. G., SPARVERO, L. J., AMOSCATO, A. A., CHU, C. T., GREENAMYRE, J. T. & KAGAN, V. E. 2009. Peroxidase mechanism of lipid-dependent cross-linking of synuclein with cytochrome C: protection against apoptosis versus delayed oxidative stress in Parkinson disease. *J Biol Chem*, 284, 15951-69.
- BAZZARI, F. H., ABDALLAH, D. M. & EL-ABHAR, H. S. 2019. Chenodeoxycholic Acid Ameliorates AICl(3)-Induced Alzheimer's Disease Neurotoxicity and Cognitive Deterioration via Enhanced Insulin Signaling in Rats. *Molecules*, 24.
- BEDUT, S., SEMINATORE-NOLE, C., LAMAMY, V., CAIGNARD, S., BOUTIN, J. A., NOSJEAN, O., STEPHAN, J.-P. & COGE, F. 2016. High-throughput drug profiling with voltage- and calcium-sensitive fluorescent probes in human iPSC-derived cardiomyocytes. *American Journal of Physiology-Heart and Circulatory Physiology*, 311, H44-H53.
- BELL, A. H., MILLER, S. L., CASTILLO-MELENDEZ, M. & MALHOTRA, A. 2020a. The Neurovascular Unit: Effects of Brain Insults During the Perinatal Period. *Frontiers in Neuroscience*, 13.
- BELL, S. M., BARNES, K., CLEMMENS, H., AL-RAFAIAH, A. R., AL-OFI, E. A., LEECH, V., BANDMANN, O., SHAW, P. J., BLACKBURN, D. J., FERRAIUOLO, L. & MORTIBOYS, H. 2018. Ursodeoxycholic Acid Improves Mitochondrial Function and Redistributes Drp1 in Fibroblasts from Patients with Either Sporadic or Familial Alzheimer's Disease. *J Mol Biol*, 430, 3942-3953.
- BELL, S. M., BURGESS, T., LEE, J., BLACKBURN, D. J., ALLEN, S. P. & MORTIBOYS, H. 2020b. Peripheral Glycolysis in Neurodegenerative Diseases. *International journal of molecular sciences*, 21, 8924.
- BENGOA-VERGNIORY, N., ROBERTS, R. F., WADE-MARTINS, R. & ALEGRE-ABARRATEGUI, J. 2017. Alpha-synuclein oligomers: a new hope. *Acta neuropathologica*, 134, 819-838.
- BERG, E. L. 2021. The future of phenotypic drug discovery. *Cell Chemical Biology*, 28, 424-430.
- BERNAL-CONDE, L. D., RAMOS-ACEVEDO, R., REYES-HERNÁNDEZ, M. A., BALBUENA-OLVERA, A. J., MORALES-MORENO, I. D., ARGÜERO-SÁNCHEZ, R., SCHÜLE, B. & GUERRA-CRESPO, M. 2020. Alpha-Synuclein Physiology and Pathology: A Perspective on Cellular Structures and Organelles. *Frontiers in neuroscience*, 13, 1399-1399.

- BHUJABAL, Z., BIRGISDOTTIR Å, B., SJØTTEM, E., BRENNE, H. B., ØVERVATN, A., HABISOV, S., KIRKIN, V., LAMARK, T. & JOHANSEN, T. 2017. FKBP8 recruits LC3A to mediate Parkin-independent mitophagy. *EMBO Rep*, 18, 947-961.
- BLESA, J., TRIGO-DAMAS, I., DEL REY, N. L. & OBESO, J. A. 2018. The use of nonhuman primate models to understand processes in Parkinson's disease. *J Neural Transm (Vienna)*, 125, 325-335.
- BOETTCHER, M. & MCMANUS, M. T. 2015. Choosing the Right Tool for the Job: RNAi, TALEN, or CRISPR. *Molecular cell*, 58, 575-585.
- BOGETOFTE, H., JENSEN, P., RYDING, M., SCHMIDT, S. I., OKARMUS, J., RITTER, L., WORM, C. S., HOHNHOLT, M. C., AZEVEDO, C., ROYBON, L., BAK, L. K., WAAGEPETERSEN, H., RYAN, B. J., WADE-MARTINS, R., LARSEN, M. R. & MEYER, M. 2019. PARK2 Mutation Causes Metabolic Disturbances and Impaired Survival of Human iPSC-Derived Neurons. *Frontiers in cellular neuroscience*, 13, 297-297.
- BOLUS, H., CROCKER, K., BOEKHOFF-FALK, G. & CHTARBANOVA, S. 2020. Modeling Neurodegenerative Disorders in *Drosophila melanogaster*. *International journal of molecular sciences*, 21, 3055.
- BONORA, M., PATERGNANI, S., RIMESSI, A., DE MARCHI, E., SUSKI, J. M., BONONI, A., GIORGI, C., MARCHI, S., MISSIROLI, S., POLETTI, F., WIECKOWSKI, M. R. & PINTON, P. 2012. ATP synthesis and storage. *Purinergic signalling*, 8, 343-357.
- BOROVAC, J. A. 2016. Side effects of a dopamine agonist therapy for Parkinson's disease: a mini-review of clinical pharmacology. *The Yale journal of biology and medicine*, 89, 37-47.
- BRAAK, H., DEL TREDICI, K., RUB, U., DE VOS, R. A., JANSEN STEUR, E. N. & BRAAK, E. 2003a. Staging of brain pathology related to sporadic Parkinson's disease. *Neurobiol Aging*, 24, 197-211.
- BRAAK, H., TREDICI, K. D., RÜB, U., DE VOS, R. A. I., JANSEN STEUR, E. N. H. & BRAAK, E. 2003b. Staging of brain pathology related to sporadic Parkinson's disease. *Neurobiology of Aging*, 24, 197-211.
- BRAGINA, O., SERGEJEVA, S., SERG, M., ŽARKOVSKY, T., MALOVERJAN, A., KOGERMAN, P. & ŽARKOVSKY, A. 2010. Smoothed agonist augments proliferation and survival of neural cells. *Neuroscience Letters*, 482, 81-85.
- BRAND, A. H. & PERRIMON, N. 1993. Targeted gene expression as a means of altering cell fates and generating dominant phenotypes. *Development*, 118, 401-15.
- BURRÉ, J., SHARMA, M. & SÜDHOF, T. C. 2018. Cell Biology and Pathophysiology of α -Synuclein. *Cold Spring Harbor perspectives in medicine*, 8, a024091.
- BURRÉ, J., SHARMA, M., TSETSENIS, T., BUCHMAN, V., ETHELTON, M. R. & SÜDHOF, T. C. 2010. Alpha-synuclein promotes SNARE-complex assembly in vivo and in vitro. *Science*, 329, 1663-7.
- CAFFREY, D. R., ZHAO, J., SONG, Z., SCHAFFER, M. E., HANEY, S. A., SUBRAMANIAN, R. R., SEYMOUR, A. B. & HUGHES, J. D. 2011. siRNA off-target effects can be reduced at concentrations that match their individual potency. *PLoS one*, 6, e21503-e21503.
- CAIAZZO, M., DELL'ANNO, M. T., DVORETSKOVA, E., LAZAREVIC, D., TAVERNA, S., LEO, D., SOTNIKOVA, T. D., MENEGON, A., RONCAGLIA, P., COLCIAGO, G., RUSSO, G., CARNINCI, P., PEZZOLI, G., GAINETDINOV, R. R., GUSTINCICH, S., DITYATEV, A. & BROCCOLI, V. 2011. Direct generation of functional dopaminergic neurons from mouse and human fibroblasts. *Nature*, 476, 224-227.
- CAMPOS, F. L., CARVALHO, M. M., CRISTOVÃO, A. C., JE, G., BALTAZAR, G., SALGADO, A. J., KIM, Y. S. & SOUSA, N. 2013. Rodent models of Parkinson's disease: beyond the motor symptomatology. *Front Behav Neurosci*, 7, 175.
- CARLING, P. J., MORTIBOYS, H., GREEN, C., MIHAYLOV, S., SANDOR, C., SCHWARTZENTRUBER, A., TAYLOR, R., WEI, W., HASTINGS, C., WONG, S., LO, C., EVETTS, S., CLEMMENS, H., WYLES, M., WILLCOX, S., PAYNE, T., HUGHES, R., FERRAIUOLO, L., WEBBER, C., HIDE, W., WADE-MARTINS, R., TALBOT, K., HU, M. T. & BANDMANN, O. 2020. Deep phenotyping of peripheral

- tissue facilitates mechanistic disease stratification in sporadic Parkinson's disease. *Progress in Neurobiology*, 187, 101772.
- CARLSON, E. A. 2013. How fruit flies came to launch the chromosome theory of heredity. *Mutat Res*, 753, 1-6.
- CARVEY, P. M., HENDEY, B. & MONAHAN, A. J. 2009. The blood-brain barrier in neurodegenerative disease: a rhetorical perspective. *J Neurochem*, 111, 291-314.
- CASTILLO-QUAN, J. I. 2011. Parkin' control: regulation of PGC-1 α through PARIS in Parkinson's disease. *Disease models & mechanisms*, 4, 427-429.
- CASTRO-CALDAS, M., CARVALHO, A. N., RODRIGUES, E., HENDERSON, C., WOLF, C. R. & GAMA, M. J. 2012a. Glutathione S-transferase pi mediates MPTP-induced c-Jun N-terminal kinase activation in the nigrostriatal pathway. *Mol Neurobiol*, 45, 466-77.
- CASTRO-CALDAS, M., CARVALHO, A. N., RODRIGUES, E., HENDERSON, C. J., WOLF, C. R., RODRIGUES, C. M. & GAMA, M. J. 2012b. Tauroursodeoxycholic acid prevents MPTP-induced dopaminergic cell death in a mouse model of Parkinson's disease. *Mol Neurobiol*, 46, 475-86.
- CHAI, J., WANG, Y., LI, H., HE, W., ZOU, W., ZHOU, Y., HU, X. & CHAI, Q. 2016. [Distribution of postsynaptic density protein 95 (PSD95) and synaptophysin during neuronal maturation]. *Xi Bao Yu Fen Zi Mian Yi Xue Za Zhi*, 32, 1619-1622.
- CHANG, E.-A., JIN, S.-W., NAM, M.-H. & KIM, S.-D. 2019. Human Induced Pluripotent Stem Cells : Clinical Significance and Applications in Neurologic Diseases. *Journal of Korean Neurosurgical Society*, 62, 493-501.
- CHEN, L., PERIQUET, M., WANG, X., NEGRO, A., MCLEAN, P. J., HYMAN, B. T. & FEANY, M. B. 2009. Tyrosine and serine phosphorylation of alpha-synuclein have opposing effects on neurotoxicity and soluble oligomer formation. *The Journal of clinical investigation*, 119, 3257-3265.
- CHESSLETT, M. F. 2008. In vivo alpha-synuclein overexpression in rodents: a useful model of Parkinson's disease? *Exp Neurol*, 209, 22-7.
- CHIA, S. J., TAN, E.-K. & CHAO, Y.-X. 2020. Historical Perspective: Models of Parkinson's Disease. *International journal of molecular sciences*, 21, 2464.
- CHIANG, J. Y. L. 2013. Bile acid metabolism and signaling. *Comprehensive Physiology*, 3, 1191-1212.
- CHO, M.-K., NODET, G., KIM, H.-Y., JENSEN, M. R., BERNADO, P., FERNANDEZ, C. O., BECKER, S., BLACKLEDGE, M. & ZWECKSTETTER, M. 2009. Structural characterization of α -synuclein in an aggregation prone state. *Protein Science*, 18, 1840-1846.
- CHOI, J., YIN, T., SHINOZAKI, K., LAMPE, J. W., STEVENS, J. F., BECKER, L. B. & KIM, J. 2018. Comprehensive analysis of phospholipids in the brain, heart, kidney, and liver: brain phospholipids are least enriched with polyunsaturated fatty acids. *Molecular and cellular biochemistry*, 442, 187-201.
- CHOI, M. L., CHAPPARD, A., SINGH, B. P., MACLACHLAN, C., RODRIGUES, M., FEDOTOVA, E., BEREZHNOV, A. V., DE, S., PEDDIE, C., ATHAUDA, D., VIRDI, G. S., ZHANG, W., EVANS, J. R., WERNICK, A., ZANJANI, Z. S., ANGELOVA, P. R., ESTERAS, N., VINIKUROV, A., MORRIS, K., JEACOCK, K., TOSATTO, L., LITTLE, D., GISSEN, P., CLARKE, D. J., KUNATH, T., COLLINSON, L., KLENERMAN, D., ABRAMOV, A. Y., HORROCKS, M. H. & GANDHI, S. 2022. Structural conversion of α -synuclein at the mitochondria induces neuronal toxicity. *bioRxiv*, 2022.06.07.494932.
- CHU, C. T., JI, J., DAGDA, R. K., JIANG, J. F., TYURINA, Y. Y., KAPRALOV, A. A., TYURIN, V. A., YANAMALA, N., SHRIVASTAVA, I. H., MOHAMMADYANI, D., WANG, K. Z. Q., ZHU, J., KLEIN-SEETHARAMAN, J., BALASUBRAMANIAN, K., AMOSCATO, A. A., BORISENKO, G., HUANG, Z., GUSDON, A. M., CHEIKHI, A., STEER, E. K., WANG, R., BATY, C., WATKINS, S., BAHAR, I., BAYIR, H. & KAGAN, V. E. 2013. Cardiolipin externalization to the outer mitochondrial membrane acts as an elimination signal for mitophagy in neuronal cells. *Nature cell biology*, 15, 1197-1205.

- CHU, Y., GOLDMAN, J. G., KELLY, L., HE, Y., WALICZEK, T. & KORDOWER, J. H. 2014. Abnormal alpha-synuclein reduces nigral voltage-dependent anion channel 1 in sporadic and experimental Parkinson's disease. *Neurobiol Dis*, 69, 1-14.
- CHUN, H. S. & LOW, W. C. 2012. Ursodeoxycholic acid suppresses mitochondria-dependent programmed cell death induced by sodium nitroprusside in SH-SY5Y cells. *Toxicology*, 292, 105-12.
- CHUNG, S. Y., KISHINEVSKY, S., MAZZULLI, J. R., GRAZIOTTO, J., MREJERU, A., MOSHAROV, E. V., PUSPITA, L., VALIULAH, P., SULZER, D., MILNER, T. A., TALDONE, T., KRAINIC, D., STUDER, L. & SHIM, J. W. 2016. Parkin and PINK1 Patient iPSC-Derived Midbrain Dopamine Neurons Exhibit Mitochondrial Dysfunction and α -Synuclein Accumulation. *Stem Cell Reports*, 7, 664-677.
- CLARK, E. H., VÁZQUEZ DE LA TORRE, A., HOSHIKAWA, T. & BRISTON, T. 2021. Targeting mitophagy in Parkinson's disease. *The Journal of biological chemistry*, 296, 100209-100209.
- COLE, N. B., DIEULIIS, D., LEO, P., MITCHELL, D. C. & NUSSBAUM, R. L. 2008. Mitochondrial translocation of alpha-synuclein is promoted by intracellular acidification. *Experimental cell research*, 314, 2076-2089.
- CONNERTH, M., TATSUTA, T., HAAG, M., KLECKER, T., WESTERMANN, B. & LANGER, T. 2012. Intramitochondrial Transport of Phosphatidic Acid in Yeast by a Lipid Transfer Protein. *Science*, 338, 815-818.
- CORTI, O. 2019. Neuronal Mitophagy: Lessons from a Pathway Linked to Parkinson's Disease. *Neurotox Res*, 36, 292-305.
- COULOM, H. & BIRMAN, S. 2004. Chronic exposure to rotenone models sporadic Parkinson's disease in *Drosophila melanogaster*. *The Journal of neuroscience : the official journal of the Society for Neuroscience*, 24, 10993-10998.
- CREED, S. & MCKENZIE, M. 2019. Measurement of Mitochondrial Membrane Potential with the Fluorescent Dye Tetramethylrhodamine Methyl Ester (TMRM). In: HAZNADAR, M. (ed.) *Cancer Metabolism: Methods and Protocols*. New York, NY: Springer New York.
- DAN DUNN, J., ALVAREZ, L. A., ZHANG, X. & SOLDATI, T. 2015. Reactive oxygen species and mitochondria: A nexus of cellular homeostasis. *Redox biology*, 6, 472-485.
- DANA, H., CHALBATANI, G. M., MAHMOODZADEH, H., KARIMLOO, R., REZAIEAN, O., MORADZADEH, A., MEHMANDOOST, N., MOAZZEN, F., MAZRAEH, A., MARMARI, V., EBRAHIMI, M., RASHNO, M. M., ABADI, S. J. & GHARAGOUZLO, E. 2017. Molecular Mechanisms and Biological Functions of siRNA. *International journal of biomedical science : IJBS*, 13, 48-57.
- DAUBNER, S. C., LE, T. & WANG, S. 2011. Tyrosine hydroxylase and regulation of dopamine synthesis. *Archives of biochemistry and biophysics*, 508, 1-12.
- DAWSON, T. M., KO, H. S. & DAWSON, V. L. 2010. Genetic animal models of Parkinson's disease. *Neuron*, 66, 646-661.
- DESALVO, M. K., MAYER, N., MAYER, F. & BAINTON, R. J. 2011. Physiologic and anatomic characterization of the brain surface glia barrier of *Drosophila*. *Glia*, 59, 1322-1340.
- DESHPANDE OA, M. S. 2021. Biochemistry, Oxidative Phosphorylation. Treasure Island (FL): StatPearls.
- DEVI, L., RAGHAVENDRAN, V., PRABHU, B. M., AVADHANI, N. G. & ANANDATHEERTHAVARADA, H. K. 2008. Mitochondrial import and accumulation of alpha-synuclein impair complex I in human dopaminergic neuronal cultures and Parkinson disease brain. *J Biol Chem*, 283, 9089-100.
- DEZSI, L. & VECSEI, L. 2017. Monoamine Oxidase B Inhibitors in Parkinson's Disease. *CNS Neurol Disord Drug Targets*, 16, 425-439.
- DI MAIO, R., BARRETT, P. J., HOFFMAN, E. K., BARRETT, C. W., ZHARIKOV, A., BORAH, A., HU, X., MCCOY, J., CHU, C. T., BURTON, E. A., HASTINGS, T. G. & GREENAMYRE, J. T. 2016. α -Synuclein binds to TOM20 and inhibits mitochondrial protein import in Parkinson's disease. *Sci Transl Med*, 8, 342ra78.

- DIEGELMANN, S., JANSEN, A., JOIS, S., KASTENHOLZ, K., VELO ESCARCENA, L., STRUDTHOFF, N. & SCHOLZ, H. 2017. The CApillary FEeder Assay Measures Food Intake in *Drosophila melanogaster*. *Journal of visualized experiments : JoVE*, 55024.
- DU, X.-Y., XIE, X.-X. & LIU, R.-T. 2020. The Role of α -Synuclein Oligomers in Parkinson's Disease. *International journal of molecular sciences*, 21, 8645.
- DURCAN, T. M. & FON, E. A. 2015. The three 'P's of mitophagy: PARKIN, PINK1, and post-translational modifications. *Genes & development*, 29, 989-999.
- EEKEN, J. C., PASTINK, A., NIVARD, M., VOGEL, E. W. & SOBELS, F. H. 1989. The nature of X-ray and chemically induced mutations in *Drosophila* in relation with DNA repair. *Ann Ist Super Sanita*, 25, 213-8.
- EICKELBERG, V., LÜERSEN, K., STAATS, S. & RIMBACH, G. 2022. Phenotyping of *Drosophila Melanogaster*—A Nutritional Perspective. *Biomolecules*, 12, 221.
- ELIA, A. E., LALLI, S., MONSURRÒ, M. R., SAGNELLI, A., TAIELLO, A. C., REGGIORI, B., LA BELLA, V., TEDESCHI, G. & ALBANESE, A. 2016. Tauroursodeoxycholic acid in the treatment of patients with amyotrophic lateral sclerosis. *Eur J Neurol*, 23, 45-52.
- ELLIS, C. E., MURPHY, E. J., MITCHELL, D. C., GOLOVKO, M. Y., SCAGLIA, F., BARCELÓ-COBLIJN, G. C. & NUSSBAUM, R. L. 2005. Mitochondrial lipid abnormality and electron transport chain impairment in mice lacking alpha-synuclein. *Molecular and cellular biology*, 25, 10190-10201.
- ELMORE, S. 2007. Apoptosis: A Review of Programmed Cell Death. *Toxicologic Pathology*, 35, 495-516.
- ELUSTONDO, P., MARTIN, L. A. & KARTEN, B. 2017. Mitochondrial cholesterol import. *Biochimica et Biophysica Acta (BBA) - Molecular and Cell Biology of Lipids*, 1862, 90-101.
- EMAMZADEH, F. N. 2016. Alpha-synuclein structure, functions, and interactions. *J Res Med Sci*, 21, 29.
- EMAMZADEH, F. N. & SURGUCHOV, A. 2018. Parkinson's Disease: Biomarkers, Treatment, and Risk Factors. *Frontiers in neuroscience*, 12, 612-612.
- ERNSTER, L. & SCHATZ, G. 1981. Mitochondria: a historical review. *J Cell Biol*, 91, 227s-255s.
- ESCHBACH, J., VON EINEM, B., MÜLLER, K., BAYER, H., SCHEFFOLD, A., MORRISON, B. E., RUDOLPH, K. L., THAL, D. R., WITTING, A., WEYDT, P., OTTO, M., FAULER, M., LISS, B., MCLEAN, P. J., SPADA, A. R., LUDOLPH, A. C., WEISHAUP, J. H. & DANZER, K. M. 2015. Mutual exacerbation of peroxisome proliferator-activated receptor γ coactivator 1 α deregulation and α -synuclein oligomerization. *Ann Neurol*, 77, 15-32.
- FALABELLA, M., VERNON, H. J., HANNA, M. G., CLAYPOOL, S. M. & PITCEATHLY, R. D. S. 2021. Cardiolipin, Mitochondria, and Neurological Disease. *Trends in endocrinology and metabolism: TEM*, 32, 224-237.
- FANG, Z., ZHAO, Z., EAPEN, V. & CLARKE, R. A. 2021. siRNA Mediate RNA Interference Concordant with Early On-Target Transient Transcriptional Interference. *Genes*, 12, 1290.
- FAUVET, B., MBEFO, M. K., FARES, M. B., DESOBRY, C., MICHAEL, S., ARDAH, M. T., TSIKA, E., COUNE, P., PRUDENT, M., LION, N., ELIEZER, D., MOORE, D. J., SCHNEIDER, B., AEBISCHER, P., EL-AGNAF, O. M., MASLIAH, E. & LASHUEL, H. A. 2012. α -Synuclein in central nervous system and from erythrocytes, mammalian cells, and *Escherichia coli* exists predominantly as disordered monomer. *J Biol Chem*, 287, 15345-64.
- FAYYAD, M., ERSKINE, D., MAJBOUR, N. K., VAIKATH, N. N., GHANEM, S. S., SUDHAKARAN, I. P., ABDESSELEM, H., LAMPROKOSTOPOULOU, A., VEKRELLIS, K., MORRIS, C. M., ATTEMS, J. & EL-AGNAF, O. M. A. 2020. Investigating the presence of doubly phosphorylated α -synuclein at tyrosine 125 and serine 129 in idiopathic Lewy body diseases. *Brain pathology (Zurich, Switzerland)*, 30, 831-843.
- FEANY, M. B. & BENDER, W. W. 2000. A *Drosophila* model of Parkinson's disease. *Nature*, 404, 394-8.

- FEDOROV, Y., ANDERSON, E. M., BIRMINGHAM, A., REYNOLDS, A., KARPILOW, J., ROBINSON, K., LEAKE, D., MARSHALL, W. S. & KHVOROVA, A. 2006. Off-target effects by siRNA can induce toxic phenotype. *RNA (New York, N.Y.)*, 12, 1188-1196.
- FERESHTEHNEJAD, S. M., ZEIGHAMI, Y., DAGHER, A. & POSTUMA, R. B. 2017. Clinical criteria for subtyping Parkinson's disease: biomarkers and longitudinal progression. *Brain*, 140, 1959-1976.
- FERNAGUT, P. O. & CHESSELET, M. F. 2004. Alpha-synuclein and transgenic mouse models. *Neurobiol Dis*, 17, 123-30.
- FERNÁNDEZ-MORENO, M. A., FARR, C. L., KAGUNI, L. S. & GARESSE, R. 2007. Drosophila melanogaster as a model system to study mitochondrial biology. *Methods in molecular biology (Clifton, N.J.)*, 372, 33-49.
- FERRAIUOLO, L., MEYER, K., SHERWOOD THOMAS, W., VICK, J., LIKHTE, S., FRAKES, A., MIRANDA CARLOS, J., BRAUN, L., HEATH PAUL, R., PINEDA, R., BEATTIE CHRISTINE, E., SHAW PAMELA, J., ASKWITH CANDICE, C., MCTIGUE, D. & KASPAR BRIAN, K. 2016. Oligodendrocytes contribute to motor neuron death in ALS via SOD1-dependent mechanism. *Proceedings of the National Academy of Sciences*, 113, E6496-E6505.
- FERRAZ-NOGUEIRA, J. P., DÍEZ-GUERRA, F. J. & LLOPIS, J. 2014. Visualization of phosphatidic acid fluctuations in the plasma membrane of living cells. *PLoS one*, 9, e102526-e102526.
- FILIUS, M., CUI, T. J., ANANTH, A. N., DOCTER, M. W., HEGGE, J. W., VAN DER OOST, J. & JOO, C. 2020. High-Speed Super-Resolution Imaging Using Protein-Assisted DNA-PAINT. *Nano letters*, 20, 2264-2270.
- FISCHER, J. A., GINIGER, E., MANIATIS, T. & PTASHNE, M. 1988. GAL4 activates transcription in Drosophila. *Nature*, 332, 853-856.
- FLETCHER, T. L., DE CAMILLI, P. & BANKER, G. 1994. Synaptogenesis in hippocampal cultures: evidence indicating that axons and dendrites become competent to form synapses at different stages of neuronal development. *The Journal of neuroscience : the official journal of the Society for Neuroscience*, 14, 6695-6706.
- FU, M., ST-PIERRE, P., SHANKAR, J., WANG, P. T., JOSHI, B. & NABI, I. R. 2013. Regulation of mitophagy by the Gp78 E3 ubiquitin ligase. *Mol Biol Cell*, 24, 1153-62.
- FUJIWARA, H., HASEGAWA, M., DOHMAE, N., KAWASHIMA, A., MASLIAH, E., GOLDBERG, M. S., SHEN, J., TAKIO, K. & IWATSUBO, T. 2002. alpha-Synuclein is phosphorylated in synucleinopathy lesions. *Nat Cell Biol*, 4, 160-4.
- GATTO, N., DOS SANTOS SOUZA, C., SHAW, A. C., BELL, S. M., MYSZCZYNSKA, M. A., POWERS, S., MEYER, K., CASTELLI, L. M., KARYKA, E., MORTIBOYS, H., AZZOUZ, M., HAUTBERGUE, G. M., MÁRKUS, N. M., SHAW, P. J. & FERRAIUOLO, L. 2021. Directly converted astrocytes retain the ageing features of the donor fibroblasts and elucidate the astrocytic contribution to human CNS health and disease. *Aging cell*, 20, e13281-e13281.
- GAUDIOSO, A., GARCIA-ROZAS, P., CASAREJOS, M. J., PASTOR, O. & RODRIGUEZ-NAVARRO, J. A. 2019. Lipidomic Alterations in the Mitochondria of Aged Parkin Null Mice Relevant to Autophagy. *Frontiers in Neuroscience*, 13.
- GEISLER, S., HOLMSTRÖM, K. M., SKUJAT, D., FIESEL, F. C., ROTHFUSS, O. C., KAHLE, P. J. & SPRINGER, W. 2010. PINK1/Parkin-mediated mitophagy is dependent on VDAC1 and p62/SQSTM1. *Nature Cell Biology*, 12, 119-131.
- GENG, X., LOU, H., WANG, J., LI, L., SWANSON, A. L., SUN, M., BEERS-STOLZ, D., WATKINS, S., PEREZ, R. G. & DRAIN, P. 2011. alpha-Synuclein binds the K(ATP) channel at insulin-secretory granules and inhibits insulin secretion. *Am J Physiol Endocrinol Metab*, 300, E276-86.
- GEORGAKOPOULOS, N. D., WELLS, G. & CAMPANELLA, M. 2017. The pharmacological regulation of cellular mitophagy. *Nature Chemical Biology*, 13, 136-146.
- GHANIM, G. E., RIO, D. C. & TEIXEIRA, F. K. 2020. Mechanism and regulation of P element transposition. *Open biology*, 10, 200244-200244.

- GHIO, S., CAMILLERI, A., CARUANA, M., RUF, V. C., SCHMIDT, F., LEONOV, A., RYAZANOV, S., GRIESINGER, C., CAUCHI, R. J., KAMP, F., GIESE, A. & VASSALLO, N. 2019a. Cardiolipin Promotes Pore-Forming Activity of Alpha-Synuclein Oligomers in Mitochondrial Membranes. *ACS Chem Neurosci*, 10, 3815-3829.
- GHIO, S., CAMILLERI, A., CARUANA, M., RUF, V. C., SCHMIDT, F., LEONOV, A., RYAZANOV, S., GRIESINGER, C., CAUCHI, R. J., KAMP, F., GIESE, A. & VASSALLO, N. 2019b. Cardiolipin Promotes Pore-Forming Activity of Alpha-Synuclein Oligomers in Mitochondrial Membranes. *ACS Chemical Neuroscience*, 10, 3815-3829.
- GINHOUX, F. & PRINZ, M. 2015. Origin of microglia: current concepts and past controversies. *Cold Spring Harbor perspectives in biology*, 7, a020537-a020537.
- GLANTZ, L. A., GILMORE, J. H., HAMER, R. M., LIEBERMAN, J. A. & JARSKOG, L. F. 2007. Synaptophysin and postsynaptic density protein 95 in the human prefrontal cortex from mid-gestation into early adulthood. *Neuroscience*, 149, 582-591.
- GLICK, D., BARTH, S. & MACLEOD, K. F. 2010. Autophagy: cellular and molecular mechanisms. *The Journal of pathology*, 221, 3-12.
- GLINKA, Y., GASSEN, M. & YODIM, M. B. 1997. Mechanism of 6-hydroxydopamine neurotoxicity. *J Neural Transm Suppl*, 50, 55-66.
- GOERS, J., MANNING-BOG, A. B., MCCORMACK, A. L., MILLETT, I. S., DONIACH, S., DI MONTE, D. A., UVERSKY, V. N. & FINK, A. L. 2003. Nuclear Localization of α -Synuclein and Its Interaction with Histones. *Biochemistry*, 42, 8465-8471.
- GOTTLIEB, R. A., PIPLANI, H., SIN, J., SAWAGED, S., HAMID, S. M., TAYLOR, D. J. & DE FREITAS GERMANO, J. 2021. At the heart of mitochondrial quality control: many roads to the top. *Cell Mol Life Sci*, 78, 3791-3801.
- GRAHAM, S. F., REY, N. L., UGUR, Z., YILMAZ, A., SHERMAN, E., MADDENS, M., BAHADO-SINGH, R. O., BECKER, K., SCHULZ, E., MEYERDIRK, L. K., STEINER, J. A., MA, J. & BRUNDIN, P. 2018a. Metabolomic Profiling of Bile Acids in an Experimental Model of Prodromal Parkinson's Disease. *Metabolites*, 8.
- GRAHAM, S. F., REY, N. L., YILMAZ, A., KUMAR, P., MADAJ, Z., MADDENS, M., BAHADO-SINGH, R. O., BECKER, K., SCHULZ, E., MEYERDIRK, L. K., STEINER, J. A., MA, J. & BRUNDIN, P. 2018b. Biochemical Profiling of the Brain and Blood Metabolome in a Mouse Model of Prodromal Parkinson's Disease Reveals Distinct Metabolic Profiles. *Journal of proteome research*, 17, 2460-2469.
- GRANT, S. M. & DEMORROW, S. 2020. Bile Acid Signaling in Neurodegenerative and Neurological Disorders. *International journal of molecular sciences*, 21, 5982.
- GRAY, M. W. 2012. Mitochondrial evolution. *Cold Spring Harbor perspectives in biology*, 4, a011403-a011403.
- GREENE, J. C., WHITWORTH, A. J., KUO, I., ANDREWS, L. A., FEANY, M. B. & PALLANCK, L. J. 2003. Mitochondrial pathology and apoptotic muscle degeneration in Drosophila parkin mutants. *Proc Natl Acad Sci U S A*, 100, 4078-83.
- GREENE JESSICA, C., WHITWORTH ALEXANDER, J., KUO, I., ANDREWS LAURIE, A., FEANY MEL, B. & PALLANCK LEO, J. 2003. Mitochondrial pathology and apoptotic muscle degeneration in Drosophila parkin mutants. *Proceedings of the National Academy of Sciences*, 100, 4078-4083.
- GREENWOOD, J., ADU, J., DAVEY, A. J., ABBOTT, N. J. & BRADBURY, M. W. 1991. The effect of bile salts on the permeability and ultrastructure of the perfused, energy-depleted, rat blood-brain barrier. *J Cereb Blood Flow Metab*, 11, 644-54.
- GREGORI-PUIGJANÉ, E., SETOLA, V., HERT, J., CREWS, B. A., IRWIN, J. J., LOUNKINE, E., MARNETT, L., ROTH, B. L. & SHOICHET, B. K. 2012. Identifying mechanism-of-action targets for drugs and probes. *Proceedings of the National Academy of Sciences of the United States of America*, 109, 11178-11183.

- GUARDIA-LAGUARTA, C., AREA-GOMEZ, E., RÜB, C., LIU, Y., MAGRANÉ, J., BECKER, D., VOOS, W., SCHON, E. A. & PRZEDBORSKI, S. 2014. α -Synuclein is localized to mitochondria-associated ER membranes. *The Journal of neuroscience : the official journal of the Society for Neuroscience*, 34, 249-259.
- GUNDERSEN, V. 2010. Protein aggregation in Parkinson's disease. *Acta Neurol Scand Suppl*, 82-7.
- GUO, Y., SUN, Y., SONG, Z., ZHENG, W., XIONG, W., YANG, Y., YUAN, L. & DENG, H. 2021. Genetic Analysis and Literature Review of SNCA Variants in Parkinson's Disease. *Frontiers in aging neuroscience*, 13, 648151-648151.
- GUSEL'NIKOVA, V. V. & KORZHEVSKIY, D. E. 2015. NeuN As a Neuronal Nuclear Antigen and Neuron Differentiation Marker. *Acta naturae*, 7, 42-47.
- GUZZO, M., CASTRO, L. K., REISCH, C. R., GUO, M. S. & LAUB, M. T. 2020. A CRISPR Interference System for Efficient and Rapid Gene Knockdown in *Caulobacter crescentus*. *mBio*, 11, e02415-19.
- HADDAD A, M. S. 2021. Biochemistry, Citric Acid Cycle. Treasure Island (FL): StatPearls Publishing.
- HAN, F., LIU, Y., HUANG, J., ZHANG, X. & WEI, C. 2021. Current Approaches and Molecular Mechanisms for Directly Reprogramming Fibroblasts Into Neurons and Dopamine Neurons. *Frontiers in aging neuroscience*, 13, 738529-738529.
- HASSANINASAB, A., HAN, G.-S. & CARMAN, G. M. 2017. Tips on the analysis of phosphatidic acid by the fluorometric coupled enzyme assay. *Analytical biochemistry*, 526, 69-70.
- HATTORI, N., TANAKA, M., OZAWA, T. & MIZUNO, Y. 1991. Immunohistochemical studies on complexes I, II, III, and IV of mitochondria in Parkinson's disease. *Ann Neurol*, 30, 563-71.
- HAWKES, C. H., DEL TREDICI, K. & BRAAK, H. 2007. Parkinson's disease: a dual-hit hypothesis. *Neuropathology and applied neurobiology*, 33, 599-614.
- HEGER, L. M., WISE, R. M., HEES, J. T., HARBAUER, A. B. & BURBULLA, L. F. 2021. Mitochondrial Phenotypes in Parkinson's Diseases-A Focus on Human iPSC-Derived Dopaminergic Neurons. *Cells*, 10, 3436.
- HEJJAOU, M., BUTTERFIELD, S., FAUVET, B., VERCRUYSE, F., CUI, J., DIKIY, I., PRUDENT, M., OLSCHESKI, D., ZHANG, Y., ELIEZER, D. & LASHUEL, H. A. 2012. Elucidating the role of C-terminal post-translational modifications using protein semisynthesis strategies: α -synuclein phosphorylation at tyrosine 125. *Journal of the American Chemical Society*, 134, 5196-5210.
- HETTIE, K. S., LIU, X., GILLIS, K. D. & GLASS, T. E. 2013. Selective catecholamine recognition with NeuroSensor 521: a fluorescent sensor for the visualization of norepinephrine in fixed and live cells. *ACS chemical neuroscience*, 4, 918-923.
- HINDLE, S. J. & BAINTON, R. J. 2014. Barrier mechanisms in the Drosophila blood-brain barrier. *Frontiers in neuroscience*, 8, 414-414.
- HOFMANN, A. F. & HAGEY, L. R. 2014. Key discoveries in bile acid chemistry and biology and their clinical applications: history of the last eight decades. *J Lipid Res*, 55, 1553-95.
- HOLMQVIST, S., CHUTNA, O., BOUSSET, L., ALDRIN-KIRK, P., LI, W., BJÖRKLUND, T., WANG, Z. Y., ROYBON, L., MELKI, R. & LI, J. Y. 2014. Direct evidence of Parkinson pathology spread from the gastrointestinal tract to the brain in rats. *Acta Neuropathol*, 128, 805-20.
- HOMEM, R. A. & DAVIES, T. G. E. 2018. An overview of functional genomic tools in deciphering insecticide resistance. *Current opinion in insect science*, 27, 103-110.
- HOUTKOOPER, R. H. & VAZ, F. M. 2008. Cardiolipin, the heart of mitochondrial metabolism. *Cell Mol Life Sci*, 65, 2493-506.
- HSIEH, C. H., SHALTOUKI, A., GONZALEZ, A. E., BETTENCOURT DA CRUZ, A., BURBULLA, L. F., ST LAWRENCE, E., SCHÜLE, B., KRAINIC, D., PALMER, T. D. & WANG, X. 2016. Functional Impairment in Miro Degradation and Mitophagy Is a Shared Feature in Familial and Sporadic Parkinson's Disease. *Cell Stem Cell*, 19, 709-724.
- HU, C., ZHU, J., MEI, H., SHI, H., GUO, H., ZHANG, G., WANG, P., LU, L. & ZHENG, X. 2018. A sensitive HPLC-MS/MS method for the analysis of fiber dyes. *Forensic Chemistry*, 11, 1-6.

- HUANG, B., BABCOCK, H. & ZHUANG, X. 2010. Breaking the diffraction barrier: super-resolution imaging of cells. *Cell*, 143, 1047-1058.
- IKEMURA, M., SAITO, Y., SENGOKU, R., SAKIYAMA, Y., HATSUTA, H., KANEMARU, K., SAWABE, M., ARAI, T., ITO, G., IWATSUBO, T., FUKAYAMA, M. & MURAYAMA, S. 2008. Lewy Body Pathology Involves Cutaneous Nerves. *Journal of Neuropathology & Experimental Neurology*, 67, 945-953.
- IMAIZUMI, Y., OKADA, Y., AKAMATSU, W., KOIKE, M., KUZUMAKI, N., HAYAKAWA, H., NIHIRA, T., KOBAYASHI, T., OHYAMA, M., SATO, S., TAKANASHI, M., FUNAYAMA, M., HIRAYAMA, A., SOGA, T., HISHIKI, T., SUEMATSU, M., YAGI, T., ITO, D., KOSAKAI, A., HAYASHI, K., SHOUJI, M., NAKANISHI, A., SUZUKI, N., MIZUNO, Y., MIZUSHIMA, N., AMAGAI, M., UCHIYAMA, Y., MOCHIZUKI, H., HATTORI, N. & OKANO, H. 2012. Mitochondrial dysfunction associated with increased oxidative stress and α -synuclein accumulation in PARK2 iPSC-derived neurons and postmortem brain tissue. *Molecular brain*, 5, 35-35.
- ISHIBASHI, A., SAGA, K., HISATOMI, Y., LI, Y., KANEDA, Y. & NIMURA, K. 2020. A simple method using CRISPR-Cas9 to knock-out genes in murine cancerous cell lines. *Scientific reports*, 10, 22345-22345.
- JAKES, R., SPILLANTINI, M. G. & GOEDERT, M. 1994. Identification of two distinct synucleins from human brain. *FEBS Lett*, 345, 27-32.
- JAN, A., GONÇALVES, N. P., VAEGTER, C. B., JENSEN, P. H. & FERREIRA, N. 2021. The Prion-Like Spreading of Alpha-Synuclein in Parkinson's Disease: Update on Models and Hypotheses. *International journal of molecular sciences*, 22, 8338.
- JANETZKY, B., HAUCK, S., YODIM, M. B. H., RIEDERER, P., JELLINGER, K., PANTUCEK, F., ZOCHLING, R., BOISSEL, K. W. & REICHMANN, H. 1994. Unaltered aconitase activity, but decreased complex I activity in substantia nigra pars compacta of patients with Parkinson's disease. *Neuroscience Letters*, 169, 126-128.
- JANKOVIC, J. & TAN, E. K. 2020. Parkinson's disease: etiopathogenesis and treatment. *Journal of Neurology, Neurosurgery & Psychiatry*, 91, 795.
- JENNINGS, B. H. 2011. Drosophila – a versatile model in biology & medicine. *Materials Today*, 14, 190-195.
- JEONG, G. R. & LEE, B. D. 2020. Pathological Functions of LRRK2 in Parkinson's Disease. *Cells*, 9, 2565.
- JIANG, H., REN, Y., YUEN, E. Y., ZHONG, P., GHAEDI, M., HU, Z., AZABDAFTARI, G., NAKASO, K., YAN, Z. & FENG, J. 2012. Parkin controls dopamine utilization in human midbrain dopaminergic neurons derived from induced pluripotent stem cells. *Nature communications*, 3, 668-668.
- JIN, H., KANTHASAMY, A., GHOSH, A., YANG, Y., ANANTHARAM, V. & KANTHASAMY, A. G. 2011. α -Synuclein negatively regulates protein kinase C δ expression to suppress apoptosis in dopaminergic neurons by reducing p300 histone acetyltransferase activity. *J Neurosci*, 31, 2035-51.
- JIN, S. M. & YOULE, R. J. 2012. PINK1- and Parkin-mediated mitophagy at a glance. *Journal of cell science*, 125, 795-799.
- JOHANSEN, K. K., TORP, S. H., FARRER, M. J., GUSTAVSSON, E. K. & AASLY, J. O. 2018. A Case of Parkinson's Disease with No Lewy Body Pathology due to a Homozygous Exon Deletion in Parkin. *Case reports in neurological medicine*, 2018, 6838965-6838965.
- JOURDAN, J.-P., BUREAU, R., ROCHAIS, C. & DALLEMAGNE, P. 2020. Drug repositioning: a brief overview. *The Journal of pharmacy and pharmacology*, 72, 1145-1151.
- JUÁREZ OLGUÍN, H., CALDERÓN GUZMÁN, D., HERNÁNDEZ GARCÍA, E. & BARRAGÁN MEJÍA, G. 2016. The Role of Dopamine and Its Dysfunction as a Consequence of Oxidative Stress. *Oxidative medicine and cellular longevity*, 2016, 9730467-9730467.
- JULIENNE, H., BUHL, E., LESLIE, D. S. & HODGE, J. J. L. 2017. Drosophila PINK1 and parkin loss-of-function mutants display a range of non-motor Parkinson's disease phenotypes. *Neurobiology of disease*, 104, 15-23.

- K HANCOCK, M., KOPP, L., KAUR, N. & HANSON, B. J. 2015. A facile method for simultaneously measuring neuronal cell viability and neurite outgrowth. *Current chemical genomics and translational medicine*, 9, 6-16.
- KAHLE, P. J., NEUMANN, M., OZMEN, L., MULLER, V., JACOBSEN, H., SCHINDZIELORZ, A., OKOCHI, M., LEIMER, U., VAN DER PUTTEN, H., PROBST, A., KREMMER, E., KRETZSCHMAR, H. A. & HAASS, C. 2000. Subcellular localization of wild-type and Parkinson's disease-associated mutant alpha -synuclein in human and transgenic mouse brain. *J Neurosci*, 20, 6365-73.
- KÁLMÁN, S., GARBETT, K. A., JANKA, Z. & MIRNICS, K. 2016. Human dermal fibroblasts in psychiatry research. *Neuroscience*, 320, 105-121.
- KAMEOKA, S., ADACHI, Y., OKAMOTO, K., IJIMA, M. & SESAKI, H. 2018. Phosphatidic Acid and Cardiolipin Coordinate Mitochondrial Dynamics. *Trends in cell biology*, 28, 67-76.
- KASSAS, N., FOUILLEN, L., GASMAN, S. & VITALE, N. 2021. A Lipidomics Approach to Measure Phosphatidic Acid Species in Subcellular Membrane Fractions Obtained from Cultured Cells. *Bio Protoc*, 11, e4066.
- KATAYAMA, H., HAMA, H., NAGASAWA, K., KUROKAWA, H., SUGIYAMA, M., ANDO, R., FUNATA, M., YOSHIDA, N., HOMMA, M., NISHIMURA, T., TAKAHASHI, M., ISHIDA, Y., HIOKI, H., TSUJIHATA, Y. & MIYAWAKI, A. 2020. Visualizing and Modulating Mitophagy for Therapeutic Studies of Neurodegeneration. *Cell*, 181, 1176-1187.e16.
- KAUFMAN, T. C. 2017. A Short History and Description of Drosophila melanogaster Classical Genetics: Chromosome Aberrations, Forward Genetic Screens, and the Nature of Mutations. *Genetics*, 206, 665-689.
- KAUR, A., BRIGDEN, K. W. L., CASHMAN, T. F., FRASER, S. T. & NEW, E. J. 2015. Mitochondrially targeted redox probe reveals the variations in oxidative capacity of the haematopoietic cells. *Organic & Biomolecular Chemistry*, 13, 6686-6689.
- KAUSAR, S., WANG, F. & CUI, H. 2018. The Role of Mitochondria in Reactive Oxygen Species Generation and Its Implications for Neurodegenerative Diseases. *Cells*, 7, 274.
- KEITA, S., MASUZZO, A., ROYET, J. & KURZ, C. L. 2017. Drosophila larvae food intake cessation following exposure to Erwinia contaminated media requires odor perception, Trpa1 channel and evf virulence factor. *J Insect Physiol*, 99, 25-32.
- KEUNE, W.-J., HAUSMANN, J., BOLIER, R., TOLENAARS, D., KREMER, A., HEIDEBRECHT, T., JOOSTEN, R. P., SUNKARA, M., MORRIS, A. J., MATAS-RICO, E., MOOLENAAR, W. H., OUDE ELFERINK, R. P. & PERRAKIS, A. 2016. Steroid binding to Autotaxin links bile salts and lysophosphatidic acid signalling. *Nature communications*, 7, 11248-11248.
- KHALAF, O., FAUVET, B., OUESLATI, A., DIKIY, I., MAHUL-MELLIER, A. L., RUGGERI, F. S., MBEFO, M. K., VERCRUYSE, F., DIETLER, G., LEE, S. J., ELIEZER, D. & LASHUEL, H. A. 2014. The H50Q mutation enhances α -synuclein aggregation, secretion, and toxicity. *J Biol Chem*, 289, 21856-76.
- KIELY, A. P., ASI, Y. T., KARA, E., LIMOUSIN, P., LING, H., LEWIS, P., PROUKAKIS, C., QUINN, N., LEES, A. J., HARDY, J., REVESZ, T., HOULDEN, H. & HOLTON, J. L. 2013. α -Synucleinopathy associated with G51D SNCA mutation: a link between Parkinson's disease and multiple system atrophy? *Acta Neuropathol*, 125, 753-69.
- KIM, E. K. & CHOI, E.-J. 2015. Compromised MAPK signaling in human diseases: an update. *Archives of Toxicology*, 89, 867-882.
- KIM, S., KWON, S. H., KAM, T. I., PANICKER, N., KARUPPAGOUNDER, S. S., LEE, S., LEE, J. H., KIM, W. R., KOOK, M., FOSS, C. A., SHEN, C., LEE, H., KULKARNI, S., PASRICHA, P. J., LEE, G., POMPER, M. G., DAWSON, V. L., DAWSON, T. M. & KO, H. S. 2019. Transneuronal Propagation of Pathologic α -Synuclein from the Gut to the Brain Models Parkinson's Disease. *Neuron*, 103, 627-641.e7.
- KIM, Y., ZHENG, X., ANSARI, Z., BUNNELL, M. C., HERDY, J. R., TRAXLER, L., LEE, H., PAQUOLA, A. C. M., BLITHIKIOTI, C., KU, M., SCHLACHETZKI, J. C. M., WINKLER, J., EDENHOFER, F., GLASS, C. K., PAUCAR, A. A., JAEGER, B. N., PHAM, S., BOYER, L., CAMPBELL, B. C., HUNTER, T.,

- MERTENS, J. & GAGE, F. H. 2018. Mitochondrial Aging Defects Emerge in Directly Reprogrammed Human Neurons due to Their Metabolic Profile. *Cell reports*, 23, 2550-2558.
- KIRIYAMA, Y. & NOCHI, H. 2019. The Biosynthesis, Signaling, and Neurological Functions of Bile Acids. *Biomolecules*, 9, 232.
- KITTAPPA, R., CHANG, W. W., AWATRAMANI, R. B. & MCKAY, R. D. G. 2007. The *foxa2* gene controls the birth and spontaneous degeneration of dopamine neurons in old age. *PLoS biology*, 5, e325-e325.
- KLEIN, C. & WESTENBERGER, A. 2012. Genetics of Parkinson's disease. *Cold Spring Harbor perspectives in medicine*, 2, a008888-a008888.
- KOCH, U., LEHAL, R. & RADTKE, F. 2013. Stem cells living with a Notch. *Development*, 140, 689-704.
- KOJIMA, R., KAKIMOTO, Y., FURUTA, S., ITOH, K., SESAKI, H., ENDO, T. & TAMURA, Y. 2019. Maintenance of Cardiolipin and Crista Structure Requires Cooperative Functions of Mitochondrial Dynamics and Phospholipid Transport. *Cell reports*, 26, 518-528.e6.
- KOKHAN, V. S., AFANASYEVA, M. A. & VAN'KIN, G. I. 2012. α -Synuclein knockout mice have cognitive impairments. *Behav Brain Res*, 231, 226-30.
- KOKOTOS, A. C., HARPER, C. B., MARLAND, J. R. K., SMILLIE, K. J., COUSIN, M. A. & GORDON, S. L. 2019. Synaptophysin sustains presynaptic performance by preserving vesicular synaptobrevin-II levels. *Journal of neurochemistry*, 151, 28-37.
- KOSICEK, M. & HECIMOVIC, S. 2013. Phospholipids and Alzheimer's disease: alterations, mechanisms and potential biomarkers. *International journal of molecular sciences*, 14, 1310-1322.
- KOSTIC, M., LUDTMANN, M. H., BADING, H., HERSHFINKEL, M., STEER, E., CHU, C. T., ABRAMOV, A. Y. & SEKLER, I. 2015. PKA Phosphorylation of NCLX Reverses Mitochondrial Calcium Overload and Depolarization, Promoting Survival of PINK1-Deficient Dopaminergic Neurons. *Cell Rep*, 13, 376-86.
- KOUKOURAKIS, M. I., KALAMIDA, D., GIATROMANOLAKI, A., ZOIS, C. E., SIVRIDIS, E., POULILIOU, S., MITRAKAS, A., GATTER, K. C. & HARRIS, A. L. 2015. Autophagosome Proteins LC3A, LC3B and LC3C Have Distinct Subcellular Distribution Kinetics and Expression in Cancer Cell Lines. *PLoS one*, 10, e0137675-e0137675.
- KRAFFE, E., SOUDANT, P., MARTY, Y., KERVAREC, N. & JEHAN, P. 2002. Evidence of a tetradocosahexaenoic cardiolipin in some marine bivalves. *Lipids*, 37, 507-514.
- KRAKAUER, D. C. & PLOTKIN, J. B. 2002. Redundancy, antiredundancy, and the robustness of genomes. *Proceedings of the National Academy of Sciences of the United States of America*, 99, 1405-1409.
- KROGH, K., OSTERGAARD, K., SABROE, S. & LAURBERG, S. 2008. Clinical aspects of bowel symptoms in Parkinson's disease. *Acta Neurologica Scandinavica*, 117, 60-64.
- KUMAR, D. & TANDON, R. K. 2001. Use of ursodeoxycholic acid in liver diseases. *J Gastroenterol Hepatol*, 16, 3-14.
- LAGE, O. M., RAMOS, M. C., CALISTO, R., ALMEIDA, E., VASCONCELOS, V. & VICENTE, F. 2018. Current Screening Methodologies in Drug Discovery for Selected Human Diseases. *Marine drugs*, 16, 279.
- LANGSTON, J. W. 2017. The MPTP Story. *Journal of Parkinson's disease*, 7, S11-S19.
- LAPASSET, L., MILHAVET, O., PRIEUR, A., BESNARD, E., BABLED, A., AÏT-HAMOU, N., LESCHIK, J., PELLESTOR, F., RAMIREZ, J.-M., DE VOS, J., LEHMANN, S. & LEMAITRE, J.-M. 2011. Rejuvenating senescent and centenarian human cells by reprogramming through the pluripotent state. *Genes & development*, 25, 2248-2253.
- LASHUEL, H. A., OVERK, C. R., OUESLATI, A. & MASLIAH, E. 2013. The many faces of α -synuclein: from structure and toxicity to therapeutic target. *Nat Rev Neurosci*, 14, 38-48.
- LASSEN, L. B., GREGERSEN, E., ISAGER, A. K., BETZER, C., KOFOED, R. H. & JENSEN, P. H. 2018. ELISA method to detect α -synuclein oligomers in cell and animal models. *PLoS one*, 13, e0196056-e0196056.

- LAZARIDIS, K. N., GORES, G. J. & LINDOR, K. D. 2001. Ursodeoxycholic acid 'mechanisms of action and clinical use in hepatobiliary disorders'. *J Hepatol*, 35, 134-46.
- LEE, B. R. & KAMITANI, T. 2011. Improved Immunodetection of Endogenous α -Synuclein. *PLOS ONE*, 6, e23939.
- LEE CLOUGH, R. & STEFANIS, L. 2007. A novel pathway for transcriptional regulation of α -synuclein. *The FASEB Journal*, 21, 596-607.
- LEE, J.-Y., NAGANO, Y., TAYLOR, J. P., LIM, K. L. & YAO, T.-P. 2010. Disease-causing mutations in parkin impair mitochondrial ubiquitination, aggregation, and HDAC6-dependent mitophagy. *The Journal of cell biology*, 189, 671-679.
- LEWITT, P. A. 2015. Levodopa therapy for Parkinson's disease: Pharmacokinetics and pharmacodynamics. *Mov Disord*, 30, 64-72.
- LI, J., QI, W., CHEN, G., FENG, D., LIU, J., MA, B., ZHOU, C., MU, C., ZHANG, W., CHEN, Q. & ZHU, Y. 2015. Mitochondrial outer-membrane E3 ligase MUL1 ubiquitinates ULK1 and regulates selenite-induced mitophagy. *Autophagy*, 11, 1216-29.
- LI, P., KILLINGER, B. A., ENSINK, E., BEDDOWS, I., YILMAZ, A., LUBBEN, N., LAMP, J., SCHILTHUIS, M., VEGA, I. E., WOLTJER, R., POSPISILIK, J. A., BRUNDIN, P., BRUNDIN, L., GRAHAM, S. F. & LABRIE, V. 2021. Gut Microbiota Dysbiosis Is Associated with Elevated Bile Acids in Parkinson's Disease. *Metabolites*, 11.
- LI, S., TAN, H. Y., WANG, N., HONG, M., LI, L., CHEUNG, F. & FENG, Y. 2016. Substitutes for Bear Bile for the Treatment of Liver Diseases: Research Progress and Future Perspective. *Evidence-Based Complementary and Alternative Medicine*, 2016, 4305074.
- LI, T., KUNG, H. J., MACK, P. C. & GANDARA, D. R. 2013. Genotyping and genomic profiling of non-small-cell lung cancer: Implications for current and future therapies. *Journal of Clinical Oncology*, 31, 1039-1049.
- LI, W. W., YANG, R., GUO, J. C., REN, H. M., ZHA, X. L., CHENG, J. S. & CAI, D. F. 2007. Localization of alpha-synuclein to mitochondria within midbrain of mice. *Neuroreport*, 18, 1543-6.
- LIM, M.-S., LEE, S. Y. & PARK, C.-H. 2015. FGF8 is Essential for Functionality of Induced Neural Precursor Cell-derived Dopaminergic Neurons. *International journal of stem cells*, 8, 228-234.
- LITTLE, D., LUFT, C., MOSAKU, O., LORVELLEC, M., YAO, Z., PAILLUSSON, S., KRISTON-VIZI, J., GANDHI, S., ABRAMOV, A. Y., KETTELER, R., DEVINE, M. J. & GISSEN, P. 2018. A single cell high content assay detects mitochondrial dysfunction in iPSC-derived neurons with mutations in SNCA. *Scientific reports*, 8, 9033-9033.
- LIU, M., VAN VOORHIS, W. C. & QUINN, R. J. 2021. Development of a target identification approach using native mass spectrometry. *Scientific reports*, 11, 2387-2387.
- LIU, X., HUANG, J., CHEN, T., WANG, Y., XIN, S., LI, J., PEI, G. & KANG, J. 2008. Yamanaka factors critically regulate the developmental signaling network in mouse embryonic stem cells. *Cell Research*, 18, 1177-1189.
- LIVAK, K. J. & SCHMITTGEN, T. D. 2001. Analysis of Relative Gene Expression Data Using Real-Time Quantitative PCR and the 2- $\Delta\Delta$ CT Method. *Methods*, 25, 402-408.
- LIVINGSTONE, A. S., POTVIN, M., GORESKY, C. A., FINLAYSON, M. H. & HINCHEY, E. J. 1977. Changes in the Blood-Brain Barrier in Hepatic Coma After Hepatectomy in the Rat. *Gastroenterology*, 73, 697-704.
- LOBO, V., PATIL, A., PHATAK, A. & CHANDRA, N. 2010. Free radicals, antioxidants and functional foods: Impact on human health. *Pharmacognosy reviews*, 4, 118-126.
- LOZANO, A. M., LIPSMAN, N., BERGMAN, H., BROWN, P., CHABARDES, S., CHANG, J. W., MATTHEWS, K., MCINTYRE, C. C., SCHLAEPFER, T. E., SCHULDER, M., TEMEL, Y., VOLKMANN, J. & KRAUSS, J. K. 2019. Deep brain stimulation: current challenges and future directions. *Nature reviews. Neurology*, 15, 148-160.

- LUDTMANN, M. H., ANGELOVA, P. R., NINKINA, N. N., GANDHI, S., BUCHMAN, V. L. & ABRAMOV, A. Y. 2016. Monomeric Alpha-Synuclein Exerts a Physiological Role on Brain ATP Synthase. *J Neurosci*, 36, 10510-10521.
- LUDTMANN, M. H. R., ANGELOVA, P. R., HORROCKS, M. H., CHOI, M. L., RODRIGUES, M., BAEV, A. Y., BEREZHNOV, A. V., YAO, Z., LITTLE, D., BANUSHI, B., AL-MENHALI, A. S., RANASINGHE, R. T., WHITEN, D. R., YAPOM, R., DOLT, K. S., DEVINE, M. J., GISSEN, P., KUNATH, T., JAGANJAC, M., PAVLOV, E. V., KLENERMAN, D., ABRAMOV, A. Y. & GANDHI, S. 2018. α -synuclein oligomers interact with ATP synthase and open the permeability transition pore in Parkinson's disease. *Nat Commun*, 9, 2293.
- MAHLKNECHT, P., SEPPI, K. & POEWE, W. 2015. The Concept of Prodromal Parkinson's Disease. *Journal of Parkinson's disease*, 5, 681-697.
- MAITRA, U. & CIESLA, L. 2019. Using *Drosophila* as a platform for drug discovery from natural products in Parkinson's disease. *MedChemComm*, 10, 867-879.
- MAKOS, M. A., KUKLINSKI, N. J., BERGLUND, E. C., HEIEN, M. L. & EWING, A. G. 2009. Chemical measurements in *Drosophila*. *Trends in analytical chemistry : TRAC*, 28, 1223-1234.
- MALIK, N. & RAO, M. S. 2013. A review of the methods for human iPSC derivation. *Methods in molecular biology (Clifton, N.J.)*, 997, 23-33.
- MANDEGAR, MOHAMMAD A., HUEBSCH, N., FROLOV, EKATERINA B., SHIN, E., TRUONG, A., OLVERA, MICHAEL P., CHAN, AMANDA H., MIYAOKA, Y., HOLMES, K., SPENCER, C. I., JUDGE, LUKE M., GORDON, DAVID E., ESKILDSEN, TILDE V., VILLALTA, JACQUELINE E., HORLBECK, MAX A., GILBERT, LUKE A., KROGAN, NEVAN J., SHEIKH, SØREN P., WEISSMAN, JONATHAN S., QI, LEI S., SO, P.-L. & CONKLIN, BRUCE R. 2016. CRISPR Interference Efficiently Induces Specific and Reversible Gene Silencing in Human iPSCs. *Cell Stem Cell*, 18, 541-553.
- MANN, V. M., COOPER, J. M., DANIEL, S. E., SRAI, K., JENNER, P., MARSDEN, C. D. & SCHAPIRA, A. H. 1994. Complex I, iron, and ferritin in Parkinson's disease substantia nigra. *Ann Neurol*, 36, 876-81.
- MANNING, B. D. & TOKER, A. 2017. AKT/PKB Signaling: Navigating the Network. *Cell*, 169, 381-405.
- MANO, N., GOTO, T., UCHIDA, M., NISHIMURA, K., ANDO, M., KOBAYASHI, N. & GOTO, J. 2004. Presence of protein-bound unconjugated bile acids in the cytoplasmic fraction of rat brain. *J Lipid Res*, 45, 295-300.
- MANZANZA, N. D. O., SEDLACKOVA, L. & KALARIA, R. N. 2021. Alpha-Synuclein Post-translational Modifications: Implications for Pathogenesis of Lewy Body Disorders. *Frontiers in aging neuroscience*, 13, 690293-690293.
- MARELLA, M., SEO, B. B., YAGI, T. & MATSUNO-YAGI, A. 2009. Parkinson's disease and mitochondrial complex I: a perspective on the Ndi1 therapy. *Journal of bioenergetics and biomembranes*, 41, 493-497.
- MARKSTEINER, J., BLASKO, I., KEMMLER, G., KOAL, T. & HUMPEL, C. 2018. Bile acid quantification of 20 plasma metabolites identifies lithocholic acid as a putative biomarker in Alzheimer's disease. *Metabolomics*, 14, 1.
- MAROTEAUX, L., CAMPANELLI, J. T. & SCHELLER, R. H. 1988. Synuclein: a neuron-specific protein localized to the nucleus and presynaptic nerve terminal. *J Neurosci*, 8, 2804-15.
- MARTIN, L. A., KENNEDY, B. E. & KARTEN, B. 2016. Mitochondrial cholesterol: mechanisms of import and effects on mitochondrial function. *J Bioenerg Biomembr*, 48, 137-51.
- MARTÍNEZ, J. H., FUENTES, F., VANASCO, V., ALVAREZ, S., ALAIMO, A., CASSINA, A., COLUCCIO LESKOW, F. & VELAZQUEZ, F. 2018. Alpha-synuclein mitochondrial interaction leads to irreversible translocation and complex I impairment. *Arch Biochem Biophys*, 651, 1-12.
- MCKINNEY, C. E. 2017. Using induced pluripotent stem cells derived neurons to model brain diseases. *Neural regeneration research*, 12, 1062-1067.
- MCLELLAND, G. L., LEE, S. A., MCBRIDE, H. M. & FON, E. A. 2016. Syntaxin-17 delivers PINK1/parkin-dependent mitochondrial vesicles to the endolysosomal system. *J Cell Biol*, 214, 275-91.

- MCLELLAND, G. L., SOUBANNIER, V., CHEN, C. X., MCBRIDE, H. M. & FON, E. A. 2014. Parkin and PINK1 function in a vesicular trafficking pathway regulating mitochondrial quality control. *Embo j*, 33, 282-95.
- MCMILLIN, M., FRAMPTON, G., QUINN, M., ASHFAQ, S., DE LOS SANTOS, M., 3RD, GRANT, S. & DEMORROW, S. 2016. Bile Acid Signaling Is Involved in the Neurological Decline in a Murine Model of Acute Liver Failure. *The American journal of pathology*, 186, 312-323.
- MCWILLIAMS, T. G., PRESCOTT, A. R., ALLEN, G. F. G., TAMJAR, J., MUNSON, M. J., THOMSON, C., MUQIT, M. M. K. & GANLEY, I. G. 2016. mito-QC illuminates mitophagy and mitochondrial architecture in vivo. *The Journal of cell biology*, 214, 333-345.
- MEDVEDEV, S. P., SHEVCHENKO, A. I. & ZAKIAN, S. M. 2010. Induced Pluripotent Stem Cells: Problems and Advantages when Applying them in Regenerative Medicine. *Acta naturae*, 2, 18-28.
- MEJIA, E. M. & HATCH, G. M. 2016. Mitochondrial phospholipids: role in mitochondrial function. *Journal of Bioenergetics and Biomembranes*, 48, 99-112.
- MEYER, K., FERRAIUOLO, L., MIRANDA, C. J., LIKHTE, S., MCELROY, S., RENUSCH, S., DITSWORTH, D., LAGIER-TOURENNE, C., SMITH, R. A., RAVITS, J., BURGHESE, A. H., SHAW, P. J., CLEVELAND, D. W., KOLB, S. J. & KASPAR, B. K. 2014. Direct conversion of patient fibroblasts demonstrates non-cell autonomous toxicity of astrocytes to motor neurons in familial and sporadic ALS. *Proceedings of the National Academy of Sciences*, 111, 829-832.
- MILIARA, X., GARNETT, J. A., TATSUTA, T., ABID ALI, F., BALDIE, H., PÉREZ-DORADO, I., SIMPSON, P., YAGUE, E., LANGER, T. & MATTHEWS, S. 2015. Structural insight into the TRIAP1/PRELI-like domain family of mitochondrial phospholipid transfer complexes. *EMBO reports*, 16, 824-835.
- MILIARA, X., TATSUTA, T., BERRY, J.-L., ROUSE, S. L., SOLAK, K., CHOREV, D. S., WU, D., ROBINSON, C. V., MATTHEWS, S. & LANGER, T. 2019. Structural determinants of lipid specificity within Ups/PRELI lipid transfer proteins. *Nature communications*, 10, 1130-1130.
- MILLER, D. E., COOK, K. R. & HAWLEY, R. S. 2019. The joy of balancers. *PLoS genetics*, 15, e1008421-e1008421.
- MILLER, J. D., GANAT, Y. M., KISHINEVSKY, S., BOWMAN, R. L., LIU, B., TU, E. Y., MANDAL, P. K., VERA, E., SHIM, J.-W., KRIKS, S., TALDONE, T., FUSAKI, N., TOMISHIMA, M. J., KRAINIC, D., MILNER, T. A., ROSSI, D. J. & STUDER, L. 2013. Human iPSC-based modeling of late-onset disease via progerin-induced aging. *Cell stem cell*, 13, 691-705.
- MILLER, S. & MUQIT, M. M. K. 2019. Therapeutic approaches to enhance PINK1/Parkin mediated mitophagy for the treatment of Parkinson's disease. *Neurosci Lett*, 705, 7-13.
- MISHIMA, T., FUJIOKA, S., MORISHITA, T., INOUE, T. & TSUBOI, Y. 2021. Personalized Medicine in Parkinson's Disease: New Options for Advanced Treatments. *Journal of personalized medicine*, 11, 650.
- MIYATA, N., GODA, N., MATSUO, K., HOKETSU, T. & KUGE, O. 2017. Cooperative function of Fmp30, Mdm31, and Mdm32 in Ups1-independent cardiolipin accumulation in the yeast *Saccharomyces cerevisiae*. *Scientific reports*, 7, 16447-16447.
- MOHS, R. C. & GREIG, N. H. 2017. Drug discovery and development: Role of basic biological research. *Alzheimer's & dementia (New York, N. Y.)*, 3, 651-657.
- MONTE, M. J., MARIN, J. J. G., ANTELO, A. & VAZQUEZ-TATO, J. 2009. Bile acids: chemistry, physiology, and pathophysiology. *World journal of gastroenterology*, 15, 804-816.
- MOREIRA, S., FONSECA, I., NUNES, M. J., ROSA, A., LEMOS, L., RODRIGUES, E., CARVALHO, A. N., OUTEIRO, T. F., RODRIGUES, C. M. P., GAMA, M. J. & CASTRO-CALDAS, M. 2017. Nrf2 activation by tauroursodeoxycholic acid in experimental models of Parkinson's disease. *Experimental Neurology*, 295, 77-87.
- MORTIBOYS, H., AASLY, J. & BANDMANN, O. 2013. Ursocholic acid rescues mitochondrial function in common forms of familial Parkinson's disease. *Brain*, 136, 3038-3050.

- MORTIBOYS, H., FURMSTON, R., BRONSTAD, G., AASLY, J., ELLIOTT, C. & BANDMANN, O. 2015. UDCA exerts beneficial effect on mitochondrial dysfunction in LRRK2(G2019S) carriers and in vivo. *Neurology*, 85, 846-52.
- MULLER, H. J. 1928. The Production of Mutations by X-Rays. *Proc Natl Acad Sci U S A*, 14, 714-26.
- MURPHY, E., ARDEHALI, H., BALABAN, R. S., DILISA, F., DORN, G. W., KITSIS, R. N., OTSU, K., PING, P., RIZZUTO, R., SACK, M. N., WALLACE, D. & YOULE, R. J. 2016. Mitochondrial Function, Biology, and Role in Disease. *Circulation Research*, 118, 1960-1991.
- NAGANA GOWDA, G. A., SHANAIAH, N., COOPER, A., MALUCCIO, M. & RAFTERY, D. 2009. Bile acids conjugation in human bile is not random: new insights from (1)H-NMR spectroscopy at 800 MHz. *Lipids*, 44, 527-35.
- NAGOSHI, E. 2018. Drosophila Models of Sporadic Parkinson's Disease. *International journal of molecular sciences*, 19, 3343.
- NAJIB, N. H. M., NIES, Y. H., ABD HALIM, S. A. S., YAHAYA, M. F., DAS, S., LIM, W. L. & TEOH, S. L. 2020. Modeling Parkinson's Disease in Zebrafish. *CNS Neurol Disord Drug Targets*, 19, 386-399.
- NARENDRA, D. P., JIN, S. M., TANAKA, A., SUEN, D.-F., GAUTIER, C. A., SHEN, J., COOKSON, M. R. & YOULE, R. J. 2010. PINK1 Is Selectively Stabilized on Impaired Mitochondria to Activate Parkin. *PLOS Biology*, 8, e1000298.
- NAVARRO-ROMERO, A., MONTPEYÓ, M. & MARTINEZ-VICENTE, M. 2020. The Emerging Role of the Lysosome in Parkinson's Disease. *Cells*, 9, 2399.
- NEWMAN, A. J., SELKOE, D. & DETTMER, U. 2013. A New Method for Quantitative Immunoblotting of Endogenous α -Synuclein. *PLOS ONE*, 8, e81314.
- NICOLAIDES NC, C. G., KINO T. 2020. *Glucocorticoid Receptor* [Online]. Endotext. Available: <https://www.ncbi.nlm.nih.gov/books/NBK279171/> [Accessed 23/06/22 2022].
- NIRENBERG, M. J., VAUGHAN, R. A., UHL, G. R., KUCHAR, M. J. & PICKEL, V. M. 1996. The dopamine transporter is localized to dendritic and axonal plasma membranes of nigrostriatal dopaminergic neurons. *J Neurosci*, 16, 436-47.
- NOLFI-DONEGAN, D., BRAGANZA, A. & SHIVA, S. 2020. Mitochondrial electron transport chain: Oxidative phosphorylation, oxidant production, and methods of measurement. *Redox biology*, 37, 101674-101674.
- NOWAKOWSKI, A. B., WOBIG, W. J. & PETERING, D. H. 2014. Native SDS-PAGE: high resolution electrophoretic separation of proteins with retention of native properties including bound metal ions. *Metallomics*, 6, 1068-78.
- NTETSICA, T., PAPATHOMA, P.-E. & MARKAKI, I. 2021. Novel targeted therapies for Parkinson's disease. *Molecular Medicine*, 27, 17.
- NUNNARI, J. & SUOMALAINEN, A. 2012. Mitochondria: in sickness and in health. *Cell*, 148, 1145-59.
- NÜSSLEIN-VOLHARD, C. & WIESCHAUS, E. 1980. Mutations affecting segment number and polarity in Drosophila. *Nature*, 287, 795-801.
- OEMER, G., KOCH, J., WOHLFARTER, Y., ALAM, M. T., LACKNER, K., SAILER, S., NEUMANN, L., LINDNER, H. H., WATSCHINGER, K., HALTMEIER, M., WERNER, E. R., ZSCHOCKE, J. & KELLER, M. A. 2020. Phospholipid Acyl Chain Diversity Controls the Tissue-Specific Assembly of Mitochondrial Cardiolipins. *Cell Reports*, 30, 4281-4291.e4.
- OEMER, G., LACKNER, K., MUIGG, K., KRUMSCHNABEL, G., WATSCHINGER, K., SAILER, S., LINDNER, H., GNAIGER, E., WORTMANN, S. B., WERNER, E. R., ZSCHOCKE, J. & KELLER, M. A. 2018. Molecular structural diversity of mitochondrial cardiolipins. *Proceedings of the National Academy of Sciences of the United States of America*, 115, 4158-4163.
- OKUMURA, M., TANIKAWA, K., CHŪMAN, Y., KŌJI, T., NAKAGAWA, S., NAKAMURA, Y., UNO, H., YAMASAKI, S. & HISATSUGU, T. 1977. Clinical studies on dissolution of gallstones using ursodeoxycholic acid. *Gastroenterologia Japonica*, 12, 469-475.
- OSMAN, C., HAAG, M., POTTING, C., RODENFELS, J., DIP, P. V., WIELAND, F. T., BRÜGGER, B., WESTERMANN, B. & LANGER, T. 2009. The genetic interactome of prohibitins: coordinated

- control of cardiolipin and phosphatidylethanolamine by conserved regulators in mitochondria. *The Journal of cell biology*, 184, 583-596.
- OSMAN, C., VOELKER, D. R. & LANGER, T. 2011. Making heads or tails of phospholipids in mitochondria. *The Journal of cell biology*, 192, 7-16.
- PAGANONI, S., HENDRIX, S., DICKSON, S. P., KNOWLTON, N., MACKLIN, E. A., BERRY, J. D., ELLIOTT, M. A., MAISER, S., KARAM, C., CARESS, J. B., OWEGI, M. A., QUICK, A., WYMER, J., GOUTMAN, S. A., HEITZMAN, D., HEIMAN-PATTERSON, T. D., JACKSON, C. E., QUINN, C., ROTHSTEIN, J. D., KASARSKIS, E. J., KATZ, J., JENKINS, L., LADHA, S., MILLER, T. M., SCELSA, S. N., VU, T. H., FOURNIER, C. N., GLASS, J. D., JOHNSON, K. M., SWENSON, A., GOYAL, N. A., PATTEE, G. L., ANDRES, P. L., BABU, S., CHASE, M., DAGOSTINO, D., HALL, M., KITTLE, G., EYDINOV, M., MCGOVERN, M., OSTROW, J., POTHIER, L., RANDALL, R., SHEFNER, J. M., SHERMAN, A. V., ST PIERRE, M. E., TUSTISON, E., VIGNESWARAN, P., WALKER, J., YU, H., CHAN, J., WITTES, J., YU, Z.-F., COHEN, J., KLEE, J., LESLIE, K., TANZI, R. E., GILBERT, W., YERAMIAN, P. D., SCHOENFELD, D. & CUDKOWICZ, M. E. 2021. Long-term survival of participants in the CENTAUR trial of sodium phenylbutyrate-taurursodiol in amyotrophic lateral sclerosis. *Muscle & Nerve*, 63, 31-39.
- PAJARES, M., I ROJO, A., MANDA, G., BOSCA, L. & CUADRADO, A. 2020. Inflammation in Parkinson's Disease: Mechanisms and Therapeutic Implications. *Cells*, 9, 1687.
- PAKHOMOV, A. G., SEMENOV, I., CASCIOLA, M. & XIAO, S. 2017. Neuronal excitation and permeabilization by 200-ns pulsed electric field: An optical membrane potential study with FluoVolt dye. *Biochimica et biophysica acta. Biomembranes*, 1859, 1273-1281.
- PALEOLOGOU, K. E., OUESLATI, A., SHAKKED, G., ROSPIGLIOSI, C. C., KIM, H.-Y., LAMBERTO, G. R., FERNANDEZ, C. O., SCHMID, A., CHEGINI, F., GAI, W. P., CHIAPPE, D., MONIATTE, M., SCHNEIDER, B. L., AEBISCHER, P., ELIEZER, D., ZWECKSTETTER, M., MASLIAH, E. & LASHUEL, H. A. 2010. Phosphorylation at S87 is enhanced in synucleinopathies, inhibits alpha-synuclein oligomerization, and influences synuclein-membrane interactions. *The Journal of neuroscience : the official journal of the Society for Neuroscience*, 30, 3184-3198.
- PAN, X., ELLIOTT, C. T., MCGUINNESS, B., PASSMORE, P., KEHOE, P. G., HÖLSCHER, C., MCCLEAN, P. L., GRAHAM, S. F. & GREEN, B. D. 2017. Metabolomic Profiling of Bile Acids in Clinical and Experimental Samples of Alzheimer's Disease. *Metabolites*, 7.
- PANDEY, U. B. & NICHOLS, C. D. 2011. Human disease models in *Drosophila melanogaster* and the role of the fly in therapeutic drug discovery. *Pharmacological reviews*, 63, 411-436.
- PANOV, A. V. & DIKALOV, S. I. 2020. Cardiolipin, Perhydroxyl Radicals, and Lipid Peroxidation in Mitochondrial Dysfunctions and Aging. *Oxidative medicine and cellular longevity*, 2020, 1323028-1323028.
- PARADIES, G., PARADIES, V., RUGGIERO, F. M. & PETROSILLO, G. 2019. Role of Cardiolipin in Mitochondrial Function and Dynamics in Health and Disease: Molecular and Pharmacological Aspects. *Cells*, 8, 728.
- PARK, J.-S., DAVIS, R. L. & SUE, C. M. 2018. Mitochondrial Dysfunction in Parkinson's Disease: New Mechanistic Insights and Therapeutic Perspectives. *Current neurology and neuroscience reports*, 18, 21-21.
- PATTERSON, M., CHAN, D. N., HA, I., CASE, D., CUI, Y., VAN HANDEL, B., MIKKOLA, H. K. & LOWRY, W. E. 2012. Defining the nature of human pluripotent stem cell progeny. *Cell research*, 22, 178-193.
- PAUL, R., CHOUDHURY, A., KUMAR, S., GIRI, A., SANDHIR, R. & BORAH, A. 2017. Cholesterol contributes to dopamine-neuronal loss in MPTP mouse model of Parkinson's disease: Involvement of mitochondrial dysfunctions and oxidative stress. *PLoS one*, 12, e0171285-e0171285.
- PAUMGARTNER, G. & BEUERS, U. 2002. Ursodeoxycholic acid in cholestatic liver disease: mechanisms of action and therapeutic use revisited. *Hepatology*, 36, 525-31.

- PAYNE, T., SASSANI, M., BUCKLEY, E., MOLL, S., ANTON, A., APPLEBY, M., MARU, S., TAYLOR, R., MCNEILL, A., HOGGARD, N., MAZZA, C., WILKINSON, I. D., JENKINS, T., FOLTYNIE, T. & BANDMANN, O. 2020. Ursodeoxycholic acid as a novel disease-modifying treatment for Parkinson's disease: protocol for a two-centre, randomised, double-blind, placebo-controlled trial, The 'UP' study. *BMJ open*, 10, e038911-e038911.
- PENG, J. & ANDERSEN, J. K. 2003. The role of c-Jun N-terminal kinase (JNK) in Parkinson's disease. *IUBMB Life*, 55, 267-71.
- PERRY, S. W., NORMAN, J. P., BARBIERI, J., BROWN, E. B. & GELBARD, H. A. 2011. Mitochondrial membrane potential probes and the proton gradient: a practical usage guide. *BioTechniques*, 50, 98-115.
- PERRY, T., HAUGHEY, N. J., MATTSON, M. P., EGAN, J. M. & GREIG, N. H. 2002a. Protection and reversal of excitotoxic neuronal damage by glucagon-like peptide-1 and exendin-4. *J Pharmacol Exp Ther*, 302, 881-8.
- PERRY, T., LAHIRI, D. K., CHEN, D., ZHOU, J., SHAW, K. T., EGAN, J. M. & GREIG, N. H. 2002b. A novel neurotrophic property of glucagon-like peptide 1: a promoter of nerve growth factor-mediated differentiation in PC12 cells. *J Pharmacol Exp Ther*, 300, 958-66.
- PESAH, Y., PHAM, T., BURGESS, H., MIDDLEBROOKS, B., VERSTREKEN, P., ZHOU, Y., HARDING, M., BELLEN, H. & MARDON, G. 2004. Drosophila parkin mutants have decreased mass and cell size and increased sensitivity to oxygen radical stress. *Development*, 131, 2183-94.
- PETERSEN, C. C. H. 2017. Whole-Cell Recording of Neuronal Membrane Potential during Behavior. *Neuron*, 95, 1266-1281.
- PETRALIA, R. S., MATTSON, M. P. & YAO, P. J. 2014. Communication breakdown: the impact of ageing on synapse structure. *Ageing research reviews*, 14, 31-42.
- PETROSKE, E., MEREDITH, G. E., CALLEN, S., TOTTERDELL, S. & LAU, Y. S. 2001. Mouse model of Parkinsonism: a comparison between subacute MPTP and chronic MPTP/probenecid treatment. *Neuroscience*, 106, 589-601.
- PETROVA, O. E. & SAUER, K. 2017. High-Performance Liquid Chromatography (HPLC)-Based Detection and Quantitation of Cellular c-di-GMP. *Methods in molecular biology (Clifton, N.J.)*, 1657, 33-43.
- PICHOT, R., WATSON, R. L. & NORTON, I. T. 2013. Phospholipids at the interface: current trends and challenges. *International journal of molecular sciences*, 14, 11767-11794.
- PISTOLLATO, F., BERNASCONI, C., MCCARTHY, J., CAMPPIA, I., DESAINTE, C., WITTWEHR, C., DECEUNINCK, P. & WHELAN, M. 2020. Alzheimer's Disease, and Breast and Prostate Cancer Research: Translational Failures and the Importance to Monitor Outputs and Impact of Funded Research. *Animals : an open access journal from MDPI*, 10, 1194.
- PISTOLLATO, F., CANOVAS-JORDA, D., ZAGOURA, D. & BAL-PRICE, A. 2017. Nrf2 pathway activation upon rotenone treatment in human iPSC-derived neural stem cells undergoing differentiation towards neurons and astrocytes. *Neurochemistry international*, 108, 457-471.
- PLOTEGHER, N., GRATTON, E. & BUBACCO, L. 2014. Number and Brightness analysis of alpha-synuclein oligomerization and the associated mitochondrial morphology alterations in live cells. *Biochim Biophys Acta*, 1840, 2014-24.
- POLINSKI, N. K., VOLPICELLI-DALEY, L. A., SORTWELL, C. E., LUK, K. C., CREMADES, N., GOTTLER, L. M., FROULA, J., DUFFY, M. F., LEE, V. M. Y., MARTINEZ, T. N. & DAVE, K. D. 2018. Best Practices for Generating and Using Alpha-Synuclein Pre-Formed Fibrils to Model Parkinson's Disease in Rodents. *J Parkinsons Dis*, 8, 303-322.
- POTASHKIN, J. A., BLUME, S. R. & RUNKLE, N. K. 2010. Limitations of animal models of Parkinson's disease. *Parkinson's disease*, 2011, 658083-658083.
- POTTING, C., TATSUTA, T., KÖNIG, T., HAAG, M., WAI, T., AALTONEN, MARI J. & LANGER, T. 2013. TRIAP1/PRELI Complexes Prevent Apoptosis by Mediating Intramitochondrial Transport of Phosphatidic Acid. *Cell Metabolism*, 18, 287-295.

- POTTING, C., WILMES, C., ENGMANN, T., OSMAN, C. & LANGER, T. 2010. Regulation of mitochondrial phospholipids by Ups1/PRELI-like proteins depends on proteolysis and Mdm35. *The EMBO journal*, 29, 2888-2898.
- POUND, P. 2020. Are Animal Models Needed to Discover, Develop and Test Pharmaceutical Drugs for Humans in the 21st Century? *Animals : an open access journal from MDPI*, 10, 2455.
- POZO DEVOTO, V. M. & FALZONE, T. L. 2017. Mitochondrial dynamics in Parkinson's disease: a role for α -synuclein? *Disease models & mechanisms*, 10, 1075-1087.
- PRASAD, E. M. & HUNG, S.-Y. 2021. Current Therapies in Clinical Trials of Parkinson's Disease: A 2021 Update. *Pharmaceuticals (Basel, Switzerland)*, 14, 717.
- PRETERRE, C., CORBILLÉ, A.-G., BALLOY, G., LETOURNEL, F., NEUNLIST, M. & DERKINDEREN, P. 2015. Optimizing Western Blots for the Detection of Endogenous α -Synuclein in the Enteric Nervous System. *Journal of Parkinson's Disease*, 5, 765-772.
- PRYDE, K. R., SMITH, H. L., CHAU, K. Y. & SCHAPIRA, A. H. 2016. PINK1 disables the anti-fission machinery to segregate damaged mitochondria for mitophagy. *J Cell Biol*, 213, 163-71.
- PRZEDBORSKI, S., VILA, M. & JACKSON-LEWIS, V. 2003. Neurodegeneration: what is it and where are we? *J Clin Invest*, 111, 3-10.
- PÜTZ, S. M., KRAM, J., RAUH, E., KAISER, S., TOEWS, R., LUENINGSCHROER-WANG, Y., RIEGER, D. & RAABE, T. 2021. Loss of p21-activated kinase Mbt/PAK4 causes Parkinson-like phenotypes in Drosophila. *Disease models & mechanisms*, 14, dmm047811.
- QI, Y., ZHANG, X.-J., RENIER, N., WU, Z., ATKIN, T., SUN, Z., OZAIR, M. Z., TCHIEU, J., ZIMMER, B., FATTAHI, F., GANAT, Y., AZEVEDO, R., ZELTNER, N., BRIVANLOU, A. H., KARAYIORGOU, M., GOGOS, J., TOMISHIMA, M., TESSIER-LAVIGNE, M., SHI, S.-H. & STUDER, L. 2017. Combined small-molecule inhibition accelerates the derivation of functional cortical neurons from human pluripotent stem cells. *Nature biotechnology*, 35, 154-163.
- QUINN, M., MCMILLIN, M., GALINDO, C., FRAMPTON, G., PAE, H. Y. & DEMORROW, S. 2014. Bile acids permeabilize the blood brain barrier after bile duct ligation in rats via Rac1-dependent mechanisms. *Digestive and liver disease : official journal of the Italian Society of Gastroenterology and the Italian Association for the Study of the Liver*, 46, 527-534.
- RAMADAN, H., ALAWI, A. A. & ALAWI, M. A. 1993. Catecholamines in Drosophila melanogaster (wild type and ebony mutant) decuticularized retinas and brains. *Cell Biol Int*, 17, 765-71.
- RASCOL, O. 2009. "Disease-modification" trials in Parkinson disease: Target populations, endpoints and study design. *Neurology*, 72, S51.
- RAY, P. D., HUANG, B.-W. & TSUJI, Y. 2012. Reactive oxygen species (ROS) homeostasis and redox regulation in cellular signaling. *Cellular signalling*, 24, 981-990.
- REHBACH, K., KESAVAN, J., HAUSER, S., RITZENHOFEN, S., JUNGVERDORBEN, J., SCHÜLE, R., SCHÖLS, L., PEITZ, M. & BRÜSTLE, O. 2019. Multiparametric rapid screening of neuronal process pathology for drug target identification in HSP patient-specific neurons. *Scientific reports*, 9, 9615-9615.
- RISIGLIONE, P., ZINGHIRINO, F., DI ROSA, M. C., MAGRÌ, A. & MESSINA, A. 2021. Alpha-Synuclein and Mitochondrial Dysfunction in Parkinson's Disease: The Emerging Role of VDAC. *Biomolecules*, 11, 718.
- ROBERTS, R. F., WADE-MARTINS, R. & ALEGRE-ABARRATEGUI, J. 2015. Direct visualization of alpha-synuclein oligomers reveals previously undetected pathology in Parkinson's disease brain. *Brain : a journal of neurology*, 138, 1642-1657.
- RODRIGUES, C. M. P., SOLA, S., NAN, Z., CASTRO, R. E., RIBEIRO, P. S., LOW, W. C. & STEER, C. J. 2003. Tauroursodeoxycholic acid reduces apoptosis and protects against neurological injury after acute hemorrhagic stroke in rats. *Proceedings of the National Academy of Sciences of the United States of America*, 100, 6087-6092.
- RODRIGUES, M. A., MARTINS, N. E., BALANCÉ, L. F., BROOM, L. N., DIAS, A. J. S., FERNANDES, A. S. D., RODRIGUES, F., SUCENA, É. & MIRTH, C. K. 2015. Drosophila melanogaster larvae make

- nutritional choices that minimize developmental time. *Journal of Insect Physiology*, 81, 69-80.
- ROGER, A. J., MUÑOZ-GÓMEZ, S. A. & KAMIKAWA, R. 2017. The Origin and Diversification of Mitochondria. *Current Biology*, 27, R1177-R1192.
- ROMORINI, L., RIVA, D. A., BLÜGUERMANN, C., VIDELA RICHARDSON, G. A., SCASSA, M. E., SEVLEVER, G. E. & MIRIUKA, S. G. 2013. Effect of antibiotics against Mycoplasma sp. on human embryonic stem cells undifferentiated status, pluripotency, cell viability and growth. *PLoS One*, 8, e70267.
- ROSA, A. I., DUARTE-SILVA, S., SILVA-FERNANDES, A., NUNES, M. J., CARVALHO, A. N., RODRIGUES, E., GAMA, M. J., RODRIGUES, C. M. P., MACIEL, P. & CASTRO-CALDAS, M. 2018. Tauroursodeoxycholic Acid Improves Motor Symptoms in a Mouse Model of Parkinson's Disease. *Mol Neurobiol*, 55, 9139-9155.
- ROSA, A. I., FONSECA, I., NUNES, M. J., MOREIRA, S., RODRIGUES, E., CARVALHO, A. N., RODRIGUES, C. M. P., GAMA, M. J. & CASTRO-CALDAS, M. 2017. Novel insights into the antioxidant role of tauroursodeoxycholic acid in experimental models of Parkinson's disease. *Biochim Biophys Acta Mol Basis Dis*, 1863, 2171-2181.
- ROSEN, A. & ZEGER, S. L. 2019. Precision medicine: Discovering clinically relevant and mechanistically anchored disease subgroups at scale. *Journal of Clinical Investigation*, 129, 944-945.
- ROSIGNOL, I., VILLAREJO-ZORI, B., TERESAK, P., SIERRA-FILARDI, E., PEREIRO, X., RODRÍGUEZ-MUELA, N., VECINO, E., VIEIRA, H. L. A., BELL, K. & BOYA, P. 2020. The mito-QC Reporter for Quantitative Mitophagy Assessment in Primary Retinal Ganglion Cells and Experimental Glaucoma Models. *International journal of molecular sciences*, 21, 1882.
- ROUSSA, E. & KRIEGLSTEIN, K. 2004. GDNF promotes neuronal differentiation and dopaminergic development of mouse mesencephalic neurospheres. *Neuroscience Letters*, 361, 52-55.
- ROUSSA, E., VON BOHLEN UND HALBACK, O. & KRIEGLSTEIN, K. 2009. TGF- β in Dopamine Neuron Development, Maintenance and Neuroprotection. In: PASTERKAMP, R. J., SMIDT, M. P. & BURBACH, J. P. H. (eds.) *Development and Engineering of Dopamine Neurons*. New York, NY: Springer New York.
- RUTTER, J. & HUGHES, A. L. 2015. Power(2): the power of yeast genetics applied to the powerhouse of the cell. *Trends in endocrinology and metabolism: TEM*, 26, 59-68.
- RYAN, B. J., HOEK, S., FON, E. A. & WADE-MARTINS, R. 2015. Mitochondrial dysfunction and mitophagy in Parkinson's: from familial to sporadic disease. *Trends in Biochemical Sciences*, 40, 200-210.
- RYAN, T., BAMB, V. V., STYKEL, M. G., COACKLEY, C. L., HUMPHRIES, K. M., JAMIESON-WILLIAMS, R., AMBASUDHAN, R., MOSSER, D. D., LIPTON, S. A., HARAUZ, G. & RYAN, S. D. 2018. Cardiolipin exposure on the outer mitochondrial membrane modulates α -synuclein. *Nat Commun*, 9, 817.
- RYDEN, L. E. & LEWIS, S. J. G. 2019. Parkinson's Disease in the Era of Personalised Medicine: One Size Does Not Fit All. *Drugs & Aging*, 36, 103-113.
- SAINI, N., GEORGIEV, O. & SCHAFFNER, W. 2011. The parkin mutant phenotype in the fly is largely rescued by metal-responsive transcription factor (MTF-1). *Molecular and cellular biology*, 31, 2151-2161.
- SALGADO-POLO, F., FISH, A., MATSOUKAS, M. T., HEIDEBRECHT, T., KEUNE, W. J. & PERRAKIS, A. 2018. Lysophosphatidic acid produced by autotaxin acts as an allosteric modulator of its catalytic efficiency. *J Biol Chem*, 293, 14312-14327.
- SALIMIAGHDAM, N., SINGH, L., SCHNEIDER, K., NALBANDIAN, A., CHWA, M., ATILANO, S. R., BAO, A. & KENNEY, M. C. 2020. Potential adverse effects of ciprofloxacin and tetracycline on ARPE-19 cell lines. *BMJ Open Ophthalmology*, 5, e000458.
- SÁNCHEZ-DANÉS, A., RICHAUD-PATIN, Y., CARBALLO-CARBAJAL, I., JIMÉNEZ-DELGADO, S., CAIG, C., MORA, S., DI GUGLIELMO, C., EZQUERRA, M., PATEL, B., GIRALT, A., CANALS, J. M., MEMO, M., ALBERCH, J., LÓPEZ-BARNEO, J., VILA, M., CUERVO, A. M., TOLOSA, E., CONSIGLIO, A. &

- RAYA, A. 2012. Disease-specific phenotypes in dopamine neurons from human iPS-based models of genetic and sporadic Parkinson's disease. *EMBO molecular medicine*, 4, 380-395.
- SANG, T.-K., CHANG, H.-Y., LAWLESS, G. M., RATNAPARKHI, A., MEE, L., ACKERSON, L. C., MAIDMENT, N. T., KRANTZ, D. E. & JACKSON, G. R. 2007. A Drosophila model of mutant human parkin-induced toxicity demonstrates selective loss of dopaminergic neurons and dependence on cellular dopamine. *The Journal of neuroscience : the official journal of the Society for Neuroscience*, 27, 981-992.
- SANTOS, D., ESTEVES, A. R., SILVA, D. F., JANUÁRIO, C. & CARDOSO, S. M. 2015. The Impact of Mitochondrial Fusion and Fission Modulation in Sporadic Parkinson's Disease. *Mol Neurobiol*, 52, 573-86.
- ŠARENAC, T. M. & MIKOV, M. 2018. Bile Acid Synthesis: From Nature to the Chemical Modification and Synthesis and Their Applications as Drugs and Nutrients. *Frontiers in pharmacology*, 9, 939-939.
- SCHÄGGER, H. 1995. Quantification of oxidative phosphorylation enzymes after blue native electrophoresis and two-dimensional resolution: normal complex I protein amounts in Parkinson's disease conflict with reduced catalytic activities. *Electrophoresis*, 16, 763-70.
- SCHAPIRA, A. H. V., COOPER, J. M., DEXTER, D., CLARK, J. B., JENNER, P. & MARSDEN, C. D. 1990. Mitochondrial Complex I Deficiency in Parkinson's Disease. *Journal of Neurochemistry*, 54, 823-827.
- SCHLAME, M., REN, M., XU, Y., GREENBERG, M. L. & HALLER, I. 2005. Molecular symmetry in mitochondrial cardiolipins. *Chemistry and Physics of Lipids*, 138, 38-49.
- SCHLAME, M., SHANSKE, S., DOTY, S., KÖNIG, T., SCULCO, T., DIMAURO, S. & BLANCK, T. J. J. 1999. Microanalysis of cardiolipin in small biopsies including skeletal muscle from patients with mitochondrial disease. *Journal of Lipid Research*, 40, 1585-1592.
- SCHMITT, K., DÄUBENER, W., BITTER-SUERMAN, D. & HADDING, U. 1988. A safe and efficient method for elimination of cell culture mycoplasmas using ciprofloxacin. *Journal of Immunological Methods*, 109, 17-25.
- SCHNITZBAUER, J., STRAUSS, M. T., SCHLICHTHAERLE, T., SCHUEDER, F. & JUNGSMANN, R. 2017. Super-resolution microscopy with DNA-PAINT. *Nature Protocols*, 12, 1198-1228.
- SCHONEWILLE, M., DE BOER, J. F. & GROEN, A. K. 2016. Bile salts in control of lipid metabolism. *Curr Opin Lipidol*, 27, 295-301.
- SCHWARTZENTRUBER, A., BOSCHIAN, C., LOPES, F. M., MYSZCZYNSKA, M. A., NEW, E. J., BEYRATH, J., SMEITINK, J., FERRAIUOLO, L. & MORTIBOYS, H. 2020. Oxidative switch drives mitophagy defects in dopaminergic parkin mutant patient neurons. *Scientific Reports*, 10, 15485.
- SCHWEITZER, J. S., SONG, B., HERRINGTON, T. M., PARK, T.-Y., LEE, N., KO, S., JEON, J., CHA, Y., KIM, K., LI, Q., HENCHCLIFFE, C., KAPLITT, M., NEFF, C., RAPALINO, O., SEO, H., LEE, I.-H., KIM, J., KIM, T., PETSKO, G. A., RITZ, J., COHEN, B. M., KONG, S.-W., LEBLANC, P., CARTER, B. S. & KIM, K.-S. 2020. Personalized iPSC-Derived Dopamine Progenitor Cells for Parkinson's Disease. *The New England journal of medicine*, 382, 1926-1932.
- SEIRAFI, M., KOZLOV, G. & GEHRING, K. 2015. Parkin structure and function. *The FEBS journal*, 282, 2076-2088.
- SESAKI, H., DUNN, C. D., IJIMA, M., SHEPARD, K. A., YAFFE, M. P., MACHAMER, C. E. & JENSEN, R. E. 2006. Ups1p, a conserved intermembrane space protein, regulates mitochondrial shape and alternative topogenesis of Mgm1p. *The Journal of cell biology*, 173, 651-658.
- SEVER, B., CIFTCI, H., DEMIRCI, H., SEVER, H., OCAK, F., YULUG, B., TATEISHI, H., TATEISHI, T., OTSUKA, M., FUJITA, M. & BAŞAK, A. N. 2022. Comprehensive Research on Past and Future Therapeutic Strategies Devoted to Treatment of Amyotrophic Lateral Sclerosis. *International journal of molecular sciences*, 23, 2400.
- SHALTOUKI, A., SIVAPATHAM, R., PEI, Y., GERENCSEK, A. A., MOMČILOVIĆ, O., RAO, M. S. & ZENG, X. 2015. Mitochondrial alterations by PARKIN in dopaminergic neurons using PARK2 patient-specific and PARK2 knockout isogenic iPSC lines. *Stem cell reports*, 4, 847-859.

- SHARMA, R., PRICHARD, D., MAJER, F., BYRNE, A. M., KELLEHER, D., LONG, A. & GILMER, J. F. 2011. Ursodeoxycholic acid amides as novel glucocorticoid receptor modulators. *J Med Chem*, 54, 122-30.
- SHELL, B. C., SCHMITT, R. E., LEE, K. M., JOHNSON, J. C., CHUNG, B. Y., PLETCHER, S. D. & GROTEWIEL, M. 2018. Measurement of solid food intake in *Drosophila* via consumption-excretion of a dye tracer. *Scientific reports*, 8, 11536-11536.
- SIDDIQUI, I. J., PERVAIZ, N. & ABBASI, A. A. 2016. The Parkinson Disease gene SNCA: Evolutionary and structural insights with pathological implication. *Scientific reports*, 6, 24475-24475.
- SIMON, D. K., TANNER, C. M. & BRUNDIN, P. 2020. Parkinson Disease Epidemiology, Pathology, Genetics, and Pathophysiology. *Clinics in geriatric medicine*, 36, 1-12.
- SINGH, F. & GANLEY, I. G. 2021. Parkinson's disease and mitophagy: an emerging role for LRRK2. *Biochemical Society transactions*, 49, 551-562.
- SOLÁ, S., AMARAL, J. D., BORRALHO, P. M., RAMALHO, R. M., CASTRO, R. E., ARANHA, M. R. M., STEER, C. J. & RODRIGUES, C. M. P. 2006. Functional Modulation of Nuclear Steroid Receptors by Tauroursodeoxycholic Acid Reduces Amyloid β -Peptide-Induced Apoptosis. *Molecular Endocrinology*, 20, 2292-2303.
- SOLÁ, S., AMARAL, J. D., CASTRO, R. E., RAMALHO, R. M., BORRALHO, P. M., KREN, B. T., TANAKA, H., STEER, C. J. & RODRIGUES, C. M. P. 2005. Nuclear translocation of UDCA by the glucocorticoid receptor is required to reduce TGF- β 1-induced apoptosis in rat hepatocytes. *Hepatology*, 42, 925-934.
- SOLTANI, M. H., PICHARDO, R., SONG, Z., SANGHA, N., CAMACHO, F., SATYAMOORTHY, K., SANGUEZA, O. P. & SETALURI, V. 2005. Microtubule-associated protein 2, a marker of neuronal differentiation, induces mitotic defects, inhibits growth of melanoma cells, and predicts metastatic potential of cutaneous melanoma. *The American journal of pathology*, 166, 1841-1850.
- SOMEKH, E., DOUER, D., SHAKED, N. & RUBINSTEIN, E. 1989. In vitro effects of ciprofloxacin and pefloxacin on growth of normal human hematopoietic progenitor cells and on leukemic cell lines. *Journal of Pharmacology and Experimental Therapeutics*, 248, 415.
- STAFSA, K., TSIKA, E., MOSER, R., MUSSO, A., GLAUSER, L., JONES, A., BISKUP, S., XIONG, Y., BANDOPADHYAY, R., DAWSON, V. L., DAWSON, T. M. & MOORE, D. J. 2014. Functional interaction of Parkinson's disease-associated LRRK2 with members of the dynamin GTPase superfamily. *Hum Mol Genet*, 23, 2055-77.
- STATHAKOS, P., JIMÉNEZ-MORENO, N., CROMPTON, L. A., NISTOR, P. A., BADGER, J. L., BARBUTI, P. A., KERRIGAN, T. L., RANDALL, A. D., CALDWELL, M. A. & LANE, J. D. 2021. A monolayer hiPSC culture system for autophagy/mitophagy studies in human dopaminergic neurons. *Autophagy*, 17, 855-871.
- STEFANIS, L., KHOLODILOV, N., RIDEOUT, H. J., BURKE, R. E. & GREENE, L. A. 2001. Synuclein-1 is selectively up-regulated in response to nerve growth factor treatment in PC12 cells. *J Neurochem*, 76, 1165-76.
- STOKER, T. B. & BARKER, R. A. 2020. Recent developments in the treatment of Parkinson's Disease. *F1000Research*, 9, F1000 Faculty Rev-862.
- SUBRAMANIAM, S. R., VERGNES, L., FRANICH, N. R., REUE, K. & CHESSELET, M. F. 2014. Region specific mitochondrial impairment in mice with widespread overexpression of alpha-synuclein. *Neurobiol Dis*, 70, 204-13.
- SUHR, S. T., CHANG, E. A., TJONG, J., ALCASID, N., PERKINS, G. A., GOISSIS, M. D., ELLISMAN, M. H., PEREZ, G. I. & CIBELLI, J. B. 2010. Mitochondrial rejuvenation after induced pluripotency. *PLoS One*, 5, e14095.
- SUN, D., GU, G., WANG, J., CHAI, Y., FAN, Y., YANG, M., XU, X., GAO, W., LI, F., YIN, D., ZHOU, S., CHEN, X. & ZHANG, J. 2017a. Administration of Tauroursodeoxycholic Acid Attenuates Early Brain Injury via Akt Pathway Activation. *Frontiers in cellular neuroscience*, 11, 193-193.

- SUN, F. F., JOHNSON, J. E., ZEIDLER, M. P. & BATEMAN, J. R. 2012. Simplified Insertion of Transgenes Onto Balancer Chromosomes via Recombinase-Mediated Cassette Exchange. *G3 (Bethesda, Md.)*, 2, 551-553.
- SUN, N., MALIDE, D., LIU, J., ROVIRA, I. I., COMBS, C. A. & FINKEL, T. 2017b. A fluorescence-based imaging method to measure in vitro and in vivo mitophagy using mt-Keima. *Nature Protocols*, 12, 1576-1587.
- SUN, N., YOULE, R. J. & FINKEL, T. 2016. The Mitochondrial Basis of Aging. *Molecular cell*, 61, 654-666.
- SZARGEL, R., SHANI, V., ABD ELGHANI, F., MEKIES, L. N., LIANI, E., ROTT, R. & ENGELENDER, S. 2016. The PINK1, synphilin-1 and SIAH-1 complex constitutes a novel mitophagy pathway. *Hum Mol Genet*, 25, 3476-3490.
- TAKAHASHI, K., TANABE, K., OHNUKI, M., NARITA, M., ICHISAKA, T., TOMODA, K. & YAMANAKA, S. 2007. Induction of Pluripotent Stem Cells from Adult Human Fibroblasts by Defined Factors. *Cell*, 131, 861-872.
- TAMBASCO, N., ROMOLI, M. & CALABRESI, P. 2018. Levodopa in Parkinson's Disease: Current Status and Future Developments. *Current neuropharmacology*, 16, 1239-1252.
- TAMURA, Y., ENDO, T., IJIMA, M. & SESAKI, H. 2009. Ups1p and Ups2p antagonistically regulate cardiolipin metabolism in mitochondria. *The Journal of cell biology*, 185, 1029-1045.
- TAMURA, Y., SESAKI, H. & ENDO, T. 2014. Phospholipid transport via mitochondria. *Traffic (Copenhagen, Denmark)*, 15, 933-945.
- TANNER, C. M., KAMEL, F., ROSS, G. W., HOPPIN, J. A., GOLDMAN, S. M., KORELL, M., MARRAS, C., BHUDHIKANOK, G. S., KASTEN, M., CHADE, A. R., COMYNS, K., RICHARDS, M. B., MENG, C., PRIESTLEY, B., FERNANDEZ, H. H., CAMBI, F., UMBACH, D. M., BLAIR, A., SANDLER, D. P. & LANGSTON, J. W. 2011. Rotenone, paraquat, and Parkinson's disease. *Environmental health perspectives*, 119, 866-872.
- THAKUR, P., BREGER LUDIVINE, S., LUNDBLAD, M., WAN OI, W., MATTSSON, B., LUK KELVIN, C., LEE VIRGINIA, M. Y., TROJANOWSKI JOHN, Q. & BJÖRKLUND, A. 2017. Modeling Parkinson's disease pathology by combination of fibril seeds and α -synuclein overexpression in the rat brain. *Proceedings of the National Academy of Sciences*, 114, E8284-E8293.
- THANVI, B., LO, N. & ROBINSON, T. 2007. Levodopa-induced dyskinesia in Parkinson's disease: clinical features, pathogenesis, prevention and treatment. *Postgraduate medical journal*, 83, 384-388.
- TILOKANI, L., NAGASHIMA, S., PAUPE, V. & PRUDENT, J. 2018. Mitochondrial dynamics: overview of molecular mechanisms. *Essays in biochemistry*, 62, 341-360.
- TOLWINSKI, N. S. 2017. Introduction: Drosophila-A Model System for Developmental Biology. *Journal of developmental biology*, 5, 9.
- TRAN, H. H., DANG, S. N. A., NGUYEN, T. T., HUYNH, A. M., DAO, L. M., KAMEI, K., YAMAGUCHI, M. & DANG, T. T. P. 2018. Drosophila Ubiquitin C-Terminal Hydrolase Knockdown Model of Parkinson's Disease. *Scientific reports*, 8, 4468-4468.
- TRAN, J., ANASTACIO, H. & BARDY, C. 2020. Genetic predispositions of Parkinson's disease revealed in patient-derived brain cells. *NPJ Parkinson's disease*, 6, 8-8.
- TRUBAN, D., HOU, X., CAULFIELD, T. R., FIESEL, F. C. & SPRINGER, W. 2017. PINK1, Parkin, and Mitochondrial Quality Control: What can we Learn about Parkinson's Disease Pathobiology? *J Parkinsons Dis*, 7, 13-29.
- TSCHUCH, C., SCHULZ, A., PSCHERER, A., WERFT, W., BENNER, A., HOTZ-WAGENBLATT, A., BARRIONUEVO, L. S., LICHTER, P. & MERTENS, D. 2008. Off-target effects of siRNA specific for GFP. *BMC molecular biology*, 9, 60-60.
- UEMURA, N., YAGI, H., UEMURA, M. T., HATANAKA, Y., YAMAKADO, H. & TAKAHASHI, R. 2018. Inoculation of α -synuclein preformed fibrils into the mouse gastrointestinal tract induces Lewy body-like aggregates in the brainstem via the vagus nerve. *Mol Neurodegener*, 13, 21.

- UMSCHEID, C. A., MARGOLIS, D. J. & GROSSMAN, C. E. 2011. Key concepts of clinical trials: a narrative review. *Postgraduate medicine*, 123, 194-204.
- URIBE, P., VILLEGAS, J. V., BOGUEN, R., TREULEN, F., SÁNCHEZ, R., MALLMANN, P., ISACHENKO, V., RAHIMI, G. & ISACHENKO, E. 2017. Use of the fluorescent dye tetramethylrhodamine methyl ester perchlorate for mitochondrial membrane potential assessment in human spermatozoa. *Andrologia*, 49, e12753.
- VAN PEER, G., MESTDAGH, P. & VANDESOMPELE, J. 2012. Accurate RT-qPCR gene expression analysis on cell culture lysates. *Scientific reports*, 2, 222-222.
- VÁRADI, C. 2020. Clinical Features of Parkinson's Disease: The Evolution of Critical Symptoms. *Biology*, 9, 103.
- VASILI, E., DOMINGUEZ-MEIJIDE, A., FLORES-LEÓN, M., AL-AZZANI, M., KANELLIDI, A., MELKI, R., STEFANIS, L. & OUTEIRO, T. F. 2022. Endogenous Levels of Alpha-Synuclein Modulate Seeding and Aggregation in Cultured Cells. *Molecular Neurobiology*, 59, 1273-1284.
- VAZ, A. R., CUNHA, C., GOMES, C., SCHMUCKI, N., BARBOSA, M. & BRITES, D. 2015. Glycoursodeoxycholic acid reduces matrix metalloproteinase-9 and caspase-9 activation in a cellular model of superoxide dismutase-1 neurodegeneration. *Mol Neurobiol*, 51, 864-77.
- VICARIO, M., CIERI, D., BRINI, M. & CALÌ, T. 2018. The Close Encounter Between Alpha-Synuclein and Mitochondria. *Frontiers in neuroscience*, 12, 388-388.
- VIJIARATNAM, N., GIRGES, C., AULD, G., CHAU, M., MACLAGAN, K., KING, A., SKENE, S., CHOWDHURY, K., HIBBERT, S., MORRIS, H., LIMOUSIN, P., ATHAUDA, D., CARROLL, C. B., HU, M. T., SILVERDALE, M., DUNCAN, G. W., CHAUDHURI, R., LO, C., DEL DIN, S., YARNALL, A. J., ROCHESTER, L., GIBSON, R., DICKSON, J., HUNTER, R., LIBRI, V. & FOLTYNIE, T. 2021a. Exenatide once weekly over 2 years as a potential disease-modifying treatment for Parkinson's disease: protocol for a multicentre, randomised, double blind, parallel group, placebo controlled, phase 3 trial: The 'Exenatide-PD3' study. *BMJ open*, 11, e047993-e047993.
- VIJIARATNAM, N., SIMUNI, T., BANDMANN, O., MORRIS, H. R. & FOLTYNIE, T. 2021b. Progress towards therapies for disease modification in Parkinson's disease. *The Lancet Neurology*, 20, 559-572.
- VILLANUEVA-PAZ, M., POVEA-CABELLO, S., VILLALÓN-GARCÍA, I., ÁLVAREZ-CÓRDOBA, M., SUÁREZ-RIVERO, J. M., TALAVERÓN-REY, M., JACKSON, S., FALCÓN-MOYA, R., RODRÍGUEZ-MORENO, A. & SÁNCHEZ-ALCÁZAR, J. A. 2020. Parkin-mediated mitophagy and autophagy flux disruption in cellular models of MERRF syndrome. *Biochimica et Biophysica Acta (BBA) - Molecular Basis of Disease*, 1866, 165726.
- VILLAR-PIQUÉ, A., LOPES DA FONSECA, T. & OUTEIRO, T. F. 2016. Structure, function and toxicity of alpha-synuclein: the Bermuda triangle in synucleinopathies. *J Neurochem*, 139 Suppl 1, 240-255.
- VINCENT, A., BRIGGS, L., CHATWIN, G. F. J., EMERY, E., TOMLINS, R., OSWALD, M., MIDDLETON, C. A., EVANS, G. J. O., SWEENEY, S. T. & ELLIOTT, C. J. H. 2012. parkin-induced defects in neurophysiology and locomotion are generated by metabolic dysfunction and not oxidative stress. *Human molecular genetics*, 21, 1760-1769.
- VINCOW, E. S., MERRIHEW, G., THOMAS, R. E., SHULMAN, N. J., BEYER, R. P., MACCOSS, M. J. & PALLANCK, L. J. 2013. The PINK1-Parkin pathway promotes both mitophagy and selective respiratory chain turnover in vivo. *Proc Natl Acad Sci U S A*, 110, 6400-5.
- VON STOCKUM, S., MARCHESAN, E. & ZIVIANI, E. 2018. Mitochondrial quality control beyond PINK1/Parkin. *Oncotarget*, 9, 12550-12551.
- VOS, M. & KLEIN, C. 2021. The Importance of Drosophila melanogaster Research to UnCover Cellular Pathways Underlying Parkinson's Disease. *Cells*, 10, 579.
- WALTER, J., BOLOGNIN, S., ANTONY, P. M. A., NICKELS, S. L., POOVATHINGAL, S. K., SALAMANCA, L., MAGNI, S., PERFEITO, R., HOEL, F., QING, X., JARAZO, J., ARIAS-FUENZALIDA, J., IGNAC, T., MONZEL, A. S., GONZALEZ-CANO, L., PEREIRA DE ALMEIDA, L., SKUPIN, A., TRONSTAD, K. J. &

- SCHWAMBORN, J. C. 2019. Neural Stem Cells of Parkinson's Disease Patients Exhibit Aberrant Mitochondrial Morphology and Functionality. *Stem cell reports*, 12, 878-889.
- WANG, D. Q. & CAREY, M. C. 2014. Therapeutic uses of animal biles in traditional Chinese medicine: an ethnopharmacological, biophysical chemical and medicinal review. *World J Gastroenterol*, 20, 9952-75.
- WANG, H., HE, M., WILLARD, B. & WU, Q. 2019. Cross-linking, Immunoprecipitation and Proteomic Analysis to Identify Interacting Proteins in Cultured Cells. *Bio-protocol*, 9, e3258.
- WANG, M., LING, K.-H., TAN, J. J. & LU, C.-B. 2020. Development and Differentiation of Midbrain Dopaminergic Neuron: From Bench to Bedside. *Cells*, 9, 1489.
- WANG, X., YAN, M. H., FUJIOKA, H., LIU, J., WILSON-DELFOSE, A., CHEN, S. G., PERRY, G., CASADESUS, G. & ZHU, X. 2012. LRRK2 regulates mitochondrial dynamics and function through direct interaction with DLP1. *Hum Mol Genet*, 21, 1931-44.
- WEI, H., LIU, L. & CHEN, Q. 2015. Selective removal of mitochondria via mitophagy: distinct pathways for different mitochondrial stresses. *Biochimica et Biophysica Acta (BBA) - Molecular Cell Research*, 1853, 2784-2790.
- WEI, P.-C., LO, W.-T., SU, M.-I., SHEW, J.-Y. & LEE, W.-H. 2012. Non-targeting siRNA induces NPGPx expression to cooperate with exoribonuclease XRN2 for releasing the stress. *Nucleic acids research*, 40, 323-332.
- WEST, R. J. H., FURMSTON, R., WILLIAMS, C. A. C. & ELLIOTT, C. J. H. 2015. Neurophysiology of Drosophila models of Parkinson's disease. *Parkinson's disease*, 2015, 381281-381281.
- WEST, R. J. H., UGBODE, C., FORT-AZNAR, L. & SWEENEY, S. T. 2020. Neuroprotective activity of ursodeoxycholic acid in CHMP2B(Intron5) models of frontotemporal dementia. *Neurobiology of disease*, 144, 105047-105047.
- WEST, R. J. H., UGBODE, C., GAO, F.-B. & SWEENEY, S. T. 2018. The pro-apoptotic JNK scaffold POSH/SH3RF1 mediates CHMP2BIntron5-associated toxicity in animal models of frontotemporal dementia. *Human molecular genetics*, 27, 1382-1395.
- WHONE, A., LUZ, M., BOCA, M., WOOLLEY, M., MOONEY, L., DHARIA, S., BROADFOOT, J., CRONIN, D., SCHROERS, C., BARUA, N. U., LONGPRE, L., BARCLAY, C. L., BOIKO, C., JOHNSON, G. A., FIBIGER, H. C., HARRISON, R., LEWIS, O., PRITCHARD, G., HOWELL, M., IRVING, C., JOHNSON, D., KINCH, S., MARSHALL, C., LAWRENCE, A. D., BLINDER, S., SOSSI, V., STOESSL, A. J., SKINNER, P., MOHR, E. & GILL, S. S. 2019. Randomized trial of intermittent intraputamenal glial cell line-derived neurotrophic factor in Parkinson's disease. *Brain*, 142, 512-525.
- WIEMERSLAGE, L. & LEE, D. 2016. Quantification of mitochondrial morphology in neurites of dopaminergic neurons using multiple parameters. *Journal of neuroscience methods*, 262, 56-65.
- WINER, J., JUNG, C. K. S., SHACKEL, I. & WILLIAMS, P. M. 1999. Development and Validation of Real-Time Quantitative Reverse Transcriptase-Polymerase Chain Reaction for Monitoring Gene Expression in Cardiac Myocytes in Vitro. *Analytical Biochemistry*, 270, 41-49.
- WONG, R., PIPER, M. D. W., WERTHEIM, B. & PARTRIDGE, L. 2009. Quantification of food intake in Drosophila. *PLoS one*, 4, e6063-e6063.
- WU, W., HODGES, E., REDELIUS, J. & HÖÖG, C. 2004. A novel approach for evaluating the efficiency of siRNAs on protein levels in cultured cells. *Nucleic acids research*, 32, e17-e17.
- WU, Y.-Y., CHIU, F.-L., YEH, C.-S. & KUO, H.-C. 2019. Opportunities and challenges for the use of induced pluripotent stem cells in modelling neurodegenerative disease. *Open biology*, 9, 180177-180177.
- XU, Z., CHU, X., JIANG, H., SCHILLING, H., CHEN, S. & FENG, J. 2017. Induced dopaminergic neurons: A new promise for Parkinson's disease. *Redox biology*, 11, 606-612.
- XUE, H., LI, J., XIE, H. & WANG, Y. 2018. Review of Drug Repositioning Approaches and Resources. *International journal of biological sciences*, 14, 1232-1244.
- YAKHINE-DIOP, S. M. S., MORALES-GARCÍA, J. A., NISO-SANTANO, M., GONZÁLEZ-POLO, R. A., URIBE-CARRETERO, E., MARTINEZ-CHACON, G., DURAND, S., MAIURI, M. C., AIASUI, A., ZULAICA,

- M., RUÍZ-MARTÍNEZ, J., LÓPEZ DE MUNAIN, A., PÉREZ-TUR, J., PÉREZ-CASTILLO, A., KROEMER, G., BRAVO-SAN PEDRO, J. M. & FUENTES, J. M. 2020. Metabolic alterations in plasma from patients with familial and idiopathic Parkinson's disease. *Aging*, 12, 16690-16708.
- YANG, H. P., TANIKAWA, A. Y., VAN VOORHIES, W. A., SILVA, J. C. & KONDRASHOV, A. S. 2001. Whole-genome effects of ethyl methanesulfonate-induced mutation on nine quantitative traits in outbred *Drosophila melanogaster*. *Genetics*, 157, 1257-1265.
- YANG, K., KOLANOWSKI, J. L. & NEW, E. J. 2017. Mitochondrially targeted fluorescent redox sensors. *Interface focus*, 7, 20160105-20160105.
- YANG, Y., LEE, M. & FAIRN, G. D. 2018. Phospholipid subcellular localization and dynamics. *The Journal of biological chemistry*, 293, 6230-6240.
- YEOW, J., KAUR, A., ANSCOMB, M. D. & NEW, E. J. 2014. A novel flavin derivative reveals the impact of glucose on oxidative stress in adipocytes. *Chemical Communications*, 50, 8181-8184.
- YU, S., LI, X., LIU, G., HAN, J., ZHANG, C., LI, Y., XU, S., LIU, C., GAO, Y., YANG, H., UÉDA, K. & CHAN, P. 2007. Extensive nuclear localization of alpha-synuclein in normal rat brain neurons revealed by a novel monoclonal antibody. *Neuroscience*, 145, 539-55.
- YU, S., ZUO, X., LI, Y., ZHANG, C., ZHOU, M., ZHANG, Y. A., UÉDA, K. & CHAN, P. 2004. Inhibition of tyrosine hydroxylase expression in alpha-synuclein-transfected dopaminergic neuronal cells. *Neurosci Lett*, 367, 34-9.
- ZHANG, L., ZHANG, C., ZHU, Y., CAI, Q., CHAN, P., UÉDA, K., YU, S. & YANG, H. 2008. Semi-quantitative analysis of alpha-synuclein in subcellular pools of rat brain neurons: an immunogold electron microscopic study using a C-terminal specific monoclonal antibody. *Brain Res*, 1244, 40-52.
- ZHENG, S., GRAY, E. E., CHAWLA, G., PORSE, B. T., O'DELL, T. J. & BLACK, D. L. 2012. PSD-95 is post-transcriptionally repressed during early neural development by PTBP1 and PTBP2. *Nature neuroscience*, 15, 381-S1.
- ZHENG, X., CHEN, T., ZHAO, A., WANG, X., XIE, G., HUANG, F., LIU, J., ZHAO, Q., WANG, S., WANG, C., ZHOU, M., PANEE, J., HE, Z. & JIA, W. 2016. The Brain Metabolome of Male Rats across the Lifespan. *Sci Rep*, 6, 24125.
- ZHU, M., QIN, Z. J., HU, D., MUNISHKINA, L. A. & FINK, A. L. 2006. Alpha-synuclein can function as an antioxidant preventing oxidation of unsaturated lipid in vesicles. *Biochemistry*, 45, 8135-42.
- ZIGONEANU, I. G., YANG, Y. J., KROIS, A. S., HAQUE, E. & PIELAK, G. J. 2012. Interaction of α -synuclein with vesicles that mimic mitochondrial membranes. *Biochimica et biophysica acta*, 1818, 512-519.